Identification of therapeutic targets in acute myeloid leukaemia expressing the mutant RAS oncogene

by

Goitseone Lucy Hopkins

2014

A thesis presented to Cardiff University in partial fulfilment of the requirement for the degree of Doctor of Philosophy

Department of Haematology,
School of Medicine,
Cardiff University,
United Kingdom.

Supervisors: Professor Richard Darley, Dr. Alex Tonks and Dr. Paul Hole
Acting Head of Department: Professor Richard Darley

Acknowledgements

My greatest thanks go to Professor R.Darley, Dr. A. Tonks and Dr. P. Hole, my supervisors for their expertise, invaluable guidance and patience throughout the study. I am also grateful to Professor Alan Burnett, Welsh Assembly (NISCHR) and Medical Research Council for funding this work. Other thanks to Cardiff University school of Medicine for giving me the chance to conclude my studies in excellent academic background providing all outstanding facilities for a proper educational carrier.

I convey my special thanks to Professor Lesley Jones, Dr. Abdul Seckam, Carol Guy and my mentor, Professor Marian Ludgate for their relentless support, enthusiasm and encouragement throughout the study.

My thanks also go to Lorna Pearn, Megan Musson, Sara Pumford and Dr. J. Zabkiewicz for their assistance in my laboratory work and all the members of Haematology department who have helped me in various aspects of this study.

Special thanks to my husband, Oliver E. Hopkins for his continuous encouragement, love, patience, cooperation and inexorable moral support throughout my entire study and my daughter, Lily-Frances Unami Hopkins for the unlimited entertainment during my write up. I would also like to express my heartfelt appreciation to all my family members for their emotional support throughout the study. Without them, this study wouldn't have been completed and I would never have reached this far.

I finally thank GOD for blessing and leading me throughout.

I dedicate this work to my daughter, Lily-Frances Unami Hopkins;
to my husband, Oliver E Hopkins
and to GOD.

Foreword

An electronic version of this document is provided on the accompanying CD (see back sleeve). In the electronic version of the document, all cross-references act as hyperlinks. Supplimentary material is also in the accompanying CD.

Publications and presentations

Publications

Hopkins G. L., Hole, P. S., Robinson A., Kreuser S., Tonks A., and Darley R. L. RAS promotes glycolysis in hematopoietic progenitor cells through the induction of reactive oxygen species. (**Manuscript in preparation 2014)**.

Hopkins, G.L., Robinson A.J., Hole, P. S., Darley, R. L., & Tonks, A. Analysis of ROS-responsive genes in mutant RAS expressing hematopoietic progenitors identifies the glycolytic pathway as a major target promoting both proliferation and survival. *American Society of Haematology Annual Meeting,* December 2014.

Abstracts

Hopkins, G.L., Pearn, L., Hole, P. S., Burnett, A. K., Darley, R. L., & Tonks, A. The role of reactive species production in acute myeloid leukaemia expressing mutant RAS. *26th Annual School of Medicine Postgraduate Research Day.* Nov 2007. (Accompanied by poster presentation).

Hopkins, G.L., Hole, P. S., Burnett, A. K., Tonks, A., & Darley, R. L.Targeting free radicals as a treatment for leukaemia, *Speaking of Science Conference, Graduate Centre, Cardiff University.* May 2011(Accompanied by oral presentation).

Hopkins, G.L., Robinson A.J., Hole, P. S., Darley, R. L., & Tonks, A. Analysis of ROS-responsive genes in mutant RAS expressing hematopoietic progenitors identifies the glycolytic pathway as a major target promoting both proliferation and survival. *American Society of Haematology Annual Meeting,* December 2014. (Accompanied by poster presentation). **ASH abstract achievement award winner. Travel sponsors awarded by Medical Research Council and British society of Haematology**.

Oral presentations

"The role of reactive oxygen species production in leukaemogenesis". *Cancer IRG seminar series*. October 2011.

"The role of reactive oxygen species production in acute myeloid leukaemia" *Haematology Departmental Seminar series*. November 2011.

"Targeting free radicals as a treatment for leukaemia". *Speaking of Science Conference, Graduate Centre, Cardiff University.* May 2011

"Does Cancer really have a sweet tooth". *3 Minutes Thesis Competition, Graduate Centre, Cardiff University.* June 2014. (**Awarded 2nd place**)

Abstract

Mutational activation of RAS is one of the most common molecular abnormalities associated with acute myeloid leukaemia (AML). Normal human haematopoietic progenitor cells (HPC) expressing mutant RAS overproduce ROS due to NADPH oxidase (NOX) activation and this promotes the proliferation of these cells as well as AML blasts. The mechanisms by which ROS promote proliferation is however unclear. The current study investigated the effect of RAS-induced ROS production on gene expression in normal HPC using gene expression profiling (GEP) and assessed whether ROS-induced gene expression changes contributed to the pro-proliferative phenotype. In order to determine the ROS-specific GEP, Affymetrix Human Exon 1.0^{ST} arrays were used for the comparison of mutant RAS and control cells cultured in the presence or absence of the NOX inhibitor, DPI, which strongly suppressed the production of ROS. This analysis showed that RAS changed the expression of 342 genes. Of these, 24 genes were specifically altered in response to ROS production by these cells and amongst these increased expressions of genes of the glycolytic pathway were prominent. To establish the functional significance of up-regulated expression of glycolytic enzymes, aldolase C (ALDOC) was investigated since it showed greatest induction with ROS. ALDOC was directly induced by physiological levels of ROS in both HPC and AML cell lines. Further, overexpression of ALDOC demonstrated that its overexpression promoted the proliferation and serum-independent survival of leukaemic cell lines. Conversely, anti-proliferative effects were observed when ALDOC was knocked-down in cells known to have high levels of constitutive ROS production. Given the high frequency of ROS production in AML, this study provides a plausible mechanism of enhanced glycolysis seen in this disease and suggests that agents restoring the redox environment could be used to correct metabolic imbalances which contribute to treatment resistance.

List of Abbreviations

7-AAD	7-aminoactinomycin D
ADP	adenosine diphosphate
Akt	v-Akt murine thymoma viral oncogene homologue (PKB)
ALDOC	Aldolase C
ALL	acute lymphoblastic leukaemia
AML	acute myeloid leukaemia
ANOVA	analysis of variance
APC	allophycocyanin
APL	acute promyelocytic leukaemia
Arg	arginine
ATP	adenosine triphosphate
ATRA	all-trans retinoic acid
BCL-2	B-cell CLL/lymphoma-2
Bis-Tris	bis (2-hydroxyethyl) imino-tris (hydroxymethyl) methane-HCl
BM	bone marrow
bp	base pair
C	Celcius
BSA	bovine serum albumin
CB	Cord blood
CBF	core binding factor
CBP	CREB-binding protein
CD	cluster of differentiation
CDK	cyclin-dependent kinase
CDKI	cyclin-dependent kinase inhibitor
CEBP	CCAAT/enhancer binding protein
CFC	colony-forming cells
CFU	colony-forming unit
Ci	Curie
CLL	chronic lymphocytic leukaemia
CML	chronic myeloid leukaemia
CMML	chronic myelomonocytic leukaemia
CMP	common myeloid progenitor
CoQ	coenzyme Q (ubiquinone)
CSF	colony stimulating factor
Cys	cysteine
Cyt c	cytochrome c
ddNTP	dideoxynucleotide triphosphate
dH_2O	distilled H_2O
DMEM	Dulbecco's Modified Eagle's Medium
DMPO	5,5-dimethyl-pyrroline-1-oxide
DMSO	dimethylsulphoxide
DNA	deoxyribonucleic acid

DNAse	deoxyribonuclease
dNTP	deoxynucleotide triphosphate
DPI	diphenyleneiodonium
DUOX	dual oxidase
DUOXA1	dual oxidase maturation factor
EBV	Epstein-Barr virus
EDTA	Ethylenediaminetetraacetic acid
EGF	epidermal growth factor
env	viral envelope and structural protein genes
EPO	erythropoietin
ERK	extracellular signal-regulated kinase
ETC	electron transport chain
ETO	Eight twenty one (protein/gene)
FAB	French-American-British
FACS™	fluorescence-activated cell sorting
FAD	flavin adenine dinucleotide
Fc	fragment crystallisable
FcR	Fc receptor
FCS	foetal calf serum
FDR	false discovery ratio
FITC	fluorescein isothiocyanate
FLT-3	FMS-like tyrosine kinase-3
FLT-3L	FLT3 ligand
FLT3-ITD	FLT-3 with internal tandem duplication mutation
FLT3-TKD	FLT-3 with tyrosine kinase domain mutation
FMN	flavin mononucleotide
FOXO	forkhead box-O
FT	farnesyl transferase
g	acceleration due to gravity; 9.8 ms^{-2}
Gab	GRB2 associated binder
gag	group-specific antigen
GAP	GTPase-activating protein
GAPDH	glyceraldehyde 3-phosphate dehydrogenase
GATA-1	GATA binding protein-1
G-CSF	granulocyte-colony stimulating factor
GDP	guanosine diphosphate
GEF	RAS guanine nucleotide exchange factor
GEP	Gene expression profiling
GFI	growth factor independent-1
GFP	green fluorescent protein
GM-CSF	granulocyte monocyte-colony stimulating factor
GMP	granulocyte-monocyte progenitors
GOX	glucose oxidase
GRB2	growth factor receptor-bound protein-2
GSH	glutathione
GTP	guanosine triphosphate
h	hours

H_2O_2	hydrogen peroxide
HBSS	Hank's balanced salt solution
HEPES	4-(2-hydroxyethyl)-1-piperazine-ethanesulfonic acid
HIF-1α	hypoxia-inducible factor-1α
HOCl	hypochlorous acid
HRP	horseradish peroxidase
HSC	haematopoietic stem cell
HX	hypoxanthine
i.v.	intravenous
IL	interleukin
IMDM	Iscove's Modified Dulbecco's Medium
ITD	internal tandem duplication
IU	international unit
JAK	Janus kinase
JMML	juvenile myelomonocytic leukaemia
Kbp	kilobase-pair
KD	Knock-down
KDa	kilo Dalton
KI	Knock-in
LB	Luria Bertani
LDS	lithium dodecyl sulphate
LN2	Liquid nitrogen
LPS	lipopolysaccharide (endotoxin)
LSC	leukaemic stem cell
LT-HSC	long term HSC
M	molarity (moles per L)
MACS	magnetic-activated cell sorting
MAPK	mitogen-activated protein kinase
MCS	multiple cloning site
M-CSF	macrophage colony-stimulating factor
MDS	myelodysplastic syndrome
MEK	mitogen-activated protein kinase
MEP	megakaryocyte-erythroid progenitor
min	minutes
MKP-3	mitogen-activated protein kinase phosphatase-3
MLL	mixed lineage leukaemia
MOPS	3-(N-morpholino) propane sulphonic acid
MPD	myeloproliferative disorder (MPN)
MPN	myeloproliferative neoplasm (MPD)
MPO	myeloperoxidase
MRD	minimum residual disease
mRNA	Messenger RNA
MSV	murine sarcoma virus
mTOR	mammalian target of rapamycin
Myc	myelocytomatosis oncogene
NADH	nicotinamide adenine dinucleotide

NAPDH	nicotinamide adenine dinucleotide phosphate
NCF	neutrophil cytosolic factor
NEB	Nuclear extraction buffer
NF1	neurofibromin
NF-κB	nuclear factor-κB
NOD/SCID	non-obese diabetic-severe combined immunodeficient (mice)
NOS	nitric oxide synthase
NOX	NADPH oxidase
NOXA1	NADPH oxidase activator-1
NOXO1	NADPH oxidase organiser-1
NPM-1	Nucleophosmin 1
N-RAS	Neuroblastoma-RAS (N-Ras or N-RasG12D)
PBS	phosphate-buffered saline
PCA	Principal component analysis
PCR	polymerase chain reaction
PDH	Pyruvate dehydrogenase
PDK1	phosphoinositide-dependent kinase-1
PE	R-phycoerythrin
PGK-1	3-phosphoglycerate kinase-1
Phox	phagocyte oxidase (NADPH oxidase complex)
PI	propidium iodide
PI3K	phosphoinositide 3-kinase
PKB	protein kinase B (Akt)
PKC	protein kinase C
PLC	phospholipase C
PMA	phorbol 12-myristate 13-acetate (TPA)
pol	viral reverse transcriptase gene
PP1	protein phosphatase-1
PP2A	protein phosphatase-2A
Pro	proline
Prx	peroxiredoxin
PS	phosphatidylserine
PTEN	phosphatase and tensin homologue
PTP	protein tyrosine phosphatase
PU.1	human homologue of murine Spi-1
PX	Phox homology domain
QA	quality assurance
QC	quality control
qRT-PCR	quantitative reverse-transcriptase PCR
RAS	rat sarcoma (Ras)
RRASGRP	RAS guanine-nucleotide release proteins
Rb	retinoblastoma protein
RIN	RNA integrity number
RMA	Robust Multichip Average
RNA	ribonucleic acid
RNAse	ribonuclease

RNS	reactive nitrogen species
ROS	reactive oxygen species
rpm	revolutions per minute
RPMI	Roswell Park Memorial Institute
RT	room temperature
RT-PCR	reverse-transcriptase PCR
S.D.	standard deviation
SCF	stem cell factor
SCT	stem cell transplant
SDS	sodium dodecyl sulphate
sec	seconds
Ser	serine
shRNA	short hairpin RNA
SiRNA	small interfering RNA
SOC	super-optimal broth (catabolite-repressing)
SOD	superoxide dismutase
SOS	son of sevenless
Spi-1	spleen focus-forming virus proviral integration oncogene-1
Src	cellular homologue of sarcoma inducing gene of Rous sarcoma virus
STAT	signal transducer and activator of transcription
ST-HSC	short term HSC
Thr	threonine
TPA	12-O-tetradecanoylphorbol-13-acetate (PMA)
TPO	thrombopoietin
Trx	thioredoxin
UC	Universal container
VLA	very late antigen
WBC	White blood cell
WHO	World Health Organisation
WT	whole transcriptome

Summary of Figures

Table of Contents

1 Introduction

1.1 NORMAL HAEMATOPOIESIS

1.1.1 OVERVIEW OF HAEMATOPOIESIS

Haematopoiesis is the formation, development and maintenance of blood cellular components. Approximately 1 x 10^{12} mature blood cells are generated daily in a healthy human body (Ogawa, 1993). These cells have biochemical and structural properties which allow them to carry out their specialized roles in living organisms. Such roles include tissue repair, blood coagulation, immunity and oxygen transport. For instance erythrocytes consist of high levels of haemoglobin and are bi-concave in shape which allows them to pass through the fine blood capillaries. On the other hand neutrophils, eosinophils and basophils (granulocytes) destroy pathogens via expression of antimicrobial proteins and inflammatory mediators and possession of a hyper-segmented flexible nucleus allows trans-endothelial migration via the blood into the site of infection. In addition, neutrophils, monocytes and macrophages produce reactive oxygen species (ROS) generating oxidases which contribute to the killing of pathogens.

The sites of haematopoiesis include, the yolk sac, liver and spleen (for foetus) vertebrae, ribs, sternum, skull, sacrum, pelvis and proximal ends of femur (for adults) (Hoffbrand and Moss, 2011). Most importantly, the bone marrow is the main source of new blood cells in normal healthy children and adults.

Haematopoiesis has been extensively studied and a considerable amount of evidence exists suggesting the hierarchical organisation of the haematopoietic system and the origin of all functionally diverse mature haematopoietic cells are attributed to the pluripotent haematopoietic stem cells (HSCs) (Figure 1.1) which are regulated by a

complex array of growth factors. According to Smithgall (1998), haematopoietic growth factors influence the proliferation, differentiation and survival of progenitor cells as well as the functional activities of the end-stage cells. Transcription factors also play an important role in lineage commitment and development and these together with growth factors govern the output of the haematopoietic system (section 1.1.2.2 and 1.1.2.3).

1.1.2 HAEMATOPOIESIS AND THE MICROENVIRONMENT

1.1.2.1 The HSC niche

HSCs are currently classified in to long term HSC (LT-HSC) and short term HSC (ST-HSC). It is important to note that LT-HSC are capable of reconstituting the whole haematopoietic system with the unique characteristic of long term self-renewal (Figure 1.1). Research on the HSC phenotype dates back to the 1960s and the broad immunophenotypic classification of human HSC was facilitated by studies in mice (Till and McCulloch 1961). Later studies defined a population of human haematopoietic cells which were able to repopulate sub-lethally irradiated non-obese diabetic-severe combined immunodeficient mice (NOD-SCID) and hence were termed human SCID-repopulating cells (SRC) (Dick, 1996; Larochelle *et al*., 1996; Bonnet and Dick, 1997) (also discussed in 1.2.1 and Figure 1.3). Using experiments such as these, human LT-HSC have been defined as lineage negative (Lin^-) $CD34^+$ $CD38^-$ and ST-HSC as Lin^-CD34^+ $CD38^+$.

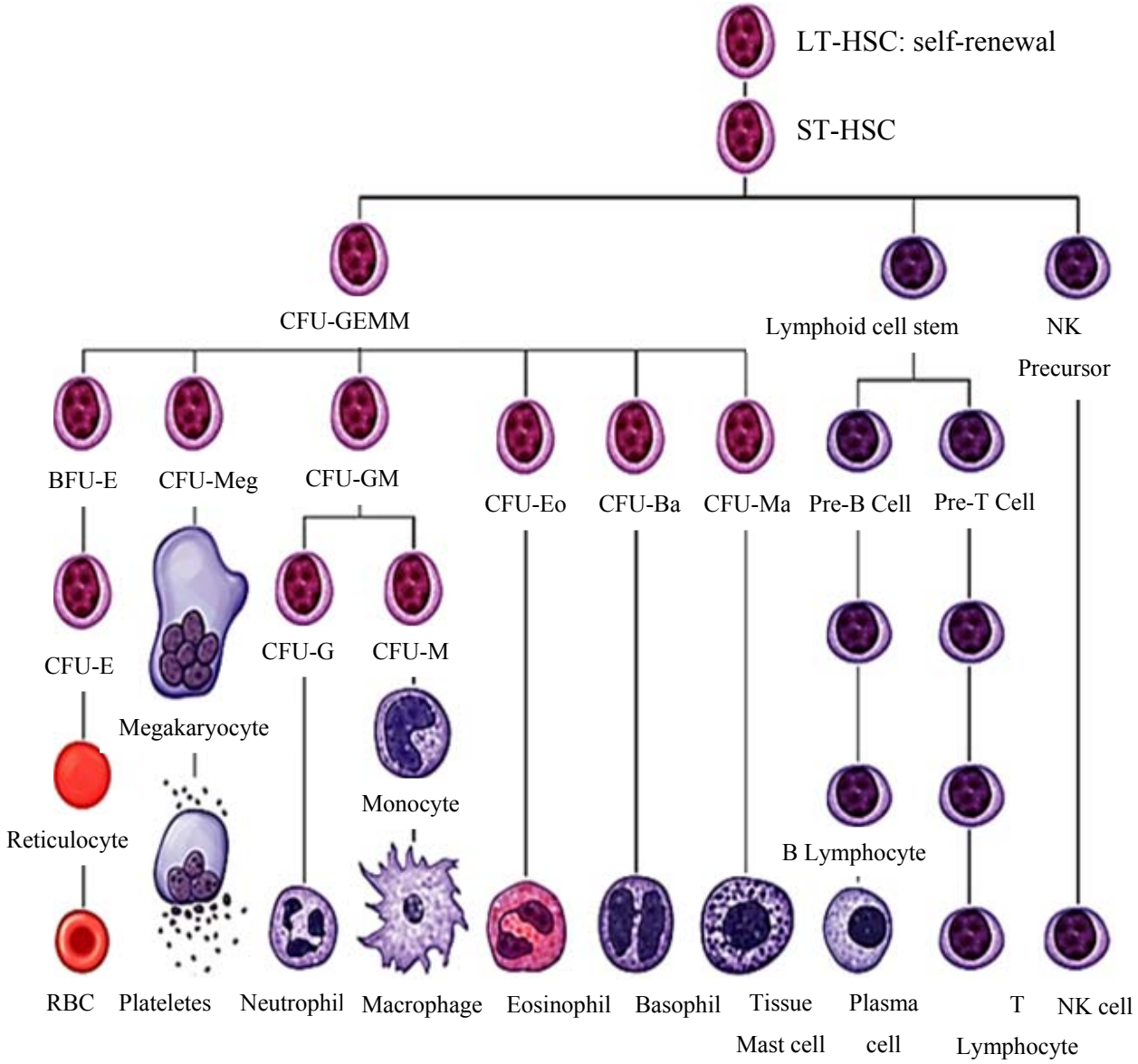

Figure 1.1 The hierarchical structure of the haematopoietic system

Diagrammatic representation of the bone marrow pluripotent, self-renewal, HSC and the mature blood cells arising from it. These cells terminally differentiate with a functionally adapted structure. Several haematopoietic progenitor cells can be identified by the type of colony they form in culture; CFU = colony forming unit; BFU = burst forming unit; GEMM = granulocyte erythroid monocyte megakaryocyte; GM = granulocyte monocyte; NK = natural killer; LT = long term; ST = short term; HSC = haematopoietic stem cell; RBC = red blood cell. Adapted from Rad, (2009).

Studies have shown that stem cells occupy specialized places in the bone marrow termed niches which are close to the blood vessels and the endosteum of the trabecular bone (Zhang *et al*., 2003; Kopp *et al*., 2005; Kiel *et al*., 2005; Orkin and Zon 2008). HSCs are known to reside in two highly specialised types of bone marrow niches namely the osteoblastic (Zhang *et al*., 2003; Yoshihara *et al*., 2007) and vascular niches (Kiel and Morrison 2006) (Figure 1.2). Quiescent HSCs are able to migrate to these sites in the bone marrow which provide a suitable environment for stem cell self-renewal and development. The bone marrow microenvironment is composed of microvascular network and stromal cells such as fibroblasts (Figure 1.2). Stromal cells secrete several growth factors necessary for HSC survival. These cells also secrete extracellular molecules essential for the formation of the extracellular matrix.

The homing of HSCs to the niche is made possible by several interactions and proteins found in the bone marrow microenvironment such as very late antigen-4 (VLA-4), very late antigen-5 (VLA-5), P-selectin and the well-studied chemokine; stromal derived factor-1 (SDF-1) (also known as CXCL12) and its receptor CXCR4 (also known as CD184) (Wilson and Trumpp, 2006; Petit *et al*., 2007). The pleiotropic chemokine, SDF-1 and its receptor, CXCR4 are widely expressed by the haematopoietic and endothelial cells of the niche (Peled *et al*., 1999). SDF-CXCR4 pathway has been reported to have a crucial role in the modulation of the trafficking and proper engraftment of the HSCs and reconstitution of haematopoiesis (Ara *et al*., 2003). In addition CXCL12 has been shown to regulate the migration of HSCs to the vascular cells (Kiel and Morrison, 2006). In summary, it is believed that stem cells depend on their microenvironment, the niche for regulation of self-renewal and differentiation (discussed in 1.1.2.2).

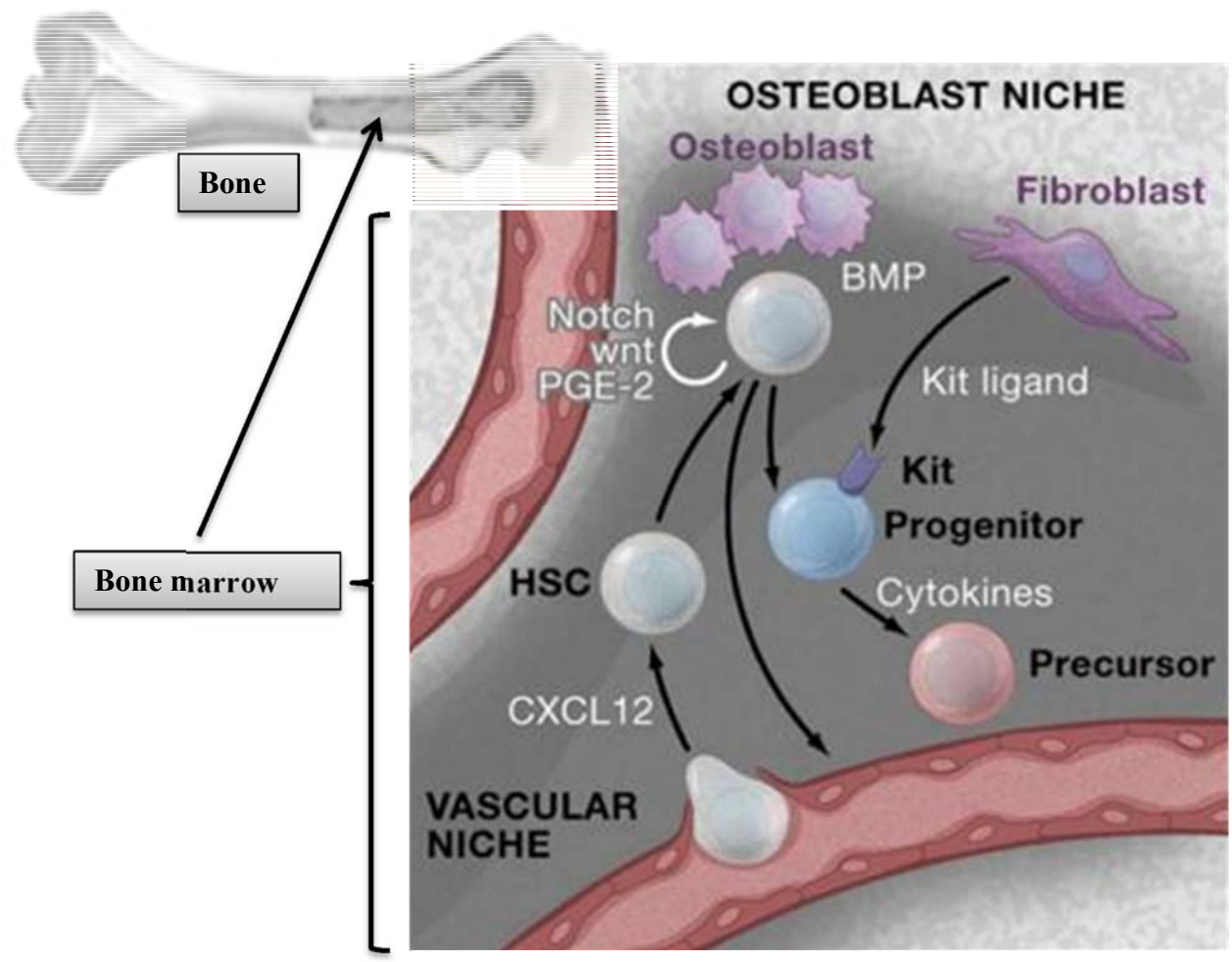

Figure 1.2 HSC Niche in the bone marrow

In the adult bone marrow, HSCs are found adjacent to osteoblasts (osteoblast niche) and blood vessels (vascular niche). HSCs in the osteoblast niche are believed to be under the regulation of bone morphogenetic protein (BMP) and CXCL12 regulates the migration of HSCs to the vascular cells in the bone marrow (reviewed by Orkin and Zon, 2008). Stromal cells, also present in the bone marrow space, secrete cytokines (c-kit and others not indicated in the figure) which influence stem cell self-renewal and survival. Curved white arrow = self-renewal. Adapted from Orkin and Zon, (2008).

1.1.2.2 Growth factors/cytokines in haematopoiesis

The stem cell niche in the adult bone marrow generates cytokines (Figure 1.2) that stimulate HSC and progenitors such as c-Kit and those that influence the progenitor survival and function; (e.g. thrombopoietin (TPO), erythropoietin (EPO) (Orkin and Zon 2008). Growth factors greatly influence proliferation, survival and terminal maturation of HSCs. For instance FLT-3 ligand and stem cell factor (SCF) act mainly on pluripotent HSCs, common myeloid progenitors (CMP`s) and common lymphoid progenitors (CLP`s) to facilitate their proliferation (Hoffbrand and Moss 2011). Cytokines such as GM-CSF, CSF-1 and EPO act primarily on a particular lineage of cells, enhancing the expansion and differentiation of macrophages, granulocytes and erythrocytes respectively. Cytokines also act synergistically, for example the combination of GM-CSF with G-CSF greatly augments the production of neutrophils compared with either cytokine alone (Lowry, 1995).

1.1.2.3 Transcription factors in haematopoiesis

Cell fate is regulated by transcription factors that control lineage development programmes, for example, GATA-binding protein 1 (GATA1), GATA 2 and FOG 1 (also known as ZFPM1) are vital for megakaryocyte-erythrocyte-basophil or mast cell-eosinophil development (Graf, 2002). The activities of transcription factors such as PU.1 have been shown to drive or direct HSCs or progenitors away from the erythroid fate to a myeloid fate (Galloway *et al*., 2005). Several studies have shown that high levels of PU.1 and GATA1 expression is necessary to generate neutrophils and monocytes (Dahl *et al*., 2003) whilst low levels of the above transcription factors are essential to enable the development of B cells (DeKoter and Singh 2000). The expression of the myelomonocytic associated factor; CCAAT/enhancer binding protein (C/EBPα) directs megakaryocyte-

erythroid progenitors to become macrophages and neutrophil-monocyte progenitors to become monocytes (Mukai *et al*., 2006). It is important to note that phosphorylation of transcription factors also play an important role in the determination of cell fate. For instance, phosphorylation of C/EBPα can inhibit its activity and can force neutrophil-eosinophil progenitors to become eosinophils (Buitenhuis *et al*., 2008). These findings together with the findings of other studies have demonstrated that the enforced expression of transcription factors can direct development towards an alternative cell fate.

Abnormal transcription factor activities are closely associated with leukaemia. Translocations frequently found in Acute Myeloid Leukaemia (AML) affect transcription factors previously shown to play vital roles in haematopoietic lineage development; for instance, the analysis of patients harbouring the most common abnormality associated with AML, the t (8; 21) translocation generating RUNX1-ETO oncogene, have shown that the expression of this oncogene leads to decreased expression of the critical granulocytic differentiation factor CEBP/α (Pabst *et al*., 2001). Researchers have therefore linked the alteration of the transcriptional machinery to the mechanisms leading to arrested differentiation (Tenen 2003). Single nucleotide polymorphisms (SNPs) can also influence transcription factor expression, for example, in AML a SNP within a highly conserved distal enhancer greatly decreases the expression of PU.1 via the blockage of chromatin-remodelling transcriptional regulator SATB1 (Steidl *et al*., 2007).

1.1.3 MODELS USED TO STUDY HAEMATOPOIESIS

Research models used to examine the haematopoietic system date back to the 1960s when it was demonstrated that bone marrow cells injected into irradiated mice resulted in spleen colonies (Till and McCulloch *et al*., 1961). Since then, several models (both *in vivo* and *in vitro*) have been developed and employed in the study of haematopoiesis, including experimental culture systems that incorporate stromal cells to aid in the generation of lymphoid (Whitlock and Witte, 1982) or myeloid cells (Dexter, 1979). For instance, the most recent and relevant model for study of haematopoiesis in mammals was generated via *in vitro* studies of primary haematopoietic cells and haematopoietic cell lines along with the *in vivo* murine studies. The ability to culture normal haematopoietic cells *in vitro* overcomes the shortcomings associated with cell lines which have limited developmental potential and harbour abnormalities including chromosome translocations (Furukawa, 2002).

1.2 ACUTE MYELOID LEUKAEMIA

1.2.1 OVERVIEW AND PATHOPHYSIOLOGY OF AML

AML is a heterogeneous malignancy of the HSC and haematopoietic progenitor cells (HPCs) characterized by a clonal expansion of immature white cells (blast cells). These are abnormal cells that have failed to differentiate into functional myeloid cells. Accumulation of leukaemic blasts results in the failure of normal haematopoiesis (Pollyea *et al*., 2011).

AML has been described as a very challenging aggressive malignancy with a very poor clinical outcome (Löwenberg 1999). It has a very high morbidity and mortality rate worldwide with an incidence of 3.4 cases per 100 000 people in the UK (Milligan *et al*., 2006). Among other types of acute leukaemia, it is the most common one in adults and

elderly people are the most affected group with a median age at diagnosis of 67 years as reported in the National cancer institute 1975-2007 report (Kohler *et al*., 2011). Therefore it is clear that the risk of AML increases with age. Other risks associated with AML include exposure to radiation, smoking, previous chemotherapy and pre-existing blood disorders (Estey and Döhner, 2006).

Advances in research have led to the identification of molecular and cytogenetic abnormalities in AML (discussed later 1.2.2 and 1.2.3). For instance, at least one chromosomal rearrangement was reported in over 80% of myeloid leukaemias (Pandolfi, 2001). In another study by Gilland and Tallman (2002), more than 100 chromosomal translocations were cloned most of which were associated with genes encoding transcription factors that play crucial roles in haematopoietic lineage development. It was also suggested that changes of the transcriptional machinery pose a potential common mechanism leading to arrested differentiation (Tenen 2003).

Despite the identification of several risk factors and abnormalities in AML, the specific cause of this disease is not clear; however the manifestation of acute leukaemia has been attributed to cooperation between the class I activating mutations such as FLT3, KIT and RAS family (1.3) and class II mutations which induce the termination of differentiation (Table 1.1), Gilland and Tallman (2002). Class I mutations confer proliferative and survival advantage to haematopoietic progenitors due to the activation of signal transduction pathways while class II mutations results in a halt in differentiation via interference with either transcription factors or co-activators. Evidence exists in support of this model. For example, it is believed that in AML, an initiating event such as chromosomal translocation (t (8; 21) which results in RUNX1-ETO fusion gene), occurs in primitive HSC and/or HPC. Such occurrence is not enough to cause leukaemia alone although it was shown to impair normal differentiation (Miyamoto *et al*., 2000; Downing,

2003) which confers the essential advantages needed to pre-dispose to subsequent transformation of the pre-malignant clone through the acquisition of class I mutations.

There is also evidence supporting the fact that myeloid leukaemia cells known as leukaemia stem cells (LSC) exist in a hierarchy similar to that of normal haematopoiesis (Figure 1.3) (Bonnet and Dick, 1997). These authors used a strain of immunocompromised mice termed non-obese diabetic mice with severe combined immunodeficiency disease (NOD/SCID mice) which allowed engraftment of human AML cells. Only a subpopulation of AML blasts-termed SCID-leukaemia initiating cell (SL-IC) was found to efficiently engraft these mice. The SL-ICs from all subtypes of AML were analysed and found to be $CD34^{+}$ $CD38^{-}$ (equivalent to the cell surface phenotype of normal HSC). Engraftment of just this subpopulation of phenotypically primitive cells subsequently recapitulated the heterogeneous phenotype of the original disease. These findings also suggested that HSC rather than committed progenitor cells are the target for leukaemic transformation and gave rise to the concept of leukaemic stem cells.

Despite these and other recent advances in the identification of recurrent mutations, the initiating mutations of AML are unknown because pre-leukaemic cells are clinically silent and are out-competed by their malignant descendants (Greaves *et al*., 2010). However recent findings have revealed pre-leukaemic HSCs which might contribute to better understanding of AML and future therapy (see 1.2.4).

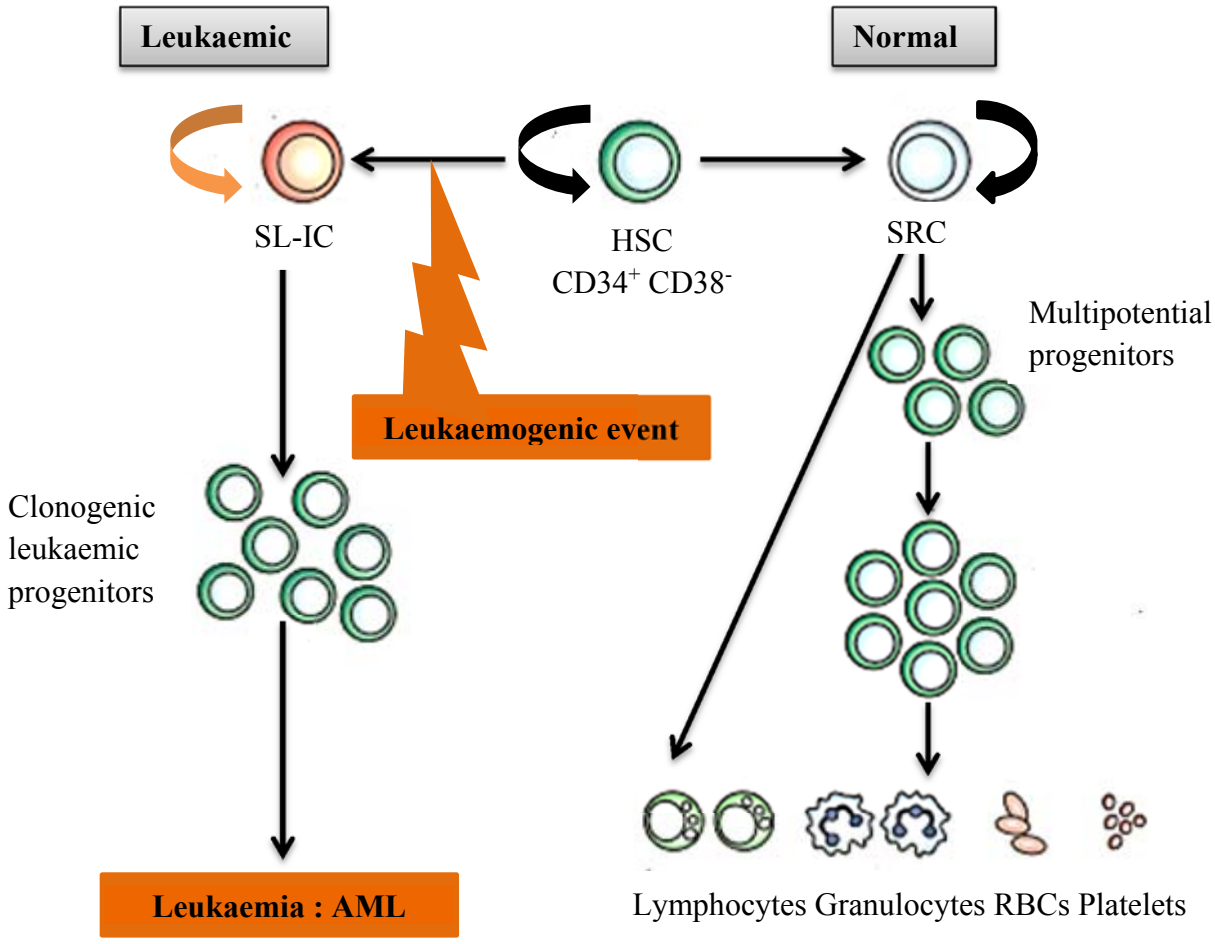

Figure 1.3 Acute myeloid leukaemia stem-cell hierarchy

Leukaemia cells are believed to be derived from HSCs which are $CD34^{+}CD38^{-}$ just like normal HSC. Normal HSC repopulating NOD/SCID mice (SCID-repopulating cells; SRC), are capable of self-renewal and production of all mature lineages through a succession of multipotent and committed progenitors. Leukaemia stem cells (LSC or SCID leukaemia-initiating cell (SL-IC)) that initiate AML express some shared surface phenotypic markers with HSC and have the capacity for producing both the clonogenic leukaemic progenitors and the non-clonogenic blast cells which make up the bulk of leukaemia. Curved arrow = self-renewal. Adapted from Bonnet and Dick, (1997).

1.2.2 MOLECULAR ABNORMALITIES IN AML

There are several molecular abnormalities associated with AML some of which are listed in Table 1.1. Mutational activation of RAS (particularly N-RAS) (section 1.3) is common (for full details see section 1.3.3). The other abnormality that frequently occurs in AML is the internal tandem duplication in the FLT3 tyrosine kinase (FLT3-ITD) with a vital role in AML prognosis (section 1.2.3), cell proliferation, survival and differentiation. Activation of FLT3 receptor by FLT3 ligand result in receptor dimerization and phosphorylation and activation of downstream signalling pathways such as Janas kinase 2 (JAK2) signal transducer activator of transcription 5 (STAT5) and mitogen activator protein kinase (MAPK) pathways (Reindl *et al*., 2006; Grundler *et al*., 2005; Lee *et al*., 2007). Mutations in the FLT3 genes, found in approximately 40% of AML patients are believed to promote its auto phosphorylation and constitutive activation resulting in ligand-independent proliferation (Frankfurt *et al*., 2007). KIT mutations have also been linked to AML (Bachas *et al*., 2010).

Mutation class	Gene involved	Frequency	Prognosis
I	RAS	15-30%	Not prognostic
	FLT-3	25-45%	bad
	c-KIT	6-10%	bad
II	NPM1	25-35%	good
	CEBPα	4-9%	good

Table 1.1 Common mutations in AML

Mutations most frequently identified in AML include: class I (signal transduction) and II (transcriptional). Reviewed by Ravandi *et al*., 2007; Dohner and Dohner, 2008).

1.2.3 CLASSIFICATION, DIAGNOSIS AND PROGNOSIS

The appearance of the blasts among patients with AML (Warner *et al*., 2004) gave rise to the French-American-British (FAB) classification (Table 1.2). This has been superseded by the World health organisation (WHO) classification which is based more heavily on the molecular characterisation of AML (Table 1.3). In the FAB classification system, AML is classified into nine FAB types according to the maturation stage of leukaemia based upon the examination of blast morphology and the expression of lineage differentiation markers (Bennet *et al*., 1976, 1982). Under the WHO classification, there are four categories of AML (detailed in Table 1.3) based upon a combination of advanced immunophenotyping, morphology assessment, clinical features and genetic data and recurring chromosomal abnormalities (Vardiman *et al*., 2002; 2009). This classification is more helpful in clinical decision making. Differences among patients that affect response to treatment are termed prognostic factors and these help in the decisions made by doctors concerning the amount of treatment required by people with certain types of leukaemia. The main prognostic factors in AML include cytogenetic status (the presence or absence of chromosome translocations, aneuploidy or deletions), age of the patient, white blood cell (WBC) count, prior blood disorders, active systemic blood infection and treatment-related AML (Estey and Dohner, 2006; Grimwade *et al*., 1998; Grimwade *et al*., 2001). Cytogenetic and molecular abnormalities (others discussed above) that have been identified in AML as of prognostic value include FLT3-ITD (Jan *et al*., 2012). This abnormality frequently occurs in AML and it indicates high risk (Schlenk *et al*., 2008).

FAB subtype	Description/Name
M0	Undifferentiated AML
M1	Acute myeloblastic leukaemia with minimal maturation
M2	Acute myeloblastic leukaemia with maturation
M3	APL
M4	Acute myelomonocytic leukaemia
M4 $_{eos}$	Acute myelomonocytic leukaemia with eosinophilia
M5	Acute monocytic leukaemia
M6	Acute erythroid leukaemia
M7	Acute megakaryoblastic leukaemia

Table 1.2 The FAB classification of AML

AML is divided into nine FAB subtypes based on the type of cell from which leukaemia developed and how mature the cells are. Abbreviations: FAB = French-American-British; APL = Acute promyelocytic leukaemia. Adapted from: Tenen *et al*., (2003).

Category of AML	Description
AML with recurrent genetic abnormalities	AML with t(8;21)(q22;q22), *AML1/ETO*
	AML with abnormal bone marrow eosinophils and inv(16)(p13q22) or t(16;16)(p13;q22),(*CBFβ-MYH11*)
	APL with t(15;17)(q22;q12), (*PML-RARα*)
	AML with t(9;11)(p22;q23), *MLLT3-MLL*
	AML with t(6;9)(p23;q34), *DEK-NUP214*
	AML with inv(3)(q21q26.2) or t(3;3)(q21;q26.2), *RPN1-EVI1*
AML with multi-lineage dysplasia	AML with changes associated with myelodysplasia or following MDS or MDS/MPD
AML and therapy related myelodysplastic syndromes	Alkylating agent/radiation- related type
AML not otherwise categorized	AML with minimal differentiation
	AML without maturation
	AML with maturation
	Acute myelomonocytic leukaemia
	Acute monocytic/monoblastic leukaemia
	Acute erythroid leukaemia (pure erythroleukaemia and erythroid/myeloid)
	Acute megakaryoblastic leukaemia
	Acute basophilic leukaemia
	Acute panmyelosis with myelofibrosis
	Myeloid sarcoma

Table 1.3 The WHO classification of AML

In the WHO classification, AML is divided into 4 subgroups/categories. Abbreviations: MDS = Myelodysplastic syndrome; APL = acute promyelocytic leukaemia Adapted from: Vardiman *et al*., (2002; 2009).

1.2.4 THERAPY

The treatment of AML occurs in two main phases: the induction phase which is aimed at reduction of tumour burden AML and consolidation treatment geared towards preventing relapse. The induction phase is based on chemotherapy using drugs such as cytarabine (Bloomfield *et al*., 1994). Sometimes a combination of different drugs is used for high risk patients. Consolidation phase follows successful remission induction and this includes more chemotherapy, donor transplant or blood stem cell transplant. It is noteworthy that doctors take into account several factors when making decisions concerning consolidation therapy including remission, patient history of other cancers and treatments. The treatment of cancer includes several health care professionals which in turn facilitates best treatment decisions. Other factors influencing cancer treatments are AML type, age and general health of a patient.

There are several challenges faced with regards to AML therapy. LSC have been shown to impact therapy in AML patients. LSC has been reported to be present after chemotherapy, thus the failure of current AML treatments has been attributed to the insufficient eradication and survival of chemotherapy resistant LSC (Van Rhenen *et al*., 2005; Ishikawa *et al*., 2007). For instance, a study by Terwijn *et al*., (2010) showed that high frequencies of $CD34^+$ $CD38^-$ LSC at diagnosis and after treatment predicted relapse in AML suggesting that the LSC are indeed clinically important (Eppert *et al*., 2011) and prognostic. Eradication of LSC may therefore prevent relapse and lead to a better long-term outcome in AML; however this presents enormous challenges. The heterogeneity of LSC phenotype within the single AML patient (Taussig *et al*., 2010) together with the similarities of both normal HSC and LSC in the same cell compartment within the AML bone marrow requires careful consideration for the tailoring and application of therapies.

In support of this, Buggins *et al*., (2001) pointed out that the extent to which LSC and HSC differ is critical to the development of LSC-targeted therapies with low toxicity. A study by (Schuurhuis *et al*., 2013) has already formed the foundation for combined immunophenotypically and functionally based identification and purification of LSC and HSC within the bone marrow which is a step towards the development of highly specific anti-LSC therapy. In this study it was shown that normal $CD34^{+}$, $CD38^{-}$ HSC found in AML bone marrow were distinct sub-population of cells with high aldehyde dehydrogenase (ALDH) activity in LSC. Therefore it was concluded that there are lower levels of ALDH activity in LSC than the normal $CD34^{+}CD38^{-}$ HSC that co-exist with these LSC in the bone marrow across all AML cases.

1.3 THE RAS FAMILY OF PROTEINS

1.3.1 OVERVIEW OF THE RAS PROTEIN SUPERFAMILY

The founding members of the RAS (rat sarcoma) protein superfamily includes Harvey-RAS (H-RAS) located on human chromosome 11p15.5, neuroblastoma-RAS (N-RAS) located on human chromosome 1p13.2 and two isoforms of Kirsten-RAS (K-RAS4A, K-RAS4B) located on human chromosome 12p12.1 (Malumbres and Barbacid, 2003; Wennerberg *et al*., 2005). Their structural similarities and differences are illustrated and discussed below (Figure 1.4). These proteins are membrane-bound GTPases that integrate signals from membrane-associated growth-factor receptors to a variety of effector molecules and have been previously shown to modulate different cellular processes (Beaupre and Kurzrock 1999; Hingorani and Tuvenson, 2003). For instance, H-RAS and K-RAS were shown to play a vital role in development (Schubbert *et al*., 2007). RAS proteins are activated when bound to guanosine triphosphate (GTP), and normally inactive when bound to guanosine diphosphate (GDP) (Mitin *et al*., 2005;Wennerberg *et al*., 2005)

which enable them to deliver an 'on' or 'off' signal, acting as binary molecular switches (Figure 1.5). X-ray crystallographic research studies of RAS proteins bound to either GDP or GTP reported large conformational changes induced in the RAS protein upon an exchange of GDP to GTP and vice versa (Schlichting *et al*., 1990). The location of these conformational changes have been attributed to switch I and II (Figure 1.4) which are flexible loop regions of the RAS superfamily responsible for their protein signalling and regulation of downstream effectors(Figure 1.5 and Figure 1.6)(Karnoub and Weinberg, 2008).

It is important to note that activated RAS molecules have the capability to self-limit their activation in an intrinsic manner via their weak intrinsic GTPase activity which enables them to hydrolyse bound GTP forming GDP and inorganic phosphate. GTPase activating proteins (GAP_S) such as neurofibromin (NF1) act as negative regulators and have been shown to enhance accumulation of GDP-bound RAS (Ahmadian *et al*., 1997) by promoting efficient GTP hydrolysis (Figure 1.5). On the other hand RAS is activated via the preferential binding of GTP. This is because the positive regulators of RAS such as the guanine nucleotide exchange factors (GEFs) (Figure 1.5) link with inactive form of the GDP-bound RAS and induce conformational changes which in turn augment the release of GDP. Usually these result in binding of GTP which is at a 10X higher concentration in the cytosol than GDP (Karnoub and Weinberg 2008).

In addition, post-translational modification is essential for RAS proteins to carry out their roles. This involves post-translational attachment of lipid molecules and prenylation of the post-translated RAS molecule in the cytosol by either farnesyl transferase (FT) or geranylgeranyl transferase which attach either farnesyl or geranylgeranyl groups to the cysteine (Cys) residue within the C-terminal motif of the RAS protein, CAAX (A = aliphatic amino acid; X = any amino acid). The farnesylated

CAAX motif then undergo palmitoylation step which involves the attachment of palmitic acid by palmitoyltransferase of the selected cysteine residues near the farnesylation site.

Mutational activation of RAS proteins has been well studied. Activating mutations of RAS proteins are clustered in codons 12, 13 and 61 (Krengel *et al*., 1990). In addition, it is now known that the most common substitutions in human cancers replace glycine with valine or aspartate at these positions. This is because several studies have shown that those positions are crucial to intrinsic GTP hydrolysis by RAS since the 12th and 13th codons in each of the RAS isoforms encode glycine (the only amino acid without a side chain). Thus any mis-sense mutation at these positions results in the inclusion of an amino acid with a side chain and substitutions at codons 12 or 13 leading to an accumulation of GTP-bound RAS (activated form) due to impairment or radical decrease in GTPase activity (Schubbert *et al*., 2007).

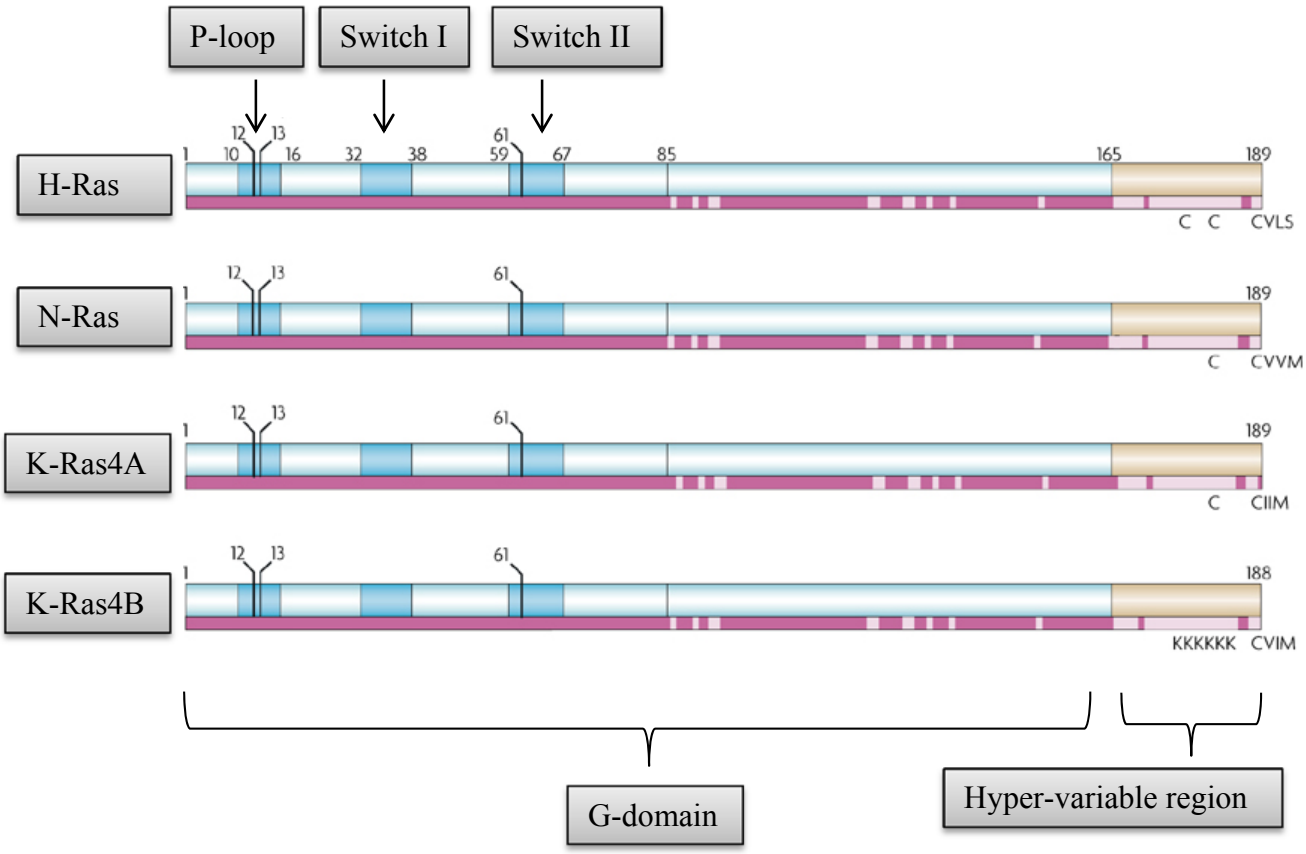

Figure 1.4 Structure of RAS proteins

The diagram illustrates the structures of the four isoforms of RAS proteins, N-RAS, H-RAS, K-RAS4A and K-RAS4B with high homology throughout the amino acid 1-165 (G-domain). The first 85 amino acids are identical in all proteins and specify binding to GDP and GTP. This includes the phosphate-binding loop (P- loop) (amino acids 10–16), which binds the γ-phosphate of GTP, and switch I (amino acids 32–38) and II (amino acids 59–67) which regulate binding to RAS regulators and effectors. Amino acids 85–165 show sequence identity (~85–90%). The C-terminal hyper-variable domain (amino acids 165–188/189) specifies membrane localization through post-translational modifications that include the farnesylation of each isoform on the C-terminal CAAX motif (CVLS, CVVM, CIIM and CVIM, respectively) and palmitoylation of key cysteines on HRAS, NRAS and KRAS4A; these cysteines are highlighted below each representation (C). Membrane localization of KRAS4B is facilitated by a stretch of lysines (KKKKKK) proximal to the CVIM motif. A box at the bottom of each isoform representation shows the conserved residues (bright pink) and the variable residues (pink) to indicate the degree of homology. Adapted from Schubbert *et al*., (2007).

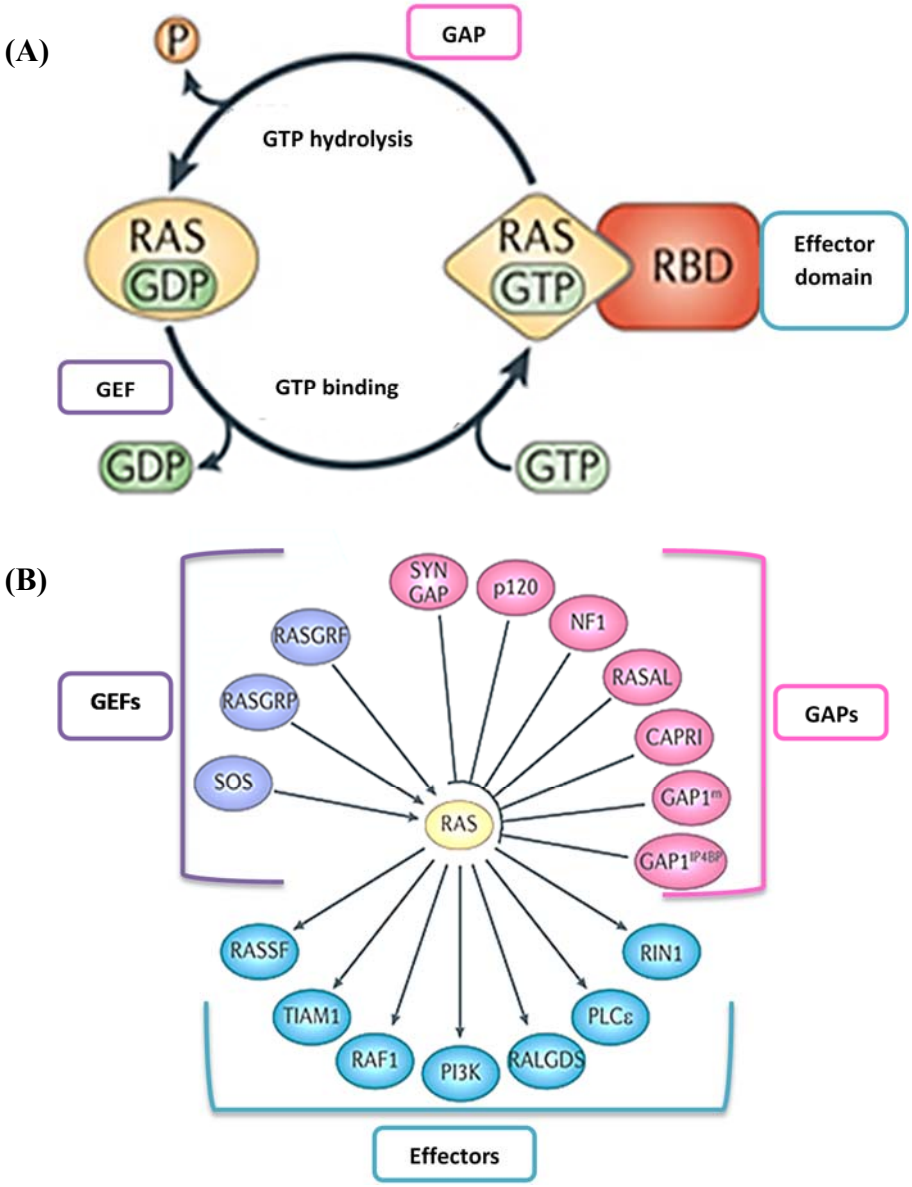

Figure 1.5 The GDP-GTP cycle and regulation of RAS

(A) An illustration of the GDP-GTP cycle of RAS. Inactive, GDP-bound RAS is activated by GEFs, which stimulates the release of GDP and permits GTP binding. GTP loading induces a marked conformational change in RAS allowing it to bind effector via their RBDs. The so called 'on' state of RAS is limited by its low intrinsic GTPase activity, which is accelerated by the binding of a GAP, allowing RAS to return to its inactive, GDP-bound state.**(B)** An illustration of several families of GEFs, GAPs and effectors that have been reported to regulate RAS or transmit signals from RAS.GTP. Abbreviations: GEF = guanine nucleotide exchange factor; GAP = GTPase-activating protein; RBD = RAS-binding domains; CAPRI = calcium-promoted RAS in-activator; $GAP1^{IP4B}$ = GAP1 $InsP_4$ –binding protein; NF1 = neurofibromin 1; P = phosphate; PI3K = phosphoinositide 3-kinase; RALGDS = RAL guanine nucleotide dissociation stimulator ; RASAL = RASGAP-activating-like; RASGRF = RAS-specific guanyl-nucleotide-releasing factor; RASGRP = RAS-specific-guanine-nucleotide-releasing protein; RASSF = RAS association domain-containing family; RIN_1 = RAS and RAB interactor 1; SYNGAP = synaptic RASGAP; $TIAM_1$ = T lymphoma invasion and metastasis-inducing 1. Adapted from Ahearn *et al*., (2011).

1.3.2 RAS SIGNALLING AND HAEMATOPOIESIS

A sequence of events occur leading to the recruitment and activation of RAS GEFs which in turn results in the accumulation of the activated GTP-bound RAS (Figure 1.6). SHP2 is recruited to the activated receptor complex along with molecules such as growth factor-receptor bound protein 2 (GRB2) linking the activated receptor to SOS family of proteins (RAS GEFs). Signalling is initiated by growth factor binding to cell surface receptors (tyrosine kinase) resulting in the activation of receptor complexes consisting of adapters such as SH2-containing protein (SHC), GRB2 and GRB2-associated binding (Gab) proteins. These proteins recruit SHP2 and SOS1, the latter increasing RAS-GTP levels by catalysing nucleotide exchange on RAS. GAPs such as NF1 bind to RAS-GTP and speed up the conversion of RAS GTP to RAS-GDP hence antagonising RAS activation resulting in the termination of its signalling. NF1 play an important role in the regulation of RAS signalling, with inactivating mutations implicated in neurofibromatosis, a congenital developmental disorder linked with the strong risk of Juvenile myelomonocytic leukaemia (JMML) development (Niemeyer *et al*., 1997; Schubbert *et al*., 2007)

Many RAS-GTP effector pathways have been described and the key ones are illustrated in Figure 1.6. The BRAF-mitogen-activated and extracellular-signal regulated kinase kinase (MEK)-extracellular signal-regulated kinase (ERK) cascade frequently governs proliferation and becomes deregulated in certain cancers and developmental disorders. In addition RAS activates other pathways such as the phosphatidylinositol 3-kinase (PI3K)-3-phosphoinositide-dependent kinase 1 (PDK1)-Akt pathway that often determines cellular survival (Figure 1.6). RAS also binds and activates the enzyme

phospholipase Cε (PLCε), the hydrolytic products of which regulate calcium signalling and the protein kinase C (PKC) family.

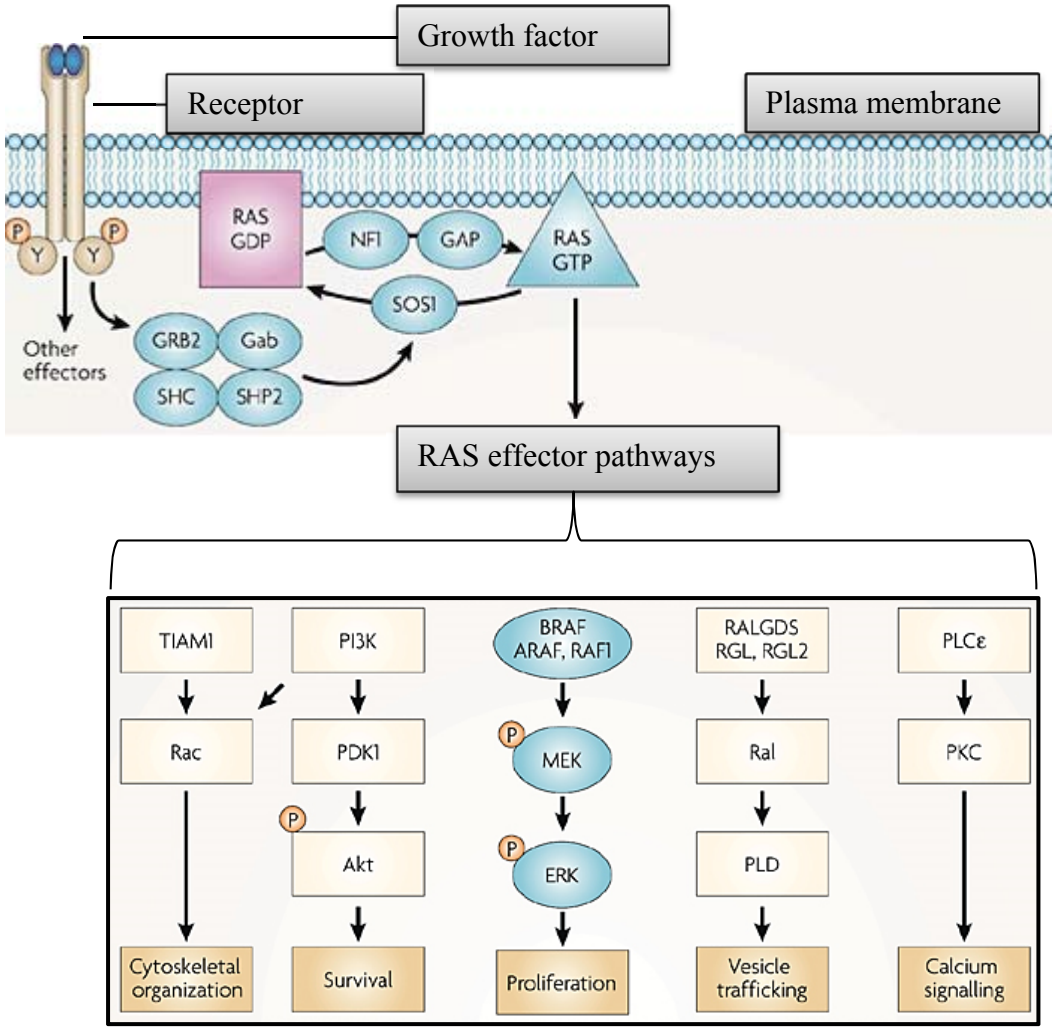

Figure 1.6 Summary of RAS activation and signalling pathways

An illustration of the events leading to RAS activation, the key effector signalling pathways initiated by activated RAS and proteins affected by mutations in developmental disorders and cancer. Abbreviations: SHC = SH2-containing protein; GRB2 = growth-factor-receptor bound protein 2; Gab = GRB2-associated binding proteins; RAS-GTP = RAS-guanosine triphosphate; GAP = GTPase-activating protein; NF1 = neurofibromin; RAS-GDP = RAS-guanosine diphosphate; MEK = mitogen-activated extracellular-signal regulated kinase; ERK = extracellular signal-regulated kinase; PI3K = phosphatidylinositol 3-kinase; PDK1 = phosphoinositide-dependent protein kinase 1; RGL = RALGDS-like gene; PLD = phospholipase D; PLCε = enzyme phospholipase Cε; PKC = protein kinase C; P = phosphate; Y = receptor tyrosine. Adapted from Schubbert *et al*., (2007)

RAS has long been linked to the haematopoietic system. H-RAS, N-RAS and K-RAS4B were all found to be expressed in mammalian haematopoietic cells with N-RAS being the most predominant according to Shen *et al*., (1987). RAS proteins play a crucial role in haematopoiesis as the downstream effectors growth factors receptors. Many haematopoietic cytokines known to influence the development of haematopoietic cells (Hoang 2004), such as IL-3, GM-CSF, FLT3-L, G-CSF and EPO act through RAS (De Koning *et al*., 1998; Itoh *et al*., 1996; Satoh *et al*., 1991) and consequently plays an important role in cell cycle progression and survival (Schubbert *et al*., 2007). Interestingly, PKC, which phosphorylates $p47^{phox}$ during activation and assembly of the NAPDH oxidase complex (section 1.4), was shown to mediate developmental dysregulation of human $CD34^{+}$ haematopoietic cells through activated RAS (Pearn *et al*., 2007). RAS signalling is therefore important in the haematopoietic system and this is further demonstrated in its contribution to leukaemogenesis (section 1.3.3).

1.3.3 THE ROLE OF RAS MUTATIONS IN AML

Activation of RAS via point mutations has long been reported to be among the most common molecular abnormalities in haematopoietic malignancy with an incidence of approximately 30% in both myeloid leukaemia and preleukaemia (Farr *et al*., 1988; Miyauchi *et al*., 1994; Niemeyer *et al*., 1997; Bos *et al*., 1989). The expression of mutant RAS including variants such as H-RAS^{G12V} and N-RAS^{G12D} has been reported in AML with the latter being the most common one (Bos *et al*., 1989). RAS mutations are among the pro-proliferative class I genes (Table 1.1) implicated in the two-hit hypothesis of leukaemogenesis (previously discussed in 1.2.1). This is because RAS oncogenes activate a variety of pathways that lead to proliferation of the haematopoietic cells (Figure 1.6) and cooperate with other gene mutations in the pathogenesis of AML (reviewed by Renneville *et al*.,2008). As highlighted previously (1.3.1), RAS mutations found in cancer cells introduce amino-acid substitutions at positions 12, 13 and 61. These changes impair the intrinsic GTPase activity and confer resistance to GAPs, thereby causing cancer-associated mutant RAS proteins to accumulate in the active, GTP-bound conformation (Trahey and McCormic, 1987). Therefore constitutively activated RAS leads to the activation of pro-proliferative pathways including Raf-MEK-ERK and survival pathways such as PI3K-Akt (Figure 1.6). It is noteworthy that inappropriate activation of RAS can also arise as a consequent of activating mutations of the FLT3 gene and loss of negative regulator of RAS, NF1, and (Zhang *et al*., 1998).

It has also been shown that mutational activation of RAS in human primary haematopoietic stem/progenitor cells give rise to deregulated development characteristic of preleukaemia (Darley *et al*., 1997; Darley *et al*., 2002; Pearn *et al*., 2007). Furthermore, H-RAS^{G12V} expression has been shown to disrupt the differentiation of these normal

haematopoietic cells (Darley *et al*., 1999) (discussed below). The fact that activating RAS mutations are also common in preleukaemia highlights their contribution to leukaemogenesis. A study by Darley *et al*., (2002) has demonstrated that N-RAS can also subvert the normal developmental cues that regulate erythropoiesis via PKC activation. This was reported to have led to the phenotypic and functional abnormalities commonly found in pre-leukaemia (Darley *et al*., 2002) suggesting a direct association between RAS mutations and the pathogenesis of preleukaemia. Other studies have shown that activated RAS can drive human $CD34^+$ cell development towards the myelomonocytic lineage at the expense of erythroid and granulocytic cells in a PKC dependent manner (Darley *et al*., 1997). In another study by and Mavilio *et al*., (1989), activated RAS was shown to block terminal granulocytic differentiation of unipotent 32D subline, which was reported to have led to self-renewal of semi-differentiated myeloid cell population. The dysregulating influence of mutant RAS on the differentiation programme of neutrophil lineages has also been demonstrated *in vitro* (Darley *et al*., 1999). In another study, mutant RAS was shown to promote a myeloproliferative disorder *in vivo* and to inhibit erythropoiesis (MacKenzie *et al*., 1999) in agreement with the observations made in the *in vitro* studies.

Taken together the above findings demonstrate that mutant RAS has the ability to disrupt haematopoietic differentiation; however the mechanisms through which it contributes to leukaemogenesis are still not completely understood. One novel observation recently made in haematopoietic cells is that both mutant H-RAS and N-RAS promote the production of reactive oxygen species (ROS) (discussed in section1.4) in human $CD34^+$ cells via increased NADPH oxidase (NOX) (section 1.4.1.1) activity (Hole *et al*., 2010) and this in turn promoted their proliferation (Hole *et al*., 2013) (discussed in 1.4.3). The mechanisms underlying this observation will be the subject of this thesis.

1.4 REACTIVE OXYGEN SPECIES

ROS are a group of inorganic molecules and free radicals including superoxide, hydrogen peroxide (H_2O_2) and hydroxyl radicals (amongst others) which possess wide spectrum of reactivity (Figure 1.7). These molecules are heterogeneous in nature (Lambeth, 2004) and have been linked to a number of cellular processes; both normal (Ray *et al*., 2012) and abnormal (Hole *et al*., 2013; Hole *et al*., 2010; Trachootham *et al*., 2009). Their role in diseases such as cancer is demonstrated in several studies and is discussed in section 1.4.3.

1.4.1 GENERATION OF ROS

The main sources of cellular superoxide are mitochondrial electron transport chain (ETC) (1.4.1.2) and the members of the NOX protein family/enzymes (1.4.1.1) (Lambeth 2004; Lambeth and Neish, 2014). Fenton chemistry has been largely implicated in the formation of hydroxyl radicals (Figure 1.7) which are generated by Fe^{2+} and Fe^{3+} ions in the presence of endogenously generated H_2O_2 (Koppenol, 2001). Specifically, Fe^{2+} ions react with H_2O_2 giving rise to a hydroxyl radical, a hydroxide ion and a Fe^{3+} ion. Superoxide (generated by ETC, NOX oxidases or reaction of H_2O_2 with hydroxyl radicals) may also react with Fe^{3+} to regenerate Fe^{2+}. It is therefore clear that iron play an important catalytic role in the generation of ROS.

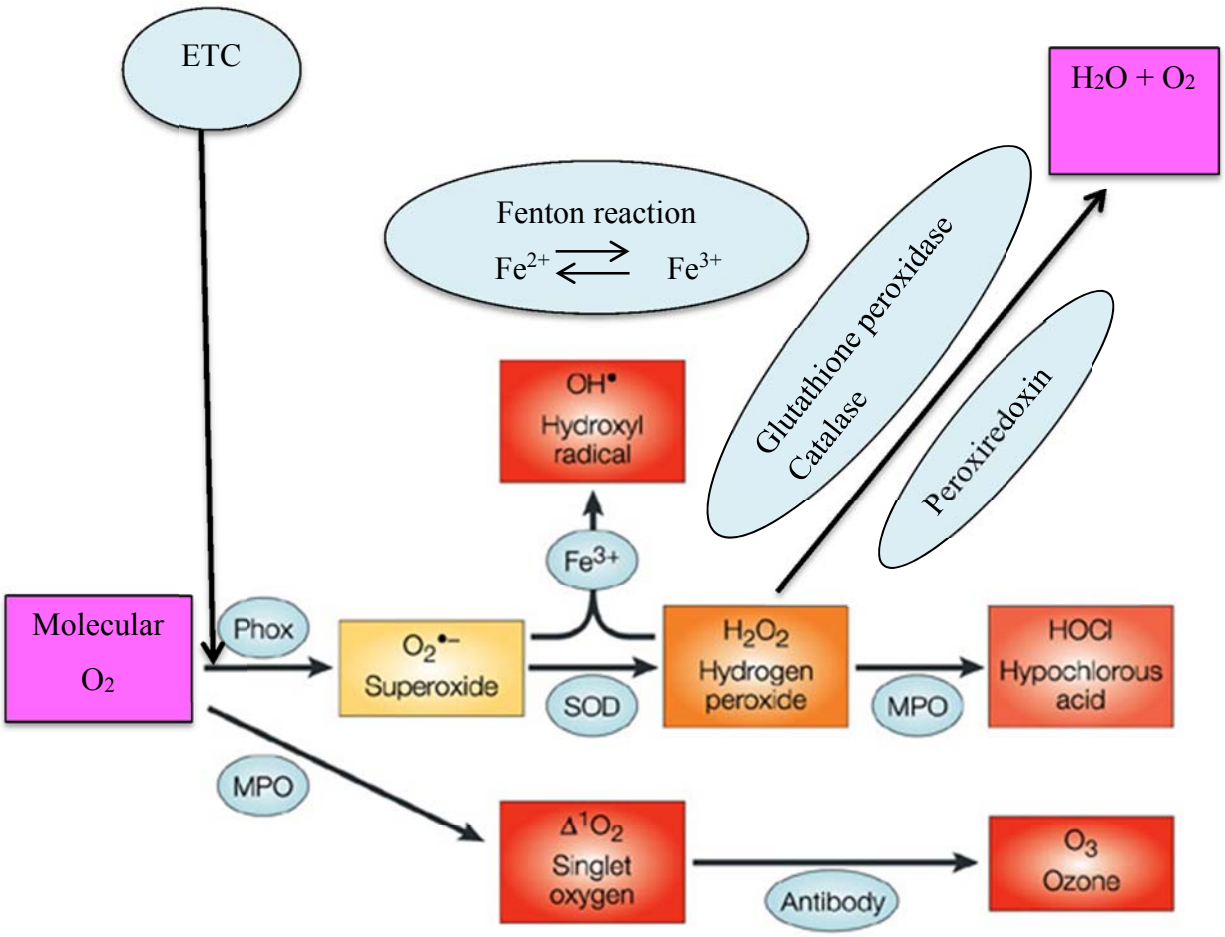

Figure 1.7 Reactive oxygen species: generation and degradation/regulation

NOX enzymes (for example Phox/NOX2) and the electron transport chain (ETC) generate ROS (superoxide) via the oxidation of molecular oxygen. Two molecules of superoxide can react to generate H_2O_2 in a reaction catalysed by superoxide dismutase (SOD). Superoxide and H_2O_2 react to generate hydroxyl radicals in the presence of iron (Fe^{3+}) (Fenton reaction). Singlet oxygen and hypochlorous acid (HOCL) may be formed from oxygen and H_2O_2 in areas of inflammation through the action of Phox/NOX and myeloperoxidase (MPO)-catalysed oxidation of halide ions and ozone can also be generated from singlet oxygen. H_2O_2 may be reduced to H_2O and O_2 in reactions catalysed by glutathione peroxidase, catalase and peroxiredoxin (Prx). The reactivity of individual molecules is colour coded in the following manner: pink = relatively unreactive; yellow = limited reactivity; orange = moderate reactivity; red = high reactivity. Adapted from Lambeth, (2004).

1.4.1.1 Generation of ROS via NOX oxidases

NOX enzymes form a part of a membrane bound complex (Figure 1.8) which generates superoxide via oxidation of molecular oxygen (Figure 1.7). Superoxide is a short lived radical but can dismutate into H_2O_2 either spontaneously or via an enzyme catalysed reaction involving superoxide dismutase (SOD) (Rahman *et al*., 2006) (Figure 1.7). The members of the NOX family include NOX1-5 and DUOX1-2 (Figure 1.8) and are widely distributed (Table 1.4). These enzymes catalyse the transfer of high energy electrons from NADPH to diatomic oxygen which yields superoxide and indirectly ROS such as H_2O_2. NOX2 (catalytic subunit of phagocyte NOX (Phox) is the founding member of the NOX family of proteins. Other sub-units of Phox include $p22^{phox}$, $p47^{phox}$, $p40^{phox}$, $p67^{phox}$ and the small GTPase Rac (Figure 1.8) associate with NOX2 to form an active complex thus regulating its activity.

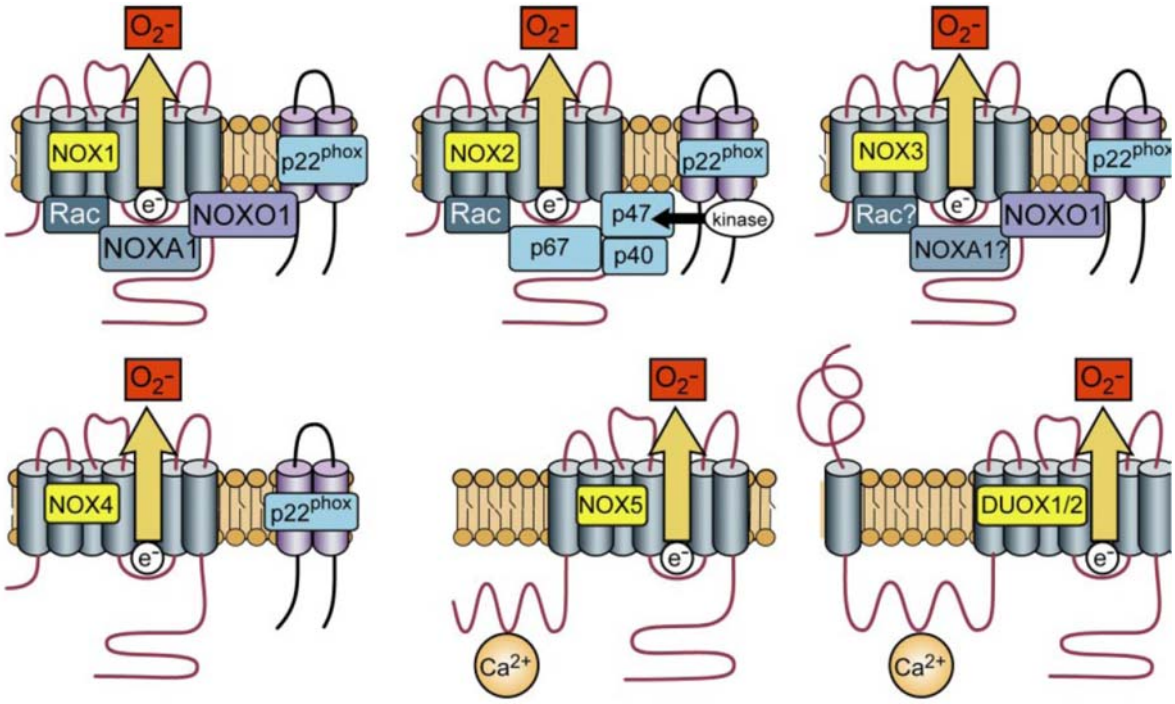

Figure 1.8 Human NOX enzymes

This figure shows the NOX enzymes (NOX1-5 and DUOX1/2) and other sub-units of the phox complex. O_2^- = superoxide. These enzymes catalyse the transfer of high energy electrons from NADPH to diatomic oxygen which yields superoxide. In order for these enzymes to perform their role, the corresponding regulatory subunits indicated above are required. Some of these subunits are common to several oxidases e.g. NOX1-4 are regulated by $p22^{phox}$ whilst some are specifically associated with a particular oxidase e.g.the p47 subunit is specific to NOX2. NOX5 and DUOX1/2 are regulated by calcium ions (Ca^{2+}). Adapted from Lambeth, (2004).

Oxidase	High-Level Expression	Intermediate- to Low-Level Expression
NOX1	Colon	Smooth muscle, endothelium, uterus, placenta, prostate, osteoclasts, retinal pericytes
NOX2	Phagocytes	B lymphocytes, neurons, cardiomyocytes, skeletal muscle, hepatocytes, endothelium, hematopoietic stem cells, smooth muscle
NOX3	Inner ear	Foetal kidney, foetal spleen, skull bone, brain
NOX4	Kidney	blood vessels Osteoclasts, endothelium, smooth muscle, hematopoietic stem cells, fibroblasts, keratinocytes, melanoma cells, neurons
NOX5	Lymphoid tissue, testis	Endothelium, smooth muscle, pancreas, foetal tissues
DUOX1	Thyroid	Airway epithelia, tongue epithelium, cerebellum, testis
DUOX2	Thyroid Salivary and rectal glands	Salivary and rectal glands, gastrointestinal epithelia, airway epithelia, uterus, gall bladder, pancreatic islets

Table 1.4 Tissue distribution of NOX enzymes

The distribution of NOX enzymes and their expression levels human tissue. Interestingly, NOX1, 2 and 4 are also expressed in the plasma membrane of human $CD34^+$ HPCs (Piccoli *et al*., 2007).

1.4.1.2 Generation of ROS via Mitochondria

The generation of ROS via mitochondrial ETC involves a number of redox-coupled proteins and complexes such as nicotinamide adenine dinucleotide (NADH) dehydrogenase (complex I) which accepts high-energy electrons from NADH (formed from pyruvate and fatty acids in the mitochondrial matrix via citric acid cycle). Electrons are passed to complex I through flavin mononucleotide (FMN) cofactor, moved to ubiquinone (coenzyme Q), transferred to cytochrome c reductase (complex III), then moved to cytochrome oxidase (complex IV) where tetravalent reduction of diatomic oxygen to water molecules takes place indicating the end of the ETC. Several studies suggest that superoxide production takes place when electrons 'leak' from the ETC before reaching their destination (Murphy, 2009). In the same study which employed the use of mitochondria isolated from mammalian cells, it was suggested that electrons may escape from the ETC predominantly at complex I forming superoxide via univalent reduction of O_2. Under similar experimental conditions, Chance and Hollunger (1961) estimated that 1-2% of the oxygen consumed by isolated mammalian mitochondria is converted to superoxide. Therefore, complex I appear to be the most common site of ROS production in the mitochondria.

1.4.1.3 Elimination of ROS

While ROS may have physiological roles (1.4.2), it can also damage biological molecules including proteins, lipid and DNA. To limit the negative consequences of ROS production, a number of enzymes and other molecules are expressed in human cells for the purpose of eliminating ROS. These include SOD, catalase, peroxiredoxins (Prxs) and glutathione (GSH) (Figure 1.7). SOD catalyses the dismutation of superoxide and as a

result, H_2O_2 is formed which is converted to O_2 and water by the action of catalase or the glutathione peroxidase (GSH) system (Lambeth, 2004). GSH, a tripeptide consisting of glutymyl, glycine and cysteine residues is the most predominant thiol in mammalian cells (Komatsu and Obata, 2003) and is used as an electron donor in the reduction of H_2O_2 to form O_2 (Poole *et al*., 2004). This is one of the important mechanisms involved in the prevention of the oxidative stress (Ballatori *et al*., 2009). Hydrogen peroxide is also reduced through the action of Prxs (Rhee *et al*., 2005). Hydrogen peroxide reacts with the N-terminal cysteine residue (cys51 in mammalian Prxs) of the Prxs generating sulphenic acid (-SOH) which reacts with the sulphydryl group (-SH) of the cys172 (cysteine residue found in the members of the 2-cys Prxs family) forming an intermolecular disulphide bond (S-S). Oxidised 2-cys Prxs are then reduced by thioredoxin. Therefore Prxs, GSH and catalase are the main antioxidants systems promoting the reduction of H_2O_2.

1.4.2 BIOLOGICAL AND PHYSIOLOGICAL FUNCTIONS OF ROS

ROS has been shown to have a crucial role in the innate immune response. For instance, it has been implicated in microbial killing (Reeves *et al*., 2002). NOX2 has a key role in innate immunity as mutations or deletions NOX2 components result in inherited conditions such as chronic granulomatous disease (CGD) (Segal *et al*., 1996). This disease is characterized by the impaired ability of neutrophils to kill microorganisms giving rise to chronic infections. Therefore it is clear that ROS plays an important role in host defence.

In addition to their expression in phagocytic cells, NOX family members have been shown to be expressed in human HPCs ($CD34^+$ cells) (Piccoli *et al*., 2007) (Table 1.4). NOX-derived H_2O_2 is well known to play crucial roles in haematopoiesis (Sardina *et al*., 2012) and haematopoietic growth factor signalling (Sattler *et al*., 1999 and Zhu *et al*., 2006). There is accumulating evidence from murine and human HSC models that ROS

management is critical for primitive haematopoietic cells. For example elevated ROS appears to drive HSCs out of quiescence and reduces self-renewal capacity, resulting in rapid bone marrow failure if not remedied (Rizo *et al*., 2009; Tothova *et al*., 2007; Ito e*t al*., 2004). In another study, an additional role of ROS in haematopoiesis was demonstrated where *in vivo* imaging technique showed that ROS-dependent expression of vascular cell adhesion protein 1 (VCAM-1) on the bone marrow endothelial cells is essential for the early stages of HSC bone marrow homing and localisation in the context of transplantation (Lewandowski *et al*., 2010). ROS signalling has also been associated with a variety of biological processes such as senescence and apoptosis (Burdon, 1995) and reviewed by Lambeth, (2004). In addition, ROS has also been shown to play an important biological role in proliferative signalling (Irani *et al*., 1997) and has been linked to diseases such as cancer (1.4.3). Excessive ROS production or a defect in antioxidant defence can lead to a state known as oxidative stress, characterized by oxidative damage to DNA and augmented ROS signalling (Block and Gorin, 2012). In addition, Hole *et al*., (2013) demonstrated that the overproduction of ROS in AML blasts showed depleted antioxidant defences but evaded the oxidative stress response through suppression of $p38^{MAPK}$ signalling (Hole *et al*., 2013).

1.4.3 ROS IN LEUKAEMIA

Though ROS have been increasingly implicated in several normal cellular processes (Ray *et al*., 2012), their overproduction have been reported in cancer cells, for example CML (Ciarcia *et al*., 2010; Ahmad *et al*., 2010), ALL (Battisti *et al*.,2008) and AML (Sallmyr *et al*., 2008; Hole *et al*., 2010; 2013). Growing evidence suggests that ROS are at least partly responsible for the mutant RAS phenotype observed in several cancers cell models (Irani *et al*., 1997; Liu *et al*., 2001; Cho *et al*., 2002; Lee *et al*., 2007). The study by Hole *et al*., (2010) was the first to show that human haematopoietic $CD34^+$

progenitor cells transduced with N-RAS^{G12D} produce excessive ROS. Given that ROS have the potential to modulate cell signalling, the direct effects of ROS on gene transcription are also unknown. It is also noteworthy that transcriptional dysregulation is a key element in leukaemogenesis. The instability in the genome of blast cells in the pathogenesis of AML has been attributed to dysregulation of genes involved in cell maintenance and DNA repair and has been reported to lead to acquisition of molecular abnormalities that contribute to the progression of this disease (Suela *et al*., 2007; Alcalay *et al*., 2003). Therefore the current study was undertaken to determine the contribution of RAS-induced ROS production on gene expression and to identify the transcriptional targets of mutant RAS which could be related the proliferative responses of cells exposed to ROS.

Additionally, in a more recent study in our group by Hole *et al*., (2013), NOX enzymes have been correlated with the increased levels of ROS in AML blasts. The authors of this study concluded that the over production of NOX-derived ROS in AML promotes proliferation and is associated with defective stress signalling (Hole *et al*., 2013). However the mechanism by which ROS or NOX family members acts is still poorly understood despite the growing literature surrounding them, warranting further research.

1.5 GLYCOLYSIS

1.5.1 OVERVIEW OF GLYCOLYSIS

Glycolysis is a metabolic process that converts glucose into pyruvate and is a sequence of enzyme catalysed reactions which results in the release of free energy used to form the high energy compounds such as reduced nicotinamide adenine dinucleotide (NADH) and adenosine triphosphate (ATP) (Stryer, 1988; Munoz-Pinedo *et al*., 2012). It is an ancient metabolic pathway occurring in the cytosol of the cells of both aerobic and anaerobic organisms (Stryer, 1988). The net products of this pathway when one molecule

of glucose is catabolized are the formation of two molecules of ATP and NADH (Figure 1.9).

$$\text{Glucose} + 2\ \text{ADP} + 2\ P_i + 2\ NAD^+ \rightarrow 2\ \text{Pyruvate} + 2\ \text{ATP} + 2\ \text{NADH} + 2\ H^+ + 2H_2O$$

Figure 1.9 Overall process of glycolysis

An equation showing the net reaction in the transformation of glucose into pyruvate. Abbreviations: P_i = Inorganic phosphate

The reactions of glycolysis are summarized in Figure 1.10. As illustrated in both figures, in the first phase of glycolysis (priming phase), two molecules of ATP are used to convert glucose to fructose-1, 6-bisphosphate through sequential reactions catalysed by hexokinase (HK/HXK), phosphoglucose isomerase (PGI) and phosphofructokinase (PFK). The second phase (energy-yielding phase), involves the stepwise conversion of fructose-1, 6-bisphosphate to pyruvate with the production of four molecules ATP and two molecules of NADH. Two ADP and two NAD^+ molecules are used up and in the absence of oxygen; NAD^+ is regenerated from NADH by reduction of pyruvate to lactic acid in a reaction catalysed by lactate dehydrogenase (LDH). It is important to note that, under aerobic conditions, pyruvate can be further oxidised to CO_2 and H_2O in the mitochondria via the tricarboxylic acid (TCA) cycle and the respiratory chain, yielding large amounts of ATP. As illustrated in Figure 1.10, each reaction in the glycolytic pathway is catalysed by a specific enzyme or enzyme complex detailed below.

1.5.1.1 Hexokinase

Hexokinases are tissue-specific isozymes that catalyse the first and rate-limiting reaction in glycolysis which involves the ATP-dependent phosphorylation of glucose to

form glucose-6-phosphate (G-6-P) which serves as the starting point for the entry of sugar into the glycolytic pathway or the pentose phosphate pathway (PPP) (Figure 1.10) or for glycogen synthesis. Four mammalian isozymes of hexokinase (Types I-IV) exist with type IV (also known as glucokinase) being responsible for the storage of excess glucose in the liver (Pelicano *et al*., 2006). Various studies have demonstrated that type II isozyme of hexokinase (HK II) play a vital role in initiating and maintaining the high glucose catabolic rates of fast growing tumours. For instance increased expression of HK II has been reported in most immortalized and malignant cells and this has been linked to elevated glycolysis (Arora *et al*., 1990; Rempel *et al*., 1996). Hexokinases have also been shown to play part in the inhibition of the apoptotic pathway (Rathmell *et al*., 2003; Majewski *et al*., 2004). Pelicano *et al*., (2006) pointed out that inhibition of these enzymes is likely to have profound effects on cellular energy metabolism and survival making them attractive targets for anticancer agents (Figure 1.15 and Table 1.5).

1.5.1.2 Phosphoglucose isomerase

Phosphoglucose isomerase (PGI) also known as glucose-6-phosphate isomerase (GPI) catalyse the inter-conversion of G-6-P and fructose-6-phosphate (Figure 1.10). Previous studies have shown that GPI can function as an autocrine motility factor (AMF), secreted from the tumour cells to promote cell proliferation (Niinaka *et al*., 1998; Sun *et al*., 1999). Interestingly, the presence of GPI in serum and urine is associated with cancer progression and indicates poor prognosis (Baumann and Brand, 1988; Baumann *et al*., 1990; Filella *et al*., 1991). It is therefore clear that GPI does not only play a role in the glycolytic pathway but also functions as a cytokine extracellularly and is linked with malignant activities.

1.5.1.3 Phosphofructokinase

PFK catalyses the second rate limiting step of glycolysis which involves the phosphorylation of fructose-6-phosphate to fructose-1,6-bisphophate using ATP as the source of energy (Figure 1.10). This enzyme is regulated by allosteric effectors and covalent modifications such as phosphorylation. It is activated by adenosine monophosphate (AMP) and fructose 2,6-bisphosphate. An abundance of ATP inhibits the activity of PFK. Nevertheless fructose 2,6-bisphosphate is capable of overriding the inhibitory effect of ATP and maintain continuous glycolytic flux. The up-regulation of fructose 2, 6-bisphosphate has been linked to cancer (Chesney *et al*., 2006). Three forms of PFK have been identified in humans namely; M (muscle), P (platelets) and L (liver), (Vora, 1983) and their involvement in cancer is unclear.

1.5.1.4 Aldolase

This enzyme catalyses the reversible conversion of fructose-1,6-bisphosphate to glyceraldehyde-3-phosphate (GLAP) and dihydroxyacetone phosphate (DHAP) (Penhoet *et al*., 1969) (Figure 1.10). There are three known distinct isozymes of aldolase namely; aldolase (ALDO) A (most highly expressed in muscle), B (highly expressed in the liver) (Penhoet *et al*., 1969; Mukai *et al*., 1986) and ALDOC which is most strongly expressed in neuronal tissues and brain (Penhoet and Rutter, 1971; Haimoto and Kato 1986; Lebherz and Rutter, 1969). These 3 mammalian aldolase isozymes have similar molecular masses but differ in structure and kinetics as well as tissue distribution. The differences in tissue and kinetics specificity among the human aldolase isozymes have been attributed to structural changes such as isozyme-specific residues (ISRs), those residues conserved among paralogs (Arakaki *et al*., 2004). The same study was the first to report the structure of human ALDOC via X-ray crystallography. In this study, a complete analysis of the ISRs

demonstrated that in several cases an amino acid residue that is conserved among ALDOC orthologs prevents an interaction that occurs in paralogs. Furthermore, the structure identified confirmed the clustering of ISRs into discrete patches on the surface and revealed the existence in ALDOC of a patch of electronegative residues localised near the C terminus. The authors of this study therefore concluded that these structural changes highlight the differences required for tissue and kinetic specificity among aldolases.

ALDOC enzyme has been linked to cancer. For example, aldolase was shown to be elevated in the serum of patients with malignant tumours (Taguchi and Takagi, 2001). In addition, proteome analysis has demonstrated that this enzyme is overexpressed in human lung squamous carcinoma (Li *et al*., 2006). Elevated levels of ALDOC have been found in cancer cells (Schapira *et al*., 1970; Skala *et al*., 1987). For more detail on the aldolase involvement in cancer see chapter 5 discussion.

Remarkably, aldolase not only plays a key role in glycolysis, but has also been demonstrated to bind macromolecules unrelated to glycolysis such as F-actin (Wang *et al*.,1996), vacuolar H^+ -ATPase (Lu *et al*.,2001) and GLUT4 (Kao *et al*.,1999). These alternative non-glycolytic functions of aldolases have been described as "moonlighting functions" (Jeffery, 1999; Copley 2003) which may be specific to each isozyme.

1.5.1.5 Glycealdehyde-3-phosphate dehydrogenase

Gyceraldehyde-3-phosphate dehydrogenase (GAPDH) enzyme catalyses a redox reaction in the glycolytic pathway which involves the conversion of glyceraldehyde-3-phosphate to 1, 3-bisphosphoglycerate coupled with the reduction of NAD^+ to NADH. The role of this enzyme in cancer remains to be defined.

1.5.1.6 Phosphoglycerate kinase

Phosphoglycerate kinase (PGK) catalyses the conversion of 1, 3-bisphosphoglycerate to 3-phosphoglycerate coupled with the generation of ATP from ADP. This enzyme consist of two domains joined by a conserved hinge with the ADP/ATP-binding site located in the N-terminal domain and a conformational rearrangement involving bending of the hinge takes place upon binding of both substrates, bringing them in position for phosphate transfer. Two isozymes of this enzyme has been identified namely; PGK-1 and PGK-2.

1.5.1.7 Phosphoglycerate mutase

This enzyme catalyses the inter-conversion of glycerate-3-phosphate and glycerate-2-phosphate and also requires D-glycerate-2, 3-diphosphate for activation by donating one of its phosphoryl groups to form a covalently linked phosphoryl enzyme. Phosphoglycerate mutase has been shown to be differentially expressed in human lung squamous carcinoma (Li *et al*., 2006).

1.5.1.8 Enolase

The conversion of 2-phosphoglycerate to phosphoenolpyruvate is catalysed by enolase (Figure 1.10). There are three major isoforms of this enzyme in mammals: non-neuronal enolase (NNE)/enolase 1/α enolase (found in a variety of tissues, including liver, brain, kidney, spleen, adipose and haematopoietic cells); muscle specific enolase (MSE)/enolase 3/ β enolase (largely restricted to muscle where it is present at very high levels); neuron-specific enolase (NSE)/enolase 2/ γ enolase (expressed at very high levels in neurons and neural tissues and at much lower levels in most mammalian cells). Proteome analysis showed that NNE is overexpressed in human lung squamous carcinoma (Li *et al*., 2006).

1.5.1.9 Pyruvate kinase

Pyruvate kinase (PK) is the enzyme that catalyses the third irreversible step in glycolysis which involves the phosphoryl group transfer from phosphoenolpyruvate to ADP, yielding ATP and pyruvate; is a vital metabolic intermediate that channels into several metabolic pathways (Figure 1.10). Therefore this enzyme controls the outflow from the glycolytic pathway. Three forms/isozymes of PK have been found in mammals: the L type predominates in the liver, M type in muscle and brain and the A type in other tissues. These isozymes have the same architectural plan and catalytic mechanism but differ in how they are regulated. PK isozyme type M2 (PKM2 or M2-PK) is the predominant pyruvate kinase isoform in proliferating cells, such as fibroblasts, embryonic cells and adult stem cells and most human tissue, including lung, bladder, kidney and thymus. M2-PK has been implicated in tumourigenesis (Mazurek *et al*., 2005; Reinacher and Eigenbrodt, 1981). Furthermore, Mazurek *et al*., (2005) pointed out that M2-PK interacts with oncoproteins which seem to cause its dimerization in tumour which is thought to allow the survival of tumour cells in environments with varying nutrients and oxygen.

1.5.1.10 Lactate dehydrogenase

Lactate dehydrogenase (LDH) catalyses the conversion of pyruvate to lactate coupled with an oxidation of NADH to NAD^+. This reaction occurs in a variety of microorganisms and higher organisms when the amount of oxygen is limiting, for example in muscle during intense activity. Major isoforms of this enzyme, LDH-A and LDH-B have been identified with the former mostly implicated in cancer. Therefore LDH-A is used as a biomarker for many malignancies including lymphoma, renal carcinoma, melanoma and prostate cancer (Augoff and Grabowki., 2004; von Eyben, 2001; Kolev *et al*.,2008; Jovanovic *et al*.,2007; Porporato *et al*., 2011; Sola-Penna, 2008).

1.5.1.11 Pyruvate dehydrogenase

Pyruvate dehydrogenase (PDH) catalyses the pyruvate decarboxylation process for the transformation of pyruvate to acetyl-CoA which is used in the TCA for cellular respiration. Therefore PDH links the glycolysis metabolic pathway to citric acid cycle.

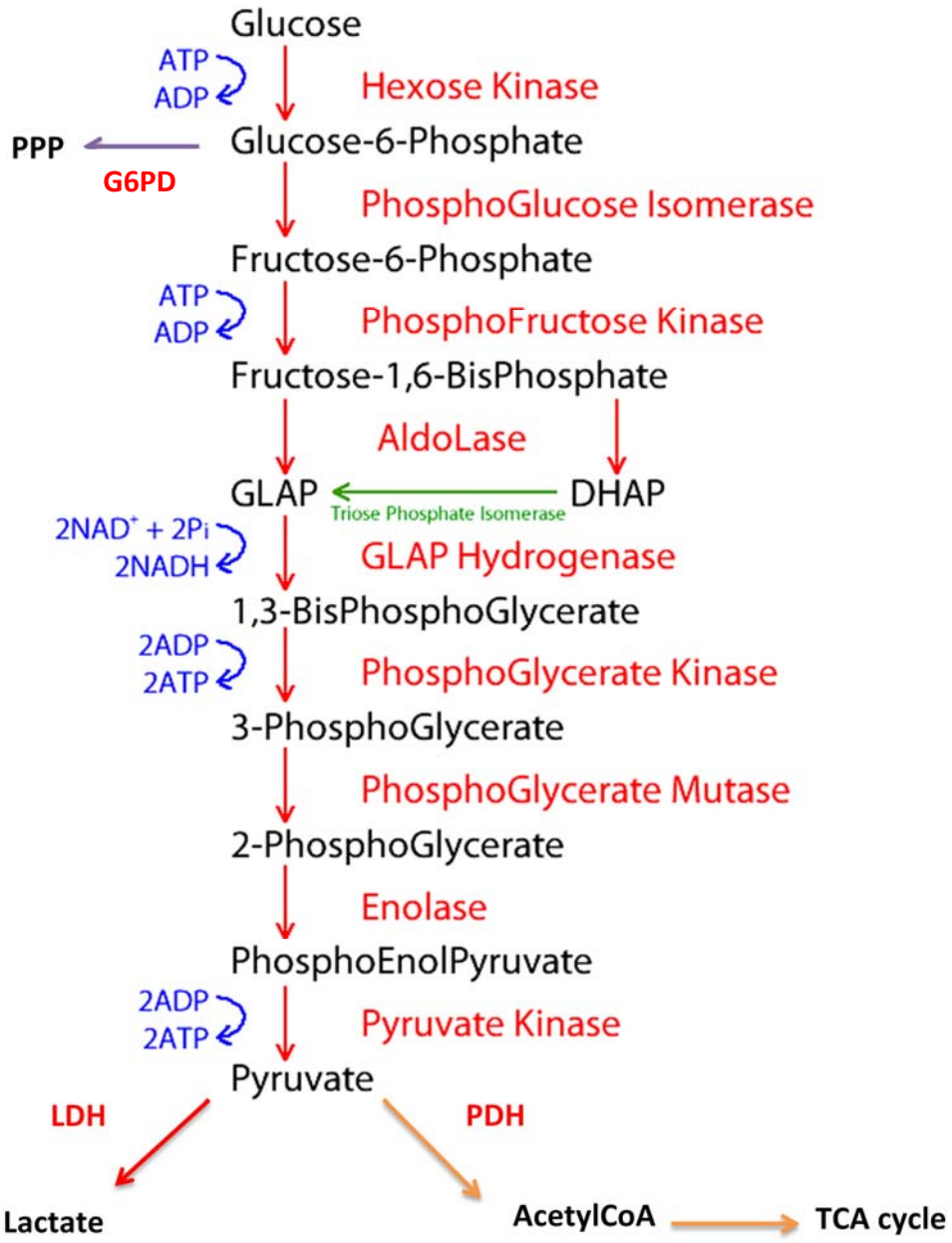

Figure 1.10 Glycolytic pathway and its metabolic interconnections with PPP and TCA cycles.

A diagrammatic representation of the glycolytic pathway. Reactions (red arrows), intermediates (black), enzymes (red), metabolic interconnection with the Pentose Phosphate Pathway (PPP) (Purple arrow), further metabolism of pyruvate downstream of glycolysis (orange arrows). Abbreviations: PDH = Pyruvate dehydrogenase; LDH = Lactate dehydrogenase; GLAP = Glycealdehyde-3-phosphate; DHAP = Dihydroxyacetone phosphate; G6PD = Glucose-6-phosphatase. Adapted from Biochem: online (http://biochem.co/2010/02/)

1.5.2 REGULATION

The regulation of glycolysis is based on the changes in the rate of particular steps in this pathway. This is achieved by the activation or inhibition of the enzymes that are involved in the process. There are several points of regulation in glycolysis which indicates that intermediates between these points enter and leave the glycolysis pathway by other processes as indicated in (Figure 1.10) and there are three key regulated enzymes in glycolysis namely phosphofructokinase (PFK), pyruvate kinase and hexokinase (HK) (discussed above).

1.5.3 POST GLYCOLYSIS PROCESSES

Glycolysis provides intermediates for other pathways which strongly rely on it as a source of metabolites. These metabolic pathways include; gluconeogenesis, lipid metabolism, pentose phosphate pathway and citric acid cycle (Figure 1.10) which leads to processes such as amino acid and nucleotide synthesis.

1.5.4 GLYCOLYSIS IN CANCER

Increased glycolysis is known to be linked to cancer and was originally described by Otto Warburg (Warburg, 1956). Normal cells obtain ATP primarily via oxidative phosphorylation (respiration) (described in section 1.5 and Figure 1.10). Cancer cells on the other hand exhibit the Warburg effect in which cancer cells exhibit increased glycolysis and use this metabolic pathway for generation of ATP as a main source of their energy supply even under aerobic conditions (Koppenol *et al*., 2011). Originally it was thought that this was driven by impairment or dysfunction in mitochondrial metabolism

(Warburg, 1956). Subsequent work suggests that the Warburg effect arises from changes in the signalling pathways that regulate glucose uptake and utilization as opposed to mitochondrial dysfunction (Jang *et al*., 2013). Furthermore, the genes of glycolysis are found to be ubiquitously overexpressed in cancers (Mikuriya *et al*., 2007; Altenberg *et al*., 2004).

In addition to solid cancers, a high level of glycolytic metabolism has also been demonstrated in AML blasts (Herst *et al*., 2011). In this study, *in vitro* dye reduction assay was used to determine the level of glycolytic metabolism in 26 bone marrow (BM) samples taken from adult patients with newly diagnosed or relapsed AML and the blasts were categorized into moderate and high levels of glycolytic metabolism. Highly glycolytic AML blasts were found to be more resistant to apoptosis induced by all-trans retinoic acid (ATRA) and/or arsenic trioxide (ATO) *in vitro* suggesting possible resistance to induction chemotherapy as for solid tumours (Herst *et al*., 2011). This study concluded that the extent of myeloblast glycolysis may be an effective and easily applied method for the determination of pre-treatment prognosis in AML.

Furthermore the importance of glycolytic phenotype in cancer has been emphasized by studies which demonstrated that increased glucose uptake coincide with transition from pre-malignant lesions to invasive cancer (Younes *et al*., 1996) which in part could explain the significant prevalence of the glycolytic phenotype in human cancers .

1.5.5 MOLECULAR MECHANISMS UNDERLYING THE WARBURG EFFECT

The exact reasons why tumour cells exhibit elevated glycolysis and use this less energy-efficient pathway to generate ATP are still unclear; however, the overall increase in aerobic glycolysis (or Warburg effect) has been attributed to several factors (Jang *et al*., 2013) such as oncogenes, hypoxic microenvironment tumour suppressors, mitochondrial

DNA (mtDNA) deletions and mutations, nuclear DNA (nDNA) mutations or abnormal gene expression (Figure 1.11, Figure 1.12 and Figure 1.13).

1.5.5.1 Role of oncogenes

Several mutations that activate oncogenes or inactivate tumour suppressers were shown to significantly affect the activities of metabolic enzymes and play a vital role in aerobic glycolysis of cancer (Elstrom *et al*., 2004; Levine and Puzio-Kuter, 2010; Bayley and Devilee 2012). Importantly, mutant RAS (in addition to the functions discussed in section 1.3.3) has been associated with the regulation of aerobic glycolysis in cancer (Blum *et al*., 2006; Mazurek *et al*., 2001a; Ramanathan *et al*., 2005). Pharmacologic inhibition of RAS was shown to result in the inhibition of RAS signalling to both the Raf, MEK, ERK and the PI3 pathways. As a consequence of this the glucose transporter, Glut-1 was substantially down regulated (Blum *et al*., 2005; Blum *et al*., 2006). Conversely, mutant H-RAS has been reported to upregulate 6-phosphofructo-1-kinase (PFK-1) activity via induction of F26bP (Kole *et al*., 1991; Telang *et al*., 2006). Similarly, Mazurek *et al*., (2001b), reported high levels of PFK-1 activity in rat kidney cells transfected with mutant RAS together with the human papillomavirus type 16 E7 (HPV-16 E7) oncoprotein led to elevated levels of fructose-1,6-bisphosphate. It was also found that the HPV-16 E7 oncoprotein, which cooperates with RAS in cell transformation, directly binds to M2-PK, induces its dimerization and thereby promotes cell proliferation. Other oncogenes including Src, P13K/Akt and Bcr-Abl have also been implicated in the promotion of glycolysis and the Warburg effect (Chapter 5 discussion and Figure 1.11). Little is known about RAS expressing leukaemias.

1.5.5.2 Role of mtDNA

High rates of human mitochondrial DNA (mtDNA) mutations observed in cancer cells are believed to lead to mitochondrial malfunction and a reduction in the ability to generate ATP through oxidative phosphorylation (Figure 1.13) (Carew and Huang 2002; Brandon *et al*., 2006). ROS has also been implicated in this. In study by Carew *et al*., (2003), primary human leukaemia cells isolated from patients were used to examine mtDNA mutations and their correlation with alteration in cellular ROS and mitochondrial mass. In this study, mtDNA mutations in leukaemia cells were found to be closely associated with increased ROS generation and altered sensitivity to drug treatment. It should be noted however that mtDNA mutations are unlikely to cause the whole defect in mitochondrial oxidative phosphorylation. In support of this, certain fast growing tumours were shown to have active ATP generation through oxidative phosphorylation which supplies a large portion of the total cellular energy (Rodriguez-Enriquez *et al*., 2000). Therefore it is likely that the Warburg effect reflects a metabolic state in cancer cells where ATP generation through mitochondrial oxidative phosphorylation is compromised by factors such as the ones indicated in (Figure 1.13) hence insufficient to support active cellular activity. Consequently cells become more reliant but not solely dependent on increased glycolysis for ATP supply. In support of this, Chen *et al*.,(2007) also pointed out that it is important to recognise that elevated glycolysis in cancer cells does not necessarily suggest that cancer cells only use the glycolytic pathway for ATP generation. In addition to its possible contribution towards the overall increase in glycolysis in cancer cells, mitochondrial respiratory malfunction has been shown to result in a change in cellular NADH/NADPH ration leading to a redox-mediated activation of the Akt survival pathway (Pelicano *et al*., 2006b) (Figure 1.13).

1.5.5.3 Role of nuclear DNA mutations or abnormal gene expression

Mutations in nuclear DNA (nDNA) or aberrant expression of certain nuclear genes may suppress mitochondrial respiratory function and/or the TCA cycle and possibly promote glycolysis (Figure 1.13). nDNA encodes for most of the mitochondrial protein components. For example, succinate dehydrogenase (SDH) and fumarate hydratase (FH) are encoded by nuclear genes and play crucial roles in the TCA cycle and mitochondrial complex II function. Germline mutations in SDH and FH are associated with tumours (Gottlieb and Tomlinson 2005) and a reduction in SDH activity may lead to increased ROS generation (Albayrak *et al*., 2003; Ishii *et al*., 2005). Accumulation of succinate due to SDH deficiency caused an inhibition of Hypoxia inducing factor (HIF)-1α prolyl hydroxylase leading to stabilization and nuclear translocation of HIF-1α (transcriptional factor that promotes the expression of glycolytic enzymes) in normoxic condition (Selak *et al*., 2005). Interestingly, overexpression of glycolytic enzymes including GAPDH, enolase 1, PK, LDH, HK2 and aldolase has been observed in a variety of cancer cells (for further details see chapter 5 discussion).

1.5.5.4 Role of tumour microenvironment

Hypoxia is frequently observed in human cancer and research has shown that that adaptation to the respiratory suppression owing to oxygen depletion possibly cause tumour cells to switch to glycolysis for ATP production, accompanied by increased generation of lactate and acidification of tumour microenvironment (Gatenby and Gillies 2004). The authors of these study speculated that this adaptation and switch to the glycolytic pathway leads to a further selection of malignant cells. HIF-1α, a key molecule that mediates cellular response to hypoxia has been shown to activate a set of genes involved in angiogenesis, glucose uptake and glycolysis (Harris, 2002). Another study by

Kim *et al*., (2006) suggest that HIF-1α may mediate a metabolic switch from mitochondria respiration to glycolysis by trans-activating pyruvate dehydrogenase kinase 1, which in turn activates pyruvate dehydrogenase leading to suppression of the TCA cycle (Figure 1.12). It should be noted that despite the fact that increased glycolysis in response to hypoxia does not exactly represent the classical Warburg effect (increased aerobic glycolysis), Chen *et al*., (2007) argued that pharmacological agents that inhibit glycolysis will not only impact cells exhibiting the Warburg effect but also cancer cells in hypoxic environment. It has also been suggested that aerobic glycolysis by proliferating cells may also be a protective mechanism against ROS (Brand and Hermfisse 1997). Although it is suggested the increased ROS generation within the cancer cells may also inhibit the respiratory chain and suppress oxidative phosphorylation forcing cells to adapt active glycolysis for ATP generation (Chen *et al*.,2007), the exact role and contribution of ROS to the Warburg effect is not well understood and still remain to be explored. Interestingly, some researchers speculate that ROS are involved in signalling to GLUT1 contributing to glucose transport activation in leukaemic cells (Maraldi *et al*., 2007); however such speculations remain inconclusive and warrant further investigation.

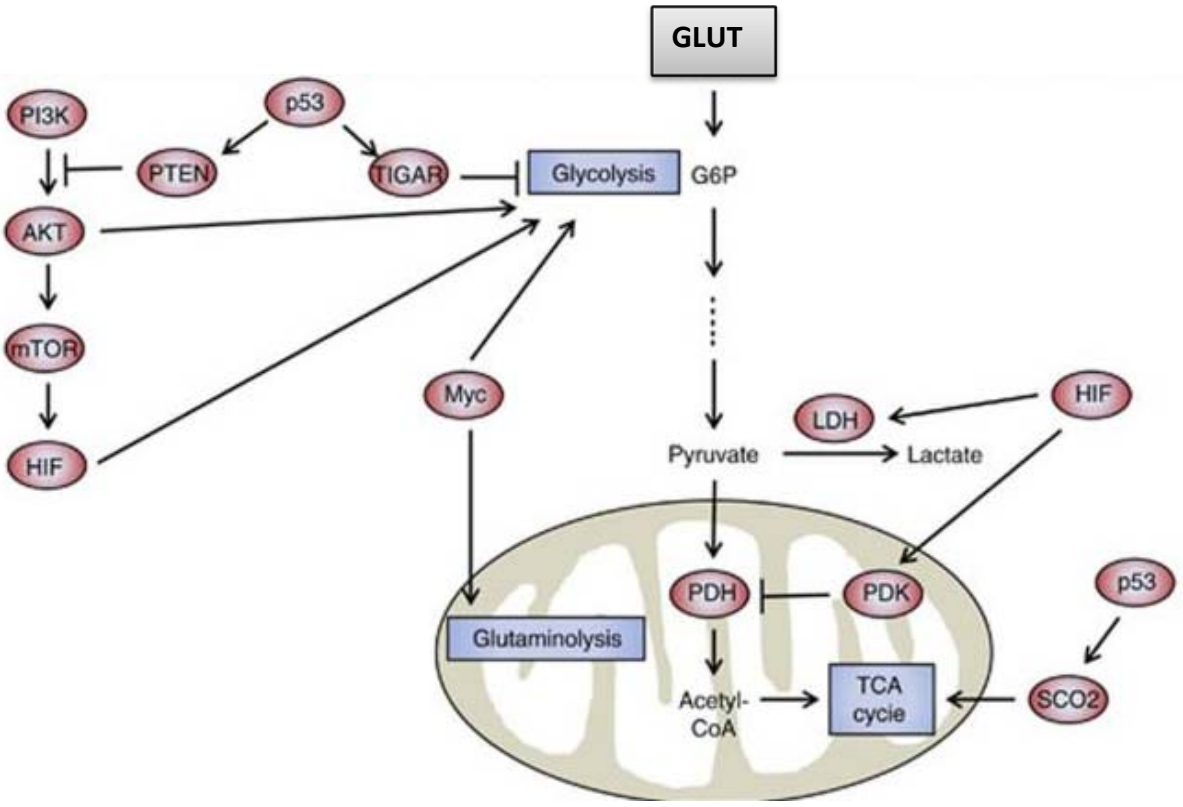

Figure 1.11 Cancer cell metabolism and signalling pathways related to oncogenes and tumour-suppressor genes.

Oncogenes and tumour suppressor genes play an important role in the signalling pathways that regulate metabolism in cancer cells. PI3K activates Akt which stimulates glucose uptake and flux by directly controlling glycolytic enzymes and activating mTOR which indirectly causes metabolic changes by activating HIF. HIF then activates PDK which inactivates the mitochondrial pyruvate dehydrogenase complex hence inhibiting the entry of pyruvate into the TCA cycle. p53 supresses glycolysis by increasing the expression of TIGAR, supporting the expression of PTEN and promoting oxidative phosphorylation via SCO2. Myc augments glycolysis by increasing transcription of glycolytic enzymes and its involvement in glutamine metabolism. Adapted from :(Jang *et al*., 2013).

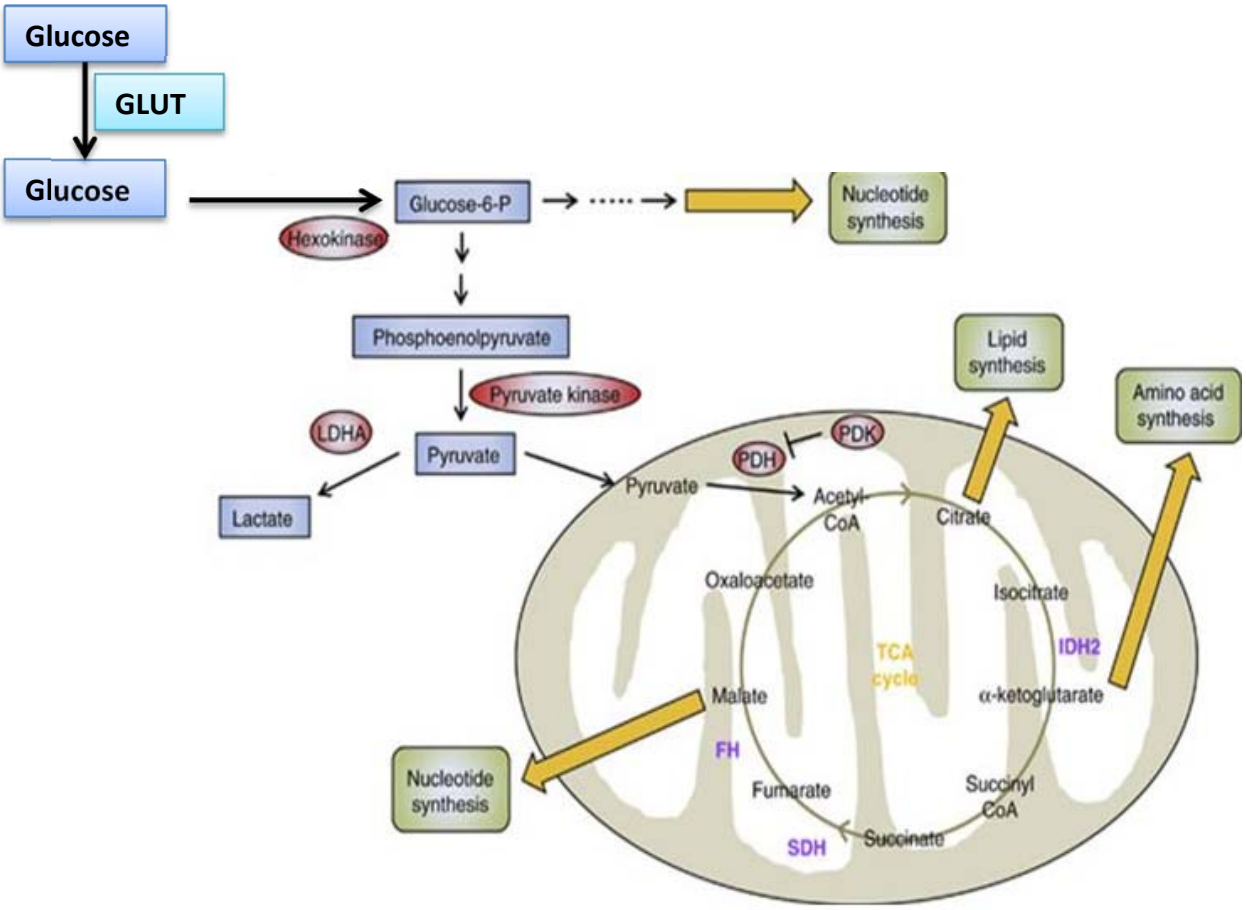

Figure 1.12 Glucose metabolism in cancer cells: Regulation

The regulation of glucose metabolism in cancer cells is via several ways. Following the entry of glucose into the cell via a glucose transporter (GLUT), it is phosphorylated by HK to glucose-6-phosphate which is further metabolized by glycolysis to pyruvate in the cytosol. Under aerobic conditions, normal cells use PDH to convert majority of pyruvate to acetyl-CoA which is then oxidised via TCA cycle, providing sources for ATP synthesis. Conversely, the metabolic pathways of glucose utilization in cancer are changed from ATP generation by oxidative phosphorylation to ATP generation via glycolysis. In addition, for cell proliferation to occur, cancer cells require the synthesis of new macromolecules such as lipids, proteins and nucleic acids. Some of the TCA cycle enzymes (purple coloured) are known to be mutated in cancer and others (highlighted in red) are potential targets for cancer therapy. Adapted from: (Jang *et al*., 2013).

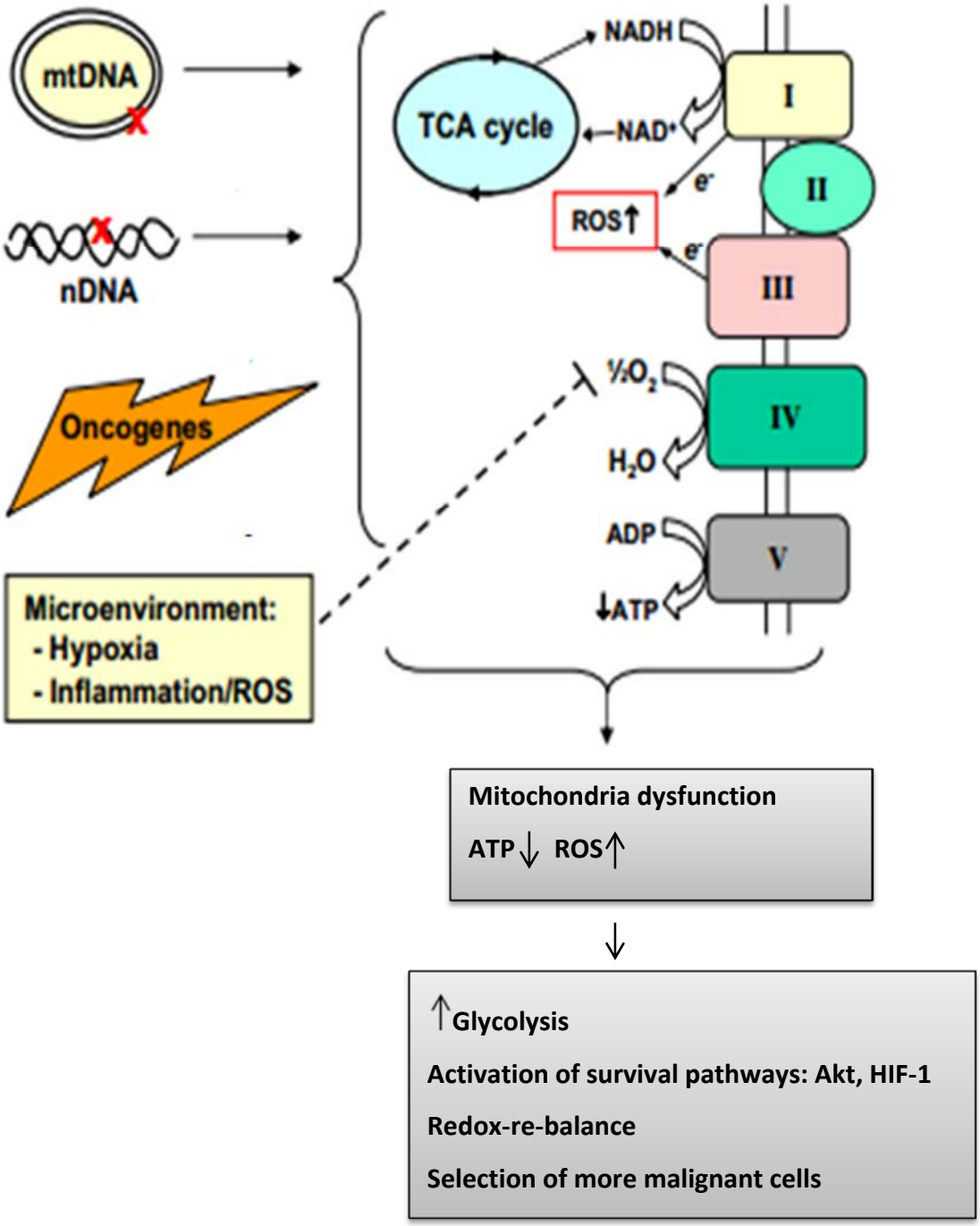

Figure 1.13 Summary of the mechanistic perspective of the Warburg

Potential mechanisms contributing to elevated glycolysis and decreased mitochondrial respiration in cancer cells. Abbreviations: mtDNA = mitochondrial DNA; nDNA = nuclear DNA; I-V = respiratory chain complexes I-V respectively. Adapted from: (Chen *et al*., 2007)

1.5.5.5 Glycolysis and cell death

In addition to the promotion of cancer cell proliferation, glycolytic metabolism has been shown to protect these cells from death. Research has shown that increased glycolytic rate renders cancer cells more resistant to apoptosis induced by growth factor withdrawal. For instance, it was shown in leukaemic cells that the overexpression of GLUT1 and hexokinase 1 was sufficient for Akt to protect against IL-3 withdrawal (Rathmell *et al*., 2003). Under normal glucose conditions, IL-3 targets the anti-apoptotic protein Mcl-1 for proteasome degradation leading to cell death (Maurer *et al*., 2006) but when glucose levels are elevated, Mcl-1 is more stable (Zhao *et al*., 2007) (Figure 1.14). Moreover, when glycolysis is inhibited, the AMPK/mTOR axis inhibits translation of Mcl-1 rendering cells more prone to death ligands (Pradelli *et al*., 2009). In addition, increased glycolytic metabolism was shown to inhibit expression or activity of the pro-apoptotic BH3-only proteins which mediate death induced by chemotherapeutic drugs and physiological agents (EI Mjiyad *et al*., 2010) (Figure 1.14). For example, overexpression of GLUT1 was shown to inhibit Puma and p53 induction upon growth factor withdrawal (Zhao *et al*., 2008). Further, hexokinase 1/GLUT1 overexpression inhibited sensitivity of cells to transfection of DNA encoding Bim (Zhao *et al*., 2007). Elevated glucose levels have been shown to promote CDK5-mediated phosphorylation and inactivation of Noxa in human leukaemic cells (Lowman *et al*., 2010) and under low glucose conditions, Bad has been shown to be dephosphorylated and induces apoptosis. These findings provide evidence that metabolic stress regulates the BH3-only proteins and that cancer cells also use glycolysis to escape cell death. In support of this, overexpression of the glycolytic enzyme GAPDH was shown to promote survival of cancer cells (Colell *et al*.,2007) and stimulation of glucose uptake

was shown to play a crucial role in the suppression of apoptosis in normal haematopoietic cells (Barnes *et al*., 2005) (for further discussion see Chapter 5).

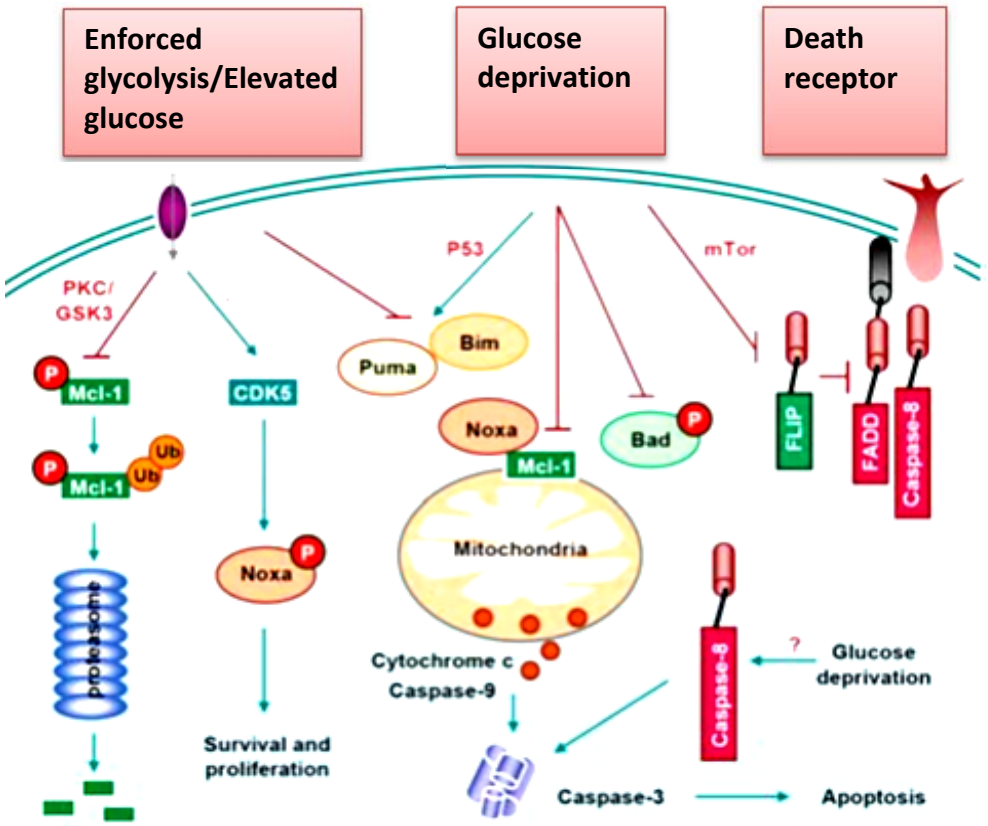

Figure 1.14 Cell death regulation by glucose metabolism

The availability of nutrients regulates cell death induced by death receptors and stimuli that kill through the mitochondrial pathway by regulating the anti-apoptotic Bcl-2 family member Mcl-1, pro-apoptotic BH3-only proteins (Bim, Noxa, Puma and Bad) and c-FLIP. Adapted from: (Munoz-Pinedo *et al*., 2012).

1.5.6 METABOLIC TARGETING FOR CANCER THERAPY

Overall, it is clear that glycolysis can indeed be blocked by inhibition of glycolytic enzymes such as HK, PFK and PK which all regulate irreversible and rate-limiting steps in glycolysis, a feature that has potential application for the metabolic targeting of cancer. Inhibition of glycolysis has also been shown to prevent cancer development, highlighting the necessity of glycolysis in proliferation, invasion and metastasis of cancer (López-Lázaro 2007; 2008 Gatenby *et al*., 2006). These findings have stimulated the search for small molecules that might specifically inhibit the key metabolic steps in glycolysis. Jang *et al*., (2013) pointed out that targeting enzymes such as lactate dehydrogenase, phosphofructokinase, pyruvate kinase and hexokinase and others indicated in (Figure 1.15) may yield therapeutic advantage and could help eradicate resistance to chemotherapy or radiotherapy. Several compounds are currently being investigated as potential therapeutic targets in glycolysis (summarised in Table 1.5)

Inhibitors of hexokinase such as 2-deoxyglucose, (2-DG) (3-bromopyruvate (3-BrPA) and lonidamine (LON, 1-[(2, 4-dichlorophenyl) methyl]-1H-indazole-3-carboxylic acid) are currently in pre-clinical and early phase clinical trials. Hexokinase mediates the first rate limiting step of glycolysis where glucose is phosphorylated with the use of ATP (Figure 1.15) hence 2-DG serves as a competitive inhibitor of hexokinase by blocking access of glucose to this enzyme. Although 2-DG showed the promising anticancer effects in preclinical models (Maher *et al*., 2004), however later studies revealed that the principal mechanisms underlying 2-DG`s anti-cancer effects vary (Kurtoglu *et al*., 2007; Zhong *et al*., 2008). Furthermore, contrary to its widely believed anticancer effects, 2-DG was shown to activate multiple pro-survival pathways in cancer cells (Zhong *et al*., 2009) and hypoxic cells were shown to be resistant to this inhibitor (Maher *et al*., 2007). Despite the

fact that the success of 2-DG as a single agent for anti-glycolytic therapy has been challenged, encouraging outcomes of its use in combination treatments were reported (Maschek *et al*., 2004; Dwarakanath *et al*., 2009).

LON, another inhibitor for hexokinase has been shown to induce apoptosis and treat multidrug resistance in several cell lines including HepG2 (Del Bufalo *et al*.,1996; Li *et al*., 2002; Ravagnan *et al*., 1999). However its clinical success has so far been impaired by significant pancreatic and hepatic toxicities reported (Price *et al*., 1996). Moreover, Phase II clinical trials of LON as a treatment for benign prostatic hyperplasia have been suspended due to its liver toxicity (Brawer, 2005; Ditonno *et al*., 2005). Despite this inhibitor is now undergoing investigation in combination treatments trials (Pelicano *et al*., 2006a; Gatenby and Gillies, 2007).

3-BrPA is a potent inhibitor of hexokinase and has been demonstrated to also affect mitochondrial respiration, leading to ATP depletion and death of cancer cells (Ko *et al*., 2001; Geschwind *et al*., 2004; Xu *et al*., 2005b). This inhibitor possesses promising anticancer property in that it is effective against hypoxic cancer and may overcome multi-drug resistance. In support of this, 3-BrPA induced severe depletion of cellular ATP and cell death in cancer cells with mitochondrial defects or under hypoxia, which normally causes a decrease in cellular sensitivity to the majority of anti-cancer agents (Xu *et al*., 2005b). Importantly, the same study showed that ATP depletion induced by 3-BrPA may disable the ATP-dependent multi-drug exporting pumps, thereby killing cells with the multi-drug resistant phenotype. It should be noted however that some researchers have pointed out that this inhibitor is unstable in solution and requires 100 μM to be effective in vitro (Chen *et al*.,2007), warranting further development of new analogues. Interestingly, it was previously reported that increased glycolysis is directly associated with glucocorticoid resistance that is associated with treatment failure in childhood acute lymphoblastic

leukaemia and inhibition of glycolysis by 2-DG, 3-BrPA or LON increases prednisolone-induced toxicity in leukaemia cells (Hulleman *et al*., 2009).

Phloretin and WZB117 (Table 1.5 and Figure 1.15) are other compounds that have demonstrated anticancer effects in preclinical models (Macheda *et al*., 2005; Liu *et al*., 2012). These compounds are believed to block the GLUTs (known to be overexpressed in most of cancer types), which would prevent glucose entry into the cancer cell and lead to the complete disruption of the glycolytic pathway. It should be noted that GLUTs are ubiquitously expressed in mammalian cells, posing a critical challenge to the selective blockade of GLUTs in tumour cells. FX11 an inhibitor of LDH diminishes intracellular ATP levels which increase oxidative stress resulting in tumour cell death (Le *et al*., 2010). Likewise, another inhibitor of LDH, oxamate (Table 1.5) sensitizes resistant cancer cells to chemotherapeutic agents such as taxol (Zhou *et al*., 2010). Both inhibitors are still in pre-clinical stages and their fate will be determined by the outcome of clinical trials.

PFK catalyses one of the rate limiting steps in glycolysis which involves the phosphorylation of fructose-6-phosphate to fructose 1,6-bisphosphate. This step is regulated by allosteric effectors involving ATP as a negative regulator and fructose-2,6-bisphosphate as a positive regulator. Strategies were previously proposed involving targeting this regulatory mechanism by suppression of PFKB3 isozyme which controls the cellular levels of fructose-2,6-bisphosphate and the glycolytic flow to preferentially kill RAS-transformed cells (Chesney, 2006). Specific inhibitors of PFKB3 are being developed and preliminary studies revealed promising anti-cancer effects (Clem *et al*., 2008) even though further research is essential to assess whether this approach could potentially be successful in clinic.

PKM2, which is highly expressed in cancer cells (Christofk *et al*.,2008; Mazurek *et al*., 2005), has been shown to be a potential therapeutic target (Chen *et al*.,2011;

Goldberg and Sharp, 2012). As a result, strategies to develop small molecule inhibitors specific for this enzyme are now in progress and their success will depend on the outcome of clinical trials.

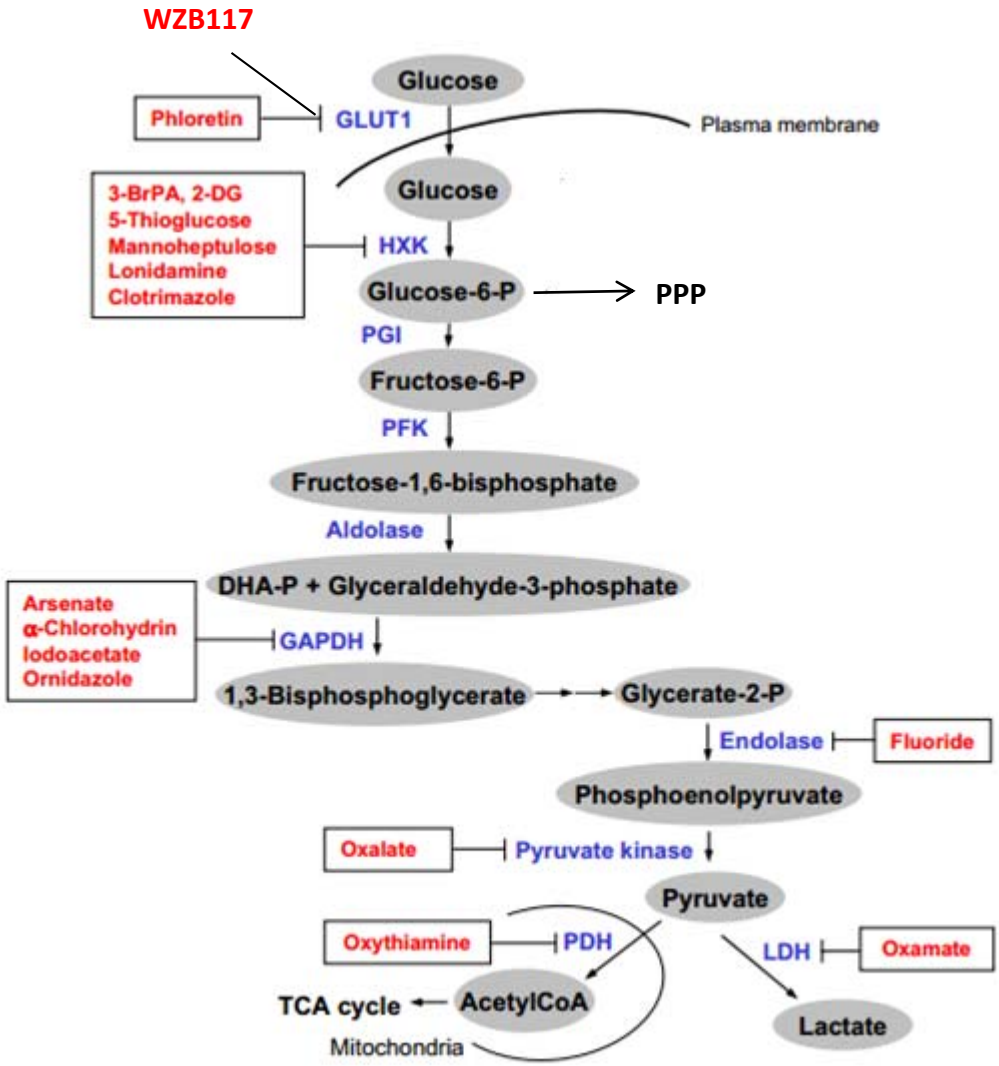

Figure 1.15 Targeting glycolysis in cancer

The enzymes that may be considered as potential targets for anti-cancer agents are indicated along with the relevant chemical inhibitors (red). Abbreviations: Glut1 = glucose transporter 1; HXK = hexokinase. Adapted from: (Chen *et al*., 2007).

Compound	Target	Mode of action
2-Deoxyglucose	Hexokinase	Inhibits glycolytic flux
3-BrPA	Hexokinase	Inhibits glycolytic flux
WZB117	GLUT1	Inhibits glucose uptake
Oxamate	Lactate dehydrogenase	Inhibits pyruvate metabolism
Phloretin	GLUT1	Inhibits glucose uptake
LON	Hexokinase	Inhibits glycolytic flux
FX11	Lactate dehydrogenase	Inhibits pyruvate metabolism

Table 1.5 Summary of compounds used for targeting glycolysis in cancer

The above figure shows the compounds used for targeting glycolysis in cancer, their target enzymes and their mode of action. Abbreviations: 2-DG = 2-Deoxyglucose; 3-BrPA = 3-bromopyruvate; GLUT = Glucose transporter; LON = Lonidamine. Adapted from Jang *et al*., (2013).

Further studies of cancer metabolic profiles are still needed together with a clear understanding of the complex metabolic alterations in cancer and mechanisms of cell death induced by the glycolysis inhibitors (Figure 1.14). So far there are no studies of how RAS and ROS induced changes impact glycolytic enzymes in haematopoietic cells. However, it has been recently demonstrated that modulating aerobic glycolysis (AG) via inhibition of either PKM2 or LDHA negatively impacted leukaemic growth, whereas normal haematopoiesis was less dependent on these enzymes (Wang *et al*., 2014). The authors of this study concluded that the differential sensitivity of normal and malignant cells to modulation of AG suggests a potential therapeutic opportunity for leukaemia intervention.

1.6 MICROARRAY ANALYSIS

1.6.1 OVERVIEW OF MICROARRAYS

A microarray is defined as a 2D array on a solid substrate such as silicon thin-film cell or glass slide that assays large amounts of biological material by the use of high-throughput screening, miniaturized, multiplexed, parallel processing and detection methods. Several types of microarrays have been invented following the initial introduction of the concept and methodology of microarray by Chang in (1983) via antibody microarray. These includes; DNA microarrays (cDNA, oligonucleotide, SNP microarrays), protein, tissue, cellular and peptide microarrays. Many companies such as Affymetrix, Illumina and Agilent have now been established and are involved in the design of the different types of microarrays.

DNA arrays are the most widely used type of microarrays. These are a collection of microscopic DNA spots attached to a solid surface which simultaneously measure the expression levels of large numbers of genes. They can be used to genotype multiple regions of a genome. Each DNA spot consists of specific DNA sequence (termed probes) which can either be a short section of a gene or other DNA element that are used to hybridize cDNA or cRNA (antisense RNA) sample (termed target). Probe-target hybridization is normally detected and quantified by the detection of fluorophore-, silver- or chemiluminescence-labelled targets for the determination of relative abundance of nucleic acid sequence in the target. In summary, the main principle behind microarray analysis is the hybridization between two DNA strands, a feature of complimentary nucleic acid sequences to specifically pair with each other via hydrogen bonds formation between complimentary nucleotide base pairs.

1.6.2 USES OF MICROARRAYS FOR GENE EXPRESSION PROFILING

DNA microarrays can be used to detect DNA (as in comparative genomic hybridization) or to detect RNA (most commonly as cDNA after reverse transcription) that may or may not be translated to proteins. The process of measuring gene expression via cDNA is called expression analysis or expression profiling. The use of miniaturized microarrays for gene expression profiling (GEP) was first reported in 1995 (Schena *et al*., 1995) and this was followed by the first publication of a complete eukaryotic genome on a microarray (Lashkari *et al*., 1997) and the emergence of the advanced different designs of microarray platforms such as Gene chip® Human Exon 1.0 ST arrays (discussed below).

1.6.3 AFFYMETRIX GENECHIP® HUMAN EXON 1.0 ST ARRAYS

The widely used Genechips® are quarts chips made by Affymetrix for the analysis of DNA microarrays. These Genechips play a vital role in research since they enable fast scanning for the presence of particular genes in a biological sample by the detection of specific pieces of mRNA. The main advantage of Affymetrix chips is that a single chip can be used to do thousands of experiments in parallel although a chip can only be used once.

Genechip® Human Exon 1.0 sense target (ST) arrays (also known as Human Exon Arrays) are a powerful new array design which are not only novel, but also have high density array manufacturing capability, offering for the first time, exon-level expression profiling at the whole-genome scale on a single array. The design of these arrays has facilitated the most comprehensive and informative coverage of the genome compared to other types that are widely used such as Genechip® Human Genome (HG) U133 Plus 2.0 arrays which measure expression only at gene level (Figure 1.16 and Table 1.6). Furthermore, Human Exon Arrays are more accurate than HG U133 Plus 2.0 arrays for

gene expression measurement (Kapur *et al*., 2007; Abdueva *et al*., 2007; Affymetrix: Online) due to a higher coverage and more evenly distributed probes (Figure 1.16 and Table 1.6). This is due to the differences in the methods used to generate the targets for amplification. In contrast to HG U133 Plus 2.0 arrays which use primers targeting the poly-A tail of mRNAs focusing on the 3' end probe selection region (PSR) the GeneChip Whole Transcript (WT) Sense Target Labelling Assay (Affymetrix :Online) applied for the Human Exon Arrays uses randomly attaching primers. Therefore bias towards the 3' end of the transcript is avoided.

Human Exon Arrays provides additional alternative splicing and transcript termination information which is beyond classical gene expression results from microarrays (Bemmo *et al*., 2008). The knowledge of changes in splicing patterns is critical to a comprehensive understanding of biological regulation and disease mechanisms. The relevance to health related studies is given by the fact that approximately 30 % of all alternatively spliced transcripts are disease related (Xi *et al*., 2008). Therefore these arrays have the ability to treat individual exons as independent objects making it possible to observe differential skipping or inclusion of exons which is impossible on arrays that focus on the transcription activities at the 3' end such as Genechip® Human Genome U133 Plus 2.0 arrays (Figure 1.16 and Table 1.6).

Furthermore Human Exon Arrays consists of sequences from cDNA-based content including the more established RefSeq and GenBank® mRNAs. Therefore each probe on this array is designed from the genomic sequence and annotated with its genome coordinates (Affymetrix: Online). Anchoring the design onto the genome enables the dynamic update of the design reflecting the new knowledge of the genomic sequence and annotations in addition to the more convenient correlation of the expression data with DNA sequence information. This is an advantage over other arrays which are typically

designed against only observed or annotated junctions. It is therefore clear that Human Exon Arrays are more advanced and greatly differ from other array types in terms of their design, coverage and density. For more detail on principles and advantages of Human Exon Arrays (Chapter 4).

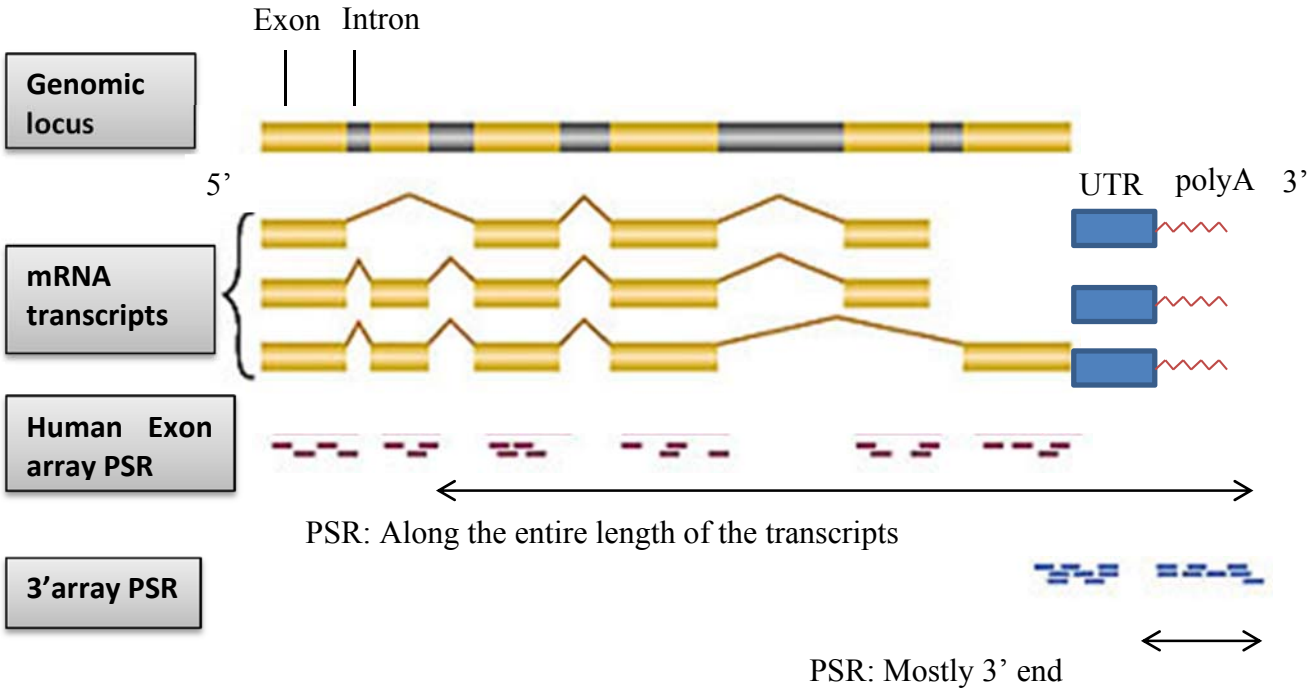

Figure 1.16 Probe coverage and distribution in Genechip® Human Exon 1.0 ST versus HG U133 Plus 2.0 arrays

Coloured regions represent exons (yellow); introns that are removed during splicing (black). The short dashes underneath the exon regions for the Human Exon Array (pink) and the 3' (HG U133 Plus 2.0) (blue) array probe selection region (PSR) indicate the individual probes representing that PSR. While the conventional HG U133 Plus 2.0 feature a probe set consisting of ~ 11 probes selected from the 3' end of the mRNA sequence, the new Human Exon Array, in contrast, has 4 probes selected from putative exon region. Abbreviations: UTR=Untranslated region. Adapted from Affymetrix: online (http://www.affymetrix.com/).

Summary of Array Statistics	Human Exon 1.0 ST Array	Human Genome U133 Plus 2.0 Array
Probe sets	1.4 million	54,000
Exon clusters	> 1 million	N/A
Supported by putative full-length mRNA	289,961 probe sets	N/A
# of perfect match probes for each probe selection region	4	11
Background subtraction strategy	Median intensity of up to 1,000 background probes with the same GC content	One mismatch probe for every PM probe
Probe selection region location	Along the entire length of the transcripts	Mostly 3' end
Probe selection region length	Median 123 bp	600 bp
Number of probes for each RefSeq Sequence	Median 30 - 40	11
Interrogated strand	Sense	Antisense

Table 1.6 Comparison of array design principles between Genechip® Human Exon 1.0 ST and Human Genome U133 Plus 2.0 arrays

Summary of the main differences in the design and performance of the Human Exon and HG U133 Plus 2.0 arrays. Abbreviations: ST = sense target; mRNA = messenger RNA. Adapted from Affymetrix: online (http://www.affymetrix.com/).

1.6.4 ADVANTAGES AND LIMITATIONS OF MICROARRAY TECHNOLOGY IN CANCER

Several GEP methods have been used in cancer research, however microarrays have become more advantageous because they are: easier to use, do not require large DNA sequencing and they allow parallel quantification of thousands of genes from multi-samples hence saving time.

Gene expression profiling of cancers using microarrays represents the largest category of research using microarray technology and seem to be the most comprehensive approach to characterize cancer at a molecular level. The importance of this approach has been demonstrated and highlighted in a number of studies performed on several malignancies such as breast, head, neck, stomach cancers and AML (for further details see Chapter 4 discussion)

Furthermore, gene expression microarrays provides a snapshot of all the transcriptional activity in a biological sample thus enable the discovery of totally novel and unexpected functional roles of genes whereas the majority of traditional molecular biology tools and techniques generally allow the study of single gene or a small set of genes. Therefore microarrays have been applied in many aspects such as the discovery of novel disease subtypes, identification of underlying mechanisms of disease or drug response and development of new diagnostic tools. In support of the above, microarrays have been referred to as a relatively new powerful tool for studying the molecular basis of interactions on a scale that is impossible using conventional analysis (Russo *et al*., 2003).

It is important to note that there are challenges and limitations to the use of microarrays that have been previously highlighted by other researchers (Murphy, 2002). These include the processing and interpretation of data generated by microarrays. However

statistical and computational tools which aid in the analysis of microarray data have now been invented and improved making microarrays more attractive in research.

Taking into consideration the emerging better designs (such as Affymetrix human exon 1.0^{ST} arrays) and advantages of microarrays, it is reasonable to conclude that microarrays will enable further improvements in diagnosis, therapy approaches and prognosis of cancer and other diseases via gene expression studies and the discovery of genes that can be targeted in the treatment of disease.

1.7 AIMS OF THE STUDY

Production of ROS in AML is frequently observed and has been shown to promote proliferation of these cells; however the mechanism through which ROS influences growth is not understood. This study will investigate how ROS influence gene expression in haematopoietic cells. A previously characterised model system based on normal human HPC will be utilised to address this. Expression of mutant RAS in these cells promotes ROS production and also drives their proliferation. The hypothesis that will be tested in this thesis is whether ROS promotes the proliferation of these cells through a transcription mechanism. The overall approach will be to identify ROS-mediated gene expression changes in RAS-transduced HPC by using a potent inhibitor of ROS production and then to analyse the functional consequences of key changes in the transcriptome induced by ROS.

Specifically the study aims to:

1) Optimise the conditions for analysis of gene expression changes attributable to ROS
2) Carry out GEP analysis using optimised conditions and validate key gene changes mediated by ROS;
3) Determine the functional consequences of key ROS-mediated changes in gene expression using knock-in and knock-down approaches.

2 General Materials and Methods

2.1 MATERIALS AND REAGENTS FORMULATIONS

2.1.1 MATERIALS

Materials used in the study and the corresponding manufacturer/supplier are listed in alphabetical order (Table 2.1, Table 2.2 and Table 2.3).

Table 2.1 General materials used in the study

Material/chemical	Manufacturer/supplier
Ampicillin	Sigma-Aldrich, Poole, UK
Bovine serum albumin fraction V (BSA)	Sigma-Aldrich, Poole, UK
Bradford's Reagent	Sigma-Aldrich, Poole, UK
Calcium chloride ($CaCl_2$)	Sigma-Aldrich, Poole, UK
Catalase	Sigma-Aldrich, Poole, UK
Chloroquine	Sigma-Aldrich, Poole, UK
Deoxyribonuclease I (DNase I)	Sigma-Aldrich, Poole, UK
Diphenyleneiodonium (DPI)	Sigma-Aldrich, Poole, UK
Dulbecco's Modified Eagle's Medium (DMEM)	Sigma-Aldrich, Poole, UK
Ethanoic acid	Sigma-Aldrich, Poole, UK
Ethanol	Sigma-Aldrich, Poole, UK
Ethylenediamine-tetraacetic acid (EDTA)	Sigma-Aldrich, Poole, UK
Foetal calf serum (FCS)	BioSera, Ringmer, UK
Ficoll-Paque®	BD Biosciences, Oxford, UK
Gentamycin	Sanofi-Aventis, Guildford, UK
Glucose oxidase (GOX)	Sigma-Aldrich, Poole, UK
Glycerol	Sigma-Aldrich, Poole, UK
Hank's Balanced Salt Solution (HBSS)	Invitrogen, Paisley, UK
Heparin	Leo Laboratories Ltd, UK
Hydrochloric acid (HCl)	Sigma-Aldrich, Poole, UK
Hypoxanthine (6-hydroxypurine)	Sigma-Aldrich, Poole, UK
Iscove's Modified Dulbecco's Medium (IMDM)	Sigma-Aldrich, Poole, UK
L-glutamine	Sigma-Aldrich, Poole, UK
Liquid nitrogen (LN_2)	BOC, Guildford, UK
Magnesium chloride ($MgCl_2$)	Sigma-Aldrich, Poole, UK
Magnesium sulphate ($MgSO_4$)	Sigma-Aldrich, Poole, UK
Methanol	Sigma-Aldrich, Poole, UK

Mini EDTA-free protease inhibitor tablets	Roche, Welwyn Garden City, UK
Penicillin	Invitrogen, Paisley, UK
Phosphate Buffered Saline (PBS)	Invitrogen, Paisley, UK
Polybrene	Sigma-Aldrich, Poole, UK
Ponceau S Reagent	Sigma-Aldrich, Poole, UK
Potassium chloride (KCl)	Sigma-Aldrich, Poole, UK
Potassium dihydrogen phosphate (KH_2PO_4)	Sigma-Aldrich, Poole, UK
Roswell Park Memorial Institute 1640 Culture medium (RPMI 1640)	Sigma-Aldrich, Poole, UK
Sodium chloride (NaCl)	Sigma-Aldrich, Poole, UK
Sodium hydroxide (NaOH)	Sigma-Aldrich, Poole, UK
Sodium orthovanadate (Na_3VO_4)	Sigma-Aldrich, Poole, UK
Sodium phosphate (Na_2HPO_4)	Sigma-Aldrich, Poole, UK
Super-Optimal medium (Catabolite-Repressing) (SOC medium)	Invitrogen, Paisley, UK
Tissue culture grade H_2O	Hameln Pharmaceuticals, Gloucester, UK
Tissue culture plastic ware	Nunc, Roskilde, Denmark and Iwaki Biosciences, Iwaki, Japan
TPA (12-O-tetradecanoylphorbol-13-acetate)	Sigma-Aldrich, Poole, UK
Tris (tris(hydroxymethyl)aminomethane)	Sigma-Aldrich, Poole, UK
Triton X-100 (4-(1,1,3,3-tetramethylbutyl)phenyl-polyethylene glycol)	Sigma-Aldrich, Poole, UK a-Aldrich, Poole, UK
Tween-20 (polyethylene glycol sorbitan monolaurate)	Sigma-Aldrich, Poole, UK
Xanthine oxidase	Sigma-Aldrich, Poole, UK

Table 2.2 Growth factors

Growth factor	Manufacturer/supplier
Human Granulocyte(G) colony-stimulating factor(CSF)	Peprotech, London, UK
Human Granulocyte-Macrophage(GM)–CSF	Peprotech, London, UK
Human interleukin(IL)-3	Peprotech, London, UK
Human IL-6	Peprotech, London, UK
Human stem cell factor (SCF)	Peprotech, London, UK
Human Fms-like tyrosine kinase-3 ligand(FLT3L)	Peprotech, London, UK

Table 2.3 Antibodies

Antibody	Use	Dilution	Catalogue No.	Manufacturer/supplier
Aldolase C (ALDOC)	Western Blotting	1/1K	Ab115212	Abcam, UK
Anti-mouse HRP	Western Blotting	1/5K	NA931	DAKO A/S, Denmark
Anti-rabbit HRP	Western Blotting	1/5K	NA934	GE Healthcare, UK
Cannabinoid receptor 2 (CNRII)	Western Blotting	1/500	Ab3561	Abcam, UK
Cbp/p300-interacting transactivator,with Glu/Asp carbox (Cited-1)	Western Blotting	1/50K	Ab92550	Abcam,UK
CD117	Flow cytometry	1/5	323408	Invitrogen ,Paisley, UK
CD32-PE	Flow cytometry	1/5	MCA1075	Serotec Oxford, UK
CD34- perCpCy5.5	Flow cytometry	1/5	X0928	Biolegend, California, USA
CD34-PE	Flow cytometry	1/5	345802	BD Biosciences, Oxford, UK
Enolase 2 (ENO2)	Western Blotting	1/5K	Ab79757	Abcam, UK
GAPDH	Western Blotting	1/10K	sc 32233	Santa Cruz, California
Glycine amidinotransferase (GATM)	Western Blotting	1/500	Ab107500	Abcam, UK
IgG1-PE	Flow cytometry	1/5	400148	BD Biosciences, Oxford, UK
IgG1-perCpCy5.5	Flow cytometry	1/5	409311	Biolegend California, USA
Protein tyrosine phosphatase receptor type D (PTPRD)	Western Blotting	1/500	Ab103013	Abcam, UK

2.1.2 REAGENTS FORMULATIONS

Table 2.4 Formulations of reagents, buffers and solutions

Reagent	Formulation
Diogenes buffer (Chapter 3)	4.6 mM $KH_2PO_4$8.0 mM Na_2HPO_4, 130.0 mM NaCl, 4.4 mM KCl, 5.5 mM glucose, 0.5 mM $MgCl_2$, 0.5 mM $CaCl_2$, 0.1% BSA, dissolved in dH_2O, pH 7.4
Loading buffer (section 2.2.4)	62.5 mg 0.25% Bromophenol blue, 62.5 mg 0.25% xylene cyanol , 7.5 ml 30% glycerol, dissolved in H_2O
Lysis byffer (section 2.9.1)	10 mM HEPES-KOH, 10 mM betamercaptoethanol, 1mM magnesium acetate, 0.5 mM EDTA, 0.5 mM EGTA, 0.25 M sucrose, 1 mM Na_3VO_4, 1 complete protease inhibitor tablet per 10 ml, dissolved in dH_2O, pH 7.2.
Magnetic activated cell sorting (MACS) buffer (section 2.4.2)	PBS consisting of 0.5% BSA, 5 mM $MgCl_2$, dissolved in dH_2O, 0.45µm filtered, degassed under negative pressure for 30 minutes.
Media mix(Table 2.6 and Chapter 5)	IMDM containing 1 % BSA fraction V, 20 % FCS, 45 µM beta-mercaptoethanol, 360 µg/ml 30% iron-saturated human transferrin
Ponceau S (section 2.9.3)	1.3 mM Ponceau S dissolved in 0.83 M ethanoic acid
Staining buffer for flow cytometry(section 2.10)	PBS consisting of 1% BSA, 3.1 mM NaN_3, dissolved in dH_2O
Selective Luria-Bertani (LB) broth(section 2.2.1)	10g Tryptone, 5g yeast extract 5g NaCl dissolved in 1 L dH_2O, pH 7. 100 µg/ml ampicillin added just before use. Selective LB agar: 35g of LB agar dissolved in 1L of dH_2O. 100 µg/ml ampicillin added just before use
TBS-Tween-20 (TBS-T) (section 2.9.3)	TBS consisting of 0.1% Tween-20. Tris-EDTA (TE) buffer: 10 mM Tris-HCl, 1 mM EDTA, pH 7.5
Tris-buffered saline (TBS) (section 2.9.1)	1 M Tris-HCl, 130.0 mM NaCl, dissolved in dH_2O, pH 7.6

2.2 RECOMBINANT DNA TECHNIQUES

2.2.1 BACTERIAL TRANSFORMATION

The generation of plasmid DNA for subsequent transfection of virus-packaging cells was achieved by DNA amplification in chemically competent *Escherichia coli* (*E.coli)*. Recombinant plasmid DNA was added directly into one freshly thawed vial of competent *E.coli* (One Shot ®Stbl3™ Invitrogen) followed by gentle tapping. The mixture was incubated on ice for 30 minutes, heat shocked for 30 seconds at 42°C in a water bath, and then placed on a rotary shaker at 225 rpm for 1 hour at 37°C in pre-warmed SOC medium. During this time, selective Luria-Bertani (LB) agar plates were prepared by melting LB agar which was allowed to cool to 42-48°C before adding the appropriate antibiotic (Table 2.5). LB agar (30 ml) was poured into 90 mm petri dishes and was allowed to cool.

Following incubation, transformed *E. coli* suspension (150 µl) was spread over selective LB agar plates using a sterile spreader and incubated for 16 h at 37°C. Single isolated colonies were picked and used to inoculate 5 ml selective LB broth cultures containing 100 µg/ml of antibiotic. The inoculated broths were incubated for 8 h at 37°C on a rotary shaker and then diluted in selective LB broth at 1:500 (300 µl of culture in 150 ml LB broth (section 2.1.2) and incubated for 16 h at 37°C on a rotary shaker. The following day DNA was purified from these bacterial cultures as described in section 2.2.3. Bacterial glycerol stocks were also prepared (section 2.2.2) and plasmid identity was verified (section 2.2.4). Purified DNA was used for transfection of Phoenix or 293T cells (section 2.5 for the method and Table 2.7 for cell line information).

Table 2.5 Plasmid DNA constructs

Plasmid DNA construct	Vector	Antibiotic resistance	Other details/source
PINCO	retroviral	Ampicillin	
pHIV ALDOC EGFP	Lentiviral	Ampicillin	2.2.5 and Chapter 5
pEXK-ALDOC	Cloning vector	Kanamycin	Eurofins, Germany
pHIV-EGFP	Lentiviral	Ampicillin	Addgene
pLJM1-EGFP	Lentiviral	Ampicillin	Addgene
pMD2	Packaging(envelope)	Ampicillin	Addgene
psPAX2	Packaging (gag/pol)	Ampicillin	Addgene

2.2.2 CRYOPRESERVATION OF TRANSFORMED BACTERIA

LB broth (850 µl) containing transformed *E. coli* cell suspension was mixed with 150 µl glycerol and transferred to -80°C freezer for long term storage. Cryopreserved *E.coli* was recovered from storage by scrapping the glycerol stock with a sterile loop and then streaking selective LB agar plates. Agar plates were incubated for 16 h at 37°C in a dry incubator. Single colonies were harvested and expanded in selective LB broth as described above (section 2.2.1).

2.2.3 ISOLATION AND QUANTITATION OF AMPLIFIED RECOMBINANT PLASMID DNA

Transformed *E.coli* which had been incubated in 150 ml selective LB broth for 16 h at 37°C on a rotary shaker were collected by centrifugation at 6,000 g for 15 min, and high-purity plasmid DNA was obtained using the HiSpeed MiniPrep and/or Maxiprep DNA isolation kit (Qiagen, Crawley, UK) as in accordance to the manufacturer's instructions. Purified DNA was quantitated using a NanoDrop spectrophotometer (Thermo Fisher Scientific, Loughborough, UK) as in accordance to the manufacturer's instructions. The purity of DNA was confirmed by A260/A280 which was in the range of 1.8-2 in all the experiments carried out in this study. The integrity of the insert and other recombinant plasmids were checked and verified by restriction enzyme digestion (section 2.2.4) and sequencing (2.2.5).

2.2.4 RESTRICTION ENZYME DIGESTION

In order to support the verification of the cDNAs insertion into the plasmid of choice and the successful transformation of *E. coli*, plasmid DNA was isolated as above (section 2.2.3) and incubated with the suitable restriction enzymes in a water bath (specific

details are in the individual chapters). An agarose gel (0.8%) was prepared by dissolving agarose powder in 1X (Tris-borate EDTA (TBE) buffer. The gel bed was cast and allowed to solidify in an electrophoresis tank. DNA samples for loading consisted of 100-500 ng DNA, in 20 µl of loading buffer) of which 12 µl was loaded per lane. Electrophoresis of the samples was carried out in 1X TBE buffer at 80V for 1 hour and DNA was visualised using peqgreen DNA dye and UV transillumination by a LAS-3000 digital imaging device (Fujifilm UK Ltd., Bedford, UK). The size of DNA plasmids or fragments was estimated using a 1 Kb DNA Ladder (New England Biolabs, NEB, UK), which was run in parallel with samples. The product of DNA restriction enzyme digestion was compared to the predicted restriction pattern obtained from pDRAW32 (http://www.acasoft.dk/acaclone/download/install.htm). Specific details are in the individual chapters.

2.2.5 GENERATION OF LENTIVIRAL EXPRESSION CONSTRUCT FOR ALDOC

ALDOC coding sequence DNA was excised from pEXK-ALDOC plasmid (Table 2.5) using both *Sma1* and *Xba1* double restriction digests (Chapter 5 for results). Plasmid DNA (pEXK-ALDOC) (7 µg) was incubated with Sma1 (70 U) at 25°C for 1 hour followed by addition of Xba1 (70 U) and further 1 hour incubation at 37 °C in a water bath. The recipient pHIV EGFP lentiviral vector (Table 2.5) (already available in our lab) was linearized using the same restriction digest. Following digestion, the insert (ALDOC) was purified using preparative electrophoresis coupled with low melting point agarose gels (1X Tris-acetate gel with Seakem GTG (1.0%)) (Section 2.2.4). Following electrophoresis, the smallest gel slice containing the insert was visualized using peqgreen DNA dye and excised from the gel. The DNA insert was extracted from the gel and purified by passing DNA sample through a QIAquick Gel extraction Spin kit (Qiagen) according to the manufacturer's instructions (section 2.2.4). DNA was finally eluted in 50 µl elution buffer

(EB). The insert (ALDOC) and vector (pHIV-EGFP) were ligated by incubation with ligase and ligase buffer at 16 °C for 4 hours in order to generate recombinant plasmid DNA, pHIV ALDOC EGFP which was used in subsequent experiments. The ligation mixture was then transformed as described in section 2.2.1.

The final construct was verified by both test digests and direct sequencing. Test digests were performed using a similar protocol to the one described in 2.2.4 and sequencing was performed using the Eurofins sequencing service, (Eurofins, Germany). The results and specific details are in the individual chapters.

2.3 CELL CULTURE

2.3.1 CRYOPRESERVATION AND THAWING OF CELL SAMPLES

Cell suspension, 500 µl in suitable growth medium was mixed with 500 µl of Iscove's Modified Dulbecco's Medium (IMDM) (Table 2.1) consisting of 30% FCS and 20% DMSO (freeze mix). Samples were transferred to 1.8 centrifuge vials and placed in controlled refrigeration containers (Mr. Frosty) where 100% isopropanol is used as the thermal interface. These controlled refrigeration containers were then placed in a -80°C freezer overnight. The following day, samples were transferred to liquid nitrogen N_2 for long term storage.

The recovery of cryopreserved $CD34^+$ cells and cord blood was achieved by rapid defrosting in a water bath at 37°C in the presence of 900 µl 0.45µm-filtered FCS and 200 µg sterile DNase I. The cells were then diluted by dropwise addition of equal volumes of MACS buffer over 3 min twice, followed by centrifugation of cells at 180 g for 10 minutes. The recovered cells were resuspended in a suitable growth medium (section 2.3.3) and allowed to recuperate for 16-24 h at 37°C in a 5% CO_2 humidified atmosphere prior to use for experimental endpoints (Chapters 3-5).

Cryopreserved cell lines, were recovered by rapid defrosting them in a 37°C water bath followed by dropwise addition of 5 ml suitable growth medium, centrifugation of cell lines at 180 g for 5 min and resuspension in growth medium (section 2.3.3). Cell lines were also allowed to recuperate for 16-24 h at 37°C in a 5% CO_2 humidified atmosphere.

2.3.2 DETERMINATION OF CELL DENSITY

Cells were counted before each passage by the use of haemocytometer (Hawksley, Brighton, UK) in order to estimate cell density (number of cells per volume of medium) before sub-culturing or for use in the experiments. The haemocytometer chamber was filled with 8 µl of cells from a known total volume of the cell suspension and placed into a counting chamber with the coverslip in place. Cell count was performed under the microscope using a hand held counter. The haemocytometer is etched with ruled lines marking a counting space which has a known volume (0.9 µl). This volume is subdivided by ruled lines into 9 cuboids equivalent to 100 nl each. The cellularity (density) of cells/ml is given by the average number of cells per cuboid multiplied by 1×10^4.

2.3.3 CULTURE OF PRIMARY CELLS AND CELL LINES

Cell lines (Table 2.6 and Table 2.7) were obtained from ATCC (Teddington, UK) unless otherwise stated, and cultured at 37°C in a humidified 5% CO_2 atmosphere in RPMI 1640 containing 10% FCS and 20 µg/ml gentamycin, unless otherwise stated. For primary cell cultures, the age of the culture is indicated in days since isolation.

2.3.3.1 Non-adherent cells

Cell lines were cultured (Table 2.6) and cell density was determined as described (section 2.3.2).

Table 2.6 Culture details for non-adherent cells

Cells	Description	Density (cells/ml)	Usual culture conditions
$CD34^+$	Primary cells from human cord blood	2-4x10^5	Media mix (section 2.1) supplemented with 5 ng/ml human(hu) IL-3, huG-CSF, huGM-CSF, 20 ng/ml huSCF
HL60	promyelocytic cell line	2-5x10^5	RPMI 1640 Sub-culturing ratio 1:2 with fresh medium as necessary or every 24-36 hours.
KG-1	Human acute myelocytic leukaemia	2-5x10^5	IMDM With 20% FCS and 4mM L-Glutamine
MV4-11	Human acute myelocytic leukaemia	2-5x10^5	IMDM With 10% FCS and 2mM L-Glutamine
K562	Human Chronic Myeloid Leukaemia	2-5x10^5	RPMI1640
THP-1	Human Monocytic Leukaemia	2-5x10^5	RPMI1640

2.3.3.2 Adherent cells

Adherent cells (Table 2.7) were cultured in DMEM with 10% FCS and 20 μg/ml gentamycin. Confluent cultures were detached from cell culture plastic ware by incubation with 1 ml 500 μg/ml trypsin solution containing 0.53 mM EDTA for 3 min. Trypsin was neutralised with 5 ml warm growth medium. Cells were disaggregated by pipetting, centrifuged for 180 g for 5 min and resuspended in fresh growth medium. The sub-culturing of cells was performed as described in the table for each type of cells.

Table 2.7 Culture details for adherent cells

Cells	Description	Source	Sub-culture details
Phoenix virus – packaging cells	retroviral-packaging cells	Garry Nolan (Stanford University)	Ratio 1:3 as necessary or every 36 hours.
HeLa	cell line derived from cervical cancer cells		Ratio 1:4 as necessary or every 72 hours.
293T	Isolated from human embryonic kidneys (HEK) and transformed with large T antigen		Ratio 1:6 as necessary or every 72 hours.

2.4 ISOLATION OF NORMAL HUMAN CD34$^+$ HAEMATOPOIETIC PROGENITOR CELLS FROM CORD BLOOD

2.4.1 ISOLATION OF HUMAN MONONUCLEAR CELLS FROM CORD BLOOD

Human cord blood was obtained from full-term pregnancies at the Maternity Unit, (University Hospital Wales, UK) with informed consent and approval from the South East Wales Research Ethics Committee. Cord blood samples were collected into tubes containing heparin (500 µl) and followed by the immediate isolation of mononuclear cells by density centrifugation using Ficoll-Paque®. Cord blood was diluted with an equal volume of Hank's balanced salt solution (HBSS) consisting of 25 mM HEPES, 100 µg/ml gentamycin and 1 U/ml heparin and 7 ml of the diluted blood was layered onto 5 ml of Ficoll-Paque® and centrifuged at 400 g for 40 min. A separate layer of mononuclear cells was formed at the plasma-Ficoll interface and was recovered, washed with RPMI 1640 containing 5% FCS and 1 U/ml heparin. These mononuclear cells were then recovered by centrifugation at 200 g for 10 min and were washed again in RPMI 1640 containing 10% FCS until there was no platelet contamination. Cells were finally counted using a haemocytometer (section 2.3.2) and stored in liquid nitrogen until when they are needed (section 2.3.1).

2.4.2 ISOLATION OF HUMAN CD34$^+$ HAEMATOPOIETIC CELLS FROM MONONUCLEAR CELLS

Human CD34$^+$ haematopoietic progenitor cells were isolated from mononuclear cells using the miniMACS® CD34$^+$ Progenitor Cell Isolation Kit (Miltenyi Biotec, Bisley, UK) by positive selection. This was performed according to the manufacturer's instructions. Previously prepared, cryopreserved mononuclear cells were thawed and resuspended in MACS buffer (section2.1.2) at 6.5x10^8 cells/ml and then incubated at 4°C

for 15 min with 50 µl anti-CD34 antibody (Table 2.3) per 10^8 cells in the presence of an FcR blocking agent. Cells were subsequently washed with 5 ml MACS buffer by centrifugation at 180 g for 5 min. These mononuclear cells were then incubated at 4°C with magnetic anti-Fc microbeads followed by washing as above. Magnetically-labelled $CD34^+$ cells were passed through an MS^+ separation column and hence were isolated from total mononuclear cells. $CD34^+$ cells were therefore eluted from the column in the absence of a magnetic field by rinsing the column with 1 ml MACS buffer.

In order to check for the purity of $CD34^+$ cells, $1x10^4$ of isolated $CD34^+$ cells were stained with anti-human CD34 antibody conjugated to R-phycoerythrin (PE) (BD Biosciences), and analysed by flow cytometry (section 2.10). Isolated $CD34^+$ cells were cultured in IMDM containing 1% BSA, 20% FCS, 45 µM beta-mercaptoethanol, 360 µg/ml 30% iron-saturated human transferrin, penicillin, 100 µg/ml streptomycin, 50 ng/ml huIL-3, huSCF, huFLT3L and 25 ng/ml huIL-6, huG-CSF and huGM-CSF (Table 2.2). These were then used in Chapter 3-Chapter 5.

2.5 GENERATION OF RETROVIRUS

The transfection of Phoenix virus-packaging cell line (Table 2.7) was achieved by the use of the previously prepared PINCO plasmid DNA (non-translated DNA stuffer fragment/GFP control or $N\text{-}RAS^{G12D}$) from transformed *E.coli* in order to generate recombinant retrovirus. A total of 6 million phoenix cells were seeded in F75 flasks for each of the DNA constructs on day 0. The following day, cell confluence was checked (~ 95 %) and the media refreshed. For transfection an aqueous solution (450 µl) containing 10-45 µg plasmid DNA and 250 mM $CaCl_2$ was added slowly-dropwise to 2× HEPES-Buffered Saline (HBS) which was bubbled at the same time using a pipette boy with 1ml pipette tip attached .The mixture was vortexted for 2-4 seconds and the precipitate was kept undisturbed for 20 minutes during which time 25 µM chloroquine was added to the

cell cultures. At the end of 20 minutes, the precipitate was added to each of the flasks and incubated overnight in a humidified CO_2 atmosphere. The next day the medium was replaced with 8ml of fresh medium in preparation for harvest the following day and incubated overnight at 33 °C. On day 3, retrovirus was harvested and the media was replaced with the fresh one for a second harvest. Medium (8 ml) was removed, transferred to a UC, centrifuged at 200 g for 10 minutes to remove residual cells, aliquoted into cryotubes, snap frozen in liquid nitrogen and then stored in a freezer at -80°C. The virus was harvested for the second time the following day as for day 3.

2.6 RETROVIRAL TRANSDUCTION OF HUMAN $CD34^+$ HAEMATOPOIETIC PROGENITOR CELLS

In order to generate human haematopoietic progenitor cells expressing mutant N- RAS (N-RAS^{G12D}), $CD34^+$ cells were isolated as above (section 2.4) from neonatal cord blood and transduced with the retroviral vector PINCO encoding full-length N-RAS^{G12D} and GFP or empty vector control (GFP alone) generated in section 2.5. Firstly, 24 well untreated tissue culture plates were coated with 150 µl retronectin (Takara, Shiga, Japan) overnight. On the first day of infection, the plates were 'blocked' with 200 µl 1% BSA solution for 30 minutes, 1ml of virus was added per coated well and centrifuged at 1400 g for 90 minutes at room temperature. At the end of the spin, the supernatant was removed, replaced with the appropriate volume of cells, centrifuged briefly at 180 g for 3 minutes and incubated at 37°C in a humidified 5% CO_2 atmosphere. The following day the infection process was repeated as above using fresh retroviruses. It is important to note that a mock control ($CD34^+$ cells treated with 1 ml of medium) was included for comparisons. Finally cell transduction frequency was assessed by flow cytometry to detect GFP expression (section 2.10) and cells were either cryopreserved (section 2.3.1) or continued in culture (Table 2.6) for determination of other experimental endpoints.

2.7 GENERATION OF LENTIVIRUS

Recombinant lentivirus was generated by the transfection of 293T cell line (Table 2.7) using previously prepared plasmid DNA (Table 2.5) from transformed *E.coli*. A total of 8.5 million 293T cells were set up in the appropriate poly-L-lysine coated F75 flasks which helped to stabilize the cell monolayer. The following day, cell confluence was checked (above 50 %) and the overnight media (15ml) was refreshed (15 ml). For transfections a mixture of appropriate volumes of water, DNA transfer vector, packaging vectors-pMD.2G (envelope plasmid) and psPAX2 (packaging plasmid) (Table 2.5) was prepared. Transfection of these DNAs was carried out as described in (section 2.5). The next day the medium was replaced with 7.5 ml of fresh medium in preparation for harvest and incubated overnight 37°C in a humidified CO_2 atmosphere. Lentivirus was harvested the following day and the medium was replaced for a second harvest the next day and cells. On the final harvest day, medium (7.5 ml) was removed, transferred to a UC, centrifuged at 200 g for 10 minutes to remove residual cells, supernatant (virus) was carefully aliquot into cryotubes, snap frozen in liquid nitrogen and then stored in a freezer at -80°C.

2.8 LENTIVIRAL TRANSDUCTION OF CELL LINES

Untreated 24 well tissue culture plates were coated with 150 µl retronectin overnight. On the first day of infection, the plates were blocked with 200 µl 1% BSA solution for a minimum of 30 minutes and 1ml of virus was added per coated well and centrifuged at 1400 g for 90 minutes at room temperature. At the end of the spin, the supernatant was removed and replaced with the appropriate number and volume of cells (4 $x10^5$ cells in 1ml) and incubated at 37°C in a humidified 5% CO_2 atmosphere. For cells

transduced with GFP, transduction frequency was assessed the following day cell by flow cytometry (section 2.10). It is noteworthy that appropriate controls (parental cell lines) were included for comparison and the determination of the thresholds (results in the individual chapters). For cells transduced with the puromycin resistance marker, see Chapter 5 section 5.2.1.3 for more detail. Cells were either cryopreserved (section 2.3.1) or continued in culture (Table 2.6) for determination of other experimental endpoints.

2.9 WESTERN BLOTTING

2.9.1 PREPARATION OF PROTEIN EXTRACTS FROM WHOLE CELLS

Cells were harvested, counted, washed twice in 20 ml of TBS then centrifuged at 180 g for 10 min and the supernatant was removed. The cell pellet was then flash frozen in liquid N_2 to enable full cell fragmentation and stored at -80°C until ready for processing. Volumes of protein extracts were recorded during extraction for use in total protein quantitation.

Whole cell protein extracts were prepared by thawing flash frozen cell pellets (prepared as described above) on ice in the presence of 10 µg DNase I per $1x10^6$ cells. Thawed cells were resuspended in a minimum of 50 µl lysis buffer containing 1% Triton X-100 per $1x10^6$ cells (section 2.1.2) and incubated on ice for 30 min with occasional vortexing to encourage protein solubilisation. Detergent-insoluble material was sedimented by centrifugation at 16,000 g for 5 min at 4°C and supernatants were transferred to pre-chilled Eppendorf tubes. Protein concentration was determined as described in (section 2.9.2) and protein extracts were stored at -80°C until when needed.

2.9.2 PROTEIN QUANTITATION

The concentration of protein in the extracts prepared above was determined using Bradford's reagent (Sigma-Aldrich, UK). Bradford's stock reagent was diluted with

an equal volume of ultra-pure water (ratio 1:1) to create enough working solution for the test (190 µl per test well). Protein extracts were diluted a minimum of 10 fold. The diluted extract (10 µl) was mixed with 190 µl diluted Bradford's reagent in a 96-well plate and samples were tested in duplicate. BSA standard solutions were assayed in duplicate as well alongside protein extract samples to create a standard curve, which allowed calculation of protein extract concentration. Absorbance was measured at 590 nm using an ASYS Hitech Expert plus spectrophotometer (Biochrom, Cambridge, UK).

2.9.3 PROTEIN ELECTROPHORESIS AND ELECTROBLOTTING

XCell SureLock™ electrophoresis and electroblotting system (Invitrogen, UK) was used for protein electrophoresis and electroblotting. All the reagents, buffers and gels used in this process were purchased from Invitrogen. All protein extracts were incubated at 70°C for 10 min in the presence of 1X LDS sample buffer and reducing agent to facilitate denaturation of proteins just before electrophoresis. Denatured protein samples (0.7-10 µg protein per lane) were loaded onto a 4-12% Bis-Tris HCl polyacrylamide gel and electrophoresis was performed at 200 V for 50 min in the XCell SureLock™ Mini-Cell in the presence of MOPS-SDS running buffer. Proteins were then electroblotted from the electrophoresis gel onto nitrocellulose membranes using the XCell SureLock™ Mini-Cell blot module. Gels were removed from their cassettes and placed into layers containing 2 blotting pads on top, the gel and membrane sandwiched between blotting filter paper and 3 additional blotting pads at the bottom. The module was placed in XCell SureLock™ Mini-Cell and with transfer buffer (1X NuPAGE® Transfer buffer, 1 ml NuPAGE® and 10% methanol). Electroblotting of proteins was carried out at 30 V for 1 hour.

At the end of electroblotting, membranes were washed twice with 20 ml of dH_2O for 5 min on a shaker to remove gel and other transfer buffer components. These membranes were then incubated with Ponceau S solution (section 2.1.2) for 30 sec to

visualise transferred protein, equal loading, and in some cases to facilitate membrane cutting between lanes. Two further washes with dH_2O were done as above, membranes were incubated with 10 ml TBS-T containing 2.5 % membrane blocking agent (Marvel) for 1 h at room temperature on a rotary shaker. Blocked membranes were rinsed twice with 10 ml TBS-T followed by one 15 min wash and three 5 min washes (with 10 ml TBS-T) on a rotary shaker.

2.9.4 IMMUNOPROBING OF ELECTROBLOTTED PROTEINS

Membranes previously blocked and rinsed above (section 2.9.3) were incubated at 4°C for 16 h (overnight) in the presence of primary antibody diluted in TBS-T containing 2.5 % blocking agent. Optimum dilutions of previously untested primary antibodies were determined. Details of specific antibodies used are in Table 2.3 and will further be given in the appropriate results sections. Outer lanes of gels were loaded with 10-20 µl of 1X LDS buffer containing a 20 fold dilution of MagicMark XP® Protein Standard (Invitrogen) for the estimation of molecular weight of proteins. To verify equal loading, membranes were incubated overnight at 4°C on a rotary shaker with one of the following antibodies: 20 ng/ml anti-GAPDH (Santa Cruz) or 10 ng/ml anti-β-actin (Abcam, Cambridge, UK) (Table 2.3).

Membranes were rinsed two times, washed once for 15 min and three times for 5 min in a rotary shaker as above after incubation with the primary antibody. Membranes were then incubated with diluted ($5x10^4$ fold) HRP-conjugated anti-mouse or anti-rabbit secondary antibody (GE Healthcare) in TBS-T containing 1% membrane blocking agent for 1 h on a rotary shaker. Membranes were finally rinsed two times, washed once for 15 min and three times for 5 min in a rotary shaker as above.

Electroblotted proteins labelled with primary and secondary antibodies were visualised using ECL Prime Advance® Western Blotting Detection Kit (GE Healthcare).

Excess wash buffer was drained from immunolabelled membranes and then incubated under low light for 5 min at room temperature with reconstituted ECL Advance®. ECL Advance® solution was then decanted, excess solution was removed using blotting paper, membranes were placed between two sheets of clean acetate and ECL Advance® chemiluminescence was detected using a LAS-3000 digital imaging device (Fujifilm UK). Digital images were processed and analysed using AIDA Image Analyzer v4.19 (Fujifilm UK) and Photoshop (Adobe Photoshop CS6 extended, UK).

2.10 FLOW CYTOMETRIC ANALYSIS

Cells were recovered from growth medium by centrifugation at 180 g for 5 min and then washed by resuspension in 1 ml staining buffer (section 2.1.2) per $1x10^6$ cells unless otherwise stated for flow cytometric data acquisition and analysis using a C6 flow cytometer (BD Bioscieces, UK). Cells were then resuspended in 25 µl staining buffer (unless otherwise stated) and incubated with primary stage antibodies or other reagents according to the experimental protocols described in the appropriate results sections.

Successive staining stages such as incubation with secondary antibodies were separated by a wash step involving resuspension in 200 µl staining buffer, centrifugation and resuspension in 25 µl of staining buffer unless otherwise stated. Background fluorescence was determined by isotype and manufacturer-matched control antibodies conjugated to the same fluorochromes for conjugated antibodies. For flow cytometric measurement of reporter gene expression, the autofluorescence of mock-infected cultures defined the threshold for GFP positivity and the threshold for positive staining was set to 95% of background fluorescence (specific details are in the individual chapters). Samples were resuspended in a maximum of 100 µl FACS flow prior to data acquisition. A C6 flow cytometer was used for data acquisition, a minimum of 10,000 events were collected and analysed using FCS Express v3 (De Novo Software, Los Angeles, CA).

2.11 STATISTICAL ANALYSES

Significance of difference was determined using Student's t-test using Minitab v17.0 (Minitab Ltd., Coventry, UK) or as indicated in the results chapters. Other statistical tests used are described in the results chapters.

3 Examination of ROS production by human CD34$^+$ haematopoietic cells and preparation of microarrays

It has previously been shown that mutational activation of RAS in human primary haematopoietic stem/progenitor cells gives rise to deregulated development characteristic of preleukaemia (Darley *et al*., 1997; Darley *et al*., 2002; Pearn *et al*., 2007). Further, mutant RAS expression has been shown to disrupt the differentiation of normal CD34$^+$ haematopoietic cells (Darley and Burnett, 1999). More recently it has been shown that both H-RAS and N-RAS promote the production of reactive oxygen species (ROS), including superoxide by these cells via increased NADPH oxidase (NOX) activity (Hole *et al*., 2010). Growing evidence suggests that ROS are at least partly responsible for the mutant RAS phenotype observed in several cell models (Irani *et al*., 1997; Liu *et al*., 2001; Cho *et al*., 2002; Lee *et al*., 1999). ROS have the potential to modulate cell signalling; however the direct effects of ROS on gene transcription are unknown. It is also noteworthy that transcriptional dysregulation is a key element in leukaemogenesis (Chapter 1). Therefore this study was undertaken to determine the contribution of ROS production to the changes in gene expression arising from expression of mutant RAS. This chapter investigates the effects of activated RAS expression on ROS production by primary human CD34$^+$ haematopoietic cells and optimises conditions for microarray analysis.

3.1 AIMS

- Optimise and validate assays for the measurement of ROS using Diogenes and its inhibiton by DPI (a NOX oxidase inhibitor).

- Determine whether mutant N-RAS^{G12D} can induce ROS production in human CD34^{+} haematopoietic progenitor cells and to confirm ROS inhibition in samples prepared for Gene Expression Profiling (GEP).

- RNA isolation and quantification from all samples prepared GEP.

- Generate GEP data using GeneChip® Human Exon 1.0ST arrays (Affymetrix UK Limited) to investigate the effect of mutant N-RAS^{G12D} and ROS on gene expression.

3.1.1 EXPERIMENTAL DESIGN

To achieve the above aims four treatment conditions: CD34^{+} cells transduced with N-RAS (test) or GFP vector (control) incubated in the presence and absence of DPI to determine the ROS-specific GEP (Figure 3.1). DPI is a NOX-inhibitor which has been previously shown to block superoxide production by NOX enzymes (Hole *et al*., 2010; O'Donnell *et al*., 1993). N-RAS cultures without DPI would detect ROS+RAS related changes, while N-RAS with DPI would detect only RAS related changes (Figure 3.1). For detailed strategy and experiments performed see Figure 3.2 and Chapter 4 for data analysis.

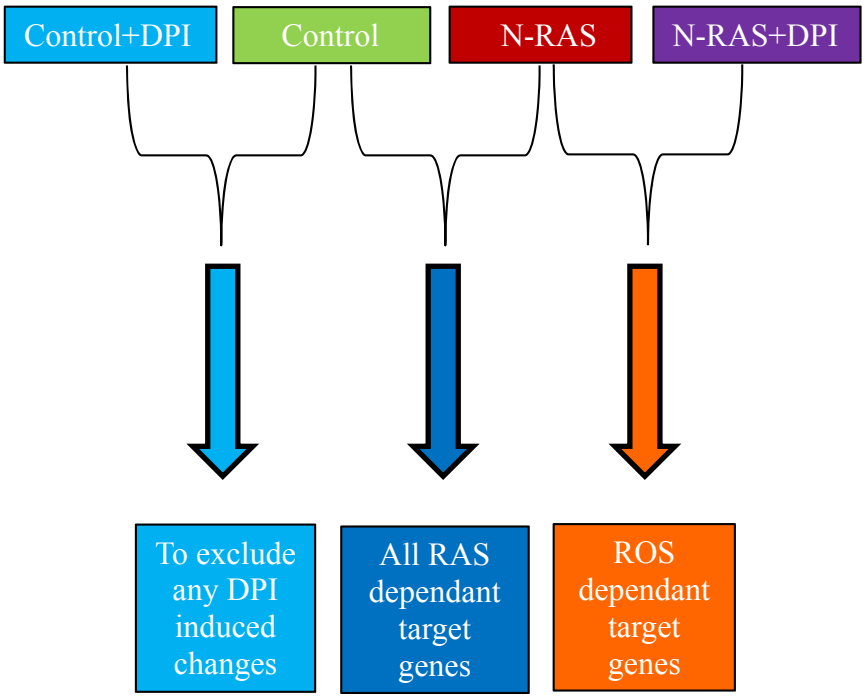

Figure 3.1 Strategy for the identification of the N-RAS^{G12D} genes changes that are mediated by ROS.

Summary flow diagram showing the simplified strategy and four treatment conditions employed for the examination of the effect of RAS and ROS on gene expression and the determination of the ROS specific gene expression profile. For detailed strategy and experiments performed see Figure 3.2 and Chapter 4 for data analysis.

3.2 MATERIALS AND METHODS

3.2.1 DETECTION OF SUPEROXIDE USING DIOGENES™

Firstly, mutant RAS expressing $CD34^+$ cells were generated and analysed for GFP positivity as outlined in Chapter 2 and summarised in Figure 3.2. In order to establish whether human $CD34^+$ haematopoietic progenitor cells over-expressing mutant N-RAS showed increased superoxide production compared to controls, chemiluminescent assays using the superoxide specific probe Diogenes (National Diagnostics, Atlanta, GA) was used (Hole *et al*., 2010). Transduced $CD34^+$ cells were washed in phosphate-buffered saline (PBS) (Gibco, Paisley, UK) and resuspended in Standard Buffer (SB) (*KH_2PO_4 4.6mM, Na_2HPO_4 8.0mM, NaCl 13mM, KCl 0.44mM, Glucose 5.5mM, BSA (low LPS) 0.1%, $MgCl_2$ 0.5mM, $CaCl_2$ 0.45mM dissolved in pure water, pH 7.3*) at $1x10^6$ cells/ml. Cell suspension (150µl) was deposited in triplicate into FluoroNunc Maxisorp 96 well plate (Thermo-Fisher Scientific) and 50 µl Diogenes (prepared according to the manufacturer's instructions) was added immediately to the wells. Chemiluminescence traces were recorded using a Hidex Chameleon (Lablogic, Sheffield, UK).

Variations on the method above are outlined below and the details are in the results section.

- In order to determine if ROS mediates oxidative stress in mutant N-RAS cells, it was necessary to block superoxide production in these cells using the NOX inhibitor DPI (Sigma, UK). Initial experiments focused on optimising the conditions of use for this inhibitor. First, the effect of DPI on superoxide production was assayed. HL60 cells were incubated for 10 seconds in the presence of 0-1000 nM DPI prior to stimulation with 1 µM 12-0-tetradecanoylphorbol-13-acetate (TPA). Diogenes chemiluminescence was

detected as outlined above. HL60 is a promyelomonocytic cell line (Table 2.6) with an NRAS mutation and was previously shown in our lab to be responsive to TPA-induced superoxide production arising from NOX oxidase activity and hence suitable for the current study.

- Determined the effect of 100 nM DPI on survival of mutant N-RAS transduced $CD34^+$ cells over time.

- Determined the effect of mutant N-RAS expression on ROS production in human haematopoietic progenitor cells,

Below is a summary of the main experimental design strategy prior to microarray experiments (Figure 3.2).

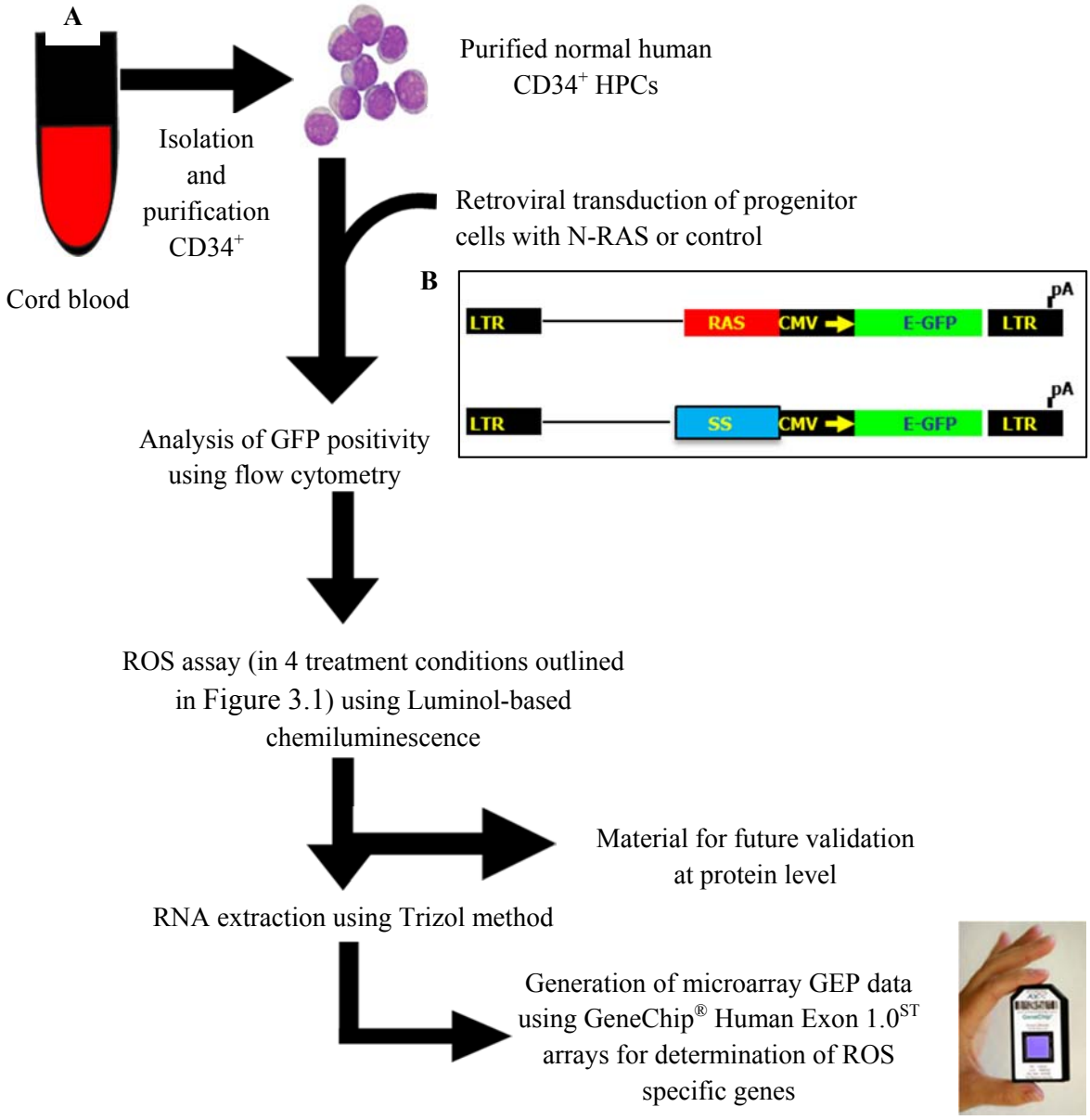

Figure 3.2 Overall experimental design and strategy prior to microarray experiments

(A) Summary flow diagram showing the experiments performed prior to the microarray experiments for the examination of the effect of the effect of N-RAS and ROS on gene expression. Human $CD34^+$ haematopoietic progenitor cells (HPCs) were isolated from whole cord blood using the MiniMACS system. $CD34^+$ cells were transduced using the PINCO retroviral vector to generate control (GFP only) and GFP + $N\text{-}RAS^{G12D}$ expressing cells. **(B)** PINCO retroviral vector DNA constructs. Top panel = $N\text{-}RAS^{G12D}$ + GFP; Bottom = GFP control; LTR = retroviral Long Terminal Repeat; SS = Stuffer sequence; CMV = cytomegalovirus promoter; RAS = *N-RAS*^{G12D} gene. Transduced cells were assessed for transduction efficiency and used for experimental end points described in the text.

3.2.2 PREPARATION OF RNA FOR MICROARRAY/GEP EXPERIMENTS

RNA was extracted and isolated from the cell cultures described in 3.2.1 using Trizol reagent (Life Technologies, California) with MaXtract high density tubes (QIAGEN, UK) as per kit method, purified using RNeasy Kit (QIAGEN, UK) and then finally quantified and checked for quality/integrity using the Agilent RNA 6000 Nano Kit (Agilent Technologies, Germany) method and Agilent 2100 bioanalyser as per manufacturer's instructions.

3.2.3 GENERATION OF GEP DATA USING HUMAN EXON 1.0^{ST} ARRAYS

3.2.3.1 GEP experiments using Human exon 1.0 Sense Target (ST) arrays

The effect of RAS and ROS on gene expression was investigated using GeneChip® Human Exon 1.0^{ST} arrays as per manufacturer's instructions. High quality RNA (in 3.2.2) was sent to the university service, CBS where microarray hybridisations were carried out. Briefly, RNA samples were processed for Affymetrix whole transcriptome microarray analysis using The Ambion WT Expression Kit protocol (Applied Biosystems, USA) by generation of cDNA from 100 ng of total RNA which was then fragmented, labelled, hybridized, washed and scanned using the Affymetrix GeneChip WT Terminal Labelling, Hybridization, wash, stain and scan kits (Affymetrix, UK) as in accordance to the manufacturer's instructions. Results obtained were imported in to Partek Genomics Suite Software (Version 6.6; Partek Inc., MO, USA) for analysis (Chapter 4).

3.2.4 DATA AND STATISTICAL ANALYSIS

All flow cytometric data were acquired using C6 flow cytometer (Accuri,UK) and analysed using FCS Express v3 (De Novo Software, Los Angeles, CA). Significance

of difference was analysed using the Student's t-test calculated in Minitabv.15 (Minitab Ltd, Coventry, UK). For the GEP data analysis please refer to Chapter 4.

3.3 RESULTS

3.3.1 MUTANT N-RAS^{G12D} EXPRESSED IN NORMAL HUMAN CD34^{+} HAEMATOPOIETIC PROGENITOR CELLS

In this study, a primary human CD34^{+} haematopoietic cell model was used to investigate the effect of mutant RAS expression on ROS production. In order to generate mutant N-RAS expressing CD34^{+} cells, a retroviral vector co-expressing N-RAS and GFP was used as previously described (Hole *et al*., 2010) (Figure 3.2). CD34^{+} cells were isolated from normal human cord blood, transduced with mutant RAS and analysed by flow cytometry (as described in Chapter 2) for GFP expression on day 3 of culture. Figure 3.3A shows that following retroviral transduction approximately 70% of cells were CD34^{+}. GFP positivity range for the control and N-RAS samples prepared for the microarray experiments was (54-84%) and (64-82%) respectively. Figure 3.3B shows example data for the samples used in the microarray experiments.

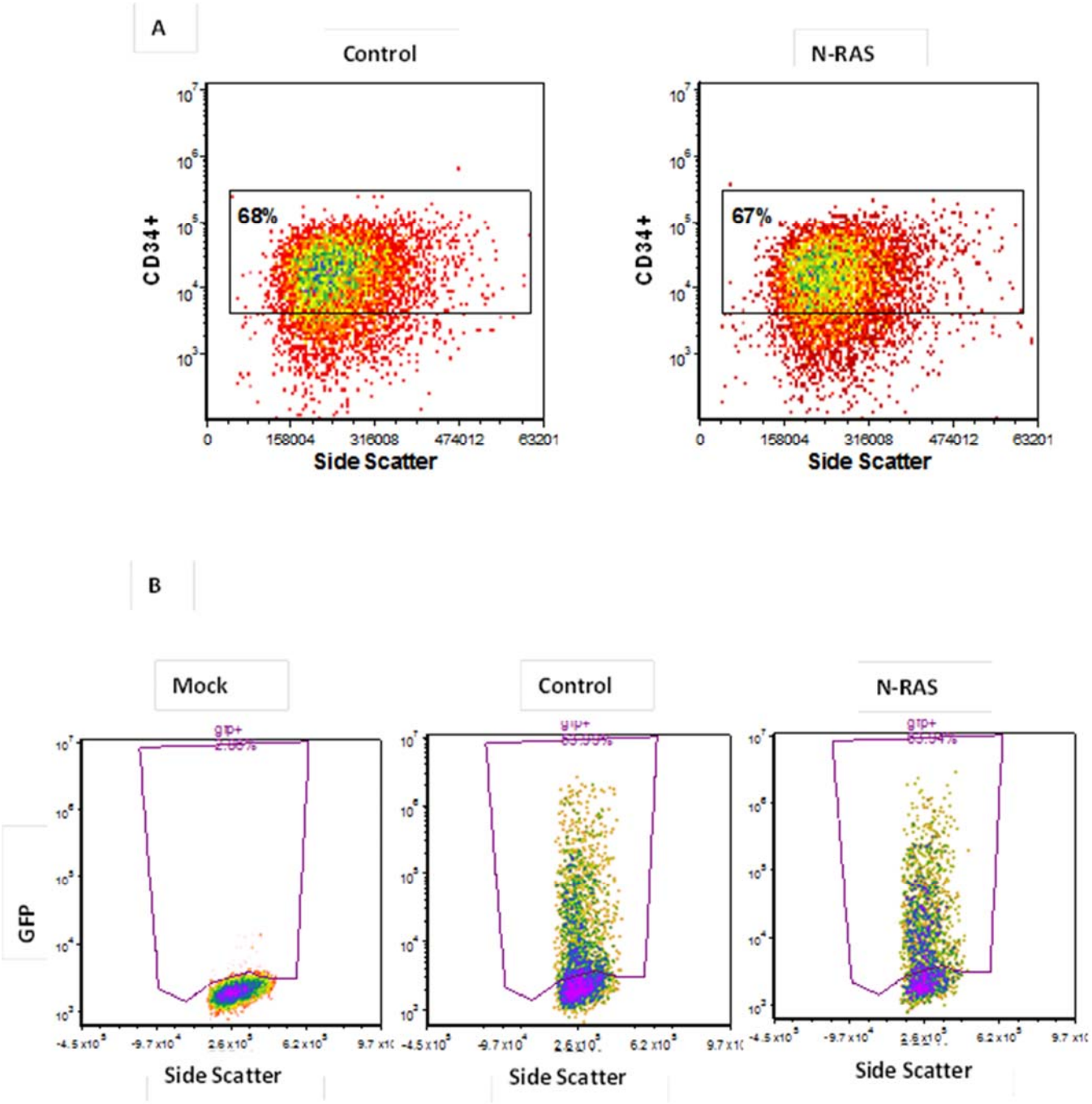

Figure 3.3 Analysis of normal human CD34$^+$ haematopoietic progenitor cells

Transduced human CD34$^+$ haematopoietic progenitor cells were analysed for CD34$^+$ and GFP expression on day 3 of development. Representative bivariate plots of transduced cells for **(A)** CD34$^+$ and (**B)** GFP expression. GFP positive threshold was defined by autofluorescence of mock-transduced cells (Mock). CD34$^+$ threshold was determined by isotype controls. Typical percentages of CD34$^+$ and GFP positive cells are shown for each culture.

3.3.2 OPTIMISATION OF ROS INHIBITION CONDITIONS

3.3.2.1 Optimisation of DPI concentration required to inhibit superoxide production in HL60 cells

To establish the lowest effective concentration of DPI needed to inhibit superoxide production, the inhibition of superoxide production in HL60 cells was investigated using the superoxide specific chemiluminecent probe Diogenes. The results showed that DPI markedly reduced superoxide production in HL60 cells at all concentrations tested compared to the control (Figure 3.4). At 100 nM DPI >90% inhibition was observed.

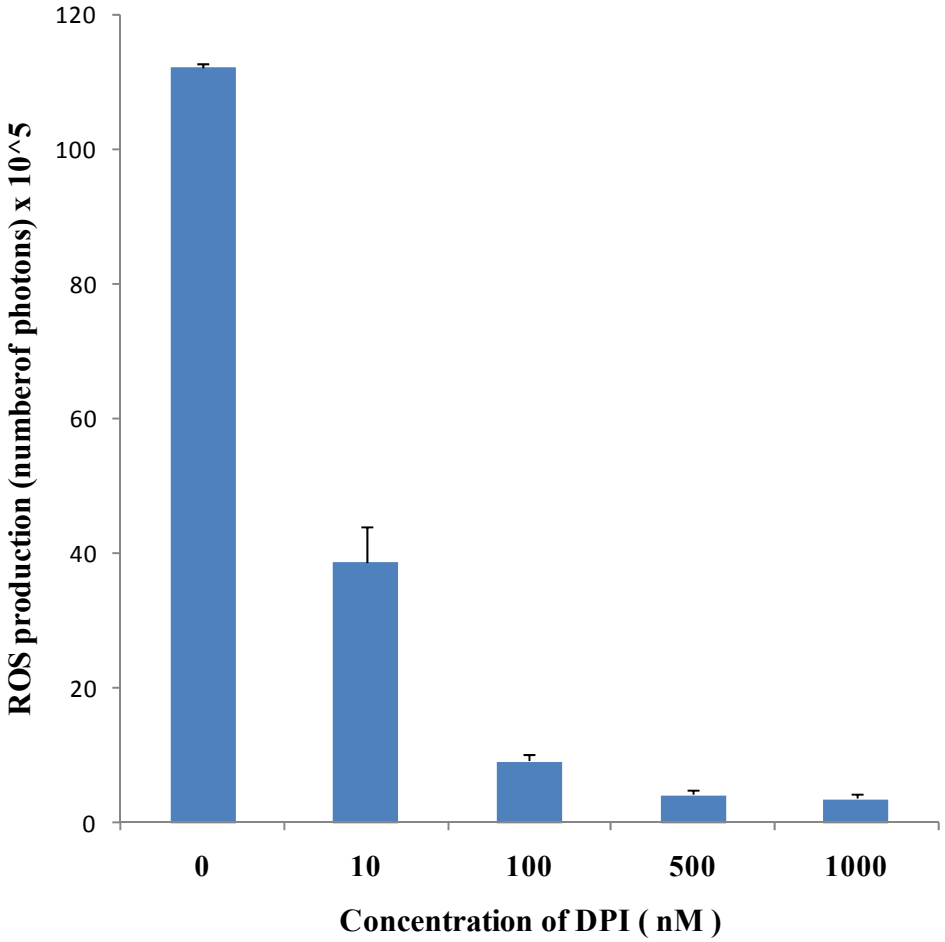

Figure 3.4 Inhibition of superoxide production in HL60 cells using DPI

HL60 cells were treated with 0 -1000 nM DPI, prior to stimulation with TPA (1000 nM), and superoxide production was assayed using Diogenes. Data represents mean± 1 SD (n=3).

3.3.2.2 Determination of the effect of 100 nM DPI on survival of mutant N-RAS transduced CD34$^+$ cells over time

In order to check that DPI at 100 nM did not affect cell viability and was not toxic to cells, cell survival assays were performed. Mutant N-RAS infected cells were incubated with 100 nM DPI for 0 - 72h followed by cell viability analysis using Annexin V and 7AAD by flow cytometry which are markers for early and late apoptosis respectively. As shown in Figure 3.5, the survival of CD34$^+$ cells was not significantly affected at any time point tested though at later time-points there was a trend to decreased cell survival compared to untreated controls. Taken together, the above data suggests that 100 nM of DPI is capable of inhibiting superoxide production in haematopoietic cells with no loss in viability up to a period of 24 hours.

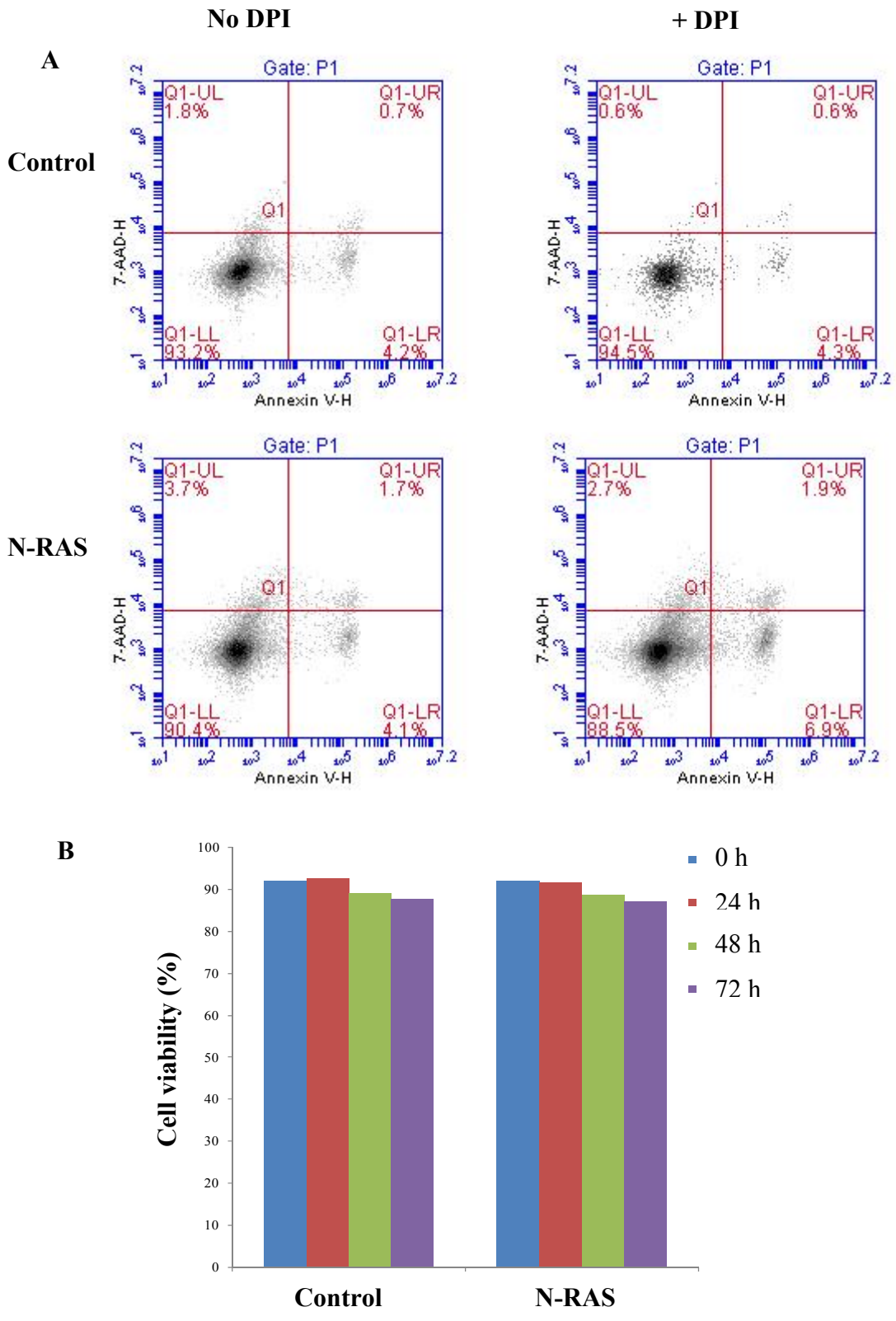

Figure 3.5 The effect of 100nM DPI on survival of mutant N-RAS transduced CD34$^+$ cells over 72 hours

N-RAS expressing cells or control cells expressing GFP alone (day 3 of culture) were incubated with 100 nM DPI for 0-72 hours followed by cell viability analysis using Annexin V and 7AAD by flow cytometry: **(A)** representative data and **(B)** summary of the overall results for both control and N-RAS. No error bars generated since n=1.

3.3.3 Optimisation of culture media conditions for the measurement of ROS directly in culture in preparation for GEP

To check whether the optimum dose of DPI in the Diogenes assay was effective in the context where the cells were harvested for microarrays it was necessary to measure ROS production directly in the cell culture medium. Three different phenol red free media formulations were investigated. As shown in Figure 3.6, medium 3 (phenol-red free media with 10% FCS and without transferrin and BME) was found to be the best medium for ROS measurement directly in culture using Diogenes probe since this showed a marked 3 fold increase in ROS production in N-RAS compared to the control whilst other media showed lower but also marked increase (2 fold and 2.5 fold for media 1 and 2 respectively).

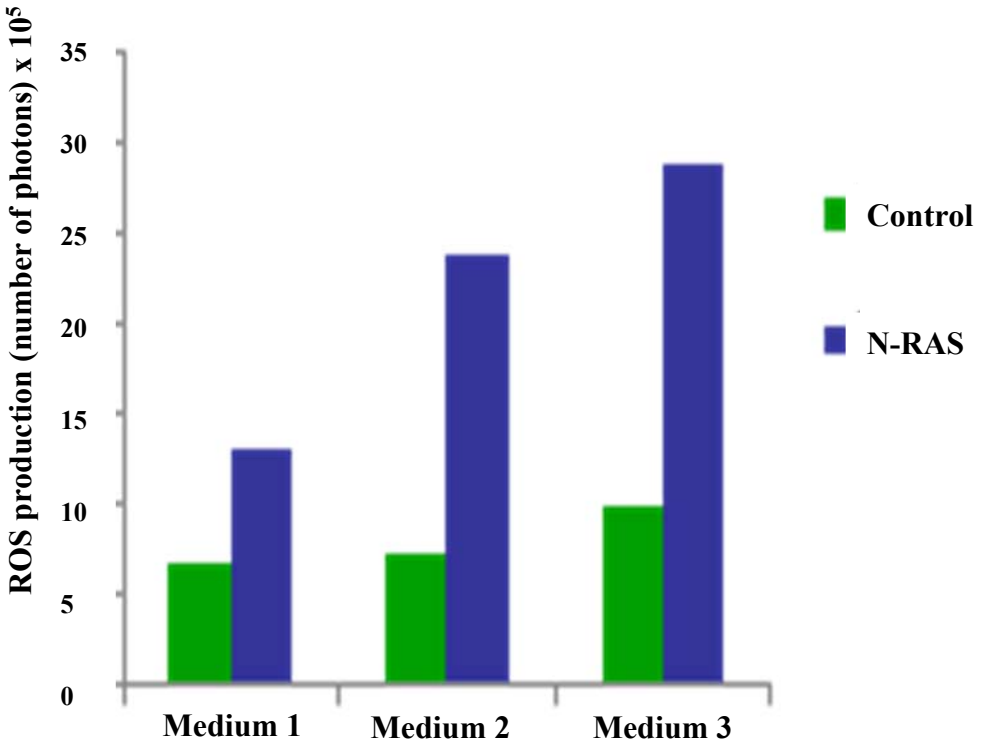

Figure 3.6 Assessment of different media for the measurement of ROS directly in culture

Diogenes chemiluminescence was measured using a luminometer directly in culture media. The graph is a representative of superoxide release by N-RAS^{G12D} expressors or control cells in 3 different phenol red free media mix (Chapter 2): Medium 1 = with transferrin, BME and 20% FCS, Medium 2 = without transferrin and BME but with 20% FCS, Medium 3 = as 2 but with 10% FCS. No error bars generated since n=1.

3.3.4 CHARACTERISATION OF CULTURES USED FOR MICROARRAY ANALYSIS

In order to confirm that human haematopoietic progenitor cells overexpressing mutant N-RAS produced elevated ROS compared to controls, chemiluminescent studies were performed using the superoxide specific probe Diogenes in the presence and absence of the 100 nM DPI. Optimised media conditions (see above) were used (medium 3). Significant 8 fold increase in superoxide production by N-RAS mutants was observed as compared to the controls (Figure 3.7). ROS (superoxide) levels were successfully and significantly inhibited by DPI (indicated by 90 % inhibition $P < 0.05$). Because DPI inhibits NOX oxidase activity, these results suggest that nearly all of the superoxide produced is derived from oxidase activity.

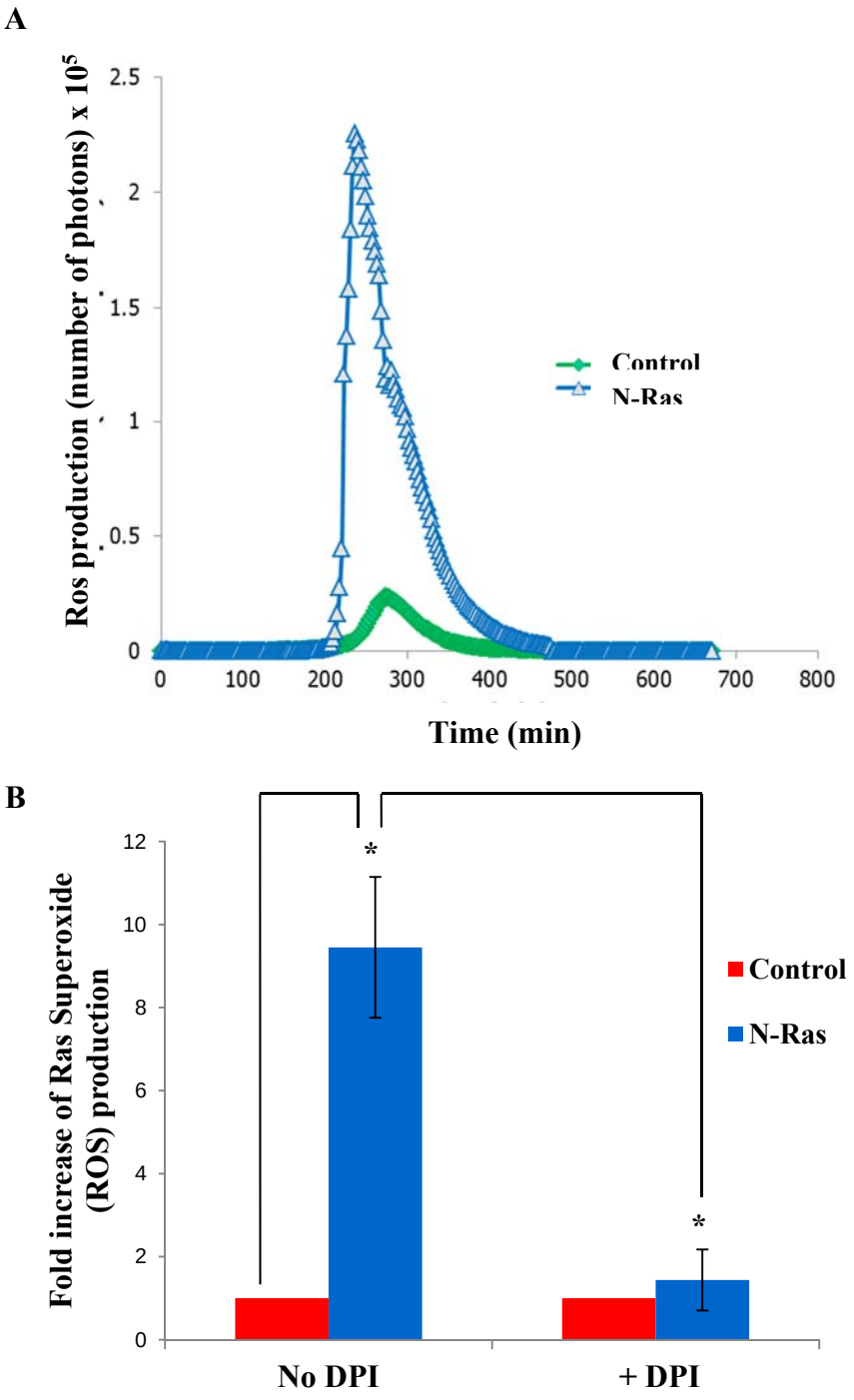

Figure 3.7 Expression of mutant N-RAS increases superoxide (ROS) production in normal human haematopoietic cells

Superoxide production was measured using Diogenes in the presence or absence of NOX family inhibitor (DPI) on day 7 of culture in medium 3. Cells were exposed to 100 nM DPI for 18 h prior to these measurements. **(A)** Representative chemiluminescence trace of superoxide production. **(B)** Summary of the overall results for both Control and N-RAS. Data represents mean ± 1SD (n=5). Statistical significance was determined by Student's t-test. * denotes statistically significant $P<0.05$.

3.3.5 RNA QUALITY AND INTEGRITY DATA

Using Trizol reagent, RNA was extracted from cell cultures described in 3.3.4 and Figure 3.7 on day 7 of culture. The quality and integrity of the RNA was assessed using the Agilent RNA 6000 Nano Kit protocol. High RNA quality and integrity (free from DNA, contaminating proteins, ethanol, phenol and salts) are required for the best microarray results. RNA sample integrity is a crucial aspect of RNA quality which is the proportion that it is full length. The mRNA is likely to be full length if the 28S and 18S rRNA bands are resolved into two descrete bands and the 28S rRNA band intensity is approximately twice the size of the 18S rRNA band which was clearly the case for all the samples tested, Figure 3.8A and B. Analysis of rRNA ratio [28S/18S] and RNA integrity number (RIN) from the bioanalyser output showed acceptable quality RNA ratio in the range 1.8-2.2 and 8.4-10 for integrity (Figure 3.8C). Therefore, the overall results suggested that all the RNA was successfully extracted and isolated with high quality and integrity for GEP and validation experiments.

A

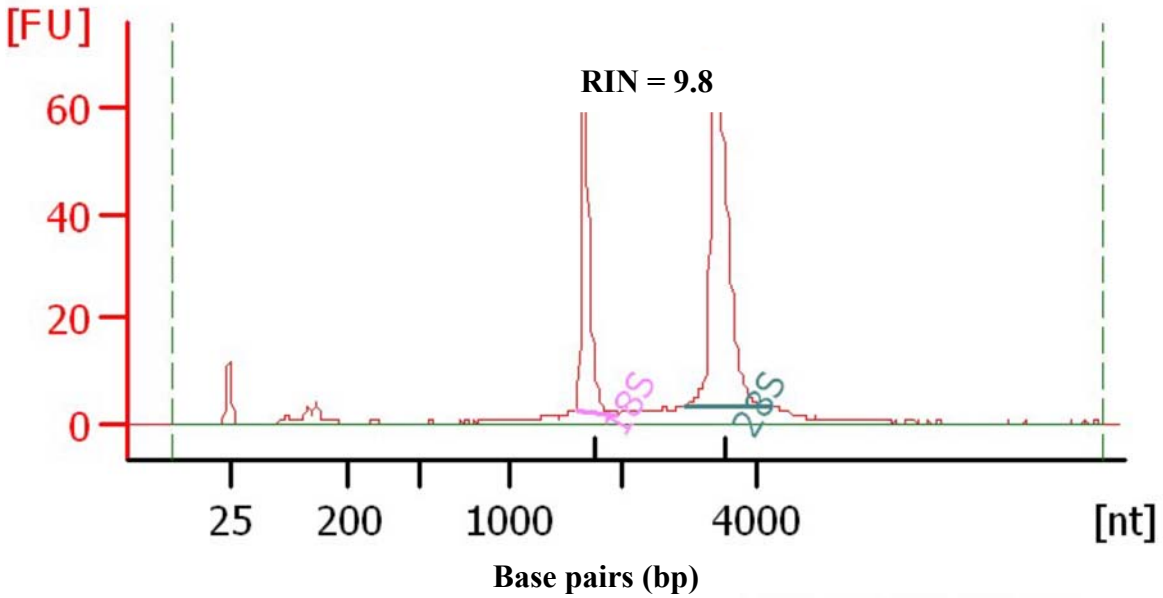
[FU]
60
40
20
0
RIN = 9.8
18S
28S
25
200
1000
4000
[nt]
Base pairs (bp)

B

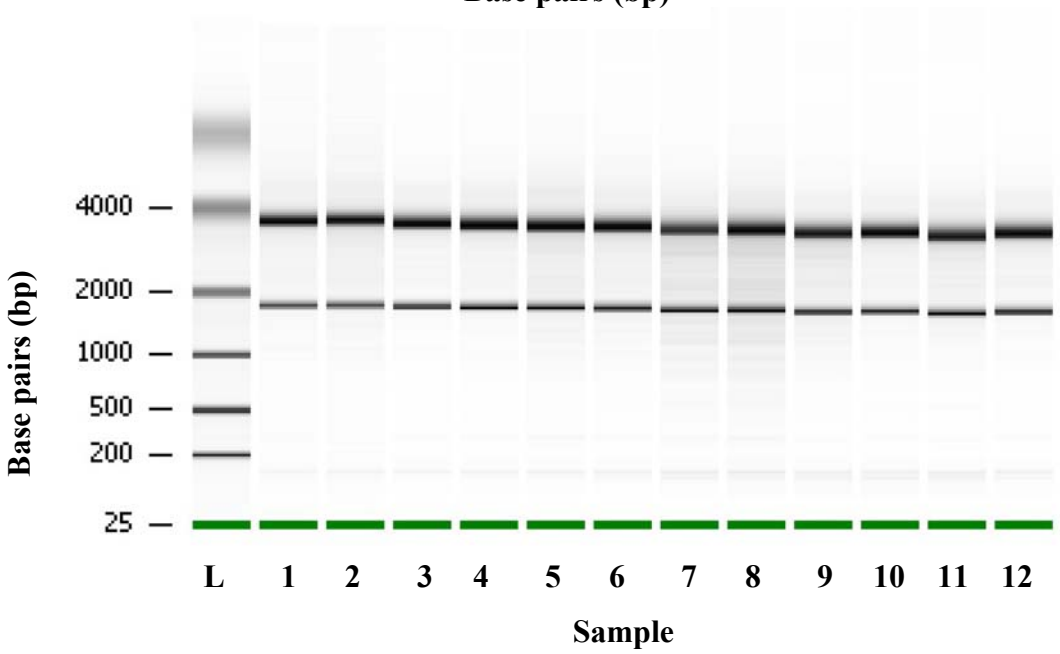
Base pairs (bp)
4000
2000
1000
500
200
25
L
1
2
3
4
5
6
7
8
9
10
11
12
Sample

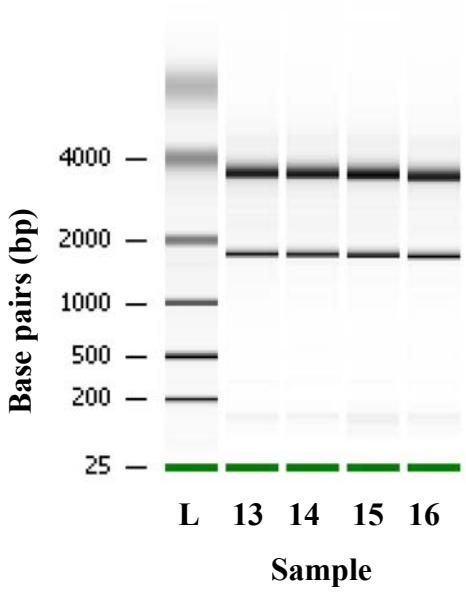
Base pairs (bp)
4000
2000
1000
500
200
25
L
13
14
15
16
Sample

C

Sample no	Details	rRNA ratio [28S/18S]	RIN
1	#1 Control,	2.0	10
2	#1 Control+DPI	1.8	10
3	#1 N-Ras	1.9	9.9
4	#1 N-Ras+DPI	2.0	9.9
5	#2 Control	2.1	9.5
6	#2 Control+DPI	1.9	9.6
7	#2 N-Ras	1.5	8.4
8	#2 N-Ras+DPI	2.2	8.9
9	#3 Control	2.2	9.4
10	#3 Control +DPI	2.0	9.8
11	#3 N-Ras	1.8	9.5
12	#3 N-Ras +DPI	2.2	9.9
13	#4 Control	1.9	9.7
14	#4 Control +DPI	1.8	9.8
15	#4 N-Ras	1.9	9.8
16	#4 N-Ras +DPI	1.8	9.8

Figure 3.8 RNA quality and integrity check

(A) Electropherogram example representing the results from the Agilent bioanalyser showing high RIN (RNA Integrity Number) indicating high integrity RNA. **(B)** Electrophoresis file run summary of successful RNA isolation from all samples tested showing the two discrete bands of 28S and 18S rRNA with former band intensity being approximately twice the size of the latter. **(C)** Summary of all RIN values which are in the range of 8.4-10 and rRNA ratios [28S/18S] range = 1.8-2.2. # indicates experimental replicate number; nt = nucleotide and L = Ladder.

3.4 DISCUSSION

A common molecular abnormality in AML and other cancers is the mutational activation of RAS observed in many AML cases (Chapter 1) and this has been linked to overproduction of ROS in several cancer models (Sallmyr *et al*., 2008). Recent studies have shown that both N-RAS and H-RAS promote ROS production via NOX and it has been shown to also promote growth factor independent proliferation by an unknown mechanism (Hole *et al*., 2010). The overall objective of this study was to determine how ROS production arising from mutationally activated RAS affects gene expression and whether this contributes to the pro-proliferative phenotype which could help in the elucidation of the mechanisms underlying ROS's contribution to leukaemogenesis. Even though both N-RAS and H-RAS have been previously shown to result in high ROS production, N-RAS^{G12D} was chosen for this study since it is the most clinically relevant. Therefore this chapter aimed to examine and confirm ROS production by human CD34^{+} haematopoietic cells expressing mutant RAS (N-RAS^{G12D}) and to optimise conditions and prepare samples for GEP microarray experiment to test whether RAS induced ROS could affect gene expression.

In this study, a model system based on normal human haematopoietic progenitor (CD34^{+}) cells was used. This model was chosen because it is well established in our lab and it is the most appropriate model to determine the effects of RAS and ROS on a normal background. To generate mutant RAS expressing cells, CD34^{+} cells were isolated from neonatal cord blood and transduced with the retroviral vector PINCO encoding full-length N-RAS^{G12D} and GFP or an empty vector control (GFP alone) as previously described (Chapter 2). Percentage GFP positivity range for the control and N-RAS samples prepared for the microarray experiments were in the range of (54-84%) and (64-82%) respectively

suggesting efficient and successful transduction. It should be noted that the overexpression of mutant RAS in this cells has previously been confirmed under the same conditions using western blotting in our lab (Hole *et al*., 2010) hence this was not done for this study.

In order to confirm that mutant RAS induced ROS production in human $CD34^+$ haematopoietic progenitor cells, chemiluminescence assays were used which had been previously optimised and validated in our lab. The inhibition of ROS production in these cells was achieved by the use of DPI, a NOX inhibitor which has also been previously shown to block superoxide production by NOX2 (Hole *et al*., 2010; O`Donnel *et al*., 1993).

Microarrays are very expensive and could be time consuming and therefore it was crucial that the optimal conditions were established prior to commencing these experiments. Firstly assays for the measurement of ROS and its inhibition by DPI were optimised and validated. The effect of different concentrations of DPI on superoxide production was investigated using HL60 cells to establish the lowest effective concentration of DPI needed to inhibit superoxide production using chemilluminescent probe, Diogenes. It was necessary to optimise DPI concentration due to its known off target effects in the cells. A concentration of 100 nM was the minimum concentration required to inhibit >90% of superoxide from mutant N-RAS infected $CD34^+$ cells. To check that this concentration of DPI did not adversely affect cell viability, DPI-treated cultures were labelled with annexin V and 7AAD. The detection of apoptosis in these cells using this assay has been previously established (Hole *et al*., 2010). Annexin V is a member of the annexin protein family which have been shown to have high avidity for a plasma-membrane phospholipid; phosphatidylserine (PS), (Van Engeland *et al*., 1998). In viable cells PS is maintained in the inner leaflet of the plasma membrane by enzymatic action of flippases. The appearance of PS on the outer leaflet however is a marker of early-intermediate stages of apoptosis (Boersma *et al*., 2005). Late stage apoptosis is

characterised by loss of membrane integrity (Wyllie, 1997) and in these cells the membrane impermeable dye, 7AAD, is able to enter cells and intercalate with DNA (Schmid *et al*., 1992), thus forming fluorescent DNA complexes (DNA/7AAD) that can be detected by flow cytometry. Therefore the incorporation of both methods enabled discrimination of early-intermediate and late stage apoptosis.

This assay confirmed that the viability of $CD34^+$ cells was not significantly affected by 100 nM DPI for 24 hours. Since longer exposure (34-72 h), showed a slight decrease in survival, an 18 hour exposure to 100 nM DPI was used as the final condition for the gene expression profiling studies.

In previous studies, ROS was measured in buffer, since culture medium components can interfere with the measurements. However, in this study it was necessary to measure ROS directly in the medium to exclude this interference and mis-interpretation of the results discussed below. Therefore this study optimised culture media conditions to measure ROS directly in culture at time of harvesting for GEP. Phenol red free media was used since this dye was interfering with the luminescence measurements. The effects of BME, transferrin and different concentrations of serum in media were checked in relation to ROS measurement sine these components might affect ROS measurements. For instance: transferrin contains iron which is likely to interfere with ROS measurement via Fenton chemistry (Chapter 1) resulting in misinterpretation of the results. In the presence of iron, superoxide and H_2O_2 react to generate hydroxyl radicals which could lead to the reduction of superoxide detectable by the chemiluminescent probe, Diogenes. This could explain lower levels (2 fold increase) of N-RAS induced ROS detected by Hole *et al*., (2010) in $CD34^+$ cells compared to higher levels detected in the current study (discussed below).

In the final optimised conditions at the time of harvest for GEP mutant, N-RAS generated a significant 8 fold increase in superoxide compared to the GFP controls

confirming the overproduction of ROS in these cells. In agreement with previous research, (Piccoli *et al*., 2007; Hole *et al*., 2010), normal human $CD34^+$ cells produced low levels of ROS (superoxide) while expression of N-RAS strongly augmented its production. Interestingly, higher levels of N-RAS induced ROS (superoxide) were observed in the current study compared to the levels reported in Hole *et al*., (2010) where ROS was measured indirectly suggesting that the indirect measurement of ROS might have underestimated the level of ROS production by these cells. DPI, a NOX inhibitor, ablated ROS production (90% inhibition) in N-RAS expressing cells suggesting the successful inhibition of ROS in these cells and that it was NOX-derived superoxide. ROS can be produced via oxidase activity (such as NOX family) or via the mitochondrial ETC (Berdad and Krausel 2007, discussed in Chapter 1). Hole *et al*., (2010) previously demonstrated that excess ROS production in these cells was derived from NOX oxidases via Diogenes probe and DPI. This is in agreement with this study and consistent with other reports of RAS-induced ROS production in a variety of cell types (Rassool *et al*., 2007; Serù *et al*., 2004; Santillo *et al*.,2001; Yang *et al*., 1999) (Chapter 1 for detail).

It was therefore concluded that ROS production in this cells was confirmed together with its inhibition making them acceptable for RNA extraction in preparation for GEP using microarrays.

RNA was extracted and isolated from cell culture models created above using Trizol reagent, purified and quantified using the optimised methods. Importantly, the quality and integrity of RNA was assessed to ensure high RNA quality and integrity for the best GEP microarray results. RNA quality and integrity is evaluated by the determination of the RNA ratio [28s/18s] and the RIN. The intensity size of 28s rRNA band was double the size of the 18 rRNA suggesting that the mRNA in all samples used in this study was full length. The RIN and rRNA ratios for all samples were found to be within the acceptable quality range of 8.4-10 and 1.8-2.2 respectively hence these results suggested

that RNA was successfully isolated and extracted. It was therefore concluded that all RNAs were of high quality and integrity thus used for GEP experiments. In addition, excess sample pellets and RNA were stored and used for the validation experiments (Chapter 4).

The experiments in this chapter have confirmed ROS overproduction and its inhibition in mutant N-RAS expressing human $CD34^+$ haematopoietic cells by direct measurement of ROS in cell culture. GEP data was also generated and analysis of this data is discussed in the next chapter.

4 Transcriptional dysregulation mediated by ROS in normal human haematopoietic progenitor cells expressing mutant N-RAS^{G12D}

The previous chapter confirmed ROS overproduction and its inhibition in mutant N-RAS expressing human CD34^{+} haematopoietic cells by direct measurement of ROS in cell culture. The main purpose of this chapter is to identify the transcriptional targets of mutant RAS and determine the contribution of RAS-induced ROS production on gene expression. This study expressed N-RAS^{G12D} in normal human haematopoietic CD34^{+} cells (Chapter 3). Using this model, cells were also treated with DPI, an inhibitor to NOX2, to determine the ROS related gene expression changes. Affymetrix microarray GEP was used to quantitate changes in mRNA gene expression. GeneChip® Human Exon 1.0ST array data were imported into and analysed using Partek Genomics Suite Software (Version 6.6; Partek Inc., MO, USA). Genego Metacore ™ software was used for the pathway and network functional analysis. A summary of the data import, processing and analysis strategy is outlined in the method section (Figure 4.1A and B).

4.1 AIMS

- Analyze microarray GEP data obtained from Chapter 3 using Partek Genomic Suite software and determine N-RAS and ROS related gene changes;

- Validate gene changes observed from microarray results using flow cytometry, and western blot methods.

4.2 METHODS

All equipment and reagents used were purchased from Affymetrix, UK Limited unless otherwise stated. GEP is a technique that measures multiple gene expression in cells, using a number of genes arrayed onto glass slides or membranes (GeneChips®) and probed with fluorescent-labelled cDNAs (Affymetrix: online) (discussed in Chapter 1). In this study, the Affymetrix Genechip whole transcriptome (WT) microarray approach was used. GeneChip® Human Exon 1.0^{ST} arrays were used where the probes on the arrays have been selected and distributed throughout the entire length of each transcript (full description, principles and illustrative figures are in 1.6). In summary, probes on different exons are summarized into an expression value of all transcripts from the same gene enabling gene level expression analysis.

4.2.1 MICROARRAY DATA IMPORT, NORMALISATION AND QUALITY CONTROL

4.2.1.1 Microarray data import and normalisation

RNA from transduced cultures were extracted and processed for hybridisation to GeneChip® Human Exon 1.0^{ST} Array for whole-transcript expression analysis and GEP data was generated as previously described (Chapter 3). All GEP data were analysed using Partek Genomics Suite (GS) Software (Version 6.6; Partek Inc., MO, USA) (See Figure 4.1A and B for summary of the analysis strategy). For Partek analysis CEL files were imported using Affymetrix annotation files (NetAffx, Version hg16, build 34, July 2003). GEP Exon-level data were filtered to include only those probe sets that are in the "core" meta-probe list which refers to probe sets that are supported by the most reliable evidence from RefSeq and full-length mRNA GenBank records containing complete CDS information. The core data include target-sequence, perfect-match, unique probe sets. The Robust Multi-Array Analysis (RMA) algorithm was used for Exon-level expression

analysis. Adjustments were made for GC content and probe sequence on pre-background-subtracted values. Background correction, quantile normalization, $\log_2$ transformation, and median polishing were used for summarization.

4.2.1.2 Quality controls

Several quality controls spikes were included during the microarray experiments in order to facilitate data quality assessment at different stages of the microarray experiments. This was done as in accordance to the manufacturer's instructions and recommendations. These included the hybridization controls such as bac_spike which is a set of probesets which hybridize to the pre-labelled bacterial spike controls (BioB, BioC, BioD and Cre) and are useful in identifying problems with the hybridization and chip, polya_spike which is the set of polyadenylated RNA spikes (Lys, Phe,Thr and Dap) which are helpful in identifying problems with the target preparation phase of the experiment. All these spikes were added at different concentrations as recommended by the manufacturer.

Following the successful completion of the import of CEL files, post import quality control (QC) spreadsheet which summarized the intensity values of the Affymetrix control probesets was generated together with the graphical representations of the probe-sets values. This was done using the QC metrics of the QA/QC section of the Partek workflow which provides quality control information from control and experimental probes on the Genechips® in order to provide confidence in the quality of the microarray data and to identify samples that do not meet the QC criteria as detailed by the manufacturer. All the image plots generated were inspected visually for any artefacts.

4.2.2 MICROARRAY DATA ANALYSIS

The Affymetrix GEP data is available as supplemental material on the attached CD. A two-arm approach was applied in order to identify statistically differentially regulated

genes. Firstly, statistically significant changing genes were identified using a 2-way ANOVA based on the following model; $Y_{ijk} = \mu + Condition_i + Cord\ blood\ replicate_j + \varepsilon_{ijk}$. Where Y_{ijk} represents the k^{th} observation on the i^{th} Condition j^{th} Cord blood replicate; μ is the common effect for the whole experiment; ε^{ijk} represents the random error present in the k^{th} observation on the i^{th} Condition j^{th} Cord blood replicate. The errors ε^{ijk} are assumed to be normally and independently distributed with mean 0 and standard deviation δ for all measurements. Cord blood replicate is a random effect and Condition represents experimental treatment e.g. mutant N-RAS^{G12D}. Fisher's Least Significant Difference (LSD) was performed for the following contrasts i) mutant N-RAS^{G12D} *vs* controls (GFP alone) or (ii) N-RAS^{G12D} *vs* N-RAS^{G12D}+DPI or iii) GFP alone *vs* GFP alone +DPI (Figure 4.1B). Where possible the Benjamini-Hochberg multiple testing correction was applied to both these strategies, otherwise the level of significance was reduced to $P<0.01$. Secondly, statistically significant genes were filtered to remove all genes that changed by less than 1.2-fold in each of the contrasts above. To identify mutant N-RAS^{G12D} gene changes that are mediated via ROS, the gene lists generated above were combined in a Venn diagram (Figure 4.6) to identify biological and statistically significant gene changes according to Figure 4.1B. No significant gene changes were observed for the control+DPI vs control hence was excluded from the Venn diagram.

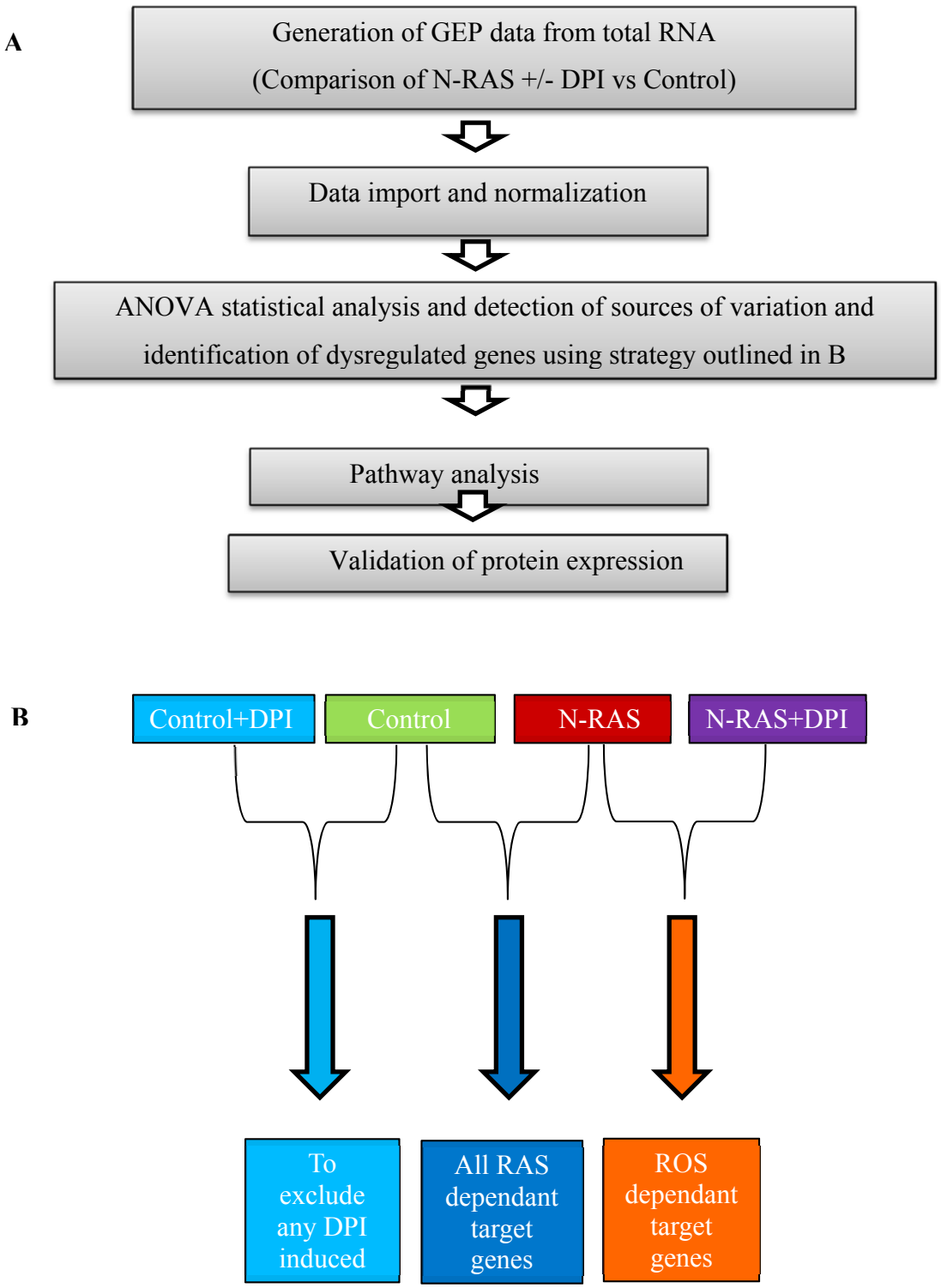

Figure 4.1 Strategy for the identification of the N-RAS^{G12D} genes changes that are mediated by ROS.

(A) is the summary of the overall experimental strategy used in this chapter and **(B)** is an outline of the specific comparisons made between treatment conditions for the determination of ROS specific genes.

4.2.3 GENEGO METACORE PATHWAY ANALYSIS

Partek GS ANOVA output (microarray gene list B) was imported into Genego Metacore ™ software (GeneGo Inc) for pathway analysis and the establishment of both direct and indirect interactions/networks between significant differentially expressed ROS target genes. This analysis also facilitates the identification and ranking of pathways and information/knowledge (including the subcellular localization) relating to the target genes. Metacore is an integrated software suite based on high-quality, manually-curated database of transcription factors, receptors, ligands, kinases, species-specific directional interactions between protein-protein-DNA, protein-RNA interactions, drug targeting, bioactive molecules and their effects with wide literature support for validity and ease reference (Metacore data-mining and pathway analysis: online). This software is therefore industry leading in reliability, accuracy and comprehensiveness hence suitable for the analysis of microarray data obtained in this study.

4.2.4 VALIDATION OF GENE CHANGES /PROTEIN EXPRESSION

4.2.4.1 Validation of protein expression using flow cytometry

The general method performed is described in Chapter 2, variations and specific details can be found in the results section (4.3.4.1).

4.2.4.2 Validation of protein expression using Western Blotting

The general method performed is described in chapter 2, variations and specific details can be found in the results section (4.3.4.2).

4.2.5 INVESTIGATION OF THE EFFECT OF GOX ON THE EXPRESSION OF ROS TARGET GENES

The general method performed is described in Hole *et al*., (2013) and Chapter 2 for treatment of cells with Glucose oxidase (GOX) and western blotting respectively. Variations and specific details can be found in the results section (4.3.5). This was done to further validate whether ROS related genes identified above (Table 4.1) were ROS responsive since ROS (in the form of H_2O_2) was generated in cultures of these cells by the addition of glucose oxidase (GOX).

4.3 RESULTS

4.3.1 MICROARRAY DATA, QC, IMPORT AND NORMALIZATION

4.3.1.1 QC assessment and Microarray Data

Prior to data analysis, a number of QC checks were performed. Only 'high quality' data (defined as data showing no indication of features that could skew or otherwise lead to data misinterpretation) were allowed to be used in subsequent analysis. In order to do this, a number of quality controls spikes (bac_and polyadenylated RNA spikes) were previously included during the microarray experiments as described in 4.2.1.2. This was also done to identify outlier arrays within the data set before the data analysis. Firstly, the raw GEP data of each sample/chip was inspected visually. As shown in Figure 4.2, the raw data were uniformly distributed with no artefacts suggesting that the GEP chip processed was of good quality and this applied to all images of all samples tested.

Secondly, to validate adequate hybridization of labelled cDNA to the GeneChip®, each GEP was analysed for increasing signal intensity of the control spikes as described in 4.2.1.2. The results of the QC data indicated that hybridization controls had signal increases following the order BioB< BioC<BioD < Cre (Figure 4.3A) and the labelling controls (RNA spikes) signal strengths followed the order Lys< Phe<Thr a< Dap (Figure 4.3 B) as expected. Signal box plots were examined for both pre and post RMA normalization and the results showed no outliers in all the 16 samples tested (Figure 4.3 C) and these data also suggested effective normalization.

The overall observations suggested successful hybridization and all the 16 samples had met the QC criteria. Thus at this stage the microarray data from all the Genechips were considered of high quality.

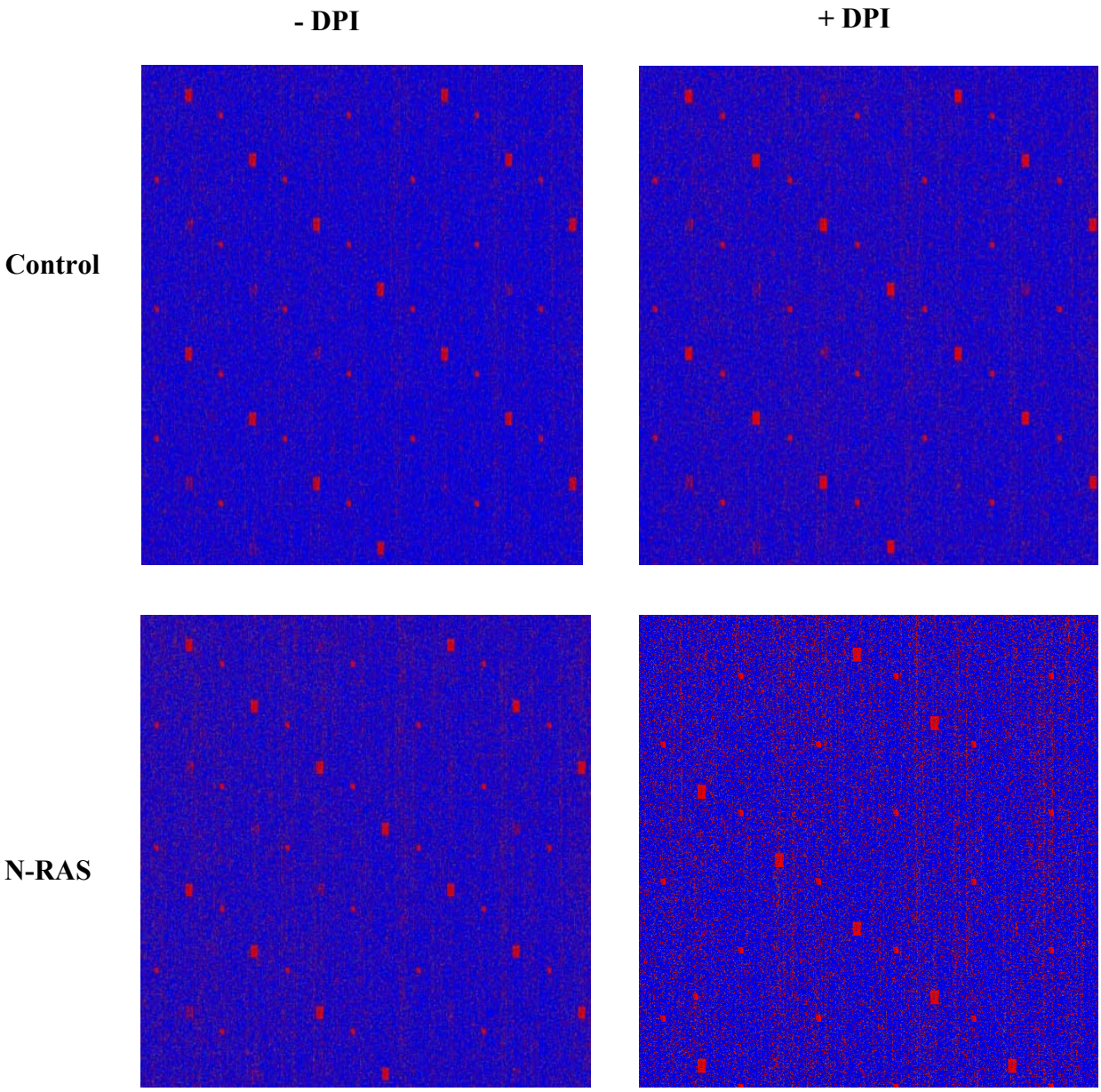

Figure 4.2 Example images of microarray data

Microarray experiments were performed using GeneChip® Human Exon 1.0ST arrays and the raw data images were generated and visualized using Partek GS software. Four independent replicate experiments were performed for both N-RAS and control with and without (+/-) DPI. Example data for visualisation from one replicate of the N-RAS and control samples +/- DPI are shown. All images were of excellent quality with no artefacts.

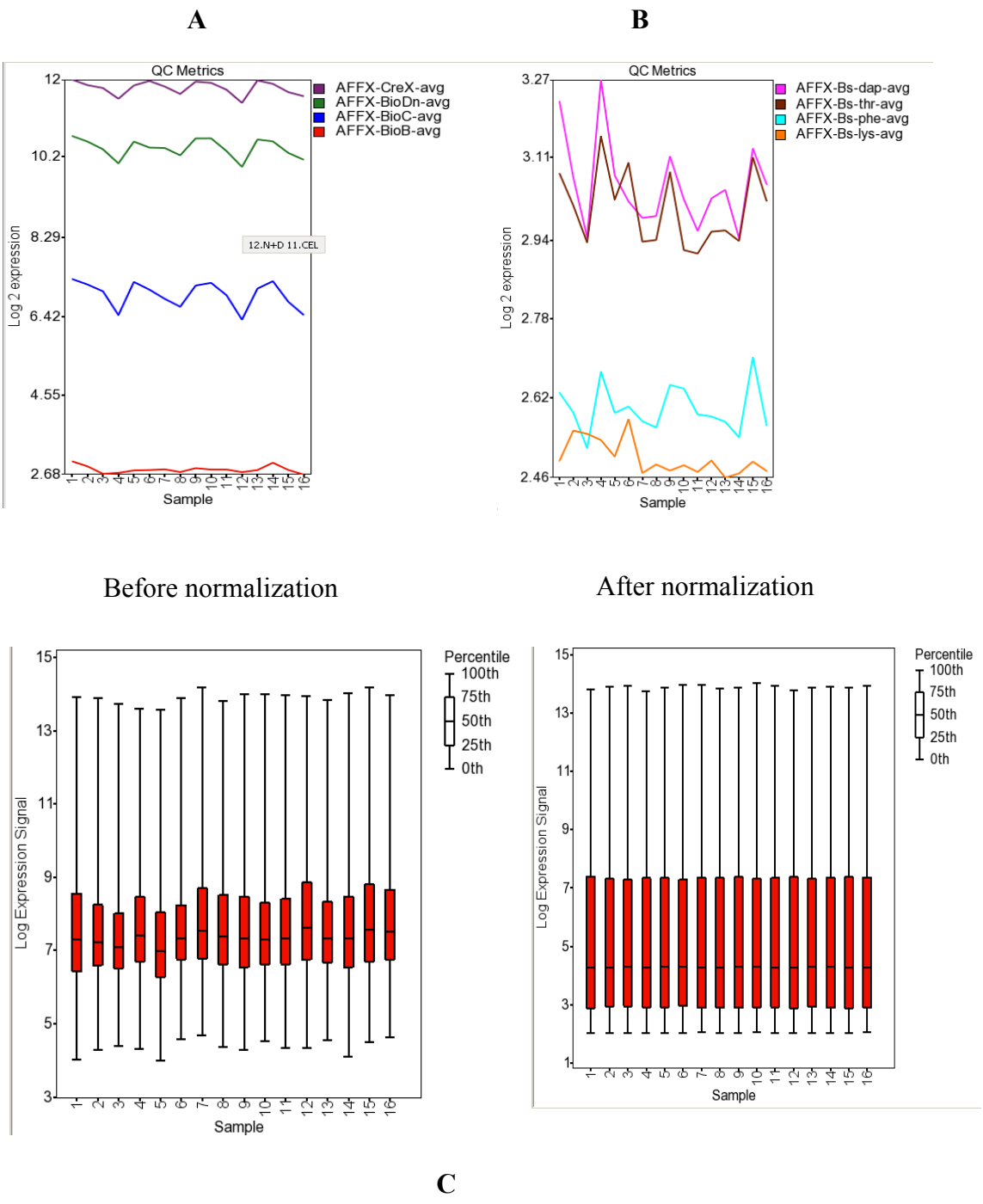

Figure 4.3 Post import QC and microarray data for quality assessment of the Exon arrays

QC graphs showing: **(A)** Log expression signal from all the samples tested for the hybridization control spikes which showed signal increases following the order BioB< BioC<BioD < Cre; **(B)** Labelling control (RNA spikes) signal strengths followed the order Lys < Phe < Thr < Dap **(C)** box plot of log expression signal from each of the 16 samples/ Genechips before and after RMA normalization indicating effective normalization.

4.3.1.2 Exploratory data analysis using Principal Components Analysis (PCA)

In order to visualize data, preliminary data analysis was performed using PCA (Figure 4.4). This was useful in identifying any outliers and major effects of samples, replicates and treatment conditions in the data and thus allowing the establishment of factors that are important in subsequent statistical analysis. As shown in Figure 4.4, the GEP of a chip groups with other data according to replicate (individual cord blood) than it does due to the sample treatment condition. These results suggested that the variation in expression of genes within individual cord bloods is driving the grouping of the samples. Therefore replicate (cord blood source) and sample treatment condition were included in the model of ANOVA selected for statistical analysis.

4.3.1.3 Generation of the statistical model used for data analysis

In order to generate the appropriate statistical model for the data analysis, sources of variation plots were generated using Partek GS to detect and visualize the factors relevant to the data obtained. The results indicated that the main sources of variation in this study were replicate (individual cord blood) and the sample treatment condition, (Figure 4.5). It is important to note that batch was not a factor tested since all samples were arrayed at once. In conclusion, replicate and sample were the two important factors relevant to the statistical data analysis in order to determine differences based on sample treatment. ANOVA 2 way analysis was therefore selected and used as a statistical model for results analysis. This model took into account both sources of variation established, replicate and sample treatment to control for the biological variation.

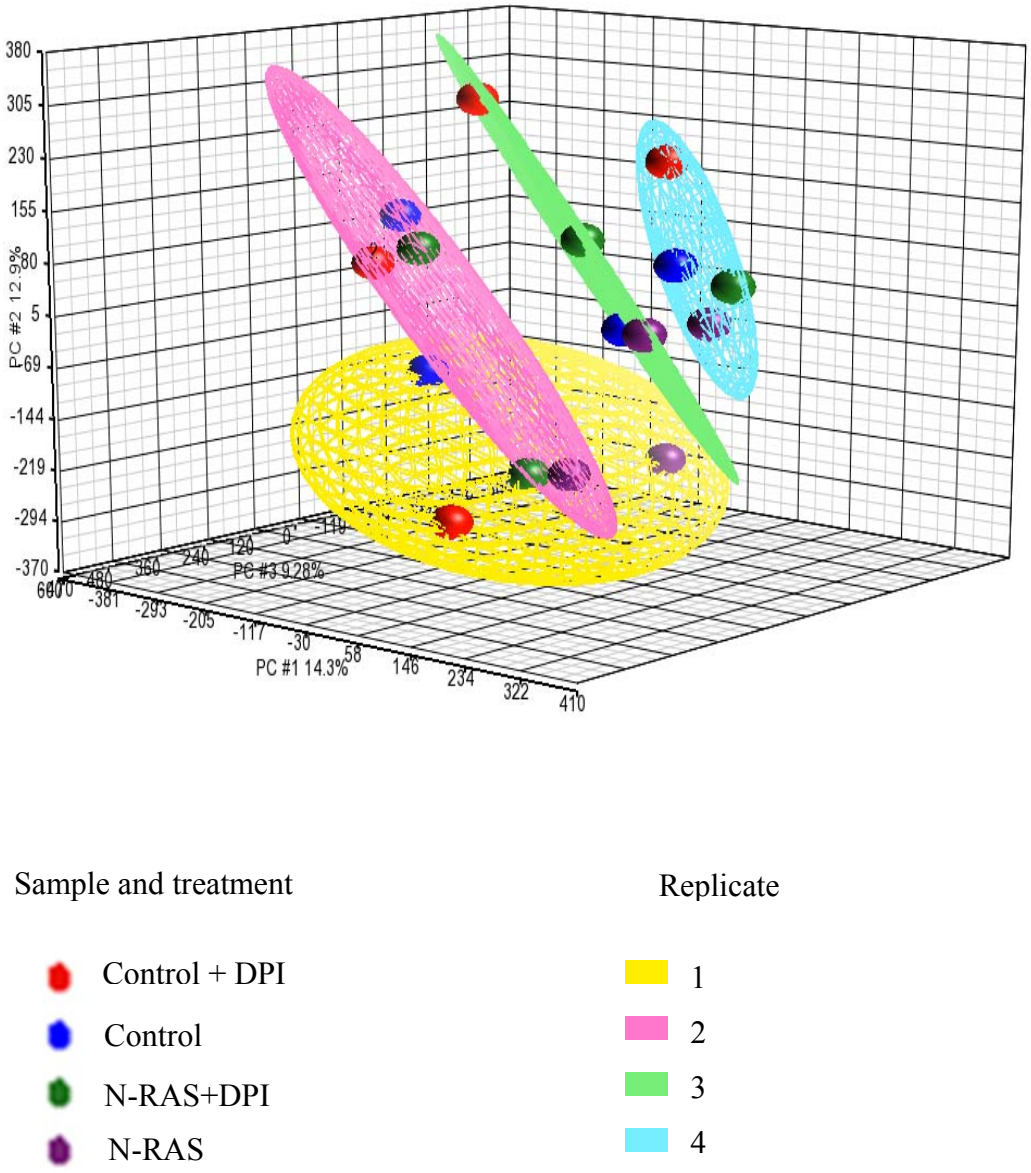

Figure 4.4 Microarray data was visualized using PCA scatter plots

Gene expression data from each sample/GeneChip are represented by coloured dots according to the legend. The coloured ellipsoids represent individual cord blood samples (or replicates) transduced with retroviral vectors and treated with or without DPI. For each replicate of the experiment, different cord blood was used and four replicates were performed per treatment condition (i.e. n=4).

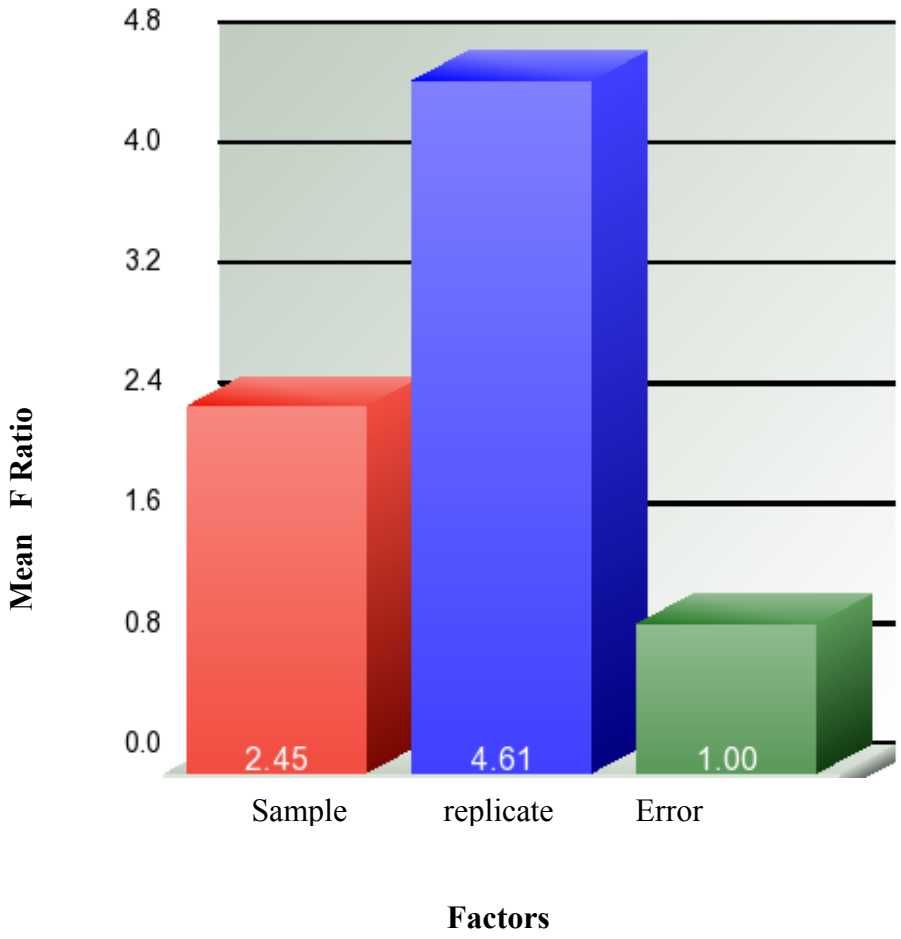

Figure 4.5 Main sources of variation

Bar graph generated from the microarray data showing that the main factors influencing the results were sample treatment condition (sample) and replicate (individual cord blood) indicated by mean F ratios.

4.3.1.4 Visualization of the direction of gene changes due to ROS using dot plots

Dot plots were generated for each of the mutant N-RAS^{G12D} gene changes that are mediated via ROS (from gene list B generated in Figure 4.6) using Partek GS for the determination and visualization of gene changes due to ROS (Figure 4.7). The results of all the dot plots were examined and the summary of the direction of gene change due to ROS was tabulated (Table 4.1). The patterns of gene expression levels in different treatment conditions were as expected with the highest expression levels in the presence of ROS and lowest leves in the absence of ROS in N-RAS cells compared to the control confirming that these genes were indeed up-regulated by ROS.

4.3.2 DETERMINATION OF GENES DYSREGULATED BY N-RAS^{G12D} AND ROS

ANOVA 2 way analysis was used to determine the differentially expressed genes between the categories described in 4.2.2 and Figure 3.1B. Lists of genes that passed the specified criteria (4.2.2) were generated for each comparison in order to identify genes that are dysregulated by N-RAS^{G12D} and ROS. According to the results, 342 gene changes were found in the control alone relative to N-RAS^{G12D} alone with FDR<0.05 (gene list C), 68 gene changes were found in the N-RAS^{G12D} alone relative to N-RAS^{G12D} + DPI with FDR<0.05 (gene list A) and no significant gene changes were found in the control + DPI relative to control alone with FDR<0.05 (Please refer to the CD for the gene lists). The lists of these differentially expressed genes were intersected using Venn diagrams as previously described (4.2.2) to identify mutant N-RAS^{G12D} significant gene changes mediated by ROS (Figure 4.6). The results showed that 25 genes (gene list B) were common between gene list A (N-RAS^{G12D} alone relative to N-RAS^{G12D} + DPI) and gene list C (control alone relative to N-RAS^{G12D} alone) suggesting that 25 mutant N-RAS^{G12D} significant gene changes were mediated via ROS (Figure 4.6 and Table 4.1).

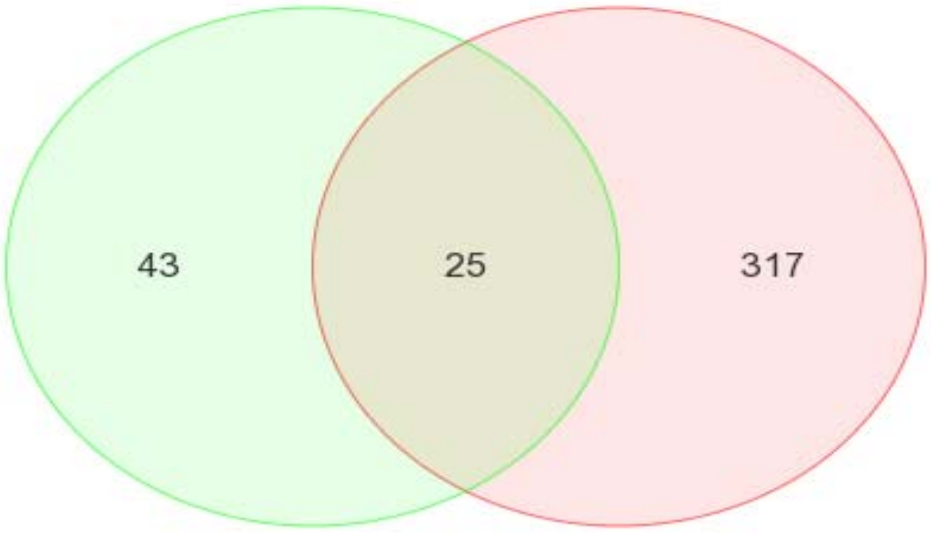

Genelist A (68) Genelist B (25) Genelist C (342)

Figure 4.6 Dysregulated gene changes in cells expressing mutant RAS

The gene lists used in this figure were generated using the statistical model already described and the lists were intersected using Venn diagrams in Partek. This figure shows number of gene changes in gene list A (N-RAS^{G12D} alone relative to N-RAS^{G12D} + DPI) and gene list C (control alone relative to N-RAS^{G12D} alone). Gene lists A and C were intersected and N-RAS^{G12D} gene changes that are mediated via ROS (gene list B) are tabulated below (Table 4.1) No gene changes were detected in control alone relative to control + DPI hence no Venn diagram shown for this comparison.

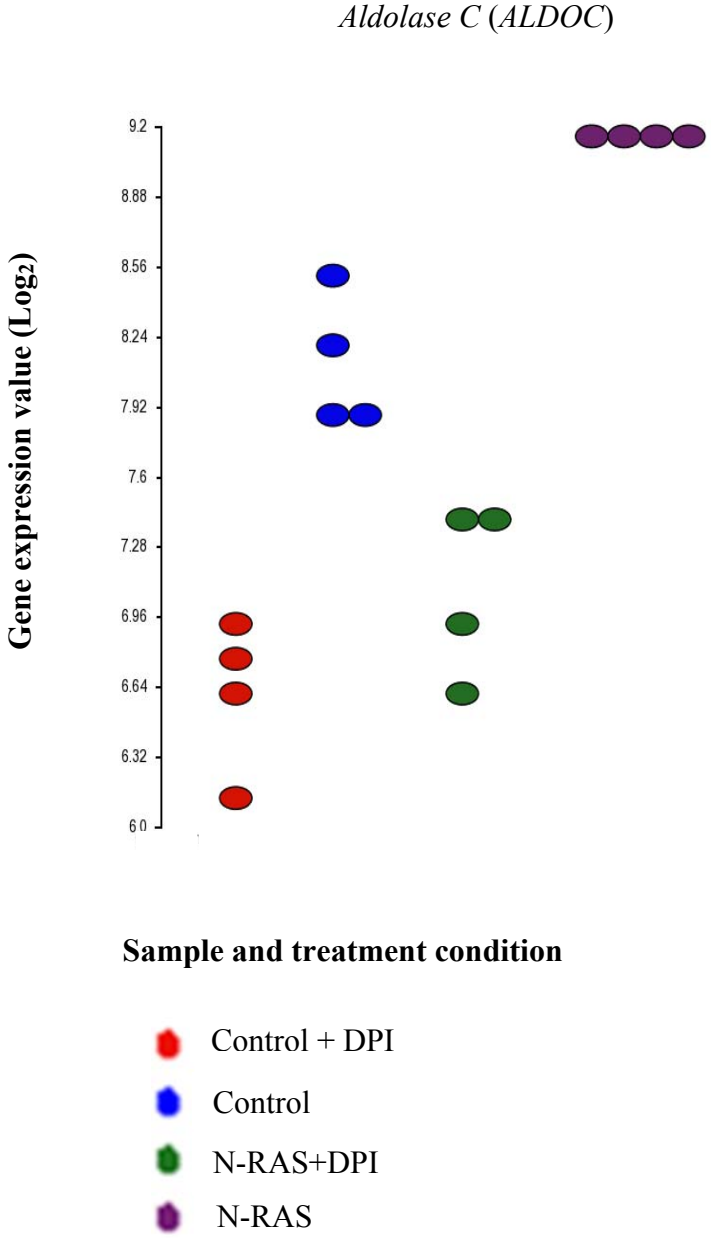

Figure 4.7 Example dot plot of the mutant N-RAS^{G12D} gene changes that are mediated via ROS

The Y-axis represents the normalised gene expression value (log_2); the X-axis represents the different sample treatment conditions and replicate data for each condition. For each treatment condition n=4. This plot shows example data for one gene (*ALDOC*) found to be dysregulated by ROS. Other images are in appendix 1. The above results demonstrate the different gene expression values associated with the sample conditions tested.

4.3.2.1 Mutant N-RAS^{G12D} gene changes that are mediated via ROS.

The number of mutant N-RAS^{G12D} gene changes that are mediated via ROS was found to be 25 (Figure 4.6). However one transcript did not have the gene assignment reducing the number to 24. Table 4.1 summarises all ROS target genes identified together with some important literature for the selection of target genes for further tests and validation experiments. The results indicated that the expression of 4 mutant N-RAS^{G12D} genes were significantly down regulated by the presence of ROS with a fold change range of 1.2-3.6 fold and 20 mutant N-RAS^{G12D} genes were significantly up-regulated by the presence of ROS with a fold change range of 1.2-4.3 fold. All the p-values of these genes were in the range of 2.26×10^{-7}-1.32×10^{-4} indicating very strong significance. ROS significantly dysregulated the expression of genes involved in several pathways such as the glycolytic, metabolism and signal transduction.These results suggested that the presence of ROS can result in the significant down or up-regulation of genes.

Gene	Affymetrix ID	RefSeq	Gene expression (fold and direction of change)	p-value	Process
ALDOC	3750767	NM_005165	+4.3	1×10^{-6}	
ENO2	3403015	NM_001975	+2.6	1×10^{-4}	
FBP1	3215570	NM_000507	+1.8	2×10^{-7}	Glycolysis
GPI	3829687	NM_000175	+1.5	2×10^{-6}	
PFKP	3232349	NM_002627	+1.4	9×10^{-6}	
GATM	3622386	NM_001482	+2.8	3×10^{-5}	
SULF2	3908358	NM_018837	+2.1	2×10^{-5}	Metabolism
CKB	3580769	NM_001823	+2.1	7×10^{-5}	
ASPH	3137530	NM_004318	+1.4	1×10^{-4}	
PTPRD	3198346	NM_002839	+2.2	2×10^{-5}	
KIT	2727587	NM_000222	-2.1	5×10^{-5}	
CD32	2363808	NM_001190828	+1.5	7×10^{-5}	
TNS1	2599153	NM_022648	+1.7	8×10^{-6}	Signal
REC8	3529725	NM_001048205	+1.4	6×10^{-5}	transduction
STARD8	3980078	NM_001142503	+1.4	3×10^{-5}	
CMTM8	2615892	NM_178868	-1.2	1×10^{-4}	
CNR2	4044363	NM_001841	-3.6	2×10^{-6}	
CD34	2453307	NM_001773	+1.7	4×10^{-5}	
CITED1	4012178	NM_001144885	+1.7	6×10^{-5}	
CYTL1	2758870	NM_018659	-1.9	6×10^{-6}	
CACNB1	3755580	NM_199247	+1.3	1×10^{-4}	Other
SLC6A8	3995804	NM_0005629	+1.7	1×10^{-5}	
JAKMIP2	2880361	NM_014790	+1.2	3×10^{-5}	
WDR54	2489228	NM_032118	+1.8	5×10^{-6}	

Table 4.1 Mutant N-RAS^{G12D} gene changes that are mediated via ROS

This table shows the ROS target genes identified (gene list B), Unique Affymetrix identifier (ID) and NM Reference sequence (RefSeq), fold and direction of gene change due to ROS (- = down regulated + = up regulated by ROS), p-value and important literature search outcomes for each gene including the description of their functions based on the Human Protein Reference database (Prasad *et al*., 2009). It was generated using the fold changes from the ANOVA microarray output results of gene list B. These genes were obtained by the intersection of the gene list A and C (Figure 4.6). The gene lists used to generate this list are provided in the CD. One transcript did not have a gene assignment. It should be noted that further information about the roles of the genes is in the Discussion (Section 4.4).

4.3.3 GENEGO METACORE PATHWAY ANALYSIS

The Partek GS ANOVA output (fold differences) of the data from gene list B Table 4.1 was imported into Genego Metacore™ software for pathway analysis and network visualization of significant mutant N-RAS^{G12D} gene changes that are mediated via ROS. As shown in Figure 4.8, a biological interaction network of the genes in question was determined. Many of the dysregulated ROS target genes identified are enzymes associated with metabolism, particularly the glycolytic pathway which confirmed the findings in Table 4.1. These include *ALDOC*, *ENO2*, *FPBP1*, *GPI*, and *PFK-1*. A common feature of these targets is that they seem to be linked to the transcription factors: SP1 and ESR (Figure 4.8). Other ROS target genes identified were associated with signal transduction and transcription. Taken together, these results and the findings in Table 4.1 suggest that N-RAS induced ROS changes gene expression of enzymes associated with transcription, signal transduction and metabolism; particularly glycolysis.

4.3.4 CONFIRMATION OF DYSREGULATED GENE EXPRESSION IN HUMAN CD34$^+$ HAEMATOPOIETIC CELLS EXPRESSING MUTANT RAS

The above GEP data analysis identified 25 target genes that are mediated via ROS production. In order to confirm the gene changes observed at protein level, western blotting or flow cytometry was performed in primary cells (detail in individual sections). The main factors considered for the selection of targets for validation experiments were: level of fold change due to ROS (high induction with ROS), availability of reagents and outcome of literature search (e.g.: novel or significant in terms of ROS or role in leukaemia). Using these criteria *CD117*, *CD34*, *CD32*, *CITED*, *ENO2*, *ALDOC*, *PTPRD, GATM* and *CNR2* were selected for validation.

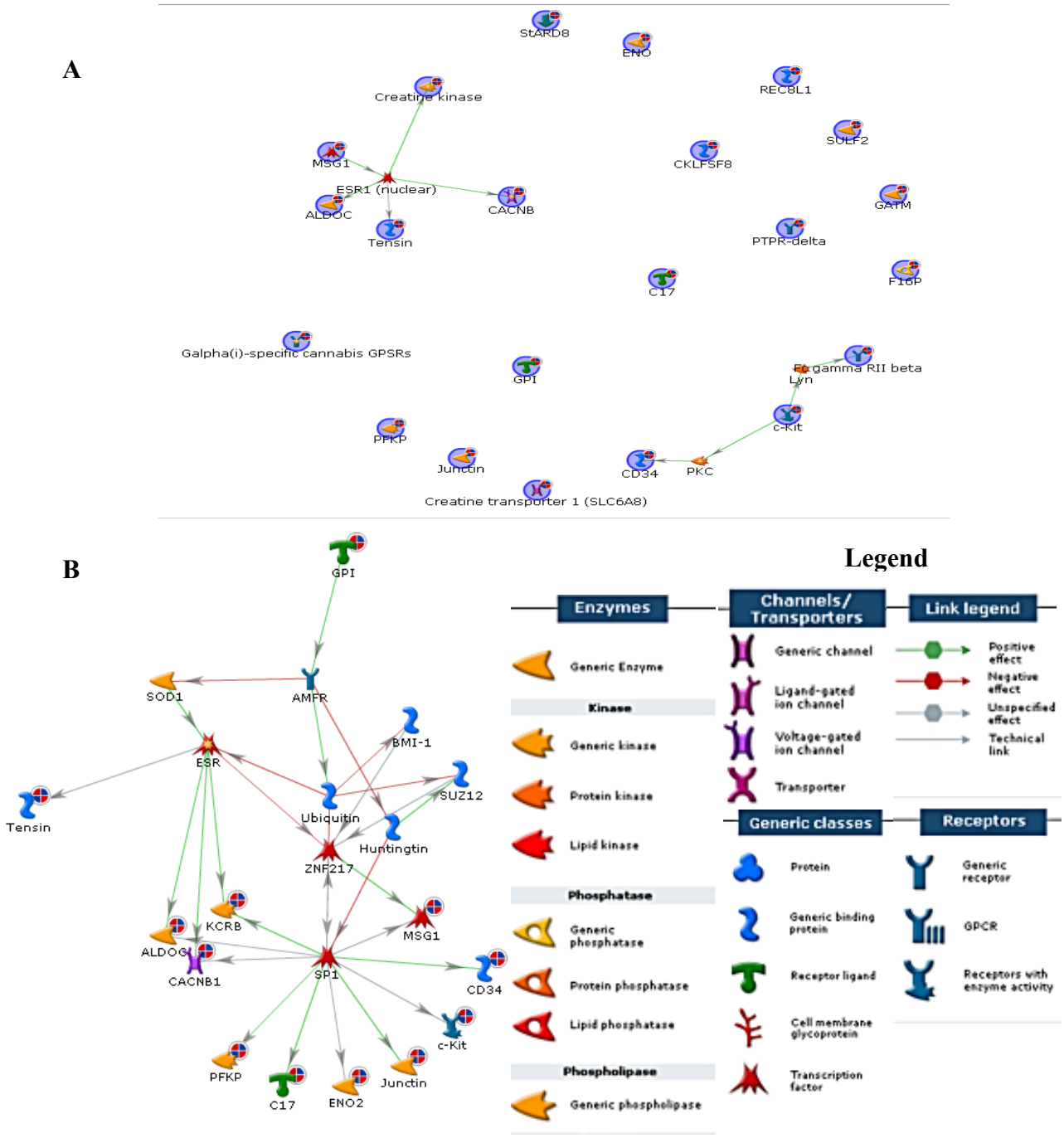

Figure 4.8 Functional and network analysis of mutant N-RAS^{G12D} gene changes that are mediated via ROS

Representation of the **(A)** direct and **(B)** indirect interactions/network between mutant N-RAS^{G12D} gene changes that are mediated via ROS. Data were generated using Genego Metacore ^{TM} as described in 4.2.3 and 4.3.3.

4.3.4.1 Flow cytometric results

In order to establish whether the changes at RNA level observed from the microarray data were also seen at protein level, flow cytometric analysis of the ROS targets *CD117*, *CD34* and *CD32* was performed in control and N-RAS^{G12D} expressing cells in the presence and absence of the inhibitor, DPI (as described in Chapter 2 and Figure 4.9). These ROS induced genes were selected for validation by flow cytometry because they showed high induction with ROS (with fold change range of 1.5-2.1 using microarray GEP), the reagents were readily available and were targets novel in terms of ROS and AML biology (Table 4.1).

The results of the histograms indicated that there is enhanced protein expression and differences between the isotype control and the test flow cytometric signals for most of the proteins. However the expression of these proteins is not influenced by RAS or DPI except for CD117 which does conform to a similar pattern to the array data (Figure 4.9 and Figure 4.10). These fold changes were measured from a very low background expression of the protein so the interpretation of this data should be treated with caution thus difficult to be confident with these data. Figure 4.10 compares the flow cytometric data and the previously obtained microarray results. It was concluded that the expression of these target genes at protein level was not validated.

(A) CD32

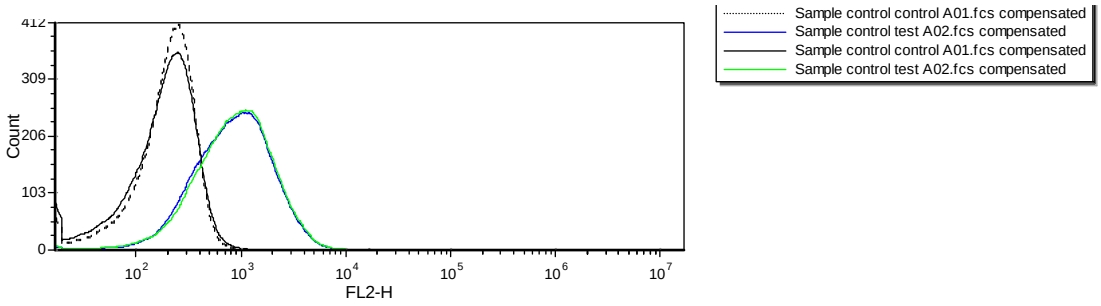
Sample control control A01.fcs compensated
Sample control test A02.fcs compensated
Sample control control A01.fcs compensated
Sample control test A02.fcs compensated
Count
FL2-H

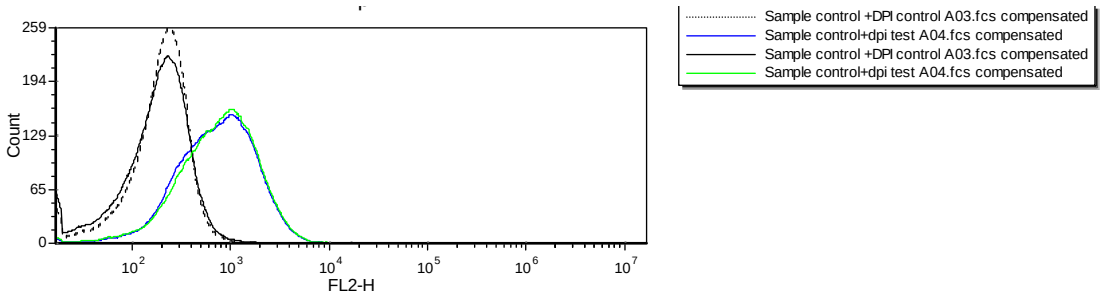
Sample control +DPI control A03.fcs compensated
Sample control+dpi test A04.fcs compensated
Sample control +DPI control A03.fcs compensated
Sample control+dpi test A04.fcs compensated
Count
FL2-H

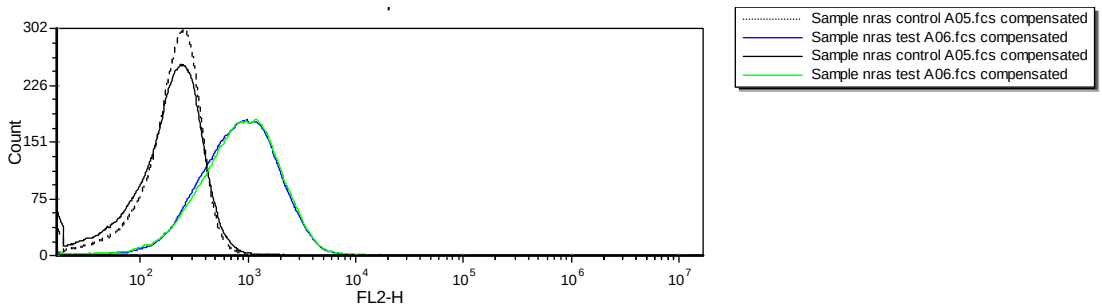
Sample nras control A05.fcs compensated
Sample nras test A06.fcs compensated
Sample nras control A05.fcs compensated
Sample nras test A06.fcs compensated
Count
FL2-H

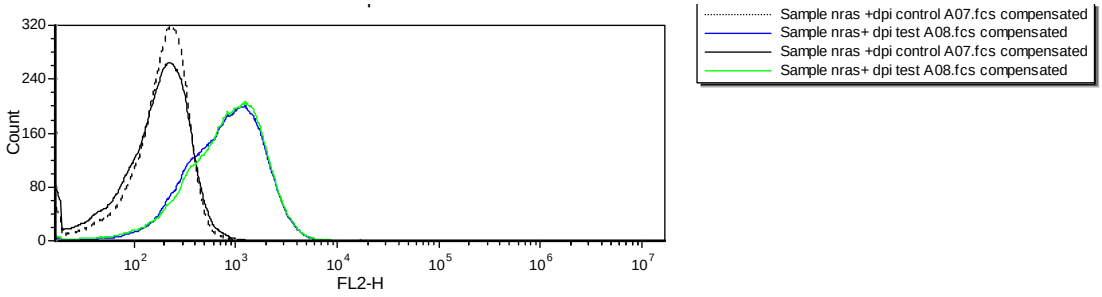
Sample nras +dpi control A07.fcs compensated
Sample nras+ dpi test A08.fcs compensated
Sample nras +dpi control A07.fcs compensated
Sample nras+ dpi test A08.fcs compensated
Count
FL2-H

(B) CD34

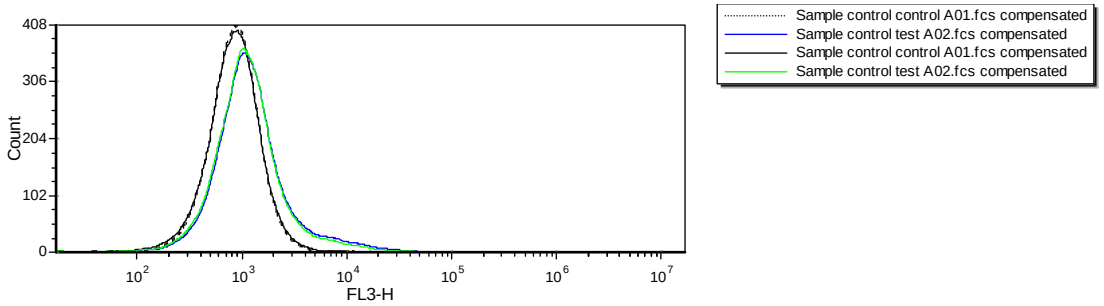
Sample control control A01.fcs compensated
Sample control test A02.fcs compensated
Sample control control A01.fcs compensated
Sample control test A02.fcs compensated
Count
FL3-H

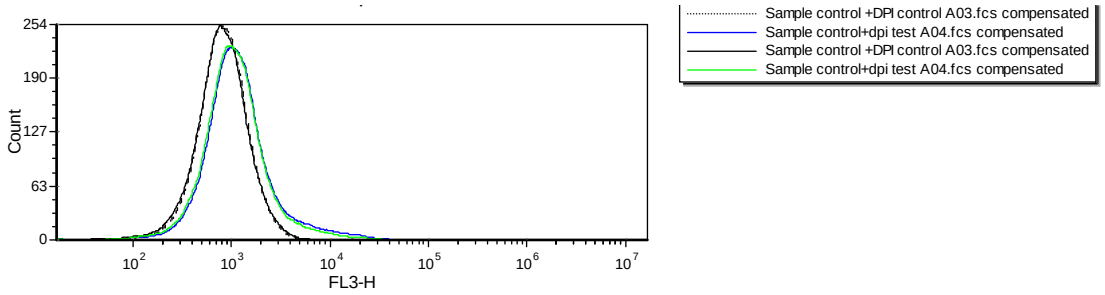
Sample control +DPI control A03.fcs compensated
Sample control+dpi test A04.fcs compensated
Sample control +DPI control A03.fcs compensated
Sample control+dpi test A04.fcs compensated
Count
FL3-H

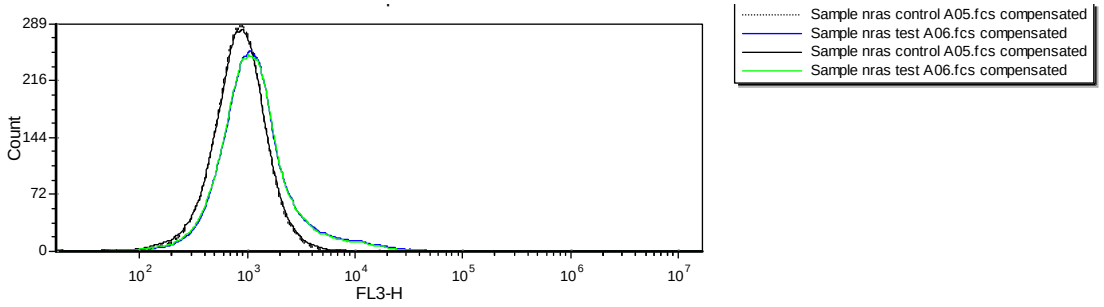
Sample nras control A05.fcs compensated
Sample nras test A06.fcs compensated
Sample nras control A05.fcs compensated
Sample nras test A06.fcs compensated
Count
FL3-H

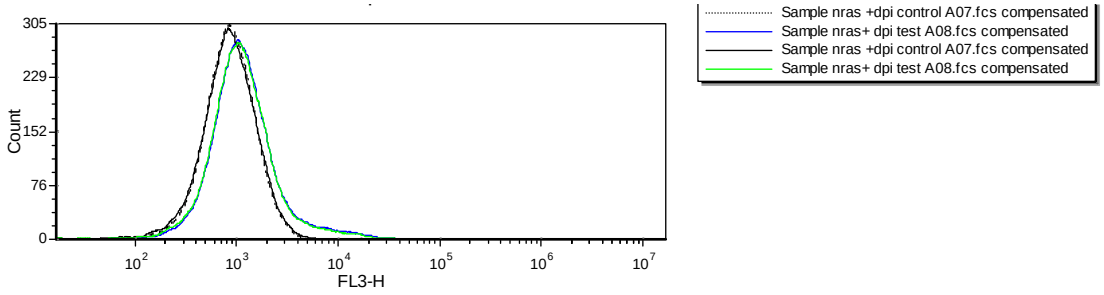
Sample nras +dpi control A07.fcs compensated
Sample nras+ dpi test A08.fcs compensated
Sample nras +dpi control A07.fcs compensated
Sample nras+ dpi test A08.fcs compensated
Count
FL3-H

(C) CD117

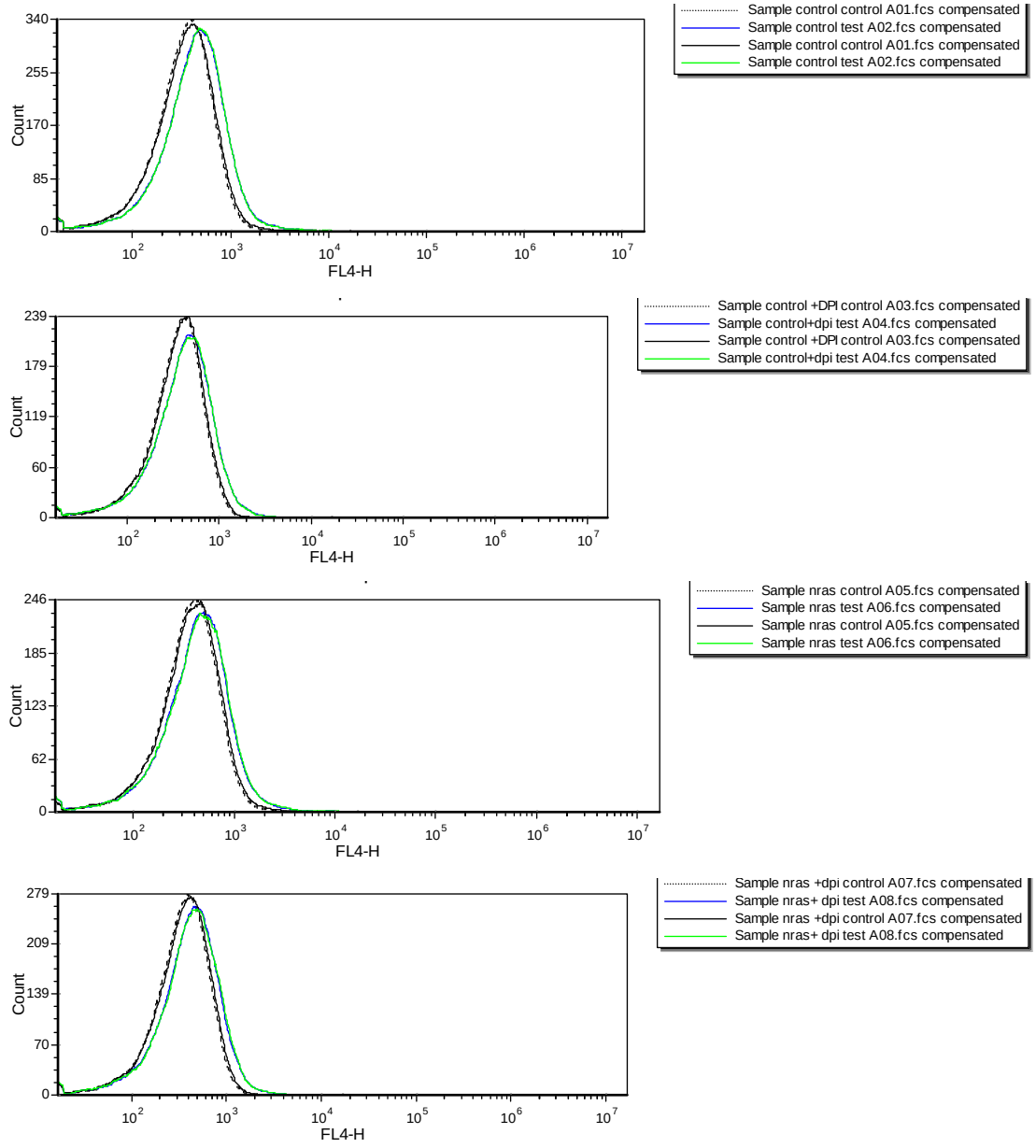

Figure 4.9 Histograms of the flow cytometric signal for target genes CD32, CD34 and CD117

N-RAS^{G12D} expressing or control CD34^{+}cells expressing GFP alone (isolated and transduced as described in chapter 2) were incubated with and without 100 nM DPI on day 6 of culture, followed by flow cytometric analysis and generation of histograms for (A) CD32; (B) CD34 and (C) CD117 protein expression on day 7. Appropriate antibodies and isotype controls were used (see Chapter 2 Table 2.3 for antibody details). n = 2

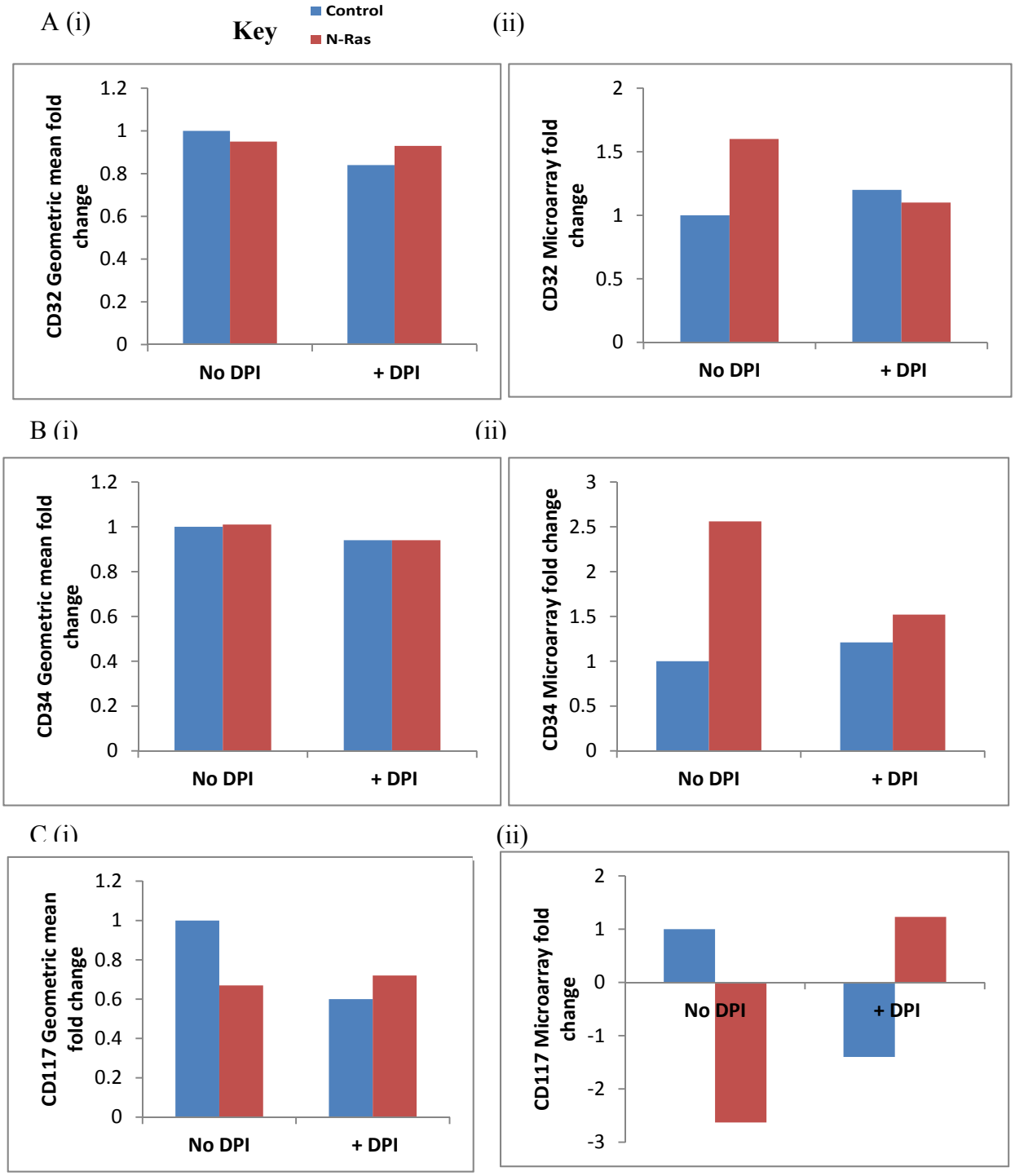

Figure 4.10 Comparison between the flow cytometric data and microarray data

The bar chats above are comparisons between (i) the flow cytometric data and (ii) microarray data for **(A)** CD32, **(B)** CD34 and **(C)** CD117 ROS target genes. Flow cytometric data = fold changes of targets levels in control and N-RAS +/-DPI calculated from the geometric means of GFP positive cells. Geometric means were obtained for each target gene from the above histograms (Figure 4.9) and the actual geometric mean signal was calculated using the formula, net geometric mean –background signal = actual signal for only GFP positive cells. Fold changes were calculated from the actual geometric signal. No error bars generated since n=1. Microarray data = fold changes for the ROS target genes obtained from the microarray data via Partek GS (Table 4.1).

4.3.4.2 Western blotting results for the validation of protein expression

Protein changes were also investigated using western blotting and performed in control and N-RAS^{G12D} expressing CD34^{+} cells in the presence and absence of DPI (as described in Chapter 2 and Figure 4.11) in order to check whether the changes seen at RNA levels were present at protein level. Six ROS target genes showing a fold change range of 1.7-4.3 using microarray (Table 4.1) were assessed by western: CITED-1, ENO2, ALDOC, PTPRD, GATM and CNR2. PKC phosphorylation is responsive to changes in the redox stress environment and was used as a control to show the effect of RAS-induced ROS and the effect of inhibition of ROS by DPI.

The results indicate that ROS induced strong protein expression signals of ALDOC (2-3 fold) and PTPRD (2.5 Fold), CITED-1 (1.5-2 fold), ENO2 (1.2 fold) and GATM (2.5 fold) in N-RAS^{G12D} expressing CD34^{+} cells compared N-RAS + DPI (no ROS) (Figure 4.11). These results were in agreement with the microarray GEP. Also consistent with the microarray data it was found that, N-RAS induced higher protein expression signals compared to the control while there was no difference in the expression signal intensities between the control and control + DPI (Figure 4.11). CNR2 was not validated since there were no bands observed with regards to its protein expression even though the control band was present (data not shown). In summary, out of the 6 targets tested, 5 were validated at protein level.

4.3.5 H_2O_2 PROMOTES THE EXPRESSION OF ROS TARGET GENES

Expressions of CITED-1, ENO2, ALDOC, PTPRD were examined further to determine whether their expression was directly promoted by ROS. These experiments employed KG-1 AML cell line as well as primary cells (CD34^{+}). ROS (in the form of H_2O_2) was generated in cultures of these cells by the addition of glucose oxidase (GOX).

The expression of these proteins was subsequently investigated using western blotting as described in Chapter 2. As above, phosphorylation of PKC was included as a positive control for ROS exposure. Phosphorylation of both these proteins was induced in KG-1 and $CD34^+$ cells treated with GOX (Figure 4.12). Direct exposure to ROS induced both ALDOC, and PTPRD in both KG-1 and $CD34^+$ cells. ENO2 was induced in KG-1 cells only and CITED-1 in $CD34^+$ cells only (Figure 4.12). Removal of GOX-derived by addition of catalase lowered protein expression but only in samples harvested after 3h. This may indicate that the amount of catalase added was insufficient to remove all the H_2O_2 during overnight culture and the PKC and $p38^{MAPK}$ phosphorylation data support this interpretation.

In conclusion all four ROS targets genes tested were directly ROS responsive in at least one context.

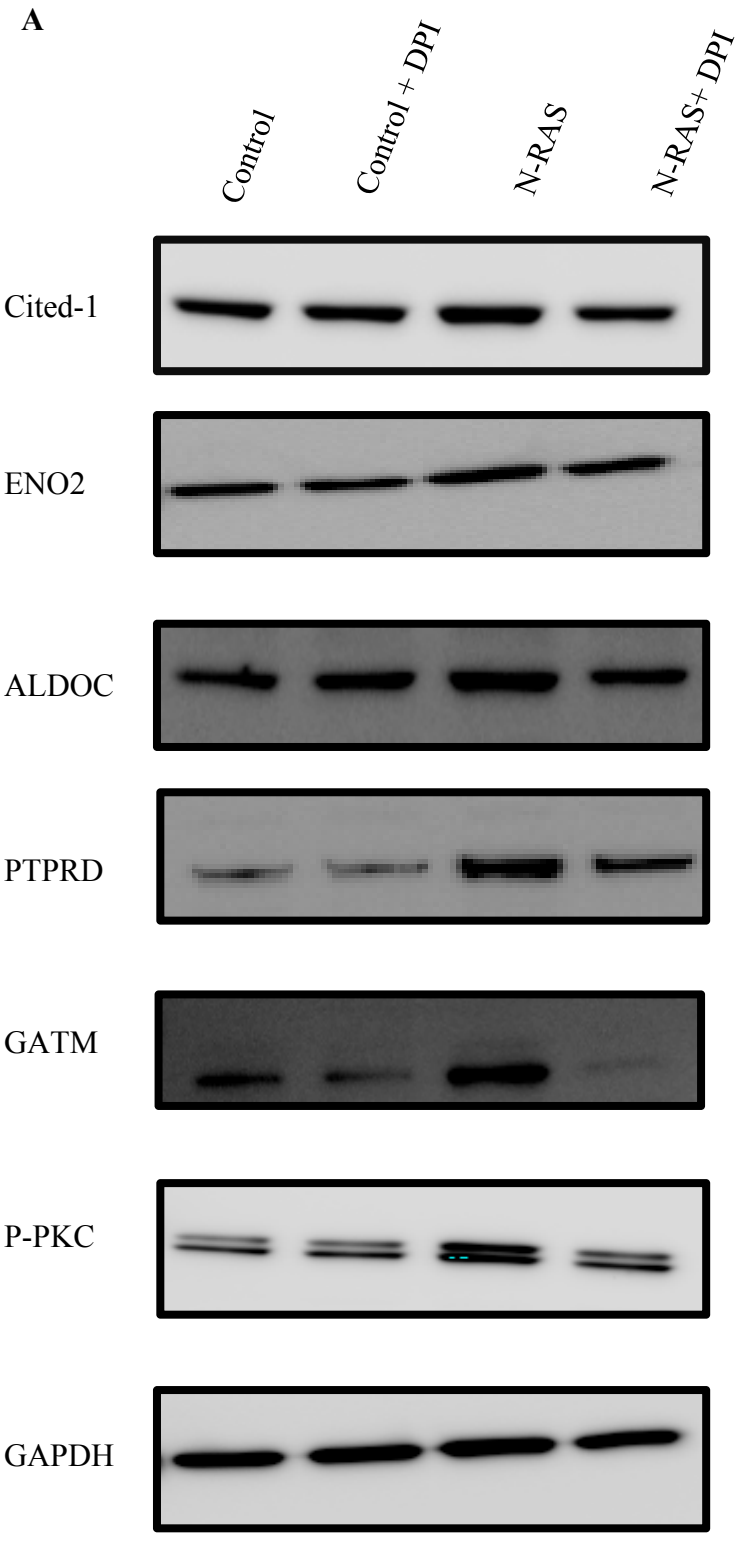
A
Control
Control + DPI
N-RAS
N-RAS+ DPI
Cited-1
ENO2
ALDOC
PTPRD
GATM
P-PKC
GAPDH

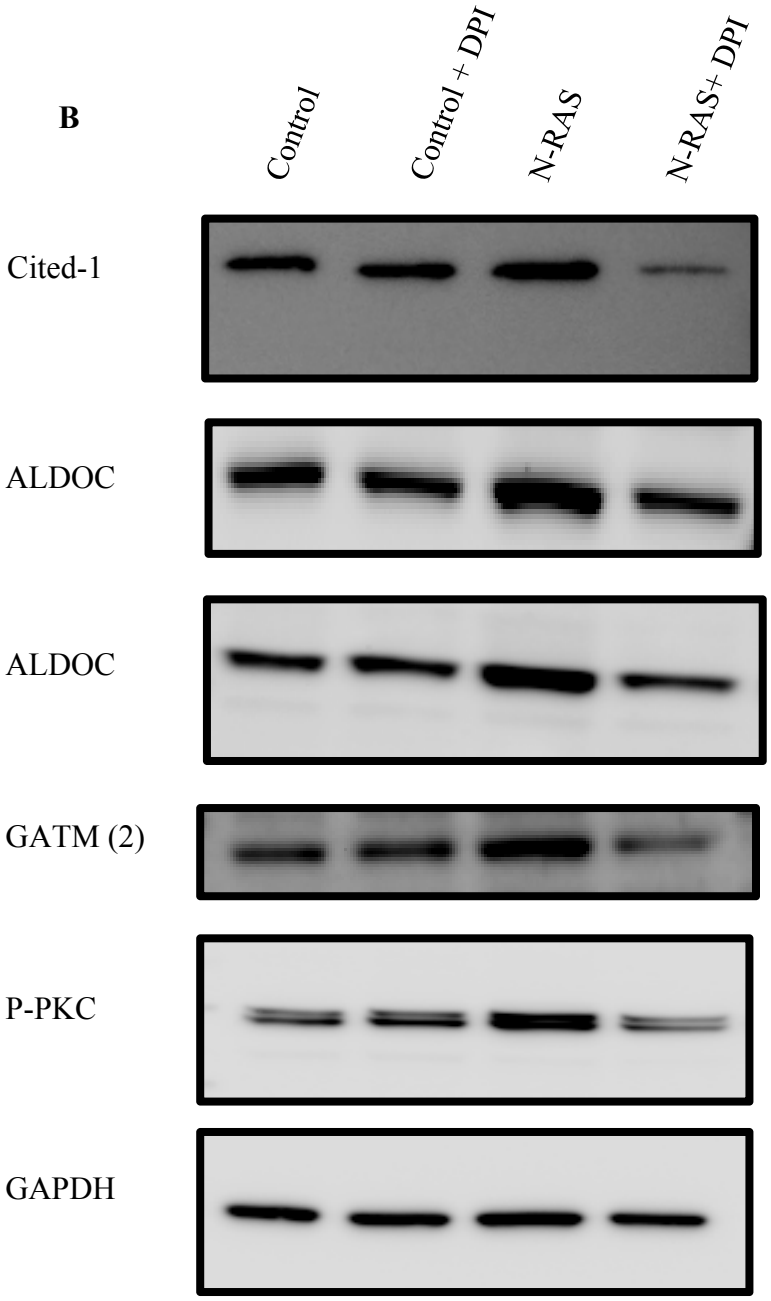

Figure 4.11 Assessment of ROS target protein expression

N-RAS^{G12D} expressing or control CD34^{+}cells expressing GFP alone (isolated and transduced as described in chapter 2) were incubated with and without 100 nM DPI on day 6 of culture. Whole cell protein extracts were prepared on day 7 of culture as described in chapter 2 and western blot analysis was performed as described in chapter 2 using (1 µg/ml) anti-ALDOC, CITED-1, GATM, PTPRD, ENO2, CNR2 and (2.9 ng/ml) P-PKC antibodies. 20 ng/ml anti-GAPDH antibody was used as a loading control. Results are representative of at least 2 independent experiments **(A)** replicate 1 and **(B)** replicate 2 including a different/alternative antibody for ALDOC and GATM.

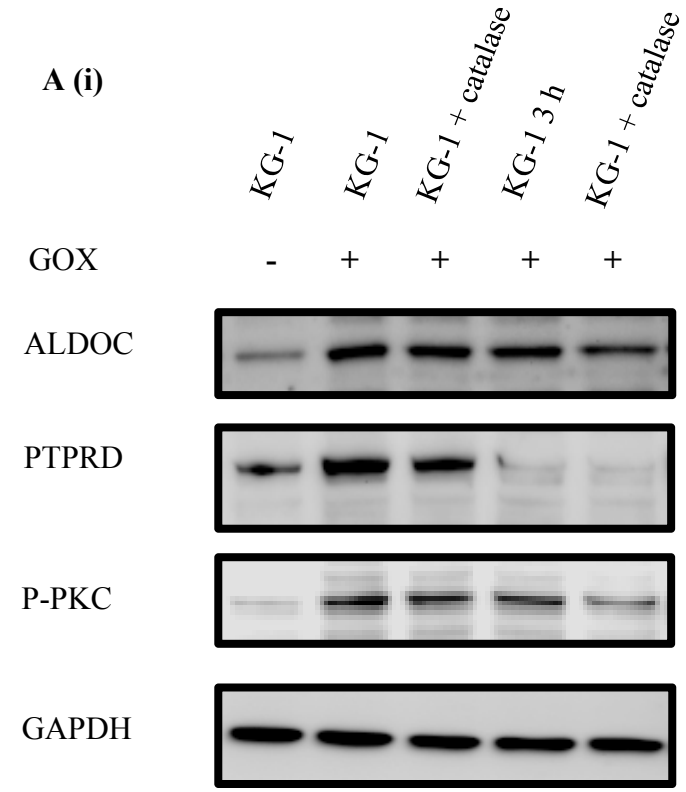
A (i)
KG-1
KG-1
KG-1 + catalase
KG-1 3 h
KG-1 + catalase
GOX
-
+
+
+
+
ALDOC
PTPRD
P-PKC
GAPDH

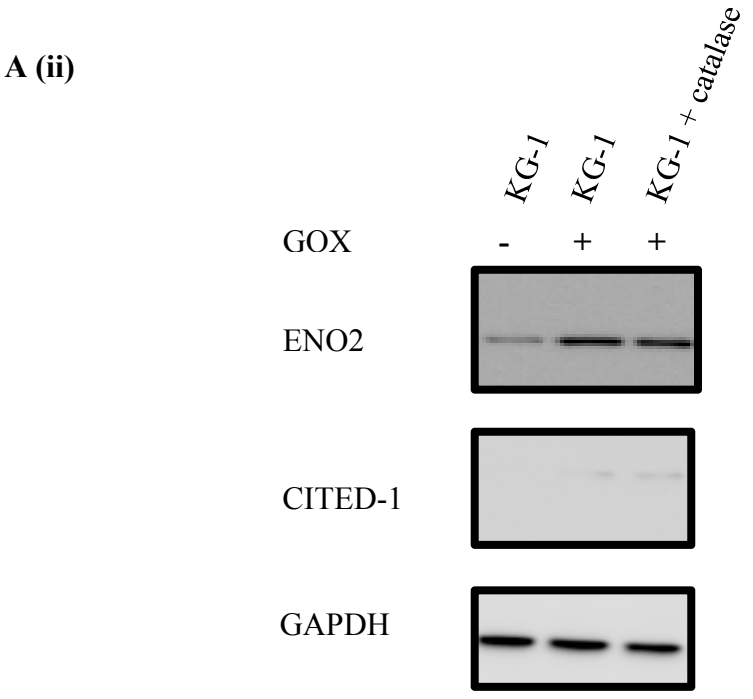
A (ii)
KG-1
KG-1
KG-1 + catalase
GOX
-
+
+
ENO2
CITED-1
GAPDH

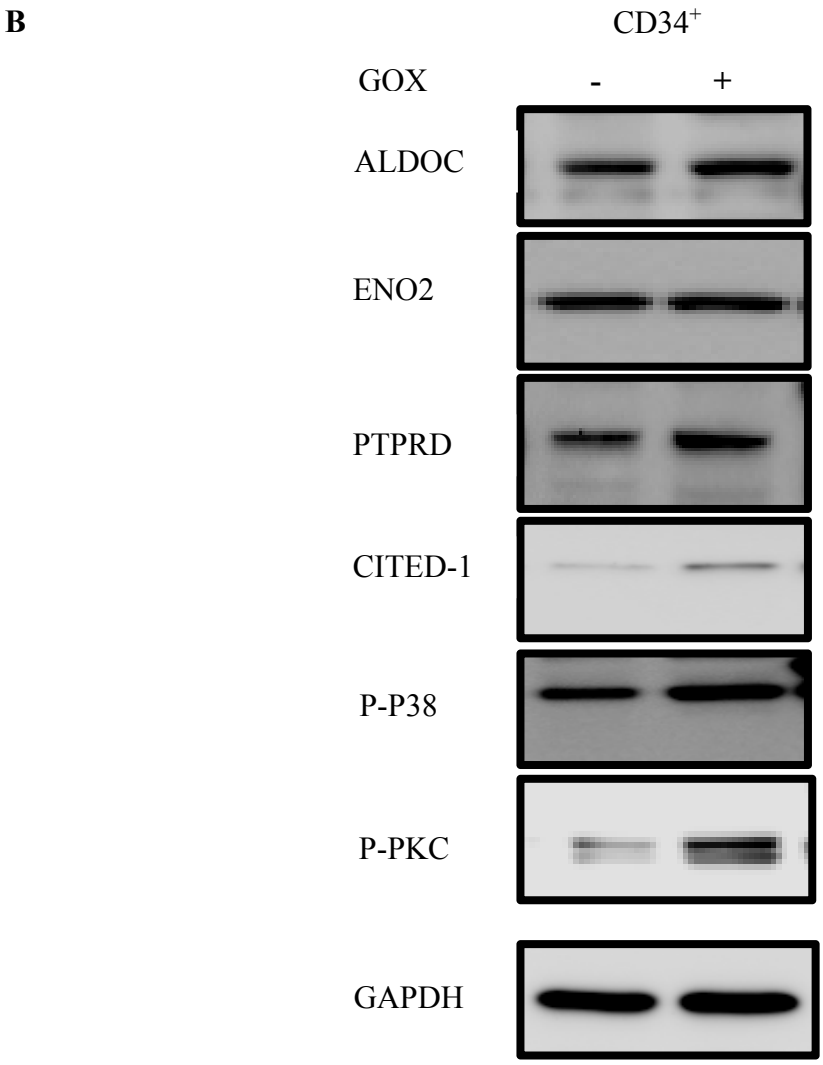

Figure 4.12 Assessment of the effects of GOX on ROS target protein expression

(A) KG-1 and (B) $CD34^+$cells (isolated and transduced as described in chapter 2) were incubated with and without (10 U/ml) GOX for 3 hours (indicated) and overnight. Catalase, which breaks down H_2O_2, was also added to some of the GOX treated cells before incubation. Whole cell protein extracts were prepared and western blot analysis was performed as above using (i) (1 µg/ml) anti-ALDOC, PTPRD, P-p38 ^{MAPK}, (2.9 ng/ml) P-PKC (ii) (1 µg/ml) ENO2 and Cited-1 antibodies. 20 ng/ml anti-GAPDH antibody was used as a loading control. Results are representative of at least 2 independent experiments.

4.4 DISCUSSION

In Chapter 3, N-RAS^{G12D} was overexpressed in normal human haematopoietic CD34^{+} cells as a model to examine the effect of ROS on gene expression in haematopoietic cells. This model was validated in terms of ROS production and inhibition of ROS production using DPI. Finally, 4 replicate samples used in the GEP studies.

In this chapter data obtained from these experiments were imported and analysed using Partek GS software for gene expression changes. In addition, functional analysis and pathway networks between genes of interest were achieved using Metacore software. Finally gene changes observed were validated using flow cytometry or western blot methods.

Genechip® Human Exon 1.0ST arrays used in this study contains probes that have been selected and distributed throughout the entire length of each transcript. They consists of 4 probes per exon and 40 probes per gene which enables both gene expression and alternative splicing analysis (Abdueva *et al*., 2007) and have also been shown to be more accurate than other arrays due to a higher coverage and more evenly distributed probes (Affymetrix Online; Kapur *et al*., 2007) as previously discussed in detail. For the analysis used in this chapter multiple probes on different exons were summarized in to an expression value of all transcripts from the same gene.

Partek GS software used in this study was also suitable for data import and GEP studies because it was already available in our department. The RMA algorithm used in this study for the exon level expression analysis includes the adjustment of GC content and probe sequence on pre-background-subtracted values. It works by estimating, for each probe set, values for the probe and chip effects that would result in the pattern of perfect matches (PM) values observed in the data (Okoniewski and Miller, 2008; Irizarry *et*

al.,2003). The fact that RMA only uses PM has made it very popular hence it has become the widest used normalization method as opposed to MAS5.0 (Hubbell *et al*., 2002).

Quality controls (QCs) used in this study during microarray experiments facilitated data quality assessment at different stages of the microarray experiments. These are useful in the identification of problems associated with hybridization and target preparation phase of the experiments to ensure excellent interpretation and confidence in the data generated before analysis. The visual inspection of image plots was also performed and this revealed that all samples tested met the QC criteria indicated by the absence of artefacts. Therefore data from all the samples were taken further for gene expression analysis with confidence.

Hierarchical clustering groups similar elements together hence can also be used as quality control. This is very helpful in the detection of bias potentially introduced for technical rather than biological reasons which should result in the exclusion of the sample in question before further analysis (Zimmermann and Leser 2010). However such bias is normally removed by normalization and taken in to account during the design of the statistical model. PCA (used in this study) on the other hand provides similar information to Hierarchical clustering apart from the fact that it preserves more information despite reports of it being computationally demanding (Zimmermann and Leser 2010). According to the PCA, Hierarchical clustering and the sources of variation plots, cord blood (replicate) is driving factor of gene expression in addition to the sample treatment. Therefore in the current study, ANOVA 2 way analysis was used which took into account the two sources of variation established namely replicate and sample treatment in order to control for the biological variation.

Gene expression analysis (Table 4.1), showed that 25 genes were significantly altered (either up or down-regulated) by ROS. However one transcript did not have gene assignment (for unknown reasons) reducing the number to 24. It was also found that of the

24 target genes identified, the expression of 4 genes was down-regulated by ROS with fold change range of 1.2-3.6 fold and 20 targets genes were up-regulated by ROS with the fold change range of 1.2-4.3 fold with ALDOC being the most strongly up-regulated. All the p-values of these gene changes were found to be in the range of 2.26×10^{-7}-1.32×10^{-4} indicating very strong significance. These results suggested that ROS can independently induce significant alteration in gene expression.

The Partek GS ANOVA output of the above 24 significant genes were then taken for pathway functional analysis using Metacore software to identify the pathways that were significantly altered and for network functional and interaction analysis. Taken together, the GEP data, manual literature searches and Metacore pathway analysis identified ROS-induced gene changes were most significantly associated with Glycolysis and Gluconeogenesis. These genes included ALDOC, PFK, GPI, FPBP1 and ENO2 and are discussed in detail in chapter 5.

Validation of gene changes at the protein level was carried out for genes which showed the biggest fold change with ROS and for which suitable antibodies were available. Of the 9 gene changes investigated 4 were not validated at the protein level suggesting that protein expression was additionally regulated at the post-transcriptional level. Five gene changes (ENO2, CITED-1, GATM, ALDOC and PTPRD) were successfully validated at protein level using western blotting.

To confirm that these genes were indeed directly responsive to ROS, KG-1 cells and primary $CD34^{+}$ cells were exposed to ROS (H_2O_2) through addition of GOX (as previously optimised for this purpose in a study by Hole *et al*., (2013). Each of these genes showed up-regulation at the protein level in at least one context. Of the glycolytic enzymes analysed ALDOC gave the most consistent up-regulation in response to ROS.

Increased glycolysis has been implicated in many cancer cells in several studies (1.5.4 and 5.4). It is now believed that cancer cells use the metabolic pathway for

generation of ATP as a main source of energy supply, "Warburg effect" (as discussed in 1.5.4) which is used to increase biosynthetic precursors for proliferation or building blocks for cell function and growth. This is considered as one of the most significant metabolic alterations during cancer development leading to malignant transformation (Pelicano *et al*., 2006a). Many researchers have shown that metabolic alterations may develop via oncogenic signalling, mitochondrial defects, adaptation to tumour microenvironment and most importantly expression of metabolic enzymes (1.5). This study supports these previous publications with regards to the significantly altered expression of most of the enzymes involved in metabolic pathways: glycolysis and gluconeogenesis, by ROS in mutant N-RAS expressing human $CD34^+$ cells. (This is fully discussed in Chapter 5).

Other ROS target genes identified in this study as significantly altered have also been previously linked to cancer including AML. For instance, it was previously shown that CNR2 (known as CB2) is frequently expressed in AML blasts and this gene either induces a neutrophilic differentiation block or confers abnormal migration properties in a ligand-dependent manner (Jorda *et al*., 2004). In the same study it was also demonstrated that CB2 receptor is aberrantly expressed in several human myeloid cell lines but not in normal bone marrow precursor cells. CB2 encodes a 7-transmembrane (7TM) protein and belongs to the family of $G_{\alpha i}$ protein-coupled receptors ($G_{\alpha i}$ PCRs) (Munro *et al*., 1993). It has been shown to be a proto oncogene involved in transformation (Valk *et al*., 1997; 1998). It should be noted however that the expression of this ROS target gene was found to be significantly down-regulated by ROS in the current study making it unlikely that its expression in AML blasts is linked to ROS production.

PTPRD, another gene which has been found to be significantly up-regulated by ROS in this study, is a tumour suppressor that has been previously reported to be mutated in glioblastoma (Veeriah *et al*., 2009) and other human cancers (Solomon *et al*., 2008; Stallings *et al*., 2006; Sato *et al*., 2005;Purdie *et al*., 2007; 2009). PTPRD was also shown

to predict poor prognosis in breast cancer and colon cancer (Chan *et al*., 2008). It is a member of the highly conserved family of the receptor protein tyrosine phosphatase (PTPs) and has not been previously linked to the pathogenesis of leukaemia.

ROS and antioxidants are known to influence the expression of a number of genes and signal transduction pathways, reviewed by Allen and Tresini (2000). For instance changes in the redox state were shown to modulate activation of transcription factors such as Myb (Myrset *et al*., 1993) and Egr-1 (Huang and Adamson 1993). In addition, numerous proto-oncogenes are known to be transcriptionally activated by increased cellular oxidation. For example, exposure of both normal and transformed cells to H_2O_2 stimulates increased expression of *jun-B*, *jun-D*, *c-fos* and *fos-B* (reviewed by Allen and Tresini (2000). However there is limited literature on the possible mechanisms through which ROS can influence gene expression. ROS was shown to regulate *ERBB2* and *ERBB3* (genes linked with cancer development and poor prognosis) expression via miR-199a/125b repression and DNA hypermethylation through DNA methyltransferase 1 (DNMT1) elevation in cancer cells and tumour tissues (He *et al*., 2012). Another study by Arnold *et al*., (2001) demonstrated that H_2O_2 mediates the cell growth and transformation caused by mitogenic oxidase NOX1 (Arnold *et al*., 2001). The same study showed that H_2O_2 triggers a genetic programme that results in altered gene expression including many genes previously associated with transformation and cancer as well as regulation of the cell cycle and signal transduction. According to the authors of this study the expression of 24 metabolism genes were altered, making it the category with the biggest change. Though the identity of these genes was not revealed the current study is not inconsistent with this previous work.

In conclusion, the results of this chapter have shown for the first time that mutant N-RAS induced ROS significantly dysregulated the expression of 24 genes in human $CD34^+$ haematopoietic cells, many of which are involved in glycolysis and

gluconeogenesis. In addition, direct addition of H_2O_2 via GOX induced/promotes the expression of some of these genes confirming that they are ROS responsive. However, it is unknown whether the dysregulation of these genes have any functional effects on haematopoietic cells. This is dealt with in the next chapter (Chapter 5).

5 Functional analysis of ALDOC in haematopoietic cells

It was previously demonstrated that endogenous ROS production has significant effects on the proliferation of human $CD34^+$ haematopoietic progenitor cells expressing mutant RAS (Hole *et al*., 2010). However, the mechanism by which ROS promote proliferation still remains unclear. Chapter 4 demonstrated that ROS significantly up regulated the expression of ALDOC (a target involved in the glycolysis pathway) in human $CD34^+$ haematopoietic progenitor cells expressing mutant RAS and also haematopoietic cell lines. It was therefore hypothesized that the pro-proliferative effect previously observed may be due to increased glycolysis via ALDOC over-expression. Therefore this chapter focused on the functional analysis of ALDOC on haematopoietic cells in order to establish whether this could be part of the mechanism through which ROS promotes proliferation in AML (Hole *et al*., 2013). This chapter also examines whether over-expression of ALDOC influences survival of human haematopoietic cells/leukaemic cell lines. MV4-11, THP-1, and KG-1 are the human AML cell lines used in this study which were chosen because they were previously shown to be responsive to ROS induced proliferation (Hole *et al*., 2013). In addition, RAS mutations have been shown to be present in all these cell lines. It was therefore concluded that all these cell lines were suitable for testing the hypothesis stated above.

In order to address these aims, ALDOC was ectopically expressed and in a complementary series of experiments ALDOC was knocked down to determine the role of ALDOC expression in proliferation and survival.

5.1 AIMS

In order to better understand the functional role of ALDOC in human leukaemic cell lines, this chapter aims:

- To overexpress and knock-down ALDOC in leukaemic cell lines using lentivirus and shRNAs for ALDOC.

- To investigate whether ALDOC overexpression/knock-down affects proliferation of leukaemic cell lines.

- To investigate the effects of ALDOC overexpression/knock-down on serum-independent survival of leukaemic cell lines.

5.2 MATERIALS AND METHODS

5.2.1 EXPRESSION AND KNOCKDOWN OF ALDOC IN LEUKAEMIC CELL LINES

5.2.1.1 Generation of the ALDOC overexpressing leukaemic cell lines

Control pHIV-EGFP (empty vector) and pHIV ALDOC EGFP lentiviruses were generated as described in (section 2.7). Specific details of the vector construction are in the results section (5.3.1.1). K562, THP-1, MV-4-11 and KG-1 cell lines were lentivirally transduced with each virus as described in (section 2.8). Cells were assessed for GFP expression by flow cytometry analysis to determine the transduction efficiency.

5.2.1.2 Fluorescence activated cell sorting of transduced cells

Discrete subpopulations of GFP positive cells were isolated using cell sorting. A minimum of 2 x10^6 transduced cells were resuspended in PBS containing 1% BSA (sterile filtered) and passed through 40 μM cell strainer into BD FACS tubes. Cells were then sorted using fluorescence activated cell sorter (FACS) (BD Aria), harvested and cultured into fresh serum replete medium for recovery and used for the determination of the experimental end points. GFP positivity was analysed using flow cytometry before and after cell sorting in order to validate successful sorting.

5.2.1.3 Generation of the ALDOC knock-down leukaemic cell lines

In order to suppress ALDOC protein expression in leukaemic cell lines and follow the effects of this loss on proliferation and survival, lentiviruses encoding shRNA control and ALDOC shRNA Table 5.1 (Sigma, UK) were generated as described in (section 2.7). K562, THP-1, MV-4-11 and KG-1 cell lines were lentivirally transduced with each virus as described in (section 2.8). The vector utilised puromycin resistance as a

selectable marker of gene transduction. Two controls (pLKO.1-puro Non-Mammalian shRNA control cells (transduction control) and puromycin sensitive/parental cells (selection control) were employed in this transduction. Puromycin (1 μg/ml for K562 and MV-4-11, 0.7 μg/ml for THP-1 and 1.5 μg/ml for KG-1) was added in all the cultures accordingly. Completion of the puromycin resistant cells selection was established by the absence of viable cells in parental cells (puromycin sensitive control). Once selection was complete, cells were harvested in to fresh medium and cultured as described in (section 2.3.3.1 Table 2.6) for recovery before use for further experimental end points.

Sequence no.	Sequence ID	Legacy Clone Name	Target Seq	Target Taxon	Target Gene	Target Gene Symbol	Vector	Match Position	Match Region	Match %	SDR Match %
AS2	TRCN0000052513	NM_005165.1-1113s1c1	GCAGCACAGTCACTCTACATT	human	230	ALDOC	pLKO.1	1113	CDS	100	100
AS1	TRCN0000052514	NM_005165.1-306s1c1	CTCTACCAGAAAGATGATAAT	human	230	ALDOC	pLKO.1	306	CDS	100	100
AS3	TRCN0000052515	NM_005165.1-647s1c1	CGACCTCAAACGTTGTCAGTA	human	230	ALDOC	pLKO.1	647	CDS	100	100
AS4	TRCN0000052516	NM_005165.1-880s1c1	AGAGCGAAGAAGAGGCATCAT	human	230	ALDOC	pLKO.1	880	CDS	100	100
AS5	TRCN0000052517	NM_005165.1-610s1c1	CTATTGTGGAACCTGAAATAT	human	230	ALDOC	pLKO.1	610	CDS	100	100

Table 5.1 Hairpins (shRNA) designed to target transcripts from ALDOC

AS = ALDOC shRNA sequence ID number/name given in the current study; % Match = percent match of hairpin target sequence (21mer) to transcript RNA sequence; % SDR Match = percent match of the "Specificity-Defining Region" of the hairpin target sequence to transcript RNA sequence. SDR is the initial 19 bases of the (21mer) target sequence. 100 % = 19/19. 230 = Target gene reference number.

Adapted from Broad institute: online (http://www.broadinstitute.org/rnai/public/gene/details?geneId=TRCG0000013892

5.2.2 INVESTIGATION OF THE EFFECTS OF ALDOC KNOCK-IN AND KNOCK-DOWN ON LEUKAEMIC CELL LINES

5.2.2.1 Preparation of cells for the analysis of proliferation and survival

Transduced K562, THP-1, and MV-4-11 cells and their corresponding controls were harvested from growth medium by centrifugation at 180 g for 10 min. To reduce background effects of serum due to left over serum from the growth medium (which would interfere with the survival assay), all traces of serum containing medium were removed by washing the cells twice by centrifugation with 20 ml and 10 ml serum-free medium at 180g for 10 min. Washed cell pellets were resuspended and set to a final density $0.5x10^5$ cells/ml (for K562) and $1.0\ x10^5$ cells/ml (for THP-1 and MV-4-11) in either serum-free, supplemented (with glutamine and gentamycin) IMDM or RPMI or in media with 10% serum and supplements (normal growth condition) for comparison. These cells were used for the proliferation and survival assays.

To determine whether ALDOC promotes proliferation in transduced K562, THP-1 and MV-4-11 (generated in 5.2.1.1 and 5.2.1.3) under normal growth conditions, cells were prepared as above and analysed as below. To determine whether ALDOC promotes serum-independent survival of ALDOC and shRNA transduced K562, THP-1, and MV-4-11 the detection of apoptosis in these cells deprived of serum was necessary. Cells (1 ml) (generated in 5.2.1.1 and 5.2.1.3) were incubated in a 24 well plate in a 5% CO_2 humidified atmosphere at 37 ^oC in the presence or absence of serum (to induce apoptosis). The incubation time was 72 h to maximise any survival differential between the controls and ALDOC or ALDOC shRNA transduced cells (i.e. for both knock-in and knock-down experiments). These cells were analysed as below. Any modifications are indicated in the appropriate figure legend. At least 3 independent replicate experiments for both knock-in and knock-down were carried out for all the assays.

The above models were used to investigate whether ALDOC KI and KD affected the proliferation of leukaemic cell lines using 2 different methods; namely MTS (5.2.2.2) and Cellometer (5.2.2.3) assays under normal growth conditions (i.e. in the presence of serum). More than one assay was carried out in order to improve confidence in the results. The MTS assay is a colorimetric method for the determination of the metabolic activity of cells in culture via the reduction of a tetrazolium compound and hence is not necessarily directly related to cell number. Assay conditions which alter metabolic activity such as the presence of ALDOC, an enzyme involved in metabolism could possibly influence the results. The advantage of this assay is that multiple readings can be taken overtime. However the MTS assay requires a lot of optimisation for each cell lines used, including the number of cells needed as well as the incubation time for formazan formation. The Cellometer method on the other hand recognizes cells based on their light scattering properties. Cells are stained with trypan blue (a dye exclusion method that utilizes membrane integrity to identify dead cells) and the instrument can thereby distinguish viable cells giving both the concentration and percentage viability of the culture. The Cellometer reports actual cell number and the percentage viability. It is a rapid analysis method for accurate viability determination and a simple method for cell proliferation studies as compared to the MTS assay. It is more accurate than manual counting of cells using a haemocytometer.

5.2.2.2 MTS assay

To determine whether ALDOC promotes proliferation under normal growth conditions, transduced K562, THP-1, and MV-4-11 cells (100 µl) and their corresponding controls harvested and prepared as above, were incubated in a 96 well plate at 37^{o}C in a

5% CO_2 humidified atmosphere for 72 h to maximise any proliferation differential between the controls and ALDOC or ALDOC shRNA transduced cells.

After incubation, MTS reagent (20 µl) (Promega, USA) was added to each well of the 96-well assay plate containing the samples in 100 µl of culture medium using a multi-channel pipette. Cells were incubated further for 4 h in a 5% CO_2 humidified atmosphere at 37 ºC and absorbance was measured after 4 h using a 96-well plate reader. Results were analysed using Microsoft Excel 2007.

5.2.2.3 Cellometer

To determine whether ALDOC promotes proliferation under normal growth conditions, transduced K562, THP-1, and MV-4-11 cells and their corresponding controls harvested and prepared as above were incubated in a 24 well plate at 37ºC in a 5% CO_2 humidified atmosphere for 72 h.

After incubation, 20 µl of the cells were harvested, stained with 20 µl of trypan blue (Sigma, UK) and the percentage and total number of viable cells was determined by Cellometer counter (Nexcelom Biosciences, USA). Results were analysed using Microsoft Excel 2010.

5.2.2.4 DNA content analysis of transduced leukaemic cell lines

To measure apoptosis, propidium iodide (PI) was used to label intracellular DNA and flow cytometry was used to analyse DNA content using a protocol similar to that described in section 5.2.2.3 with some slight modifications (indicated where appropriate).

After incubation, cells were washed with 15 ml PBS by centrifugation at 180 g for 10 min and the pellet was resuspended in 300 µl PBS and left on ice for 5 min. Ice cold ethanol (700 µl) was added to the cell suspension and the mixture was incubated on ice for further 30 min followed by incubation overnight at -20 ºC. Following incubation, 10 ml of PBS was added to the cell suspension and then centrifuged at 300 g for 10 min. The cell

pellet was resuspended in 75 µl PBS and 25 µl of staining solution consisting of PI at 40 µg/ml and RNase at 0.1 µg/ml (Sigma, UK) was added and the mixture was incubated for 30 min at 37 ^{o}C in a water bath. PI labelled cells were analysed by flow cytometry. The results were further analysed using multi-cycle on FCS express version 4 (De Novo Software, Los Angeles, CA) for the determination of the percentage of the cells that were apoptotic (sub G0/G1 events) which was determined by the subtraction of the background apoptotic frequency (from 10% serum growth condition) to correct for the low level of background apoptosis in normal growth condition.

5.2.2.5 7-AAD method

Given the fact that loss of homeostasis and membrane integrity are some of the indications of late stage apoptosis (Wyllie, 1997), and that 7-AAD, a known membrane – impermeable molecule can enter cells with defective plasma membranes and interpolates with DNA resulting in the fluorescent complexes (Schmid *et al*., 1992), this facilitated the use of this molecule (7-AAD) in conjunction with flow cytometry for the detection of apoptosis. In addition this assay was also previously validated in our lab for the detection of apoptosis in $CD34^{+}$ cells.

After incubation, 100 µl of the remaining cells were harvested, labelled with 1 µg/ml 7-AAD (Sigma-Aldrich) for 30 min and analysed by flow cytometry and the results were further analysed using FCS Express version 4 (De Novo Software, Los Angeles, CA). 7-AAD enabled the discrimination of apoptotic and viable cells.

5.3 RESULTS

5.3.1 GENERATION OF ALDOC OVEREXPRESSING LEUKAEMIC CELL LINES

5.3.1.1 Construction of ALDOC lentiviral expression vector

ALDOC lentivirus vector (pHIV ALDOC EGFP) was generated as described in (section 2.2.5 and Figure 5.1 and Figure 5.2). In summary, ALDOC coding sequence DNA was excised from pEXK-ALDOC plasmid (Table 2.5) using *SmaI* and *XbaI* double restriction digest (Figure 5.1). The expected fragments sizes corresponding to the ALDOC sequence (1.2 kb) and pEXK sequence (2.5 kb) were generated. The ALDOC coding sequence was excised from a preparative agarose gel and purified as described in section 2.2.5. The recipient pHIV EGFP lentiviral vector (Table 2.5) was linearized using the same restriction digest (Figure 5.1). The insert (ALDOC) and the vector (pHIV-EGFP) were ligated by incubation with ligase in ligase buffer in order to generate the recombinant plasmid, pHIV ALDOC EGFP (Figure 5.1). The ligation was transformed as described in section 2.2.1. Following ligation and transformation six clearly distinct ampicillin-resistant colonies were isolated, and cultured for DNA isolation. To identify colonies harbouring pHIV ALDOC EGFP DNA, *NcoI* restriction enzyme test digest was performed using a similar protocol to the one described in section 2.2.4, on all plasmid DNAs isolated from the above colonies. pHIV EGFP contains three *NcoI* enzyme recognition sites and ALDOC insert contains one *NcoI* recognition site. Therefore as shown in Figure 5.1 pHIV ALDOC EGFP contains four *NcoI* enzyme restriction sites hence four fragments are expected in the colonies containing pHIV ALDOC EGFP DNA whereas the parent vector would only generate 3 fragments (Figure 5.2). Four colonies (C1, C2, C4 and C5) were identified via test digest as potentially expressing the relevant pHIV ALDOC EGFP DNA (Figure 5.2) indicated by the expected fragment numbers and sizes. Finally one colony (C1) was taken as the definitive colony and DNA from this colony was used for sequence verification using Eurofins sequencing service (Eurofins Genomics, Germany). The results

were as predicted (data not shown) and hence DNA derived from this colony was used in subsequent experiments.

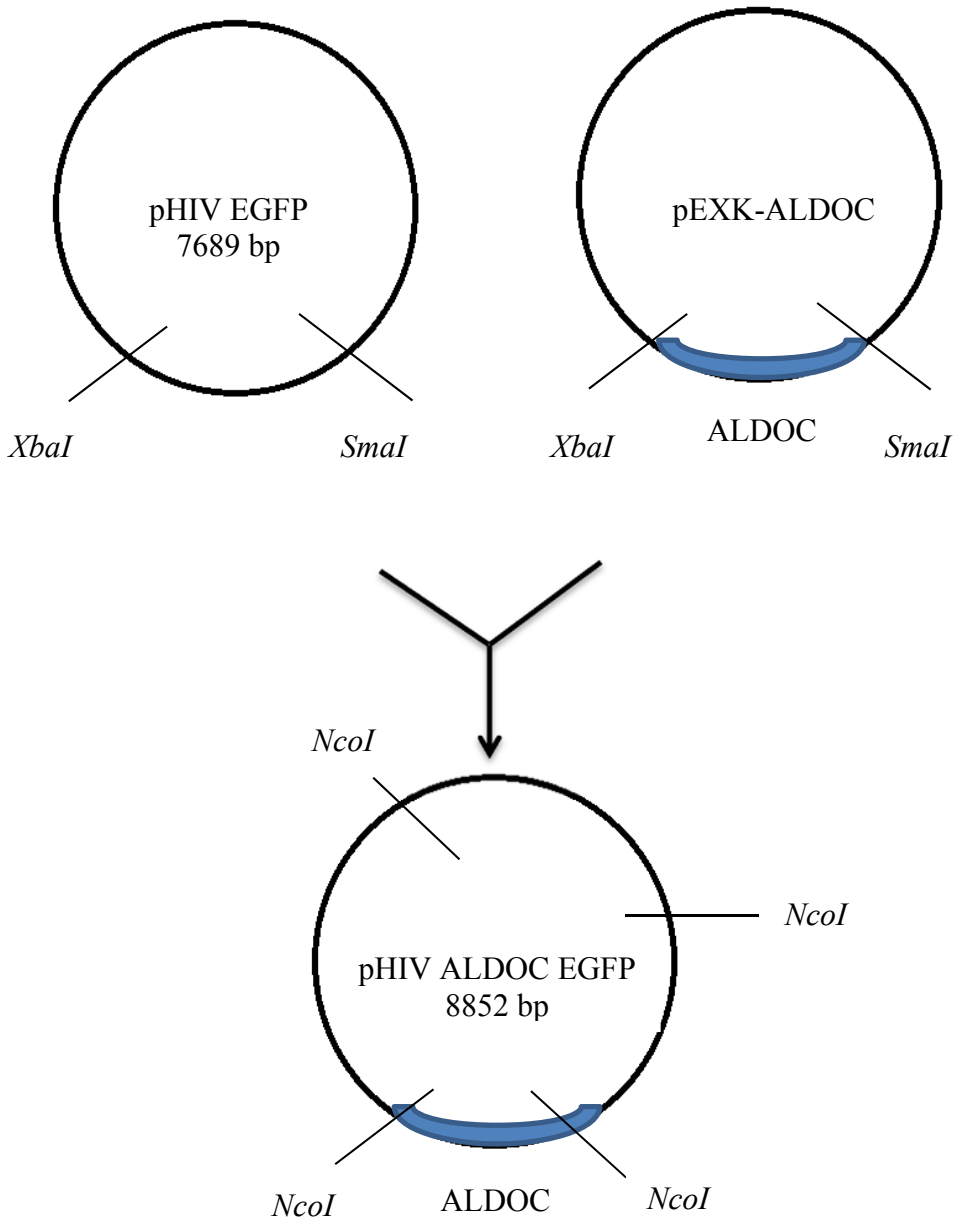

Figure 5.1 Generation of pHIV ALDOC EGFP

The ALDOC lentivirus vector (pHIV ALDOC EGFP) was generated by excision of ALDOC coding sequence DNA from pEXK-ALDOC using double restriction digest, *SmaI* and *XbaI*. Locations of restriction enzyme recognition sequences and the insert sequence are shown. The recipient pHIV EGFP lentiviral vector was linearized using the same restriction digest. Ligation and transformation yielded the final pHIV ALDOC EGFP which was verified using *NcoI* restrictive enzyme digestion (Figure 5.2) and then used for the generation of lentivirus encoding ALDOC.

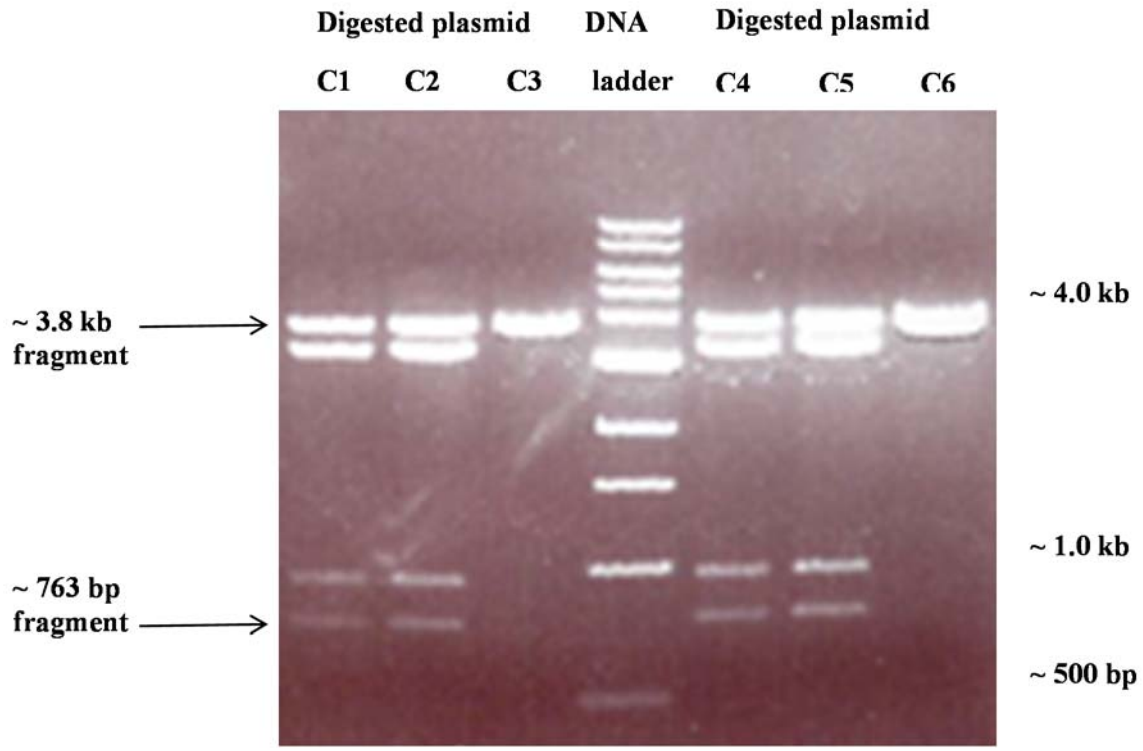

Figure 5.2 Recombinant plasmid DNA verification by restriction enzyme digestion

Six clearly distinct colonies generated as described above (5.3.2) were analysed for their plasmid DNA content. Test digests were carried out using *NcoI* and agarose gel electrophoresis as described in Chapter 2. The insert-derived band at 763bp indicated successful subcloning in 4/6 of the colonies. 300 ng DNA was loaded per lane.

5.3.1.2 The overexpression of ALDOC protein in leukaemic cell lines

To establish whether ALDOC promotes proliferation in leukaemic cell lines, it was important to overexpress (knock-in) ALDOC in leukaemic cell lines. K562, THP-1, KG-1 and MV-4-11 cells were lentivirally transduced with either GFP control or ALDOC DNA constructs generated above (section 5.3.1.1). Transduced cells were analysed for GFP expression by flow cytometry (section 5.2.1.1). All cell lines with GFP positivity of less than 70% were enriched for GFP expression by cell sorting as described in 5.2.1.2. ALDOC and control MV-4-11 cells exhibited a pre-sort GFP positivity in the range (36-75%) and a post-sort GFP positivity in the range (93-94 %) (Figure 5.3A). Since the GFP positivity of K562 and THP-1 cultures were in the range (70-99%) for both ALDOC and control these were not taken for cell sorting (Figure 5.3A). KG-1 cells showed a very low GFP expression (less than 1%) and demonstrated instability in GFP expression post-sort; hence these cells were not studied further.

Following gene transduction, confirmation of ALDOC overexpression was carried out via western blotting. The results of the western blots (Figure 5.3B) showed that ALDOC was overexpressed in THP-1, MV-4-11 and K562 cells indicated by approximately 2 fold increase of ALDOC protein levels in ALDOC transduced cultures as compared to the corresponding controls in each of the cell lines. These results should be interpreted with caution since the loading control used, GAPDH is an enzyme involved in the glycolytic pathway just like ALDOC. However, this was similar to the overexpression of ALDOC observed in $CD34^+$ N-RAS cells, protein levels (2-3 fold) (Chapter 4). It was therefore concluded that the ALDOC DNA construct used in this study was effective.

A

i) CONTROL **ii) ALDOC**

MV-4-11 Pre-sort

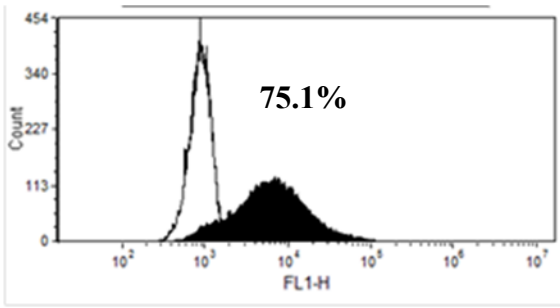

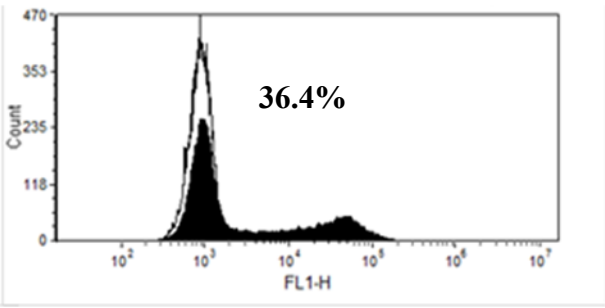

MV-4-11 Post-sort

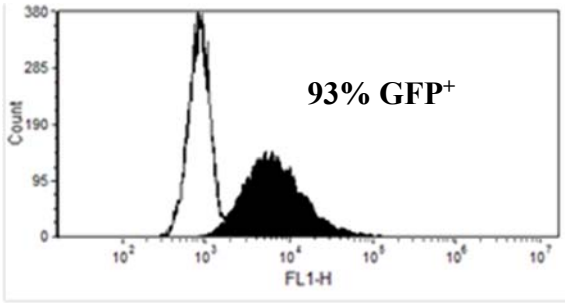

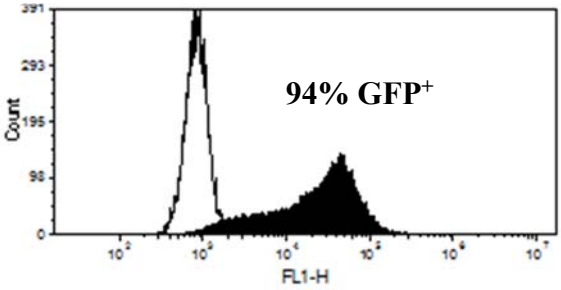

K562

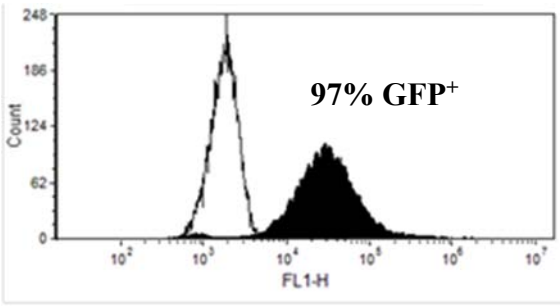

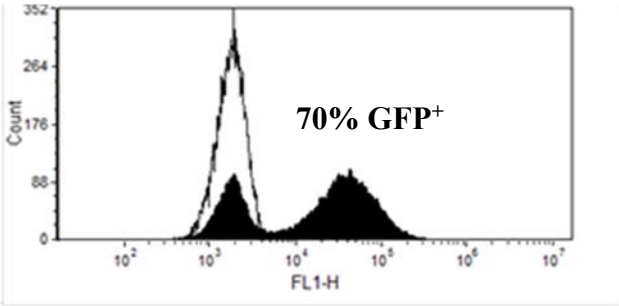

Thp-1

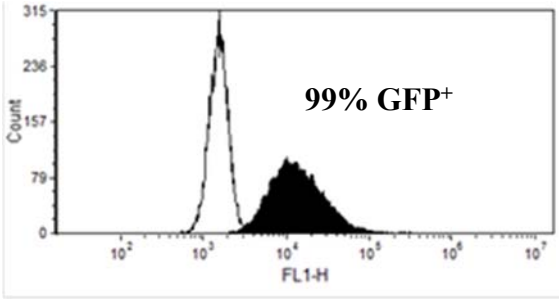

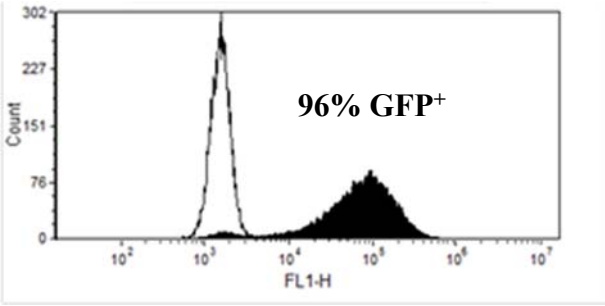

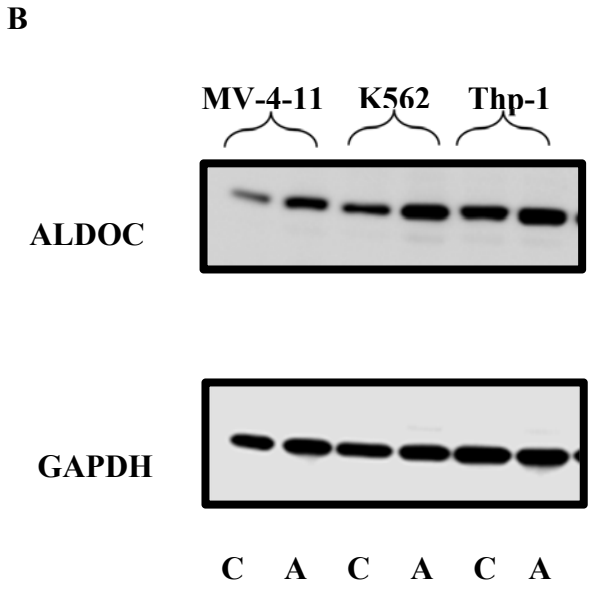

Key:

C = Control

A = ALDOC

Figure 5.3 The assessment of ALDOC overexpression

(A) Analysis of GFP positivity; ALDOC and GFP control transduced cultures of K562, THP-1 and MV-4-11 were analysed for GFP positivity (filled histograms) post transduction. Threshold for positivity was determined by autofluoroscence (open histograms) of parental cells, and percentages of GFP^+ are shown for **i)** control cells and **ii)** ALDOC cells. GFP was analysed pre and post-cell sorting for both the control and ALDOC MV-4-11 cells. **(B)** Assessment KI efficiency of ALDOC in K562, THP-1 and MV-4-11 cells; Whole cell protein extracts of ALDOC and GFP control transduced cultures of K562, THP-1 and MV-4-11 were prepared as described in section 2.9.1 and western blot analysis was performed as described in section 2.9 using (1000 ng/ml) anti-ALDOC antibody (Abcam). 20 ng/ml anti-GAPDH (Santa Cruz) was used as a loading control.

5.3.2 GENERATION OF ALDOC KNOCK-DOWN LEUKAEMIC CELL LINES

In order to establish the functional role of ALDOC in leukaemic cell line observed above (section5.3.1.2) it was important to knock down the endogenous levels of ALDOC protein within the leukaemic cell lines and examine the consequences on the proliferation and survival of these cells. To optimise and validate this approach, K562 cells were used in the initial stage of this study because of their tractability and high endogenous levels of ALDOC. The western blot (Figure 5.4A) show that the knockdown (by approximately 3.5 fold) was greatest in cells expressing ALDOC shRNA2 (AS2) (sequence ID TRCN0000052513). This construct was then also used to knock-down ALDOC in other cell lines (THP-1, MV-4-11 and KG-1). KG-1 cells grew very poorly after the infections with the ALDOC shRNA, hence were not studied further. Western Blot analysis (Figure 5.4B) showed that ALDOC was also successfully knocked down in THP-1 and MV-4-11 by approximately 1.5 fold.

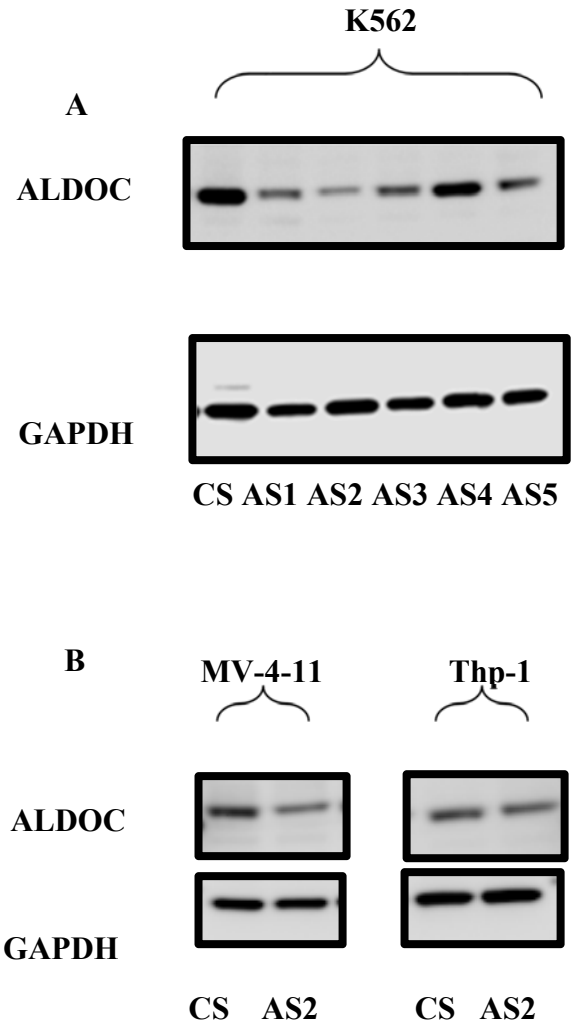

Kev:
C = Control
A= ALDOC
S= sh RNA

Figure 5.4 Assessment of ALDOC shRNA knockdown

(A) Assessment KD efficiency of ALDOC shRNA in K562 cells; K562 cell line was initially transduced with 5 clones of ALDOC shRNA, AS1, AS2, AS3, AS4 and AS5. **(B)** Assessment KD efficiency of successful ALDOC ShRNA in THP-1 and MV-4-11 cells; 1 shRNA clone (AS2) was used to knock-down ALDOC in MV-4-11 and THP-1 cells. Whole cell protein extracts of ALDOC shRNA and the corresponding control shRNA transduced cultures of K562, THP-1 and MV-4-11 were prepared and western blot analysis was performed under the same conditions described above (Figure 5.3).

5.3.3 THE ROLE OF ALDOC IN PROLIFERATION

Given the previous findings of the ability of ROS to promote proliferation, this study investigated whether the overexpression of ALDOC that occurs in response to ROS (Chapters 3 and 4) could play any role in promoting proliferation of K562, THP-1 and MV-4-11 cell lines by studying the effect of both ALDOC overexpression (knock-in) and knock-down .

5.3.3.1 ALDOC knock-in promotes proliferation of human leukaemic cell lines

In order to establish whether ALDOC promotes proliferation of human leukaemic cells, MTS and Cellometer counts assays described in 5.2.2.2 and 5.2.2.3 were used. Under normal culture conditions THP-1 and MV-4-11 cells overexpressing ALDOC showed a significant increase in relative proliferation over 72 h compared to the corresponding controls. MV-4-11 showed significant ~2.4 and 1.4 fold increases with the Cellometer and MTS assays respectively while THP-1 showed significant ~2.7 and 1.5 fold increases with the Cellometer and MTS assays respectively. ALDOC also modestly enhanced proliferation in K562 cells (<1.5 fold) which was not significant with regards to both the Cellometer and MTS assays. The trend of the results was consistent across all the cell lines with regards to both MTS and Cellometer data despite greater effects in proliferation with the Cellometer (Figure 5.5). Taken together these data demonstrates that ALDOC knock-in is sufficient to promote proliferation of these leukaemic cell lines.

5.3.3.2 ALDOC knock-down impairs the proliferation of human leukaemic cell lines

Considering the results obtained above (5.3.3.1), it was then tested whether ALDOC expression was also necessary for proliferation of these cells by examining the effects of ALDOC knock-down. To investigate this, a similar version of the protocol used

in 5.3.3.1 was used to establish whether ALDOC knock-down affected the proliferation of K562, THP-1 and MV-4-11 cells using ALDOC knock-down cell lines and shRNA control cell lines (generated as described in 5.2.1.3) and validated in (5.3.2) .

Under the conditions of the experiments above, ALDOC knock-down in THP-1 and MV-4-11 cells showed a significant decrease in relative proliferation over 72 h compared to the corresponding controls. MV-4-11 showed significant ~2 fold decrease with both the Cellometer and MTS assays while THP-1 showed significant ~5 fold decrease with both Cellometer and MTS assays. Finally K562 showed the modest effect on proliferation with less than 2 fold decrease with both assays and was not statistically significant (Figure 5.6) The results were consistent across all the cell lines with regards to both MTS and Cellometer data (Figure 5.6). Taken together these data demonstrate that ALDOC knock-down can impair proliferation of THP-1 and MV-4-11 cell lines.

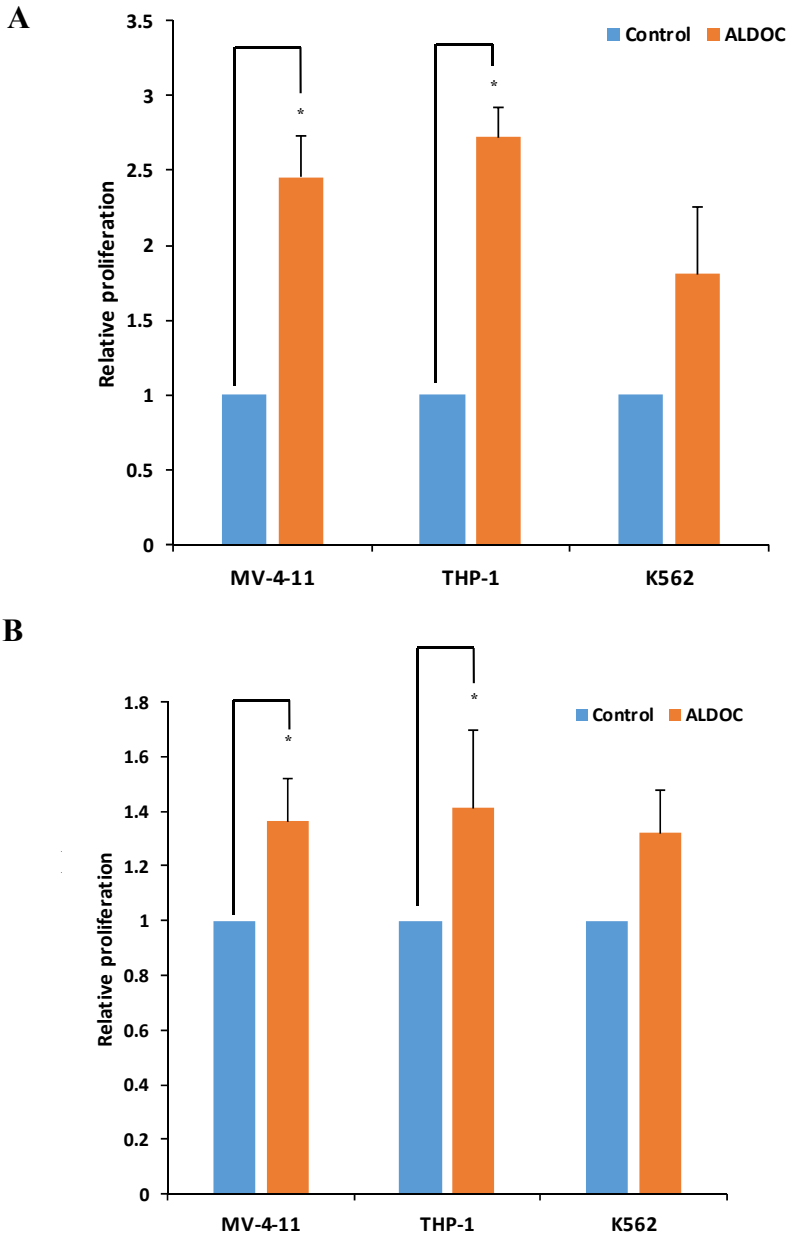

Figure 5.5 The effect of ALDOC knock-in on proliferation of transduced leukaemic cells

Leukaemic cell lines (MV-4-11, THP-1, K562) overexpressing ALDOC and their corresponding control were cultured in serum-replete (10%) media for 72 h and proliferation was measured using **(A)** Cellometer and **(B)** MTS assay (experiment was carried out in quadruplicate for each treatment condition). Data are normalised relative to control cells hence there are no error bars on controls. Statistical significance was calculated using the Student's t-test.*P<0.05 n=3 for Cellometer and n=4 for MTS assay; error bars represent SD.

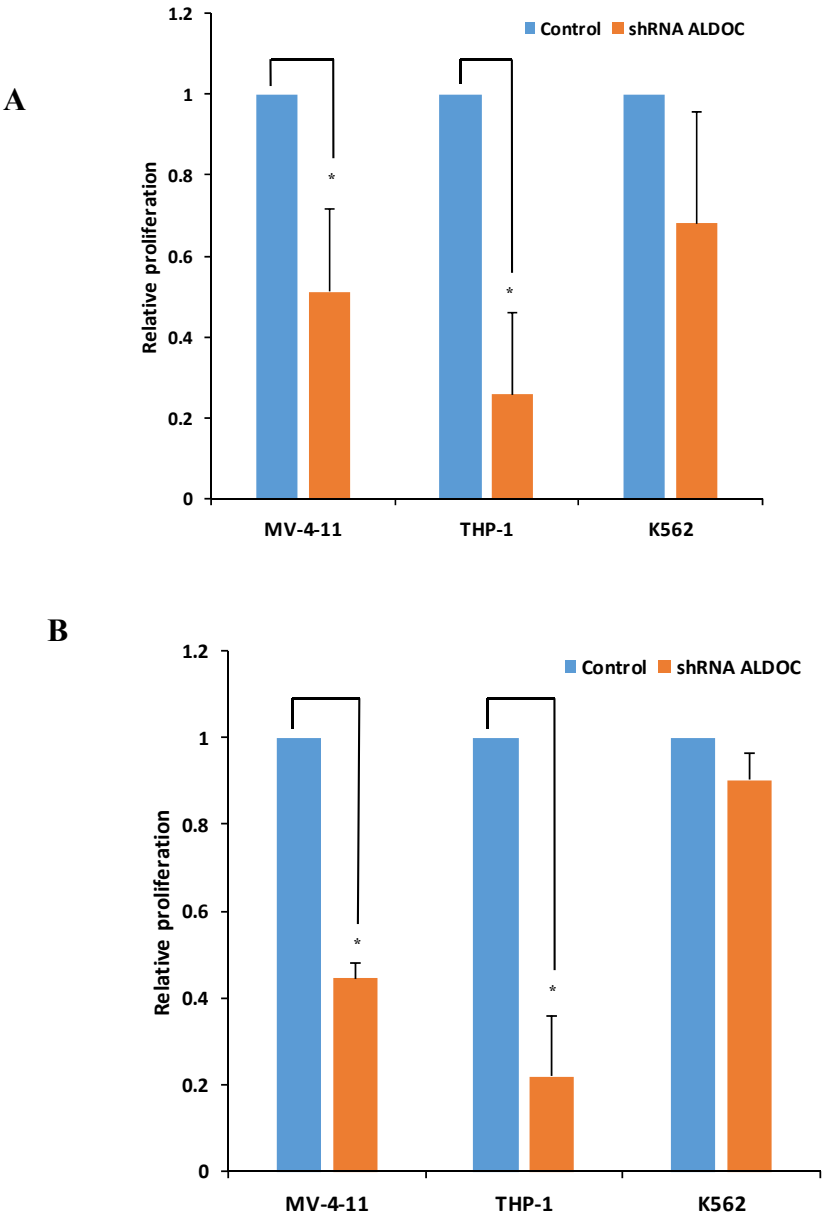

Figure 5.6 The effect of ALDOC knock-down on proliferation of transduced leukaemic cells

ALDOC knock-down lines (MV-4-11, THP-1, and K562) and their corresponding control were cultured in the same conditions as above (Figure 5.5) and proliferation was measured using **(A)** Cellometer and **(B)** MTS assay. Data are normalised relative to control cells hence there are no error bars on controls. Statistical significance was calculated using the Student's t-test.*P<0.05 n=3 for each assay; error bars represent SD.

5.3.4 THE ROLE OF ALDOC IN CELL SURVIVAL

5.3.4.1 ALDOC overexpression promotes serum-independent survival of human leukaemic cell lines

Given the effects of ALDOC on proliferation (5.3.3.1 and 5.3.3.2) it was then examined whether ALDOC ectopic expression also influenced cell survival. To test this, cells were cultured in the absence of serum and apoptosis was determined using two different methods namely 7AAD assay (described in section 5.2.2.5) and the DNA content assay (section 5.2.2.4) for the determination of the frequency of cells with sub G0/G1 DNA content (a well-established feature of apoptotic cells).

Under culture conditions previously described (absence of serum), THP-1 cells overexpressing ALDOC showed a significant ~1.2 fold and marked ~2.5 fold decrease in apoptosis over 72 h compared to the corresponding controls using the 7AAD and DNA content methods respectively. MV-4-11 showed non-significant ~1.2 and ~1.1 fold decreases using the 7AAD and DNA content methods respectively and finally K562 showed significant ~1.5 and marked 2.5 fold decreases with the 7AAD and DNA content methods respectively (Figure 5.7A and Figure 5.8A). All ALDOC KI cell lines therefore showed some resistance to apoptosis with the highest significant effect in THP-1 cells (Figure 5.7A and Figure 5.8A). It was therefore concluded that ALDOC overexpression is able to promote serum-independent survival of human leukaemic cells.

5.3.4.2 ALDOC protein knockdown inhibits the survival of human leukaemic cell lines

Considering the results obtained (5.3.4.1), it was then examined whether ALDOC expression was also necessary for survival of these cells by examining the effects of ALDOC knock-down. To investigate this a similar version of the protocol used in 5.3.4.1 was used to establish whether ALDOC knock-down affected the survival of K562,

THP-1 and MV-4-11 cells using ALDOC knocked-down cell lines and shRNA control cell lines (generated as described in 5.2.1.3 and validated in 5.3.2).

Under the conditions of the experiments above, ALDOC knock-down showed a significant effect on apoptosis in THP-1 cells only. ALDOC KD THP-1 cells showed ~1.7 fold increase in apoptosis over 72 h compared to the corresponding controls using 7AAD method (Figure 5.7B) and a ~2.5 fold increase in the sensitivity to apoptosis using DNA content method (Figure 5.8B) though this increase was not statistically significant. MV-4-11 and K562 showed smaller changes in sensitivity to apoptosis but these were not significant. These results taken together with the results of the ALDOC knock-in (5.3.4.1) suggested that ALDOC exhibit pro-survival properties with the highest effects in THP-1 cells since cells were able to survive under no serum condition and ALDOC enhanced the survival of these cells. Moreover these cells were more sensitive to apoptosis in the absence of ALDOC. It was therefore concluded that ALDOC exhibit both the pro-survival and pro-proliferative effects which might help in understanding the role of ALDOC, ROS and RAS in leukaemogenesis.

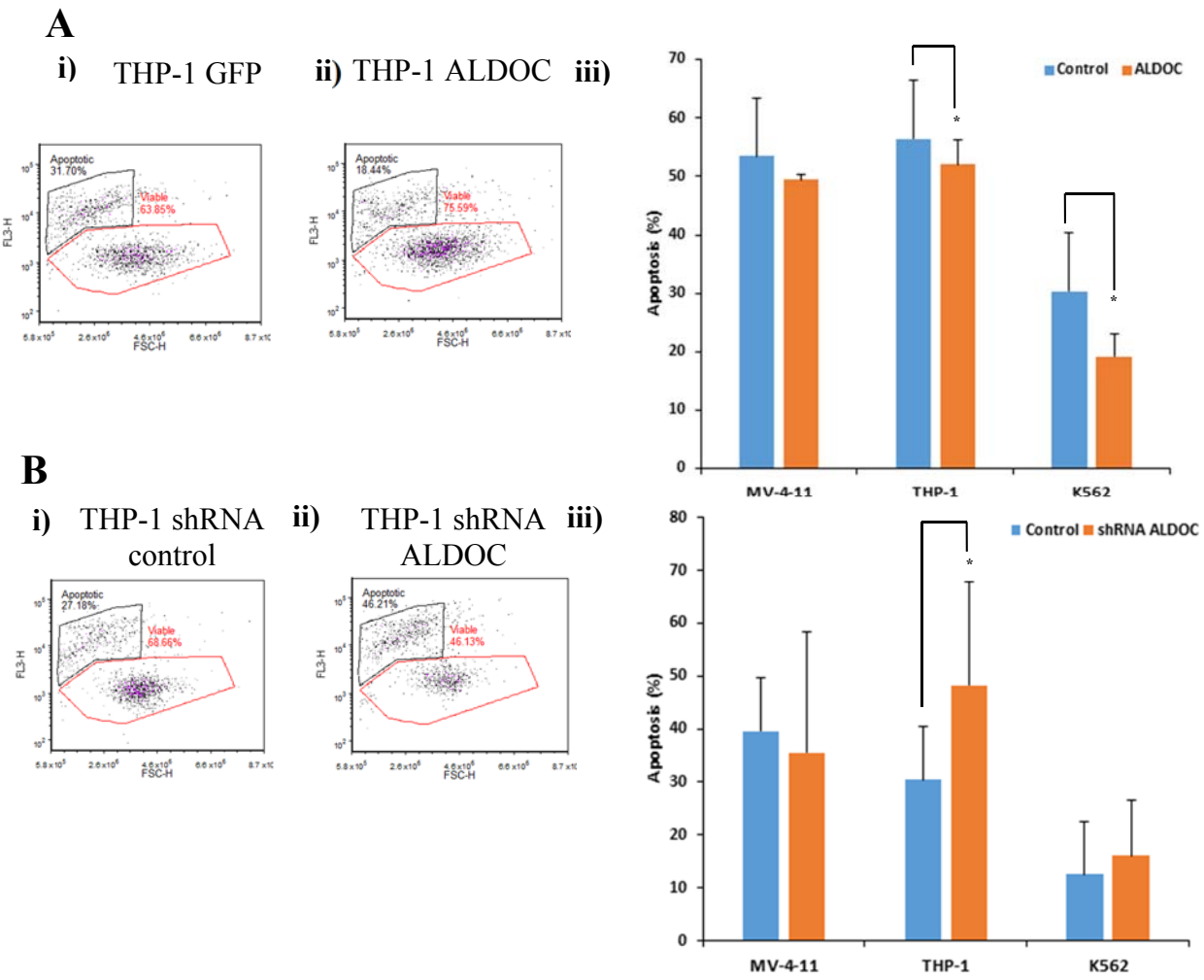

Figure 5.7 Summary of the 7AAD flow cytometric data showing apoptotic transduced leukaemic cells after serum deprivation for 72 h

(A) Effect of ALDOC knock-in on survival of MV-4-11, THP-1 and K562 cells **i)** Representative flow cytometric plots showing apoptotic cells in control, **ii)** ALDOC transduced cells and **iii)** A summary of the flow cytometric data. **(B)** Effect of ALDOC knock-down on survival of MV-4-11, THP-1 and K562 cells **i)** Representative flow cytometric plots showing apoptotic cells in shRNA control, **ii)** shRNA ALDOC transduced cells and **iii)** Summary data are expressed as mean percentage apoptotic cells. Statistical significance was calculated using the Student's t-test.*P<0.05 n=4 for knock-in and n=3 for knock-down; error bars represent SD.

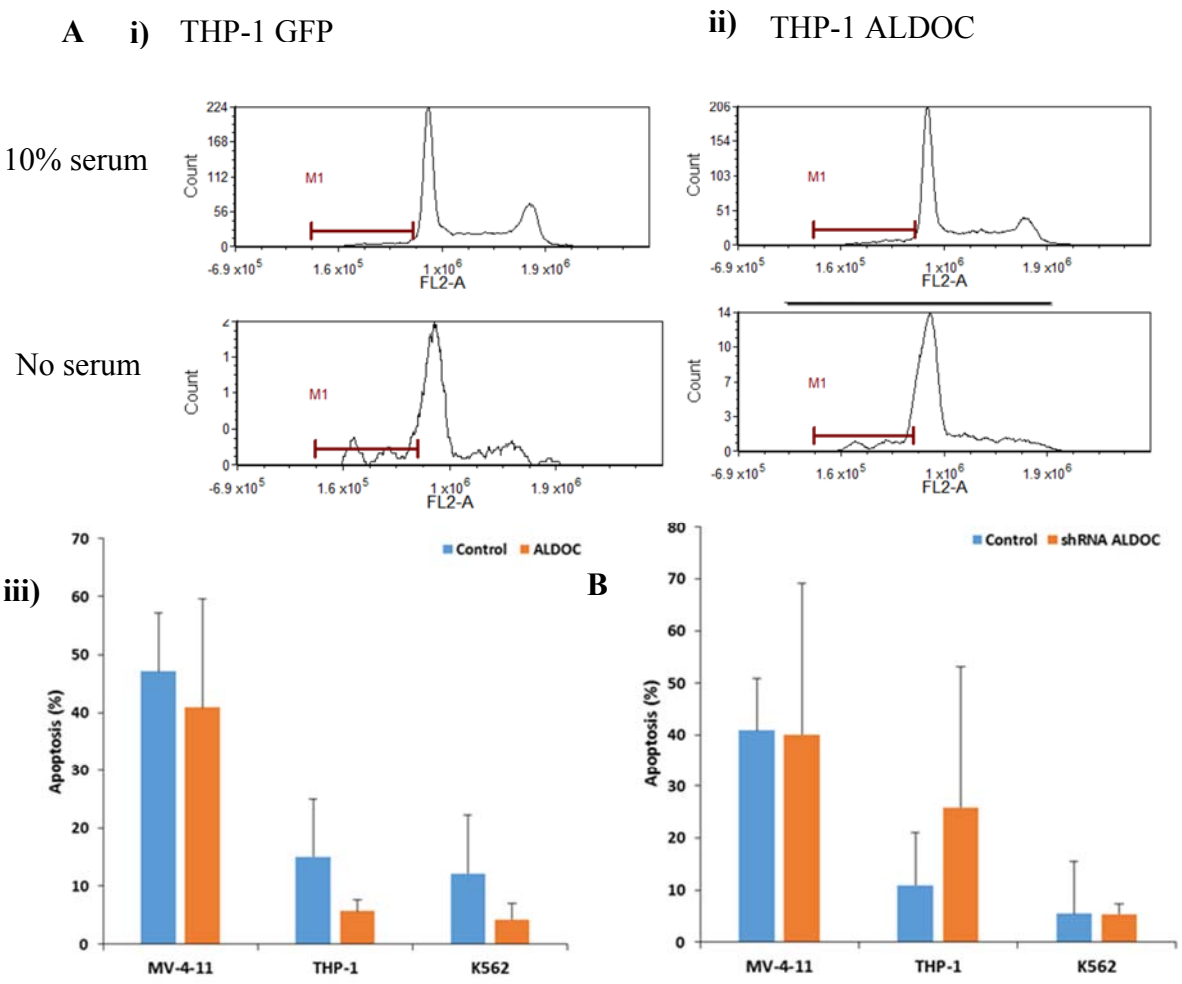

Figure 5.8 Summary of the DNA content sub-G0/G1 data showing apoptotic transduced leukaemic cells after serum deprivation over 72 h

(A) Effect of ALDOC knock-in on survival of MV-4-11, THP-1 and K562 cells **i)** Representative histograms showing apoptotic cells (indicated by the sub G0/G1 DNA content data) in control, **ii)** ALDOC transduced cells and **iii)** A summary of the apoptosis DNA content data. **(B)** Effect of ALDOC knock-down on survival of MV-4-11, THP-1 and K562 cells. A summary of the apoptosis DNA content data showing apoptotic cells following serum deprivation and staining with PI. % apoptotic cells (sub G0/G1 events) were determined by the subtraction of the background apoptotic frequency (from 10% serum growth condition). Data are expressed as mean percentage apoptotic cells. Statistical significance was calculated using the Student's t-test.*P<0.05 n=3 for each assay; error bars represent SD.

5.4 DISCUSSION

It was previously shown that ROS production has significant effects on the proliferation of human $CD34^+$ haematopoietic cells expressing mutant RAS (Hole *et al*., 2010); however, the mechanism by which ROS promotes proliferation remained unclear. Data in Chapter 4 demonstrated that N-RAS-induced ROS significantly up regulated the expression of 24 genes in $CD34^+$ haematopoietic cells many of which were associated with glycolysis and gluconeogenesis as revealed by Exon Microarray and Metacore pathway analysis; for example ALDOC (4.3 fold), GPI (1.5 fold), PFK-1 (1.4 fold), ENO2 (2.6 fold), FBP1 (1.8 fold). Amongst the genes identified, five were validated using Western Blotting of which ALDOC and ENO2 were analysed in further experiments to test directly whether these genes were ROS responsive. Both of them were indeed ROS responsive and ALDOC was selected for further functional studies since it showed the strongest expression in the presence of GOX in both cell lines and $CD34^+$ cells. This chapter aimed to test whether ALDOC could mediate some of the previously observed functional effects of ROS particularly the ability of ROS to promote proliferation.

To understand the role of ALDOC in human leukaemic cell lines, an ALDOC lentiviral construct vector (pHIV ALDOC EGFP) was generated and this was used to knock-in ALDOC into KG-1, THP-1, K562 and MV-4-11 cells. On the other hand ALDOC knock-down in the same cell lines was achieved using shRNA for ALDOC. KG-1 cells showed very low and unstable GFP expression in both the control and ALDOC cultures following infections. Moreover these cells did not grow well following infections with shRNA hence were not studied further. Though, these cells would have been the ideal ones to use for functional studies (since they were previously shown to be responsive to GOX (Chapter 4), their lack of stability of lentiviral expression following infections means

that they are not a useful model for these studies. On the other hand the KI and KD of ALDOC in THP-1, K562 and MV-4-11 cells were successful as confirmed by Western Blotting.

5.4.1 EFFECTS ON PROLIFERATION

The data generated from this study using the above models and methods have shown that ALDOC expression can influence proliferation. The overexpression of ALDOC resulted in the significant increase in proliferation of MV-4-11 (1.4-2.4 fold) and THP-1 cells (1.5-2.7 fold). Conversely a significant decrease in proliferation was observed when ALDOC was knocked-down in MV-4-11 (2 fold) and THP-1 cells (5 fold) with both the MTS and Cellometer methods. There were no significant effects of ALDOC in the proliferation of K562 cells suggesting that ALDOC does not regulate the proliferation of these cells. The proliferation data for ALDOC KI were consistent across the MTS and the Cellometer assays in terms of the trend of effect despite a slightly bigger effect size observed with regards to the Cellometer. A possible cause of this variation could be the differences in end points measured by the two assays (discussed above); however, variation in assay results (between MTS and the Cellometer) were not observed in the KD proliferation assays suggesting that the former differences could be due to experimental variation rather than to differences in end points used. Interestingly MV-4-11 and THP-1 cell lines were previously shown to respond to ROS induced proliferation in our lab and both contain RAS mutations. Therefore it is possible that ALDOC, a ROS responsive gene, specifically promotes the proliferation in the context of mutant RAS. This might then explain the failure of a pro-proliferative reponse in K562 cell lines (which do not contain mutant RAS).

Taken together the above data suggest that ALDOC expression could mediate the changes in proliferation observed as a consequence of ROS production and also highlight for the first time a potential role of ALDOC in leukaemic cell proliferation.

The expression of the aldolase isozymes have been reported in cancer with ALDOA commonly overexpressed in pancreatic and digestive tract cancers demonstrated by elevated levels in patient's serum (Asaka *et al*., 1983). Tissue ALDOC levels were found elevated in patients with lung cancer (Ojika *et.al*., 1991). A study by Hatakeyama *et al*., (2011), demonstrated that mRNA levels of ALDOC gene was 30-fold higher in the highly metastatic gastric cancer cell line MKN45P than in the lower metastatic cell line MKN45 (Hatakeyama et al., 2011). Recently the up-regulation of ALDOB was reported in the bone marrow blasts from AML patients with low prognosis-risk score (PRS) which the authors of this study concluded that it verified the modified glucose metabolism of this patients (Chen *et al*., 2014). According to the authors of this study, a low PRS was able to predict patients with poor survival. In the same study, *in vitro* results demonstrated enhanced glycolysis contributed to decreased sensitivity to anti-leukaemic agent Ara-C, whereas inhibition of glycolysis suppressed AML cell proliferation and potential cytotoxicity of Ara-C. Therefore this study provides evidence for the use of metabolic pathways as novel prognostic markers and potential therapeutic targets for AML. Despite these reports of overexpression of aldolases, their specific role in cancer cell proliferation was not addressed; however, dysregulation of glycolysis generally has been widely reported in cancer.

Glycolysis is a metabolic process that occurs in the cytoplasm which involves the production of energy from glucose. In normal cells the rate of glycolysis is low and the products of this process are further processed in the mitochondria via oxidative phosphorylation. However, cancer cells display a metabolic shift from oxidative phosphorylation in the mitochondria to glycolysis in the cytosol or lactate fermentation

even in the presence of oxygen, a phenomenon known as the "Warburg effect" (Warburg, 1956a and b) (Chapter 1 section 1.5). This has been further shown to result in biosynthetic precursors from glycolytic intermediates thus supporting rapid tumour progression (Hu *et al*., 2011; Hanahan and Weinberg, 2011; Kroemer and Pousyssegur, 2008; Vander Heiden *et al*., 2009). Cancer cells exhibiting increased aerobic glycolysis are dependent on both glucose and glutamine as a source of carbon and the up-regulation of GLUT1, GLUT3 (glucose transporters) and hexokinase I and II (key enzymes for the regulation of the first rate limiting steps in glycolysis) have been implicated in this (Bos *et al*., 2002; Burt *et al*., 2001). High rates of glycolysis and glucose uptake have been demonstrated and reported in many tumours including AML (Chapter 1). For instance, use of FdGPET imaging for the clinical diagnosis of cancer has demonstrated that the elevated glucose uptake is observed in the majority of human cancers (Mochiki *et al*., 2004; Kaira *et al*., 2011; Vergez *et al*., 2010).

There is evidence that oncogenic mutations (discussed below) promote the up-regulation of glucose transporters thus facilitating increased glucose consumption by cancer cells, which in turn increases the rate of glycolysis. Several molecules such as mutant RAS, c-Myc, HIF-1α, Akt have been implicated in this (Vafa *et al*., 2002; Kim and Dang, 2006).

MYC, an oncogene involved in the regulation of cellular proliferation, has also been shown to also contribute to the Warburg effect by increasing glycolysis and lactate production via enhancement of the overexpression of GLUT 1 and lactate dehydrogenase A (LDHA) in cancer (Dang and Gao 2009). Metabolic changes in c-Myc driven oncogenesis were reported to have preceded tumour formation and modulated by inactivation of c-myc (Hu *et al*., 2011). The same study also emphasised the additional importance of glucose metabolism or high rates of glycolysis as a source of biosynthetic precursors for cancer cells since modifications of glycolysis and alanine (amino acid

synthesized from glycolytic intermediates) synthesis pathways were identified in pre-tumour stages.

Mutant RAS has been shown to contribute to an increase in glycolysis and proliferation in cancer cells (Chapter 1). For example, mutant RAS transfection in Fisher rat 3T3 (FR3T3) fibroblasts stimulates glucose uptake, increases glycolysis, inhibits oxygen consumption and weakens mitochondrial respiration (Flier *et al*., 1987). Another study has demonstrated that BJ fibroblasts cell line expressing H-RAS exhibit increased glycolysis and become more sensitive to the glycolytic inhibitor, 2-deoxyglucose (Ramanathan *et al*., 2005). It was also demonstrated that K-RAS^{G12V} transformation leads to mitochondrial dysfunction and a metabolic switch from oxidative phosphorylation to elevated glycolysis and generation of ROS in human embryonic kidney (HEK 293) cells (Hu *et al*., 2012). Activated RAS has been reported to increase glycolysis in several ways. For example, activation of Akt by RAS has been shown to promote the increased expression and membrane localization of the glucose transporter GLUT 1, stimulation of phosphofructokinase activity and the association of hexokinases 1 and 2 with the mitochondria thus increasing glucose uptake and glycolysis in haematopoietic cell line FL5.12 (Rathmell *et al*., 2003), mouse hepatoma (Hepa1c1c7) cells (Barthel *et al*., 1999), and Rat 1a cells, (Gottlob et *al*., 2001).

Although it is clear that oncogenes such as these contribute to the Warburg effect, the mechanisms involved in the transition from oxidative phosphorylation to aerobic glycolysis in cancer cells were not addressed in detail by any of these studies. The current study suggests that increased glycolysis may arise from up-regulated glycolytic genes triggered by RAS-induced ROS. In accord with this subsequent work has demonstrated increased glycolysis in N-RAS cells (Hopkins *et al*., 2014) indicating that N-RAS also promotes the Warburg effect in the haematopoietic context. Increased rates of glycolysis have also been implicated in AML patients (Chen *et al*., 2014). This coupled with the

observation that over-production of ROS occurs in 60% of AML patients due to NOX oxidase activation (Hole *et al*., 2013) suggests that this may also be a mechanism of increased glycolysis in AML. In support of analysis of a GEP database of 139 AML patients; this showed that those with high ROS (defined by high NOX2 oxidase expression; Hole *et al*., 2013) had a distinct profile of glycolytic enzyme overexpression, particularly *ALDOC* ($r=0.4$; $p=2x10^{-25}$), *GPI* ($r=0.4$; $p=2x10^{-8}$) and *FBP1*($r=0.7$; $p=5x10^{-8}$) (Hopkins *et al*., 2014). These are amongst the most significant ROS-responsive genes in Table 4.1 and suggest that promotion of glycolysis through extracellular ROS production is also seen in AML blasts.

5.4.2 EFFECTS ON SURVIVAL

In addition to the proliferation, analysis of the influence of ALDOC on cell survival was carried out. The 7-AAD and DNA content methods were used for these studies. 7-AAD is a membrane-impermeable molecule that can enter cells with defective plasma membranes and interpolate with DNA resulting in the fluorescent complexes (Schmid *et al*., 1992) and hence is suitable for the measurement of late stage apoptosis (section 5.2.2.5). The DNA content method was used to determine sub G0/G1 events and is based on the univariate analysis of cellular DNA content following cell staining with PI and analysis using flow cytometry. This approach enables the detection of apoptotic cells with fractional DNA content (sub G0/G1 events) and is a complementary method for measuring apoptosis.

The overexpression of ALDOC resulted in the significant decrease in apoptosis of THP-1 cells (1.2-2.5 fold) and K562 (1.5-2.5 fold) under serum-free conditions. Conversely a significant increase in apoptosis was observed when ALDOC was knocked-down for THP-1 cells (1.7-2.5 fold) and to some extent for K562 cells (1.3 fold). No significant effects on MV-4-11 survival were seen for either KI or KD. The survival data

for ALDOC KI and KD were consistent across the 7AAD and the DNA content method in terms of the trend of effect despite the lack of significance/statistical power in data due to the low number of replicate samples.

Overall, these results suggest that ALDOC overexpression can promote survival and that ALDOC expression was also necessary for survival of THP-1 cells. This is a novel finding and the mechanism underlying this is still yet to be elucidated; however, existing literature suggest that this might be related to glycolysis. Munoz-Pinedo (2012) pointed out that cancer cells may benefit from keeping an active metabolism not only for proliferation but also as a mechanism to escape cell death. Interestingly, stimulation of glucose uptake has been linked to the suppression of apoptosis in normal haematopoietic cells (Barnes *et al*., 2005) and increased tumour aggressiveness has been linked to elevated glucose uptake (Mochiki *et al*., 2004; Kunkel *et al*., 2003). Hypoxic tumours such as pancreatic cancer and melanoma are dependent upon raised glycolysis for survival (Postovit *et al*., 2002; He *et al*., 2004; Büchler *et al*., 2003; Postovit *et al*., 2004). In addition it has been previously demonstrated that increased glycolytic rate renders cancer cells more resistant to apoptosis induced by growth factor withdrawal. For instance, in leukaemic cells overexpression of hexokinase 1 and GLUT 1 was sufficient to protect against IL-3 withdrawal (Rathmell *et al*., 2003). IL-3 withdrawal targets the anti- apoptotic protein Mcl-1 for proteasome degradation leading to cell death (Maurer *et al*., 2006) but Mcl-1 has been shown to be stable when glucose levels are high (Zhao *et al*., 2007). Another study has demonstrated that AMPK/mTOR axis (Chapter 1) inhibits translation of Mcl-1 if glycolysis is inhibited, thus making cells more susceptible to death ligands (Pradelli *et al*., 2009). Increased glycolysis also inhibits expression and activity of many pro-apoptotic BH3-only proteins, which mediate death induced by physiological agents and chemotherapeutic drugs (El Mjiyad *et al*., 2010). For example over expression of GLUT 1 was shown to inhibit Puma induction in the early haematopoietic precursor (murine pro-lymphocytic) cell line, FL5.12

upon growth factor withdrawal (Zhao *et al*., 2008). Metabolic stress was shown to regulate the pro-apoptotic BH3-only proteins, Noxa and Bad. High glucose levels has been shown to promote CDK5-mediated phosphorylation and inactivation of Noxa in leukaemic cells (Lowman *et al*., 2010) and Bad was shown to be dephosphorylated and induced apoptosis under low glucose conditions (Danial *et al*.,2003). Besides the BH3-only proteins, it was also shown that glucose deprivation induced a drop in the cFLIP levels and sensitization to death receptors in HeLa cells (Munoz-Pinedo *et al*., 2003). Interestingly, it was shown that maintenance of ATP production or overexpression of the glycolytic enzyme GAPDH promotes survival of cancer cells (Colell *et al*., 2007; Ferraro *et al*., 2008; Ricci *et al*., 2004).

Glycolytic rate has also been linked to chemotherapy resistance and poor prognosis Increased glycolysis has been shown to be associated with resistance to apoptosis induction by a combination of ATRA and ATO in AML cell lines (Herst *et al*., 2008). The authors of this study suggested that the extent of myeloblast glycolysis may be an effective and easily applied method to determine the pre-treatment prognosis of AML. Elevated glycolysis and treatment resistance is also a feature of ALL (Beesley *et al*., 2009 and Hulleman *et al*., 2009). The fact that most tumours are highly dependent on glucose have led to the development of inhibitors against almost every step of glycolysis some of which are currently being tested *in vitro*, *in vivo* and in clinical trials (see Chapter 1 and 6).

5.4.3 CONCLUSION

In conclusion data from this study show for the first time that a major target of ROS are enzymes of the glycolytic pathway. Evidence that ROS promotes glycolysis in both cell lines and in AML patients and that myeloid leukemia cells show dependency on ALDOC, for their growth and survival has also been shown. Thus results of this study also highlight the duality of ALDOC effects, concurrently enhancing proliferation while

hampering apoptosis. These data suggest a possible mechanism for the enhanced glycolysis seen in AML and also indicate that agents restoring the redox environment could be used to correct metabolic imbalances which contribute to treatment resistance in this disease. Further work would however be required to substantiate these conclusions and this is discussed in Chapter 6.

6 General Discussion and Further Work

AML is characterised by accumulation of blasts with an unrestrained proliferative capacity and a block at various stages of myeloid differentiation (Löwenberg *et al*., 1999). Its development has been attributed to alterations in genes that confer proliferative advantage or differentiation arrest (Gilliland *et al*., 2004) and mutational activation of RAS, particularly N-RAS is one of the most common molecular abnormalities associated with AML (section 1.2.2). Mutant RAS has also been linked to overproduction of ROS in several cancers including AML (Sallmyr *et al*., 2008; Kumar *et al*., 2008). It was previously demonstrated that normal human $CD34^+$ haematopoietic cells expressing mutant RAS overproduce ROS due to NOX activation and this has been shown to promote the proliferation of these cells (Hole *et al*., 2010). More recently, NOX derived ROS was shown to promote proliferation in AML blasts (Hole *et al*., 2013). The mechanisms by which ROS promote proliferation are unclear. Therefore the main aim of this study was to examine the effects of RAS induced ROS on gene expression and to determine the functional consequences of the key changes in gene expression.

The results of this study have shown for the first time that extracellular ROS driven by $N\text{-}RAS^{G12D}$ drives significant expression of several glycolytic enzymes in human $CD34^+$ haematopoietic cells including ALDOC (Chapters 3 and 4) and that ALDOC promotes both proliferation and survival of myeloid leukaemia cell lines (Chapter 5). Taken together, the results of this study and other findings in our lab (Hopkins *et al*., 2014) suggest that extracellular ROS promote glycolysis in $CD34^+$ haematopoietic cells and AML blasts (discussed in Chapter 5).

The results of the current study raise a question as to whether ALDOC or other glycolytic enzymes found in this study and/or NOX induced ROS may be relevant therapeutic targets in AML. The extent of ALDOC expression and levels of glucose metabolism in AML particularly in leukaemias with mutant RAS or high NOX2 activity is currently unknown; however, analysis of our GEP database of 139 AML patient blasts has shown that those with high ROS (defined by high NOX2 oxidase expression; Hole *et al*., 2013) had a distinct profile of glycolytic enzyme overexpression, particularly *ALDOC, GPI* and *FBP1* (Hopkins *et al*., 2014) which are amongst the most significant ROS responsive genes identified in this current study. To strengthen the argument for targeting ALDOC in AML, future studies could involve the analysis of ALDOC protein expression in AML blasts and association with clinical outcome with the hope of discovering a prognostic association with ALDOC overexpression, especially given that (Chen *et al*., 2014) recently showed that aldolase B enzyme (ALDOB) overexpression was associated with elevated glycolysis and poor prognosis in AML. The effect of KI and KO of other glycolytic genes (such as GPI, FBP1 and PFK-1) found in this study on proliferation and survival is another area of interest.

To substantiate the effect of ALDOC overexpression on glucose metabolism, measurement of glucose uptake, lactate production, oxygen consumption and cellular ATP production would need to be carried out. Other methods such as GC-TOF-MS, LC-MS and NMR may also be used for metabolic profiling to help in the identification and quantification of the metabolites which would provide information on multiple metabolic pathways. Similarly, metabolic profiling of AML blasts would also establish whether the changes that have been observed in the model system are characteristic of patients' disease. Further, the analysis of this material would not be influenced by the high nutrients and oxygen conditions which is a concern with the *in vitro* model described here.

The high levels of glycolysis that have been shown in many types of cancer has provided a biochemical basis for the design of therapeutic strategies to preferentially kill cancer cells by pharmacological inhibition of glycolysis (section 1.5.6). A variety of molecules now exist that have a potential anticancer activity *in vitro* and *in vivo* as a single agent or in combination with other therapeutic strategies. These data suggest that such approaches would also be applicable to AML, particularly those expressing high levels of ROS. Alternatively, given that ROS drives the expression of these glycolytic enzymes, targeting ROS or NOX2 for the purpose of restoring the metabolic imbalance in AML would be another potential therapeutic approach.

References

Abdueva, D. et al. 2007. Experimental comparison and evaluation of the Affymetrix exon and U133Plus2 GeneChip arrays. *PLoS One* 2(9), p. e913.

Affymetrix. 2014. *GeneChip Exon Array Design* [Online]. Available at: http://www.affymetrix.com/products/arrays/specific/exon.affx .

Ahearn, I. M. et al. 2011. Regulating the regulator: post-translational modification of RAS. *Nature Reviews Molecular Cell Biology* 13(1), pp. 39-51.

Ahmad, R. et al. 2010. Studies on lipid peroxidation and non-enzymatic antioxidant status as indices of oxidative stress in patients with chronic myeloid leukaemia. *Singapore medical journal* 51(2), p. 110.

Ahmadian M.R., Stege P., Scheffzek K., Wittinghofer A. 1997. Confirmation of the arginine-finger hypothesis for the GAP-stimulated GTP-hydrolysis reaction of Ras. *Nat.Struct.Biol.* 4(9), pp. 686-689

Albayrak, T. et al. 2003. The tumour suppressor cybL, a component of the respiratory chain, mediates apoptosis induction. *Molecular Biology of the Cell* 14(8), pp. 3082-3096.

Alcalay, M. et al. 2003. Acute myeloid leukaemia fusion proteins deregulate genes involved in stem cell maintenance and DNA repair. *Journal of Clinical Investigation* 112(11), pp. 1751-1761.

Allen, R. and Tresini, M. 2000. Oxidative stress and gene regulation. *Free Radical Biology and Medicine* 28(3), pp. 463-499.

Altenberg, B. and Greulich, K. O. 2004. Genes of glycolysis are ubiquitously overexpressed in 24 cancer classes. *Genomics* 84(6), pp. 1014-1020.

Ara, T. et al. 2003. Long-term hematopoietic stem cells require stromal cell-derived factor-1 for colonizing bone marrow during ontogeny. *Immunity* 19(2), pp. 257-267.

Arakaki, T. L. et al. 2004. Structure of human brain fructose 1, 6-(bis) phosphate aldolase: Linking isozyme structure with function. *Protein science* 13(12), pp. 3077-3084.

Arnold, R. S. et al. 2001. Hydrogen peroxide mediates the cell growth and transformation caused by the mitogenic oxidase Nox1. *Proceedings of the National Academy of Sciences of the United States of America* 98(10), pp. 5550-5555.

Arora, K. K. et al. 1990. Glucose phosphorylation in tumor cells: Cloning, sequencing, and overexpression in active form of a full-length cDNA encoding a mitochondrial bindable form of hexokinase. *Journal of Biological Chemistry* 265(11), pp. 6481-6488.

Asaka, M. and Alpert, E. 1983. Subunit -specific radioimmunoassay for aldolase A, B and C subunits: clinical significance. *Annals of the New York Academy of Sciences* 417(1), pp. 359-367.

Augoff, K. and Grabowski, K. 2004. Significance of lactate dehydrogenase measurements in diagnosis of malignancies. *Polski merkuriusz lekarski: organ Polskiego Towarzystwa Lekarskiego* 17(102), pp. 644-647.

Bachas, C. et al. 2010. High-frequency type I/II mutational shifts between diagnosis and relapse are associated with outcome in paediatric AML: implications for personalized medicine. *Blood* 116(15), pp. 2752-2758.

Ballatori, N. et al. 2009. Glutathione dysregulation and the aetiology and progression of human diseases. *Biological chemistry* 390(3), pp. 191-214.

Barnes, K. et al. 2005. Chronic myeloid leukaemia: An investigation into the role of Bcr-Abl-induced abnormalities in glucose transport regulation. *Oncogene* 24(20), pp. 3257-3267.

Barthel, A. et al. 1999a. Regulation of GLUT1 gene transcription by the serine/threonine kinase Akt1. *Journal of Biological Chemistry* 274(29), pp. 20281-20286.

Battisti, V. et al. 2008. Measurement of oxidative stress and antioxidant status in acute lymphoblastic leukemia patients. *Clinical biochemistry* 41(7), pp. 511-518.

Baumann, M. and Brand, K. 1988. Purification and characterization of phosphohexose isomerase from human gastrointestinal carcinoma and its potential relationship to neuroleukin. *Cancer Research* 48(24 I), pp. 7018-7021.

Baumann, M. et al. 1990. The diagnostic validity of the serum tumor marker phosphohexose isomerase (PHI) in patients with gastrointestinal, kidney, and breast cancer. *Cancer Investigation* 8(3-4), pp. 351-356.

Bayley, J.-P. and Devilee, P. 2012. The Warburg effect in 2012. *Current opinion in Oncology* 24(1), pp. 62-67.

Beaupre, D. M. and Kurzrock, R. 1999. RAS and leukemia: From basic mechanisms to gene-directed therapy. *Journal of Clinical Oncology* 17(3), pp. 1071-1079.

Beesley, A. H. et al. 2009. Glucocorticoid resistance in T-lineage acute lymphoblastic leukaemia is associated with a proliferative metabolism. *British Journal of Cancer* 100(12), pp. 1926-1936.

Bemmo, A. et al. 2008. Gene expression and isoform variation analysis using Affymetrix Exon Arrays. *BMC genomics* 9(1), p. 529.

Bennett, J. M. et al. 1982. Proposals for the classification of the myelodysplastic syndromes. *British journal of haematology* 51(2), pp. 189-199.

Bennett, J. M. et al. 1976. Proposals for the classification of the acute leukaemias. *British Journal of Haematology* 33(4), pp. 451-458.

Block, K., & Gorin, Y. (2012). Aiding and abetting roles of NOX oxidases in cellular transformation. *Nature Reviews Cancer*, *12*(9), 627-637.

Bloomfield, C. et al. eds. 1994. Curative impact of intensification with high-dose cytarabine (hidac) in acute myeloid-leukemia (aml) varies by cytogenetic group. *Blood.* WB Saunders co independence square west Curtis Center, ste 300, Philadelphia, pa 19106-3399.

Blum, R. et al. 2005. Ras inhibition in glioblastoma down-regulates hypoxia-inducible factor-1α, causing glycolysis shutdown and cell death. *Cancer Research* 65(3), pp. 999-1006.

Blum, R. et al. 2006. E2F1 identified by promoter and biochemical analysis as a central target of glioblastoma cell-cycle arrest in response to ras inhibition. *International Journal of Cancer* 119(3), pp. 527-538.

Boersma, H. H., Kietselaer, B. L., Stolk, L. M., Bennaghmouch, A., Hofstra, L., Narula, J., ... & Reutelingsperger, C. P. (2005). Past, Present, and Future of Annexin A5: From Protein Discovery to Clinical Applications*. *Journal of nuclear medicine*, *46*(12), 2035-2050.

Bonnet, D. and Dick, J. E. 1997. Human acute myeloid leukemia is organized as a hierarchy that originates from a primitive hematopoietic cell. *Nature Medicine* 3(7), pp. 730-737.

Bos, J. L. 1989. Ras oncogenes in human cancer: a review. *Cancer research* 49(17), pp. 4682-4689.

Bos, R. et al. 2002. Biologic correlates of 18fluorodeoxyglucose uptake in human breast cancer measured by positron emission tomography. *Journal of Clinical Oncology* 20(2), pp. 379-387.

Brand, K. A. and Hermfisse, U. 1997. Aerobic glycolysis by proliferating cells: A protective strategy against reactive oxygen species. *FASEB Journal* 11(5), pp. 388-395.

Brandon, M. et al. 2006. Mitochondrial mutations in cancer. *Oncogene* 25(34), pp. 4647-4662.

Brawer, M. K. 2005. Lonidamine: basic science and rationale for treatment of prostatic proliferative disorders. *Reviews in urology* 7(Suppl 7), p. S21.

Buggins, A. G. et al. 2001. Microenvironment produced by acute myeloid leukemia cells prevents T cell activation and proliferation by inhibition of NF-κB, c-Myc, and pRb pathways. *The Journal of Immunology* 167(10), pp. 6021-6030.

Buitenhuis, M. et al. 2008. Protein kinase B (c-akt) regulates hematopoietic lineage choice decisions during myelopoiesis. *Blood* 111(1), pp. 112-121.

Burdon, R. H. 1995. Superoxide and hydrogen peroxide in relation to mammalian cell proliferation. *Free Radical Biology and Medicine* 18(4), pp. 775-794.

Burt, B. M. et al. 2001. Using positron emission tomography with [18F]FDG to predict tumor behavior in experimental colorectal cancer. *Neoplasia* 3(3), pp. 189-195.

Büchler, P. et al. 2003. Hypoxia-inducible factor 1 regulates vascular endothelial growth factor expression in human pancreatic cancer. *Pancreas* 26(1), pp. 56-64.

Carew, J. S. and Huang, P. 2002. Mitochondrial defects in cancer. *Molecular Cancer* 1.

Carew, J. S. et al. 2003. Mitochondrial DNA mutations in primary leukemia cells after chemotherapy: Clinical significance and therapeutic implications. *Leukemia* 17(8), pp. 1437-1447.

Chan, T. A. et al. 2008. Convergence of mutation and epigenetic alterations identifies common genes in cancer that predict for poor prognosis. *PLoS Medicine* 5(5), pp. 0823-0837.

Chance, B. and Hollunger, G. 1961. The interaction of energy and electron transfer reactions in mitochondria I. General properties and nature of the products of succinate-linked reduction of pyridine nucleotide. *Journal of Biological Chemistry* 236(5), pp. 1534-1543.

Chang, T.-W. 1983. Binding of cells to matrixes of distinct antibodies coated on solid surface. *Journal of immunological methods* 65(1), pp. 217-223.

Chen, J. et al. 2011. Shikonin and its analogs inhibit cancer cell glycolysis by targeting tumor pyruvate kinase-M2. *Oncogene* 30(42), pp. 4297-4306.

Chen, W. L. et al. 2014. Erratum: A distinct glucose metabolism signature of acute myeloid leukemia with prognostic value. (Blood (2014) 124:10 (1645-1654)). *Blood* 124(18), p. 2893.

Chen, Z. et al. 2007. The Warburg effect and its cancer therapeutic implications. *Journal of bioenergetics and biomembranes* 39(3), pp. 267-274.

Chesney, J. 2006. 6-Phosphofructo-2-kinase/fructose-2,6-bisphosphatase and tumor cell glycolysis. *Current Opinion in Clinical Nutrition and Metabolic Care* 9(5), pp. 535-539.

Cho, H.-J. et al. 2002. Oncogenic H-Ras Enhances DNA Repair through the Ras/Phosphatidylinositol 3-Kinase/Rac1 Pathway in NIH3T3 Cells evidence for association with reactive oxygen species. *Journal of Biological Chemistry* 277(22), pp. 19358-19366.

Christofk, H. R. et al. 2008. The M2 splice isoform of pyruvate kinase is important for cancer metabolism and tumour growth. *Nature* 452(7184), pp. 230-233.

Ciarcia, R. et al. 2010. Dysregulated calcium homeostasis and oxidative stress in chronic myeloid leukemia (CML) cells. *Journal of cellular physiology* 224(2), pp. 443-453.

Clem, B. et al. 2008. Small-molecule inhibition of 6-phosphofructo-2-kinase activity suppresses glycolytic flux and tumor growth. *Molecular cancer therapeutics* 7(1), pp. 110-120.

Colell, A. et al. 2007. GAPDH and Autophagy Preserve Survival after Apoptotic Cytochrome c Release in the Absence of Caspase Activation. *Cell* 129(5), pp. 983-997.

Copley, S. D. 2003. Enzymes with extra talents: moonlighting functions and catalytic promiscuity. *Current opinion in chemical biology* 7(2), pp. 265-272.

Dahl, R. et al. 2003. Regulation of macrophage and neutrophil cell fates by the PU.1:C/EBPα ratio and granulocyte colony-stimulating factor. *Nature Immunology* 4(10), pp. 1029-1036.

Dang, C. V., Le, A., & Gao, P. (2009). MYC-induced cancer cell energy metabolism and therapeutic opportunities. *Clinical Cancer Research*, *15*(21), 6479-6483.

Danial, N. N. et al. 2003. BAD and glucokinase reside in a mitochondrial complex that integrates glycolysis and apoptosis. *Nature* 424(6951), pp. 952-956.

Darley, R. L. and Burnett, A. K. 1999. Mutant RAS inhibits neutrophil but not macrophage differentiation and allows continued growth of neutrophil precursors. *Experimental hematology* 27(11), pp. 1599-1608.

Darley, R. L. et al. 1997. Mutant N-RAS induces erythroid lineage dysplasia in human CD34+ cells. *Journal of Experimental Medicine* 185(7), pp. 1337-1347.

Darley, R. L. et al. 2002. Protein kinase C mediates mutant N-Ras-induced developmental abnormalities in nonformal human erythroid cells. *Blood* 100(12), pp. 4185-4192.

De Koning, J. P. et al. 1998. Proliferation signalling and activation of Shc, p21Ras, and Myc via tyrosine 764 of human granulocyte colony-stimulating factor receptor. *Blood* 91(6), pp. 1924-1933.

DeKoter, R. P. and Singh, H. 2000. Regulation of B lymphocyte and macrophage development by graded expression of PU.1. *Science* 288(5470), pp. 1439-1442.

Del Bufalo, D. et al. 1996. Lonidamine induces apoptosis in drug-resistant cells independently of the p53 gene. *Journal of Clinical Investigation* 98(5), p. 1165.

Dexter, T. M. 1979. Hemopoiesis in long-term bone marrow cultures. A review. *Acta Haematologica* 62(5-6), pp. 299-305.

Dick, J. E. 1996. Normal and leukemic human stem cells assayed in SCID mice. *Seminars in Immunology* 8(4), pp. 197-206.

Ditonno, P. et al. 2005. Clinical evidence supporting the role of lonidamine for the treatment of BPH. *Reviews in urology* 7(Suppl 7), p. S27.

Downing, J. R. (2003). The core-binding factor leukemias: lessons learned from murine models. *Current opinion in genetics & development*, *13*(1), 48-54.

Dwarakanath, B. and Jain, V. 2009. Targeting glucose metabolism with 2-deoxy-D-glucose for improving cancer therapy. *Future Oncology* 5(5), pp. 581-585.

Döhner, K. and Döhner, H. 2008. Molecular characterization of acute myeloid leukemia. *Haematologica* 93(7), pp. 976-982.

El Mjiyad, N. et al. 2010. Sugar-free approaches to cancer cell killing. *Oncogene* 30(3), pp. 253-264.

Elstrom, R. L. et al. 2004. Akt stimulates aerobic glycolysis in cancer cells. *Cancer research* 64(11), pp. 3892-3899.

Eppert, K., Takenaka, K., Lechman, E. R., Waldron, L., Nilsson, B., van Galen, P., ... & Dick, J. E. (2011). Stem cell gene expression programs influence clinical outcome in human leukemia. *Nature medicine*, *17*(9), 1086-1093.

Estey, E. and Döhner, H. 2006. Acute myeloid leukaemia. *The Lancet* 368(9550), pp. 1894-1907.

Farr, C. J. et al. 1988. Analysis of RAS gene mutations in acute myeloid leukemia by polymerase chain reaction and oligonucleotide probes. *Proceedings of the National Academy of Sciences of the United States of America* 85(5), pp. 1629-1633.

Ferraro, E. et al. 2008. Apoptosome-deficient cells lose cytochrome c through proteasomal degradation but survive by autophagy-dependent glycolysis. *Molecular Biology of the Cell* 19(8), pp. 3576-3588.

Filella, X. et al. 1991. Serum phosphohexose isomerase activities in patients with colorectal cancer. *Tumor Biology* 12(6), pp. 360-367.

Flier, J. S. et al. 1987a. Elevated levels of glucose transport and transporter messenger RNA are induced by ras or src oncogenes. *Science* 235(4795), pp. 1492-1495.

Frankfurt, O. et al. 2007. Molecular characterization of acute myeloid leukemia and its impact on treatment. *Current opinion in Oncology* 19(6), pp. 635-649.

Furukawa Y. 2002. Cell cycle control genes and hematopoietic cell differentiation. *Leuk.Lymphoma* 43(2), pp. 225-231

Galloway, J. L. et al. 2005. Loss of Gata1 but not Gata2 converts erythropoiesis to myelopoiesis in zebrafish embryos. *Developmental Cell* 8(1), pp. 109-116.

Gatenby, R. A. et al. 2006. Acid-mediated tumor invasion: a multidisciplinary study. *Cancer research* 66(10), pp. 5216-5223.

Gatenby, R. A. and Gillies, R. J. 2004. Why do cancers have high aerobic glycolysis? *Nature Reviews Cancer* 4(11), pp. 891-899.

Gatenby, R. A. and Gillies, R. J. 2007. Glycolysis in cancer: a potential target for therapy. *The international journal of biochemistry & cell biology* 39(7), pp. 1358-1366.

Geschwind, J. F. et al. 2004. Novel therapy for liver cancer: direct intraarterial injection of a potent inhibitor of ATP production. *Cancer Research* 62, pp. 3909-3913.

Gillies, R. J. et al. 2008. Causes and consequences of increased glucose metabolism of cancers. *Journal of Nuclear Medicine* 49(Suppl 2), pp. 24S-42S.

Gilliland, D. G. et al. 2004. The molecular basis of leukemia. *ASH Education Program Book* 2004(1), pp. 80-97.

Gilliland, D. G. and Tallman, M. S. 2002. Focus on acute leukemias. *Cancer cell* 1(5), pp. 417-420.

Goldberg, M. S. and Sharp, P. A. 2012. Pyruvate kinase M2-specific siRNA induces apoptosis and tumor regression. *The Journal of experimental medicine* 209(2), pp. 217-224.

Gottlieb, E. and Tomlinson, I. P. M. 2005. Mitochondrial tumour suppressors: A genetic and biochemical update. *Nature Reviews Cancer* 5(11), pp. 857-866.

Gottlob, K. et al. 2001. Inhibition of early apoptotic events by Akt/PKB is dependent on the first committed step of glycolysis and mitochondrial hexokinase. *Genes and Development* 15(11), pp. 1406-1418.

Graf, T. 2002. Differentiation plasticity of hematopoietic cells. *Blood* 99(9), pp. 3089-3101.

Greaves, M. ed. 2010. *Cancer stem cells: back to Darwin?* Seminars in cancer biology. Elsevier.

Grimwade, D. et al. 2001. The predictive value of hierarchical cytogenetic classification in older adults with acute myeloid leukemia (AML): analysis of 1065 patients entered into the United Kingdom Medical Research Council AML11 trial. *Blood* 98(5), pp. 1312-1320.

Grimwade, D. et al. 1998. The importance of diagnostic cytogenetics on outcome in AML: analysis of 1,612 patients entered into the MRC AML 10 trial. *Blood* 92(7), pp. 2322-2333.

Grundler, R. et al. 2005. FLT3-ITD and tyrosine kinase domain mutants induce 2 distinct phenotypes in a murine bone marrow transplantation model. *Blood* 105(12), pp. 4792-4799.

Haimoto, H. and Kato, K. 1986. Highly sensitive enzyme immunoassay for human brain aldolase C. *Clinica chimica acta* 154(3), pp. 203-211.

Hanahan, D., & Weinberg, R. A. (2011). Hallmarks of cancer: the next generation. *Cell*, *144*(5), 646-674.

Harris, A. L. 2002. Hypoxia—a key regulatory factor in tumour growth. *Nature Reviews Cancer* 2(1), pp. 38-47.

Hatakeyama, K. et al. 2011. Identification of a novel protein isoform derived from cancer-related splicing variants using combined analysis of transcriptome and proteome. *Proteomics* 11(11), pp. 2275-2282.

He, J., Xu, Q., Jing, Y., Agani, F., Qian, X., Carpenter, R., ... & Jiang, B. H. (2012). Reactive oxygen species regulate ERBB2 and ERBB3 expression via miR-199a/125b and DNA methylation. *EMBO reports*, *13*(12), 1116-1122

He, X. et al. 2004. Hypoxia increases heparanase-dependent tumor cell invasion, which can be inhibited by antiheparanase antibodies. *Cancer Research* 64(11), pp. 3928-3933.

Herst, P. M. et al. 2008. Glycolytic metabolism confers resistance to combined all-trans retinoic acid and arsenic trioxide-induced apoptosis in HL60ρ0 cells. *Leukemia Research* 32(2), pp. 327-333.

Herst, P. M. et al. 2011. The level of glycolytic metabolism in acute myeloid leukemia blasts at diagnosis is prognostic for clinical outcome. *Journal of Leukocyte Biology* 89(1), pp. 51-55.

Hingorani, S. R. and Tuveson, D. A. 2003. Ras redux: rethinking how and where Ras acts. *Current opinion in genetics & development* 13(1), pp. 6-13.

Hoang, T. 2004. The origin of hematopoietic cell type diversity. *Oncogene* 23(43 REV. ISS. 6), pp. 7188-7198.

Hoffbrand, V. and Moss, P. 2011. *Essential haematology*. John Wiley & Sons.

Hole, P. S. et al. 2010. Ras-induced reactive oxygen species promote growth factor–independent proliferation in human CD34+ hematopoietic progenitor cells. *Blood* 115(6), pp. 1238-1246.

Hole, P. S. et al. 2013. Overproduction of NOX-derived ROS in AML promotes proliferation and is associated with defective oxidative stress signaling. *Blood* 122(19), pp. 3322-3330.

Hopkins, G. L. et al. eds. 2014. *2210 Analysis of ROS-responsive genes in mutant RAS expressing hematopoietic progenitors identifies the glycolytic pathway as a major target promoting both proliferation and survival*. San Francisco, CA. 56th ASH Annual Meeting and Exposition.

Horecker, B. et al. 1980. Aldolase and fructose bisphosphatase: key enzymes in the control of gluconeogenesis and glycolysis. *Current topics in cellular regulation* 18, pp. 181-197.

Hu, S. et al. 2011. 13 C-Pyruvate Imaging Reveals Alterations in Glycolysis that Precede c-Myc-Induced Tumor Formation and Regression. *Cell metabolism* 14(1), pp. 131-142.

Hu, Y. et al. 2012. K-ras G12V transformation leads to mitochondrial dysfunction and a metabolic switch from oxidative phosphorylation to glycolysis. *Cell Research* 22(2), pp. 399-412.

Huang, R. P. and Adamson, E. D. 1993. Characterization of the DNA-binding properties of the early growth response-1 (Egr-1) transcription factor: evidence for modulation by a redox mechanism. *DNA and cell biology* 12(3), pp. 265-273.

Hubbell, E., Liu, W. M., & Mei, R. (2002). Robust estimators for expression analysis. *Bioinformatics*, *18*(12), 1585-1592.

Hulleman, E. et al. 2009. Inhibition of glycolysis modulates prednisolone resistance in acute lymphoblastic leukemia cells. *Blood* 113(9), pp. 2014-2021.

Irani, K. et al. 1997. Mitogenic signaling mediated by oxidants in Ras-transformed fibroblasts. *Science* 275(5306), pp. 1649-1652.

Irizarry, R. A. et al. 2003. Exploration, normalization, and summaries of high density oligonucleotide array probe level data. *Biostatistics* 4(2), pp. 249-264.

Ishii, T. et al. 2005. A mutation in the SDHC gene of complex II increases oxidative stress, resulting in apoptosis and tumorigenesis. *Cancer Research* 65(1), pp. 203-209.

Ishikawa, F., Yoshida, S., Saito, Y., Hijikata, A., Kitamura, H., Tanaka, S., ... & Shultz, L. D. (2007). Chemotherapy-resistant human AML stem cells home to and engraft within the bone-marrow endosteal region. *Nature biotechnology*,*25*(11), 1315-1321.

Ito, K. et al. 2004. Regulation of oxidative stress by ATM is required for self-renewal of haematopoietic stem cells. *Nature* 431(7011), pp. 997-1002.

Itoh, T. et al. 1996. Granulocyte-macrophage colony-stimulating factor provokes RAS activation and transcription of c-fos through different modes of signaling. *Journal of Biological Chemistry* 271(13), pp. 7587-7592.

Jan, M. et al. 2012. Clonal evolution of preleukemic hematopoietic stem cells precedes human acute myeloid leukemia. *Science translational medicine* 4(149), pp. 149ra118-149ra118.

Jang, M. et al. 2013. Cancer cell metabolism: implications for therapeutic targets. *Experimental & molecular medicine* 45(10), p. e45.

Jeffery, C. J. 1999. Moonlighting proteins. *Trends in biochemical sciences* 24(1), pp. 8-11.

Jordà, M. A. et al. 2004. The peripheral cannabinoid receptor Cb2, frequently expressed on AML blasts, either induces a neutrophilic differentiation block or confers abnormal migration properties in a ligand-dependent manner. *Blood* 104(2), pp. 526-534.

Jovanović, S. et al. 2007. M-LDH Serves as a Regulatory Subunit of the Cytosolic Substrate-channelling Complex< i> in Vivo</i>. *Journal of Molecular Biology* 371(2), pp. 349-361.

Kaira, K. et al. 2011. Biologic correlates of 18F-FDG uptake on PET in pulmonary pleomorphic carcinoma. *Lung Cancer* 71(2), pp. 144-150.

Kao, A. W. et al. 1999. Aldolase mediates the association of F-actin with the insulin-responsive glucose transporter GLUT4. *Journal of Biological Chemistry* 274(25), pp. 17742-17747.

Kapur, K. et al. 2007. Exon arrays provide accurate assessments of gene expression. *Genome Biol* 8(5), p. R82.

Karnoub, A. E. and Weinberg, R. A. 2008. Ras oncogenes: split personalities. *Nature reviews Molecular cell biology* 9(7), pp. 517-531.

Kiel, M. J. and Morrison, S. J. 2006. Maintaining Hematopoietic Stem Cells in the Vascular Niche. *Immunity* 25(6), pp. 862-864.

Kiel, M. J. et al. 2005. SLAM family receptors distinguish hematopoietic stem and progenitor cells and reveal endothelial niches for stem cells. *Cell* 121(7), pp. 1109-1121.

Kim, J.-w. et al. 2006. HIF-1-mediated expression of pyruvate dehydrogenase kinase: a metabolic switch required for cellular adaptation to hypoxia. *Cell metabolism* 3(3), pp. 177-185.

Kim, J. W. and Dang, C. V. 2006. Cancer's molecular sweet tooth and the warburg effect. *Cancer Research* 66(18), pp. 8927-8930.

Ko, Y. H. et al. 2001. Glucose catabolism in the rabbit VX2 tumor model for liver cancer: Characterization and targeting hexokinase. *Cancer Letters* 173(1), pp. 83-91.

Kohler, B. A., Ward, E., McCarthy, B. J., Schymura, M. J., Ries, L. A., Eheman, C., ... & Edwards, B. K. (2011). Annual report to the nation on the status of cancer, 1975–2007, featuring tumors of the brain and other nervous system. *Journal of the National Cancer Institute*.

Kole, H. K. et al. 1991. Regulation of 6-phosphofructo-1-kinase activity in ras-transformed rat-1 fibroblasts. *Archives of Biochemistry and Biophysics* 286(2), pp. 586-590.

Kolev, Y. et al. 2008. Lactate dehydrogenase-5 (LDH-5) expression in human gastric cancer: association with hypoxia-inducible factor (HIF-1α) pathway, angiogenic factors production and poor prognosis. *Annals of surgical oncology* 15(8), pp. 2336-2344.

Komatsu, H. and Obata, F. 2003. An optimized method for determination of intracellular glutathione in mouse macrophage cultures by fluorimetric high-performance liquid chromatography. *Biomedical Chromatography* 17(5), pp. 345-350.

Kopp, H.-G. et al. 2005. The bone marrow vascular niche: home of HSC differentiation and mobilization. *Physiology* 20(5), pp. 349-356.

Koppenol, W. H. et al. 2011. Otto Warburg's contributions to current concepts of cancer metabolism. *Nature Reviews Cancer* 11(5), pp. 325-337.

Koppenol, W. H. (2001). The Haber-Weiss cycle–70 years later. *Redox Report*,*6*(4), 229-234

Krengel U., Schlichting I., Scherer A., Schumann R., Frech M., John J., Kabsch W., Pai E.F., Wittinghofer A. 1990. Three-dimensional structures of H-ras p21 mutants: molecular basis for their inability to function as signal switch molecules. *Cell* 62(3), pp. 539-548

Kroemer, G. and Pouyssegur, J. 2008. Tumor cell metabolism: cancer's Achilles' heel. *Cancer cell* 13(6), pp. 472-482.

Kumar, B. et al. 2008. Oxidative stress is inherent in prostate cancer cells and is required for aggressive phenotype. *Cancer research* 68(6), pp. 1777-1785.

Kunkel, M. et al. 2003. Overexpression of Glut-1 and increased glucose metabolism in tumors are associated with a poor prognosis in patients with oral squamous cell carcinoma. *Cancer* 97(4), pp. 1015-1024.

Kurtoglu, M. et al. 2007. Under normoxia, 2-deoxy-D-glucose elicits cell death in select tumor types not by inhibition of glycolysis but by interfering with N-linked glycosylation. *Molecular cancer therapeutics* 6(11), pp. 3049-3058.

Lambeth, J. D. 2004. NOX enzymes and the biology of reactive oxygen. *Nature Reviews Immunology* 4(3), pp. 181-189.

Lambeth, J. D. and Neish, A. S. 2014. Nox enzymes and new thinking on reactive oxygen: a double-edged sword revisited. *Annual Review of Pathology: Mechanisms of Disease* 9, pp. 119-145.

Larochelle, A. et al. 1996. Identification of primitive human hematopoietic cells capable of repopulating NOD/SCID mouse bone marrow: implications for gene therapy. *Nature medicine* 2(12), pp. 1329-1337.

Lashkari, D. A. et al. 1997. Yeast microarrays for genome wide parallel genetic and gene expression analysis. *Proceedings of the National Academy of Sciences* 94(24), pp. 13057-13062.

Le, A. et al. 2010. Inhibition of lactate dehydrogenase A induces oxidative stress and inhibits tumor progression. *Proceedings of the National Academy of Sciences* 107(5), pp. 2037-2042.

Lebherz, H. G. and Rutter, W. J. 1969. Distribution of fructose diphosphate aldolase variants in biological systems. *Biochemistry* 8(1), pp. 109-121.

Lee, A. C. et al. 1999. Ras proteins induce senescence by altering the intracellular levels of reactive oxygen species. *Journal of Biological Chemistry* 274(12), pp. 7936-7940.

Lee, B. H. et al. 2007. FLT3 Mutations Confer Enhanced Proliferation and Survival Properties to Multipotent Progenitors in a Murine Model of Chronic Myelomonocytic Leukemia. *Cancer Cell* 12(4), pp. 367-380.

Levine, A. J. and Puzio-Kuter, A. M. 2010. The control of the metabolic switch in cancers by oncogenes and tumor suppressor genes. *Science* 330(6009), pp. 1340-1344.

Lewandowski, D. et al. 2010. In vivo cellular imaging pinpoints the role of reactive oxygen species in the early steps of adult hematopoietic reconstitution. *Blood* 115(3), pp. 443-452.

Li, C. et al. 2006. Proteome analysis of human lung squamous carcinoma. *Proteomics* 6(2), pp. 547-558.

Li, Y. et al. 2002. Mitochondrial targeting drug lonidamine triggered apoptosis in doxorubicin-resistant HepG2 cells. *Life sciences* 71(23), pp. 2729-2740.

Liu, R. et al. 2001. Elevated superoxide production by active H-ras enhances human lung WI-38VA-13 cell proliferation, migration and resistance to TNF-alpha. *Oncogene* 20(12), pp. 1486-1496.

Liu, Y. et al. 2012. A small-molecule inhibitor of glucose transporter 1 downregulates glycolysis, induces cell-cycle arrest, and inhibits cancer cell growth in vitro and in vivo. *Molecular cancer therapeutics* 11(8), pp. 1672-1682.

Lowman, X. H. et al. 2010. The proapoptotic function of Noxa in human leukemia cells is regulated by the kinase Cdk5 and by glucose. *Molecular cell* 40(5), pp. 823-833.

Lowry, P. A. 1995. Hematopoietic stem cell cytokine response. *Journal of Cellular Biochemistry* 58(4), pp. 410-415.

Lu, M. et al. 2001. Interaction between Aldolase and Vacuolar H+-ATPase Evidence for direct coupling of glycolysis to the atp-hydrolyzing proton pump. *Journal of Biological Chemistry* 276(32), pp. 30407-30413.

López-Lázaro, M. 2007. Why do tumors metastasize? *Cancer Biology and Therapy* 6(2), p. 141.

López-Lázaro,, M. 2008. The warburg effect: why and how do cancer cells activate glycolysis in the presence of oxygen? *Anti-Cancer Agents in Medicinal Chemistry (Formerly Current Medicinal Chemistry-Anti-Cancer Agents)* 8(3), pp. 305-312.

Löwenberg, B. et al. 1999. Acute myeloid leukemia. *New England Journal of Medicine* 341(14), pp. 1051-1062.

Macheda, M. L. et al. 2005. Molecular and cellular regulation of glucose transporter (GLUT) proteins in cancer. *Journal of cellular physiology* 202(3), pp. 654-662.

MacKenzie, K. L. et al. 1999. Mutant N-ras induces myeloproliferative disorders and apoptosis in bone marrow repopulated mice. *Blood* 93(6), pp. 2043-2056.

Maher, J. C. et al. 2004. Greater cell cycle inhibition and cytotoxicity induced by 2-deoxy-D-glucose in tumor cells treated under hypoxic vs aerobic conditions. *Cancer chemotherapy and pharmacology* 53(2), pp. 116-122.

Maher, J. C. et al. 2007. Hypoxia-inducible factor-1 confers resistance to the glycolytic inhibitor 2-deoxy-D-glucose. *Molecular cancer therapeutics* 6(2), pp. 732-741.

Majewski, N. et al. 2004. Akt Inhibits Apoptosis Downstream of BID Cleavage via a Glucose-Dependent Mechanism Involving Mitochondrial Hexokinases. *Molecular and Cellular Biology* 24(2), pp. 730-740.

Malumbres, M. and Barbacid, M. 2003a. RAS oncogenes: the first 30 years. *Nature Reviews Cancer* 3(6), pp. 459-465.

Maraldi, T. et al. 2007. Glucose-transport regulation in leukemic cells: how can H2O2 mimic stem cell factor effects? *Antioxidants & Redox Signaling* 9(2), pp. 271-279.

Maschek, G. et al. 2004. 2-deoxy-D-glucose increases the efficacy of adriamycin and paclitaxel in human osteosarcoma and non-small cell lung cancers in vivo. *Cancer research* 64(1), pp. 31-34.

Maurer, U. et al. 2006. Glycogen synthase kinase-3 regulates mitochondrial outer membrane permeabilization and apoptosis by destabilization of MCL-1. *Molecular Cell* 21(6), pp. 749-760.

Mavilio, F. et al. 1989. Alteration of growth and differentiation factors response by Kirsten and Harvey sarcoma viruses in the IL-3-dependent murine hematopoietic cell line 32D C13(G). *Oncogene* 4(3), pp. 301-308.

Mazurek, S. et al. eds. 2005. *Pyruvate kinase type M2 and its role in tumor growth and spreading*. Seminars in cancer biology. Elsevier.

Mazurek, S. et al. 2001b. Effects of the human papilloma virus HPV-16 E7 oncoprotein on glycolysis and glutaminolysis: Role of pyruvate kinase type M2 and the glycolytic-enzyme complex. *Biochemical Journal* 356(1), pp. 247-256.

Mazurek, S. et al. 2001a. Metabolic cooperation between different oncogenes during cell transformation: Interaction between activated ras and HPV-16 E7. *Oncogene* 20(47), pp. 6891-6898.

MetaCore. 2014. *Data mining and pathway analysis* [Online]. Available at: http://thomsonreuters.com/metacore/ [Accessed]

Mikuriya, K. et al. 2007. Expression of glycolytic enzymes is increased in pancreatic cancerous tissues as evidenced by proteomic profiling by two-dimensional electrophoresis and liquid chromatography-mass spectrometry/mass spectrometry. *International Journal of Oncology* 30(4), pp. 849-855.

Mitin, N. et al. 2005. Signaling interplay in ras superfamily function. *Current Biology* 15(14), pp. R563-R574.

Milligan D.W., Grimwade D., Cullis J.O., Bond L., Swirsky D. et al. 2006. Guidelines on the management of acute myeloid leukaemia in adults. *Br.J.Haematol.* 135(4), pp. 450-474

Miyamoto, T. et al. 2000. AML1/ETO-expressing nonleukemic stem cells in acute myelogenous leukemia with 8; 21 chromosomal translocation. *Proceedings of the National Academy of Sciences* 97(13), pp. 7521-7526.

Miyauchi, J. et al. 1994. Mutations of the N-ras gene in juvenile chronic myelogenous leukemia. *Blood* 83(8), pp. 2248-2254.

Mochiki, E. et al. 2004. Evaluation of 18F-2-deoxy-2-fluoro-D-glucose Positron Emission Tomography for Gastric Cancer. *World Journal of Surgery* 28(3), pp. 247-253.

Mukai, H. Y. et al. 2006. Transgene insertion in proximity to the c-myb gene disrupts erythroid-megakaryocytic lineage bifurcation. *Molecular and Cellular Biology* 26(21), pp. 7953-7965.

Mukai, T. et al. 1986. Tissue-specific expression of rat aldolase A mRNAs. Three molecular species differing only in the 5'-terminal sequences. *Journal of Biological Chemistry* 261(7), pp. 3347-3354.

Munoz-Pinedo, C. et al. 2012. Cancer metabolism: current perspectives and future directions. *Cell death & disease* 3(1), p. e248.

Munro, S., Thomas, K. L., & Abu-Shaar, M. (1993). Molecular characterization of a peripheral receptor for cannabinoids. Nature, 365, 51-65.

Murphy, D. 2002. Gene expression studies using microarrays: principles, problems, and prospects. *Advances in Physiology education* 26(4), pp. 256-270.

Murphy, M. 2009. How mitochondria produce reactive oxygen species. *Biochem. J* 417, pp. 1-13.

Muñoz-Pinedo, C. et al. 2003. Inhibition of glucose metabolism sensitizes tumor cells to death receptor-triggered apoptosis through enhancement of death-inducing signaling complex formation and apical procaspase-8 processing. *Journal of Biological Chemistry* 278(15), pp. 12759-12768.

Myrset, A. H. et al. 1993. DNA and redox state induced conformational changes in the DNA-binding domain of the Myb oncoprotein. *The EMBO journal* 12(12), p. 4625.

Niemeyer, C. M. et al. 1997. Chronic myelomonocytic leukemia in childhood: A retrospective analysis of 110 cases. *Blood* 89(10), pp. 3534-3543.

Niinaka, Y. et al. 1998. Expression and secretion of neuroleukin/phosphohexose isomerase/maturation factor as autocrine motility factor by tumor cells. *Cancer Research* 58(12), pp. 2667-2674.

O'Donnell, B. et al. 1993. Studies on the inhibitory mechanism of iodonium compounds with special reference to neutrophil NADPH oxidase. *Biochem. J* 290, pp. 41-49.

Ogawa, M. 1993. Differentiation and proliferation of hematopoietic stem cells. *Blood* 81(11), pp. 2844-2853.

Ojika, T. et al. 1991. Immunochemical and immunohistochemical studies on three aldolase isozymes in human lung cancer. *Cancer* 67(8), pp. 2153-2158.

Okoniewski, M. J. and Miller, C. J. 2008. Comprehensive analysis of affymetrix exon arrays using BioConductor. *PLoS computational biology* 4(2), p. e6.

Orkin, S. H. and Zon, L. I. 2008. Haematopoiesis: an evolving paradigm for stem cell biology. *Cell* 132(4), pp. 631-644.

Pabst, T. et al. 2001. AML1–ETO downregulates the granulocytic differentiation factor C/EBPα in t (8; 21) myeloid leukemia. *Nature medicine* 7(4), pp. 444-451.

Pandolfi, P. P. 2001. In vivo analysis of the molecular genetics of acute promyelocytic leukemia. *Oncogene* 20(40), pp. 5726-5735.

Pearn, L. et al. 2007. The role of PKC and PDK1 in monocyte lineage specification by Ras. *Blood* 109(10), pp. 4461-4469.

Peled, A. et al. 1999. The chemokine SDF-1 stimulates integrin-mediated arrest of CD34+ cells on vascular endothelium under shear flow. *Journal of Clinical Investigation* 104(9), pp. 1199-1211.

Pelicano, H. et al. 2006a. Glycolysis inhibition for anticancer treatment. *Oncogene* 25(34), pp. 4633-4646.

Pelicano, H. et al. 2006b. Mitochondrial respiration defects in cancer cells cause activation of Akt survival pathway through a redox-mediated mechanism. *Journal of Cell Biology* 175(6), pp. 913-923.

Penhoet, E. E. et al. 1969. Isolation of fructose diphosphate aldolases A, B, and C. *Biochemistry* 8(11), pp. 4391-4395.

Penhoet, E. E. and Rutter, W. J. 1971. Catalytic and immunochemical properties of homomeric and heteromeric combinations of aldolase subunits. *Journal of Biological Chemistry* 246(2), pp. 318-323.

Petit, I. et al. 2007. The SDF-1–CXCR4 signaling pathway: a molecular hub modulating neo-angiogenesis. *Trends in immunology* 28(7), pp. 299-307.

Piccoli, C. et al. 2007. Bone-marrow derived hematopoietic stem/progenitor cells express multiple isoforms of NADPH oxidase and produce constitutively reactive oxygen species. *Biochemical and Biophysical Research Communications* 353(4), pp. 965-972.

Pollyea, D. A. et al. 2011. Acute myeloid leukaemia in the elderly: a review. *British journal of haematology* 152(5), pp. 524-542.

Poole, L. B. et al. 2004. Protein sulfenic acids in redox signaling. *Annual Review of Pharmacology and Toxicology*. pp. 325-347.

Porporato, P. E. et al. 2011. Anticancer targets in the glycolytic metabolism of tumors: a comprehensive review. *Frontiers in pharmacology* 2.

Postovit, L. M. et al. 2002. Oxygen-mediated regulation of tumor cell invasiveness: Involvement of a nitric oxide signaling pathway. *Journal of Biological Chemistry* 277(38), pp. 35730-35737.

Postovit, L. M. et al. 2004. Nitric oxide-mediated regulation of hypoxia-induced B16F10 melanoma metastasis. *International Journal of Cancer* 108(1), pp. 47-53.

Pradelli, L. et al. 2009. Glycolysis inhibition sensitizes tumor cells to death receptors-induced apoptosis by AMP kinase activation leading to Mcl-1 block in translation. *Oncogene* 29(11), pp. 1641-1652.

Prasad, T. K., Goel, R., Kandasamy, K., Keerthikumar, S., Kumar, S., Mathivanan, S., ... & Pandey, A. (2009). Human protein reference database—2009 update. *Nucleic acids research*, *37*(suppl 1), D767-D772.

Price, G. S. et al. 1996. Pharmacokinetics and toxicity of oral and intravenous lonidamine in dogs. *Cancer chemotherapy and pharmacology* 38(2), pp. 129-135.

Purdie, K. J. et al. 2009. Single nucleotide polymorphism array analysis defines a specific genetic fingerprint for well-differentiated cutaneous SCCs. *Journal of Investigative Dermatology* 129(6), pp. 1562-1568.

Purdie, K. J. et al. 2007. Allelic imbalances and microdeletions affecting the PTPRD gene in cutaneous squamous cell carcinomas detected using single nucleotide polymorphism microarray analysis. *Genes Chromosomes and Cancer* 46(7), pp. 661-669.

Rad, A. 2009. Hematopoiesis human diagram. p. Simplified haematopoiesis.

Rahman, I. et al. 2006. Oxidant and antioxidant balance in the airways and airway diseases. *European journal of pharmacology* 533(1), pp. 222-239.

Ramanathan, A. et al. 2005. Perturbational profiling of a cell-line model of tumorigenesis by using metabolic measurements. *Proceedings of the National Academy of Sciences of the United States of America* 102(17), pp. 5992-5997.

Rassool, F. V. et al. 2007. Reactive oxygen species, DNA damage, and error-prone repair: a model for genomic instability with progression in myeloid leukemia? *Cancer research* 67(18), pp. 8762-8771.

Rathmell, J. C. et al. 2003. Akt-directed glucose metabolism can prevent Bax conformation change and promote growth factor-independent survival. *Molecular and Cellular Biology* 23(20), pp. 7315-73Chang28.

Ravagnan, L. et al. 1999. Lonidamine triggers apoptosis via a direct, Bcl-2-inhibit effect on the mitochondrial permeability transition pore. *Oncogene* 18, pp. 2537-2546.

Ravandi, F. et al. 2007. Progress in the treatment of acute myeloid leukemia. *Cancer* 110(9), pp. 1900-1910.

Ray, P. D. et al. 2012. Reactive oxygen species (ROS) homeostasis and redox regulation in cellular signaling. *Cellular signalling* 24(5), pp. 981-990.

Reeves, E. P. et al. 2002. Killing activity of neutrophils is mediated through activation of proteases by K+ flux. *Nature* 416(6878), pp. 291-297.

Reinacher, M. and Eigenbrodt, E. 1981. Immunohistological demonstration of the same type of pyruvate kinase isoenzyme (M2-Pk) in tumors of chicken and rat. *Virchows Archiv B* 37(1), pp. 79-88.

Reindl, C. et al. 2006. Point mutations in the juxtamembrane domain of FLT3 define a new class of activating mutations in AML. *Blood* 107(9), pp. 3700-3707.

Rempel, A. et al. 1996. Glucose catabolism in cancer cells: Amplification of the gene encoding type II hexokinase. *Cancer Research* 56(11), pp. 2468-2471.

Renneville, A. et al. 2008. Cooperating gene mutations in acute myeloid leukemia: a review of the literature. *Leukemia* 22(5), pp. 915-931.

Rhee, S. G. et al. 2005. Intracellular messenger function of hydrogen peroxide and its regulation by peroxiredoxins. *Current Opinion in Cell Biology* 17(2), pp. 183-189.

Ricci, J.-E. et al. 2004. Disruption of mitochondrial function during apoptosis is mediated by caspase cleavage of the p75 subunit of complex I of the electron transport chain. *Cell* 117(6), pp. 773-786.

Rizo, A. et al. 2009. Repression of BMI1 in normal and leukemic human CD34+ cells impairs self-renewal and induces apoptosis. *Blood* 114(8), pp. 1498-1505.

Rodríguez-Enríquez, S., Torres-Márquez, M. E., & Moreno-Sánchez, R. (2000). Substrate oxidation and ATP supply in AS-30D hepatoma cells. *Archives of biochemistry and biophysics*, *375*(1), 21-30.

Russo, G. et al. 2003. Advantages and limitations of microarray technology in human cancer. *Oncogene* 22(42), pp. 6497-6507.

Sallmyr, A. et al. 2008. Genomic instability in myeloid malignancies: Increased reactive oxygen species (ROS), DNA double strand breaks (DSBs) and error-prone repair. *Cancer Letters* 270(1), pp. 1-9.

Santillo, M. et al. 2001. Opposing functions of< i> Ki-</i> and< i> Ha-Ras</i> genes in the regulation of redox signals. *Current Biology* 11(8), pp. 614-619.

Sardina, J. L., López-Ruano, G., Sánchez-Sánchez, B., Llanillo, M., & Hernández-Hernández, A. (2012). Reactive oxygen species: Are they important for haematopoiesis?. *Critical reviews in oncology/hematology*, *81*(3), 257-274.

Sato, M. et al. 2005. Identification of chromosome arm 9p as the most frequent target of homozygous deletions in lung cancer. *Genes Chromosomes and Cancer* 44(4), pp. 405-414.

Satoh, T. et al. 1991. Involvement of ras p21 protein in signal-transduction pathways from interleukin 2, interleukin 3, and granulocyte/macrophage colony-stimulating factor, but not from interleukin 4. *Proceedings of the National Academy of Sciences of the United States of America* 88(8), pp. 3314-3318.

Sattler, M. et al. 1999. Hematopoietic growth factors signal through the formation of reactive oxygen species. *Blood* 93(9), pp. 2928-2935.

Schapira, F. et al. 1970. Resurgence of two fetal-type of aldolases (A and C) in some fast-growing hepatomas. *Biochemical and biophysical research communications* 40(2), pp. 321-327.

Schena, M. et al. 1995. Quantitative monitoring of gene expression patterns with a complementary DNA microarray. *Science* 270(5235), pp. 467-470.

Schlenk, R. F., Döhner, K., Krauter, J., Fröhling, S., Corbacioglu, A., Bullinger, L., ... & Döhner, H. (2008). Mutations and treatment outcome in cytogenetically normal acute myeloid leukemia. *New England Journal of Medicine*, *358*(18), 1909-1918.

Schlichting, I. et al. 1990. Time-resolved X-ray crystallographic study of the conformational change in Ha-Ras p21 protein on GTP hydrolysis. *Nature* 345(6273), pp. 309-315.

Schmid, I. et al. 1992. Dead cell discrimination with 7-amino-actinomcin D in combination with dual color immunofluorescence in single laser flow cytometry. *Cytometry* 13(2), pp. 204-208.

Schubbert, S. et al. 2007. Hyperactive Ras in developmental disorders and cancer. *Nature Reviews Cancer* 7(4), pp. 295-308.

Schuurhuis, G. J. et al. 2013. Normal hematopoietic stem cells within the AML bone marrow have a distinct and higher ALDH activity level than co-existing leukemic stem cells. *PloS one* 8(11), p. e78897.

Segal, A. W. 1996. The NADPH oxidase and chronic granulomatous disease. *Molecular medicine today* 2(3), pp. 129-135.

Selak, M. A. et al. 2005. Succinate links TCA cycle dysfunction to oncogenesis by inhibiting HIF-α prolyl hydroxylase. *Cancer Cell* 7(1), pp. 77-85.

Serù, R. et al. 2004. HaRas activates the NADPH oxidase complex in human neuroblastoma cells via extracellular signal-regulated kinase 1/2 pathway. *Journal of neurochemistry* 91(3), pp. 613-622.

Shen, W. P. V. et al. 1987. Expression of normal and mutant ras proteins in human acute leukemia. *Oncogene* 1(2), pp. 157-165.

Skala, H. et al. 1987. Molecular cloning and expression of rat aldolase C messenger RNA during development and hepatocarcinogenesis. *European Journal of Biochemistry* 163(3), pp. 513-518.

Smithgall, T. E. 1998. Signal transduction pathways regulating hematopoietic differentiation. *Pharmacological reviews* 50(1), pp. 1-20.

Sola-Penna, M. 2008. Metabolic regulation by lactate. *IUBMB life* 60(9), pp. 605-608.

Solomon, D. A. et al. 2008. Mutational inactivation of PTPRD in glioblastoma multiforme and malignant melanoma. *Cancer Research* 68(24), pp. 10300-10306.

Stallings, R. L. et al. 2006. High-resolution analysis of chromosomal breakpoints and genomic instability identifies PTPRD as a candidate tumor suppressor gene in neuroblastoma. *Cancer Research* 66(7), pp. 3673-3680.

Steidl, U. et al. 2007. A distal single nucleotide polymorphism alters long-range regulation of the< i> PU. 1</i> gene in acute myeloid leukemia. *Journal of Clinical Investigation* 117(9), pp. 2611-2620.

Stryer, L. 1988. *Biochemistry*. 3rd ed. New York: WH Freeman & Co.

Suela, J. et al. 2007. DNA profiling analysis of 100 consecutive de novo acute myeloid leukemia cases reveals patterns of genomic instability that affect all cytogenetic risk groups. *Leukemia* 21(6), pp. 1224-1231.

Sun, Y. J. et al. 1999. The crystal structure of a multifunctional protein: Phosphoglucose isomerase/autocrine motility factor/neuroleukin. *Proceedings of the National Academy of Sciences of the United States of America* 96(10), pp. 5412-5417.

Taguchi, K. and Takagi, Y. 2001. Aldolase. *Rinsho byori. The Japanese journal of clinical pathology* Suppl 116, pp. 117-124.

Taussig, D. C., Vargaftig, J., Miraki-Moud, F., Griessinger, E., Sharrock, K., Luke, T., ... & Bonnet, D. (2010). Leukemia-initiating cells from some acute myeloid leukemia patients with mutated nucleophosmin reside in the CD34− fraction. *Blood*, *115*(10), 1976-1984.

Telang, S. et al. 2006. Ras transformation requires metabolic control by 6-phosphofructo-2-kinase. *Oncogene* 25(55), pp. 7225-7234.

Tenen, D. G. 2003. Disruption of differentiation in human cancer: AML shows the way. *Nature Reviews Cancer* 3(2), pp. 89-101.

Terwijn M, Rutten AP, Kelder A, Snel AN, Scholten WJ, et al.. (2010) Accurate detection of residual leukemic stem cells in remission bone marrow predicts relapse in acute myeloid leukemia patients. Blood ASH Annu Meet Abstr 759

Till, J. E. and McCulloch, E. A. 1961. A direct measurement of the radiation sensitivity of normal mouse bone marrow cells. *Radiat Res* 14, pp. 213-222.

Tothova, Z. et al. 2007. FoxOs are critical mediators of hematopoietic stem cell resistance to physiologic oxidative stress. *Cell* 128(2), pp. 325-339.

Trachootham, D. et al. 2009. Targeting cancer cells by ROS-mediated mechanisms: A radical therapeutic approach? *Nature Reviews Drug Discovery* 8(7), pp. 579-591.

Trahey, M. and McCormick, F. 1987. A cytoplasmic protein stimulates normal N-ras p21 GTPase, but does not affect oncogenic mutants. *Science* 238(4826), pp. 542-545.

Vafa, O. et al. 2002. c-Myc can induce DNA damage, increase reactive oxygen species, and mitigate p53 function: A mechanism for oncogene-induced genetic instability. *Molecular Cell* 9(5), pp. 1031-1044.

Valk, P. J., Hol, S., Vankan, Y., Ihle, J. N., Askew, D., Jenkins, N. A., ... & Delwel, R. (1997). The genes encoding the peripheral cannabinoid receptor and alpha-L-fucosidase are located near a newly identified common virus integration site, Evi11. *Journal of virology*, *71*(9), 6796-6804.

Valk, P. J., & Delwel, R. (1998). The peripheral cannabinoid receptor, Cb2, in retrovirally-induced leukemic transformation and normal hematopoiesis.*Leukemia & lymphoma*, *32*(1-2), 29-43.

Van Engeland, M., Nieland, L. J., Ramaekers, F. C., Schutte, B., & Reutelingsperger, C. P. (1998). Annexin V-affinity assay: a review on an apoptosis detection system based on phosphatidylserine exposure. *Cytometry*,*31*(1), 1-9.

Van Rhenen, A., Feller, N., Kelder, A., Westra, A. H., Rombouts, E., Zweegman, S., ... & Schuurhuis, G. J. (2005). High stem cell frequency in acute myeloid leukemia at diagnosis predicts high minimal residual disease and poor survival. *Clinical Cancer Research*, *11*(18), 6520-6527.

Vander Heiden, M. G. et al. 2009. Understanding the Warburg effect: the metabolic requirements of cell proliferation. *science* 324(5930), pp. 1029-1033.

Vardiman, J. W. et al. 2002. The World Health Organization (WHO) classification of the myeloid neoplasms. *Blood* 100(7), pp. 2292-2302.

Vardiman, J. W. et al. 2009. The 2008 revision of the World Health Organization (WHO) classification of myeloid neoplasms and acute leukemia: rationale and important changes. *Blood* 114(5), pp. 937-951.

Veeriah, S. et al. 2009. The tyrosine phosphatase PTPRD is a tumor suppressor that is frequently inactivated and mutated in glioblastoma and other human cancers. *Proceedings of the National Academy of Sciences* 106(23), pp. 9435-9440.

Vergez, S. et al. 2010. Preclinical and clinical evidence that deoxy-2-[18F]fluoro-D-glucose positron emission tomography with computed tomography is a reliable tool for the detection of early molecular responses to erlotinib in head and neck cancer. *Clinical Cancer Research* 16(17), pp. 4434-4445.

von Eyben, F. E. 2001. A systematic review of lactate dehydrogenase isoenzyme 1 and germ cell tumors. *Clinical biochemistry* 34(6), pp. 441-454.

Vora, S. 1983. Isozymes of human phosphofructokinase: biochemical and genetic aspects. *Isozymes* 11, pp. 3-23.

Wang, Y. H., Israelsen, W. J., Lee, D., Vionnie, W. C., Jeanson, N. T., Clish, C. B., ... & Scadden, D. T. (2014). Cell-state-specific metabolic dependency in haematopoiesis and leukemogenesis. *Cell*, *158*(6), 1309-1323.

Wang, J. et al. 1996. The molecular nature of the F-actin binding activity of aldolase revealed with site-directed mutants. *Journal of Biological Chemistry* 271(12), pp. 6861-6865.

Warburg, O. 1956a. On respiratory impairment in cancer cells. *Science* 124(3215), pp. 269-270.

Warburg, O. 1956b. On the origin of cancer cells. *Science* 123(3191), pp. 309-314.

Warner, J. K. et al. 2004. Concepts of human leukemic development. *Oncogene* 23(43), pp. 7164-7177.

Wennerberg, K. et al. 2005. The Ras superfamily at a glance. *Journal of cell science* 118(5), pp. 843-846.

Whitlock, C. A. and Witte, O. N. 1982. Long-term culture of B lymphocytes and their precursors from murine bone marrow. *Proceedings of the National Academy of Sciences of the United States of America* 79(11 I), pp. 3608-3612.

Wilson, A. and Trumpp, A. 2006. Bone-marrow haematopoietic-stem-cell niches. *Nature Reviews Immunology* 6(2), pp. 93-106.

Wyllie, A. H. 1997. Apoptosis: an overview. *British Medical Bulletin* 53(3), pp. 451-465.

Xi, L. et al. 2008. Whole genome exon arrays identify differential expression of alternatively spliced, cancer-related genes in lung cancer. *Nucleic acids research* 36(20), pp. 6535-6547.

Xu, R. H. et al. 2005b. Inhibition of glycolysis in cancer cells: A novel strategy to overcome drug resistance associated with mitochondrial respiratory defect and hypoxia. *Cancer Research* 65(2), pp. 613-621.

Yang, J.-Q. et al. 1999. Superoxide Generation in v-Ha-rasąTransduced Human Keratinocyte HaCaT Cells. *Molecular carcinogenesis* 26, p. 180ą188.

Yoshihara, H. et al. 2007. Thrombopoietin/MPL Signaling Regulates Hematopoietic Stem Cell Quiescence and Interaction with the Osteoblastic Niche. *Cell Stem Cell* 1(6), pp. 685-697.

Younes, M. et al. 1996. Overexpression of the human erythrocyte glucose transporter occurs as a late event in human colorectal carcinogenesis and is associated with an increased incidence of lymph node metastases. *Clinical Cancer Research* 2(7), pp. 1151-1154.

Zhang, J. et al. 2003. Identification of the haematopoietic stem cell niche and control of the niche size. *Nature* 425(6960), pp. 836-841.

Zhang, Y. Y. et al. 1998. Nf1 regulates hematopoietic progenitor cell growth and ras signaling in response to multiple cytokines. *Journal of Experimental Medicine* 187(11), pp. 1893-1902.

Zhao, Y. et al. 2007. Glycogen synthase kinase 3α and 3β mediate a glucose-sensitive antiapoptotic signaling pathway to stabilize Mcl-1. *Molecular and cellular biology* 27(12), pp. 4328-4339.

Zhao, Y. et al. 2008. Glucose metabolism attenuates p53 and Puma-dependent cell death upon growth factor deprivation. *Journal of Biological Chemistry* 283(52), pp. 36344-36353.

Zhong, D. et al. 2008. 2-Deoxyglucose induces Akt phosphorylation via a mechanism independent of LKB1/AMP-activated protein kinase signaling activation or glycolysis inhibition. *Molecular cancer therapeutics* 7(4), pp. 809-817.

Zhong, D. et al. 2009. The glycolytic inhibitor 2-deoxyglucose activates multiple prosurvival pathways through IGF1R. *Journal of Biological Chemistry* 284(35), pp. 23225-23233.

Zhou, M. et al. 2010. Warburg effect in chemosensitivity: targeting lactate dehydrogenase-A re-sensitizes taxol-resistant cancer cells to taxol. *Mol Cancer* 9(1), p. 33.

Zhu, Q. S. et al. 2006. G-CSF induced reactive oxygen species involves Lyn-PI3-kinase-Akt and contributes to myeloid cell growth. *Blood* 107(5), pp. 1847-1856.

Zimmermann, K. and Leser, U. 2010. Analysis of Affymetrix exon arrays.

Appendices

Appendix 1

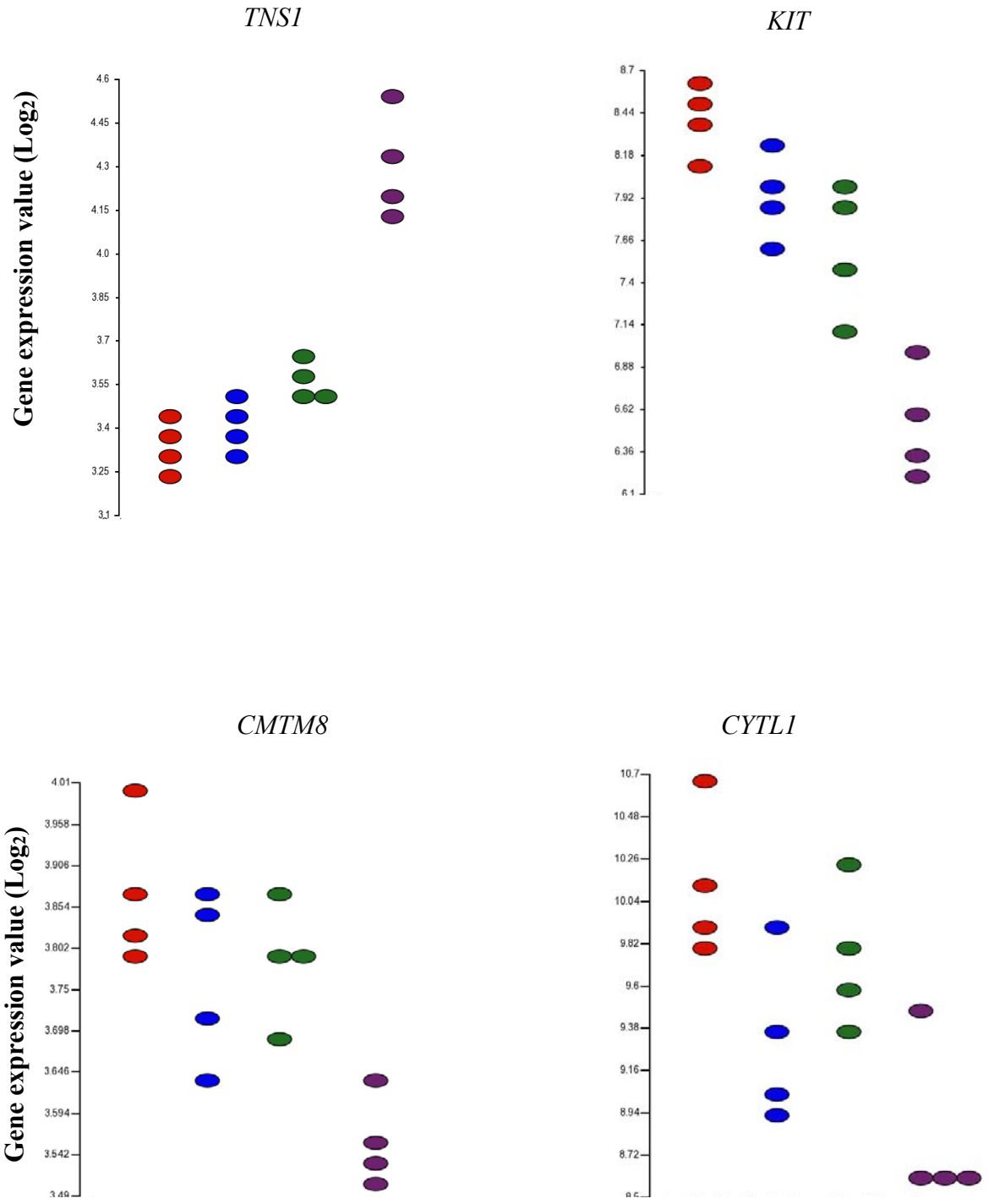

CNR2

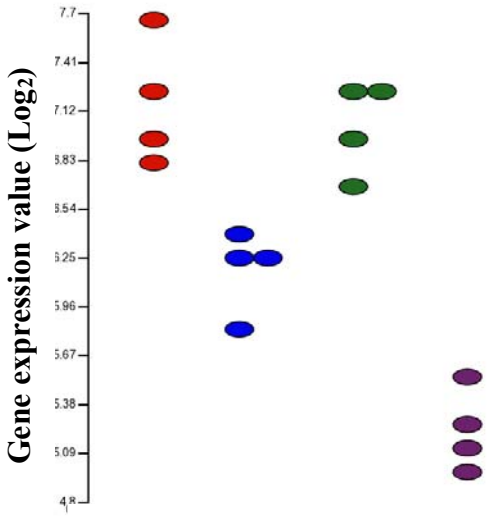

CD32

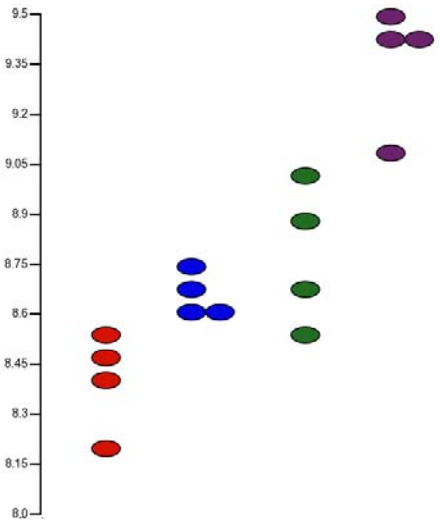

CD34

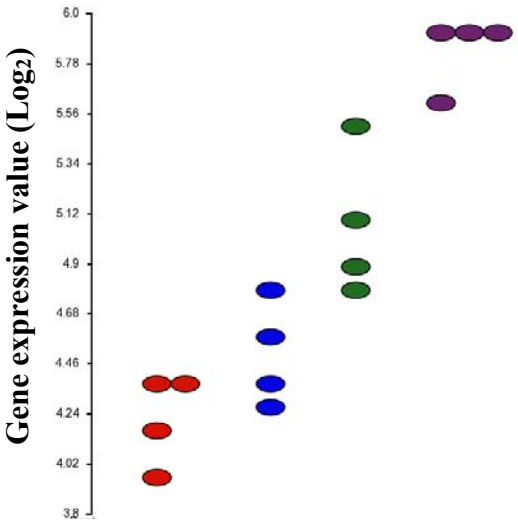

WDR54

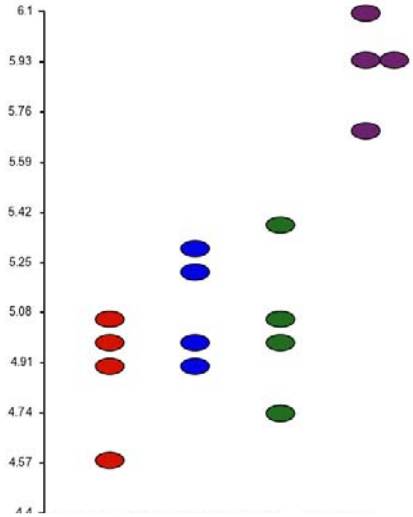

JAKMIP2

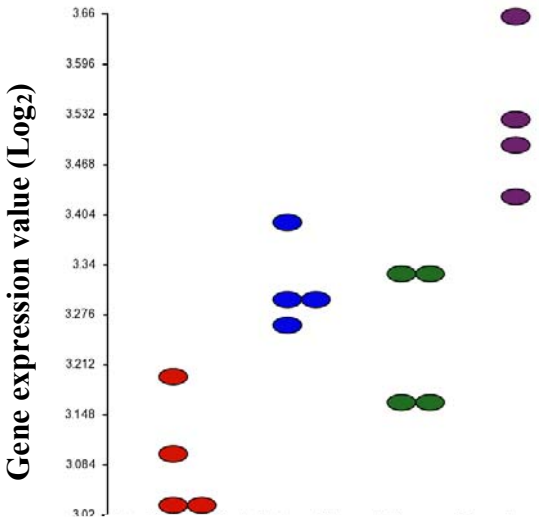

PTPRD

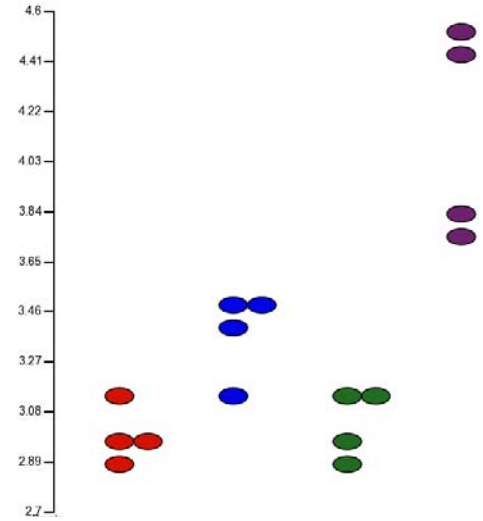

ASPH

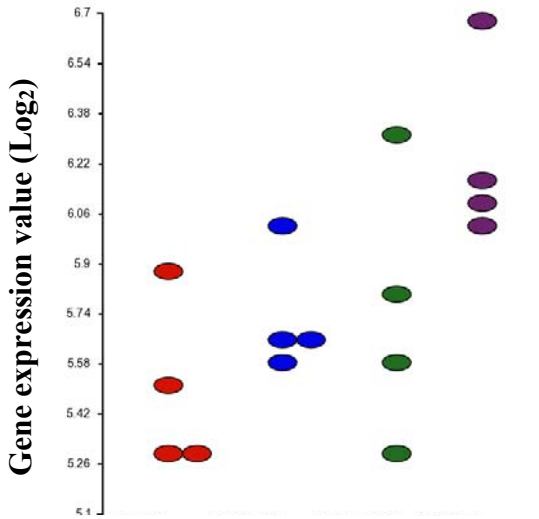

FBP1

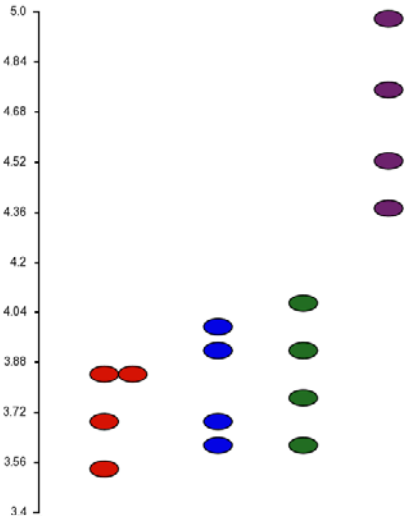

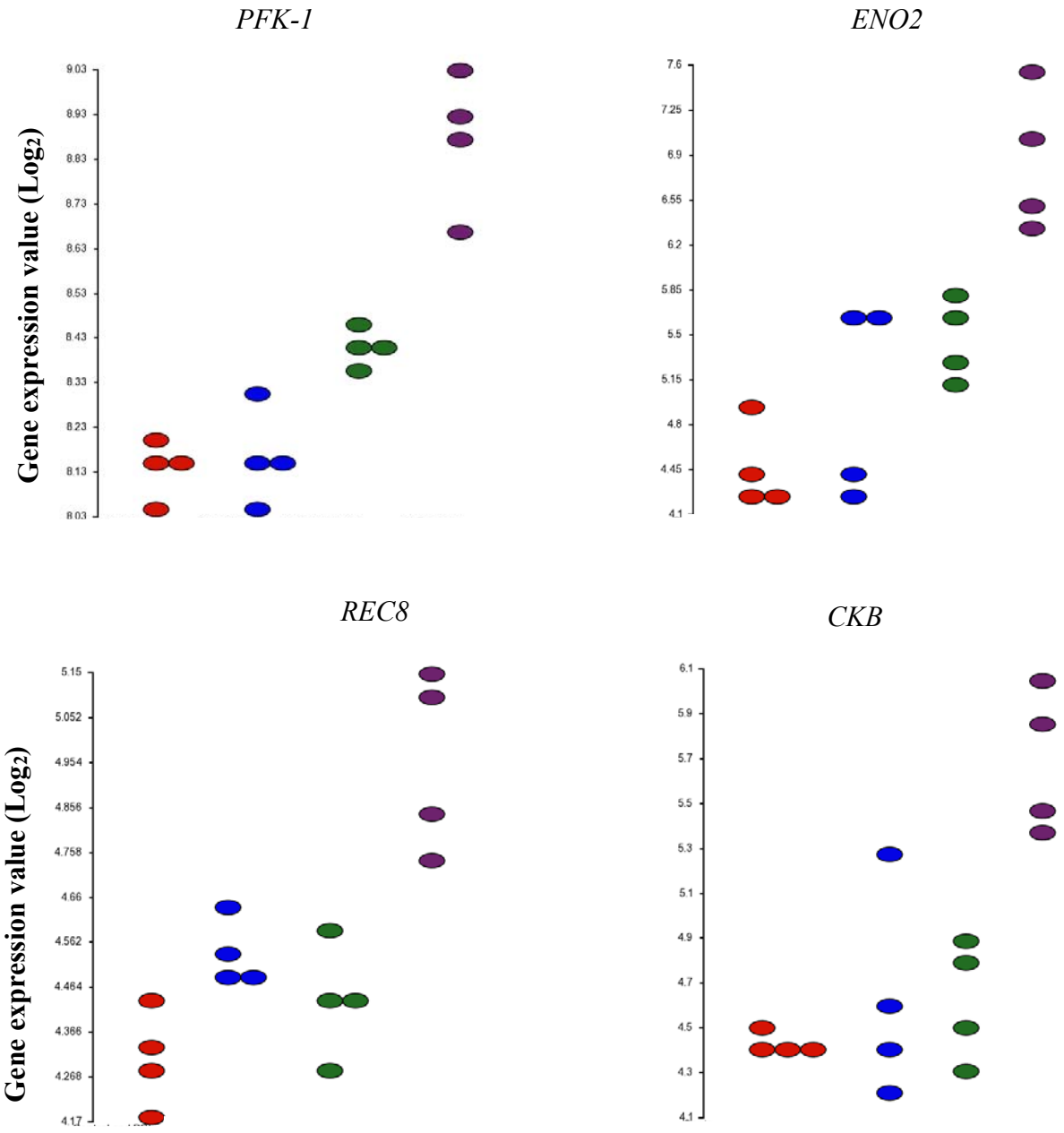
PFK-1
ENO2
REC8
CKB
Gene expression value (Log2)
Gene expression value (Log2)
9.03
8.93
8.83
8.73
8.63
8.53
8.43
8.33
8.23
8.13
8.03
7.6
7.25
6.9
6.55
6.2
5.85
5.5
5.15
4.8
4.45
4.1
5.15
5.052
4.954
4.856
4.758
4.66
4.562
4.464
4.366
4.268
4.17
6.1
5.9
5.7
5.5
5.3
5.1
4.9
4.7
4.5
4.3
4.1

GATM

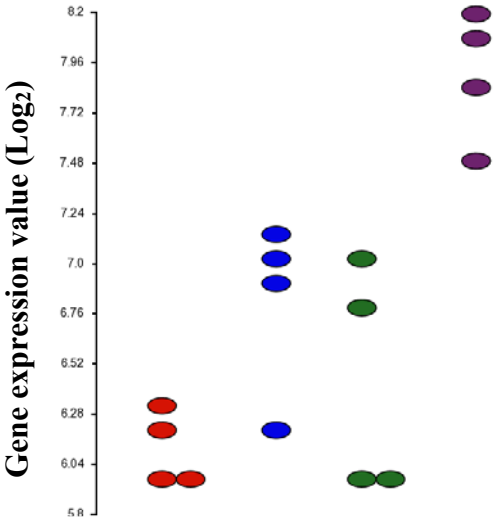

GPI

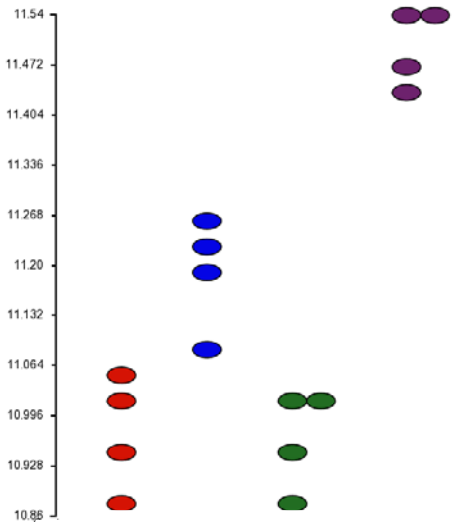

CACNB1

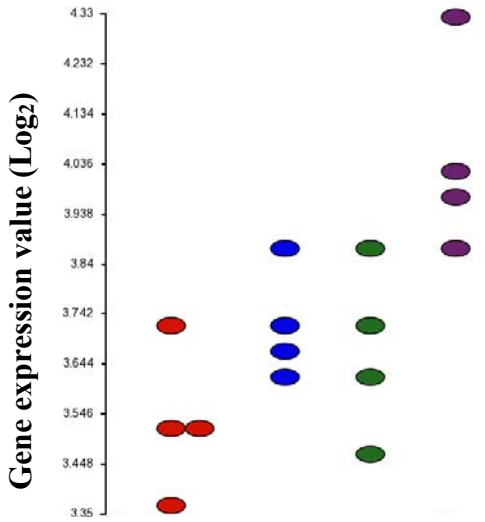

Un-identified

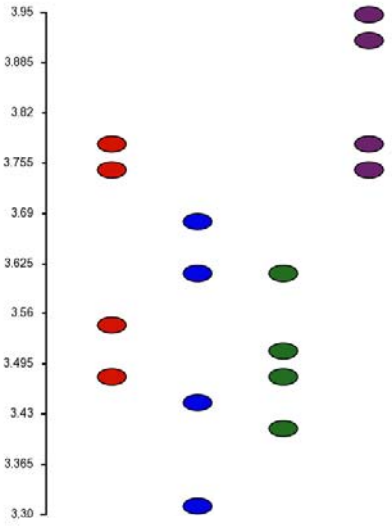

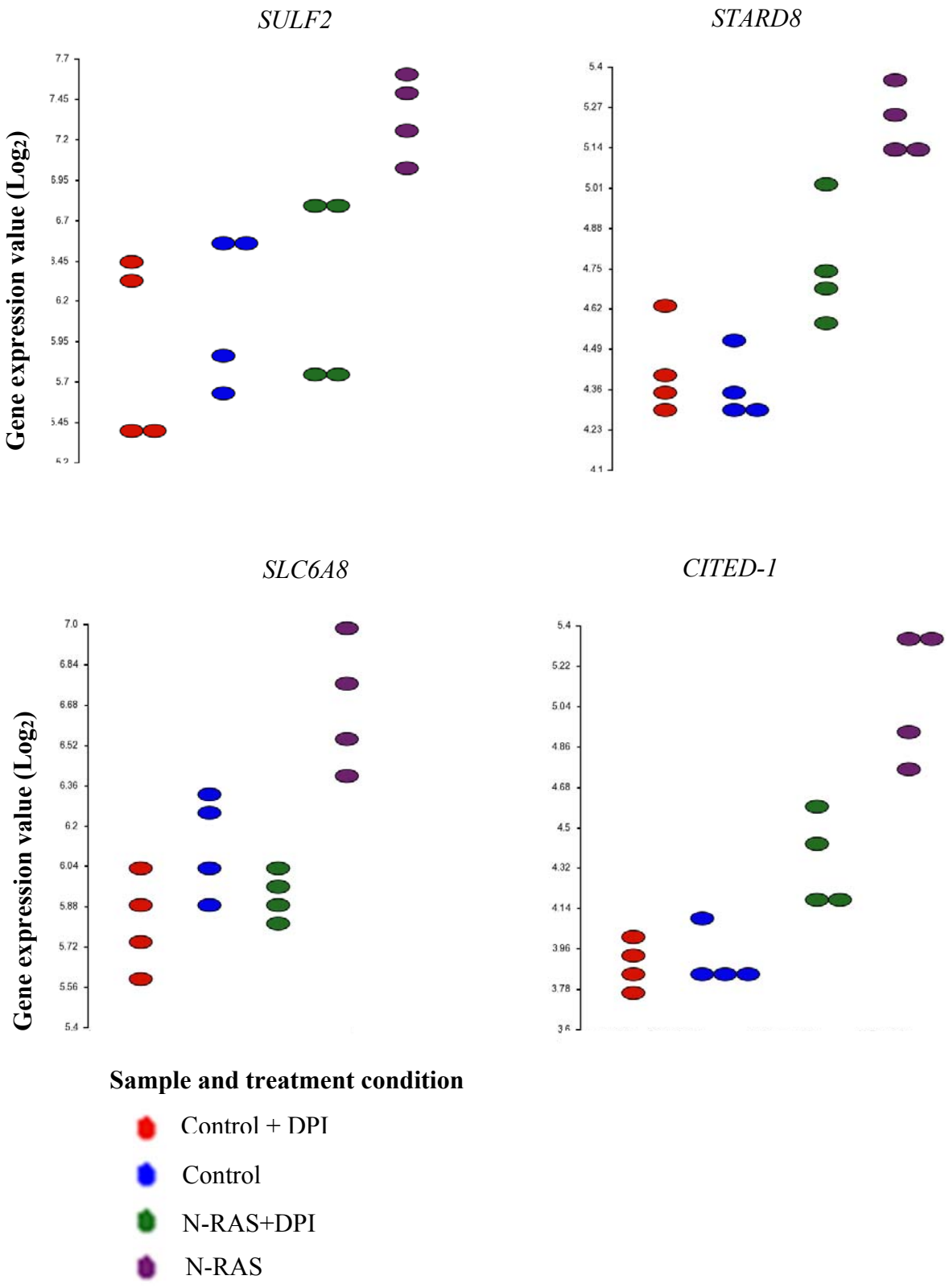

Dot plots of mutant N-RAS gene changes mediated by ROS

The Y-axis represents the normalised gene expression value (log_2); the X-axis represents the different sample treatment conditions and replicate data for each condition (coloured dots). For each treatment condition n=4. These plots are data for all genes found to be dysregulated by ROS (see chapter 4).